AN INVESTIGATION OF THE PROPAGATION OF RADIO WAVES AT FREQUENCIES IN THE VHF AND UHF BANDS WITHIN CERTAIN BRITISH CITIES

by

Keith Allsebrook

This report is submitted for the degree of Doctor of Philosophy to the Faculty of Science and Engineering at the University of Birmingham.

January 1977

Department of Electronic and Electrical Engineering

University of Birmingham

SYNOPSIS

Unmodulated carrier waves at frequencies of 75.375, 85.875, 167.2 and 441.025 MHz have been radiated by aerials mounted on tall buildings or prominent terrain features in the British cities of Birmingham, Bath and Bradford. The spatial distribution of the r.f. signal envelope existing within urban and suburban areas at these frequencies has been recorded using a vehicle-mounted receiver with a aerial fixed to the vehicle's roof. An analysis of these measurements has shown the distance over which the envelope may be anticipated to be Rayleigh distributed to be less than 75 m.

A median signal prediction model is derived from the measured data and its performance is statistically assessed with the experimental values. The measurements and the predictions have been found to be in close agreement.

Comparison of the Okumura model with measured values has demonstrated that the proposed model exhibits similar prediction errors to those obtained by the more widely used Okumura model. The Okumura model is therefore concluded to be more complex, and hence more costly to use, than is necessary for applications in British cities.

ACKNOWLEDGEMENTS

The author wishes to thank Mr J.D. Parsons of the University of Birmingham for his advice, guidance and moral support during the course of this research project and also to acknowledge the many useful technical discussions which took place, particularly with Dr. C.J.Hall (AWRE Aldermaston) and Mr. C. Felix (BAC Bristol). The author is also grateful to Professors E.D.R. Shearman (University of Birmingham), W. Gosling (University of Bath) and D.P. Howson (University of Bradford) for the use of equipment and facilities at their respective Universities.

CONTENTS

APPENDICES

LIST OF PRINCIPAL SYMBOLS

a	The Earth's Effective Radius
a_o	The Earth's True Radius (approximately 6370 km)
b	The Mode of a Rayleigh Distribution
c	Velocity of Propagation
d	A Distance Variable
d_{km}	Distance expressed in kilometres
f	Frequency
f_{MHz}	Frequency expressed in Megahertz
f_m	Maximum Doppler Frequency
h	A Height Variable
h_r	Height of Receiving Aerial
h_t	Height of Transmitting Aerial
i	An Index or Counter
j	$\sqrt{-1}$
k	A Constant
n	An Exponent
n_s	Refractive Index of the Earth's Atmosphere
$p(x)$	Probability Density Function
r	A Range Variable
s	Standard Deviation
t	A Time Variable
u	Vehicle Velocity
v	Fresnel v-parameter
$w(t)$	Filter Impulse Response
x	A General Variable
y	A General Variable
z	A General Variable

A	Attenuation
$A(P-Q-R)$	Attenuation over the Diffracted Path Joining Points P,Q and R
C	Phase Change on Reflection from a Conducting Surface in Excess of π
D	Distance
E	Electric Field Component
E_o	RMS Electric Field
E_z	Vertical Component of the Electric Field
$F(x)$	A Function of x
G	Aerial Gain
G_r	Gain of Receiving Aerial
G_t	Gain of Transmitting Aerial
H	Magnetic Field Component
H_o	RMS Magnetic Field
H_x	x - component of the Magnetic Field
H_y	y - component of the Magnetic Field
L	Loss (in dB)
L_b	Basic Transmission Loss (dB)
L_B	Diffraction Loss over Buildings (dB)
L_D	Diffraction Loss (dB)
L_F	Free-Space Path Loss (dB)
L_P	Plane-Earth Path Loss (dB)
L_T	Total Loss (dB)
N	The Total Number of Events in a Set
N_S	Surface Refractivity of the Earth's Atmosphere
N_X	Level Crossing Rate
P	Power
P_r	Power Received
P_t	Power Transmitted

$P(x)$	Probability of Event 'x'
Q	Divergence Factor
R	Reflection Coefficient
R_e	Effective Reflection Coefficient
S	Power Spectral Density
T	Total Time Elapsed
$U(x)$	Correction Factor for Diffraction over a Cylindrical Obstacle
$V(\tau)$	Covariance Function
W	Street Width
X	A General Variable
Y	A General Variable

$E(x)$	The Complete Elliptic Integral of the Second Kind
$J_n(x)$	The Bessel Function of the First Kind, of n^{th} Order
$K(x)$	The Complete Elliptic Integral of the First Kind

α	Street Orientation
β	Urban Clutter Factor
β'	Frequency Corrected Urban Clutter Factor
γ	UHF Correction Factor
δ	Error Parameter for Double Knife-Edge Diffraction
ϵ	Permittivity
λ	Wavelength
θ	The Diffraction Angle
η	Normalised Amplitude (x/x_{rms})
σ	Conductivity
$\sum$	The sum of

ψ	Azimuthal Angle of Arrival of Signals at the Receiver
ϕ	A Phase Angle
Φ	The Grazing Angle of Reflection
τ	A Time Duration
Δ	A small change of
Δr	Path Length Difference
ρ	Curvature
ξ	A Correction Factor
ω	Angular Frequency
ω_c	Angular Carrier Frequency
ω_m	Maximum Angular Doppler Frequency

ψ	Azimuthal Angle of Arrival of Signals at the Receiver
ϕ	A Phase Angle
Φ	The Grazing Angle of Reflection
τ	A Time Duration
Δ	A small change of
Δr	Path Length Difference
ρ	Curvature
ξ	A Correction Factor
ω	Angular Frequency
ω_c	Angular Carrier Frequency
ω_m	Maximum Angular Doppler Frequency

CHAPTER 1

INTRODUCTION

The radiotelephone, in its many guises, is rapidly becoming an everyday item of electronic equipment. This development is hardly surprising when one considers that the benefits afforded to the users by such systems are many and varied and, in general, far outweigh any disadvantages they might impose. For example, a taxi can be directed by a central controller to collect a passenger without it having to return to base for instructions. Each taxi in the fleet therefore has the capability of making more paying journeys during a given time period when fitted with a radiotelephone than would be possible without. Similarly, a police patrol vehicle can be redirected away from its routine duties to deal with an emergency as, and when, it happens. Furthermore, it is possible for the base station controller to locate those police vehicles closest to the scene of the incident which are most ably equipped to handle it and to divert only those vehicles to the required location, thereby dealing quickly and efficiently with the situation. This ability to operate with dynamic assignment can provide a large increase in the efficiency of each vehicle, thus making the mobile radiotelephone extremely popular with the operators of large fleets of vehicles.

The rapid increase in the quantity of operational radiotelephones brought about by this popularity has created a number of problems, however. For instance, in Great Britain during the late 1960's the UHF civil land mobile frequency band extended from 450 MHz to 470 MHz and was allocated to users at 50 kHz channel spacing. The total number of UHF channels available in any city therefore amounted to

only 400, insufficient to meet the rising demand at that time. Even with the inclusion of the VHF bands the frequency spectrum can be seen to be easily congested. Immediate solutions which have been adopted have been to reduce the channel spacing to as low as 12½ kHz for voice communications and to increase the width of the frequency bands. Nevertheless, the attainment of the maximum number of channels in any band by optimum spectrum usage is of great importance. A large amount of interest[1.1] has accordingly been aroused in the application of single sideband modulation techniques to mobile systems with the ultimate intention of achieving the minimum practicable value of r.f. bandwidth for a voice link of approximately 3 kHz. The problems concerned with the implementation of s s b systems in electrically noisy, urban environments are numerous, however, and much research is still needed before a viable system can be made commercially available.

The range to which a radio link can operate depends largely upon the aerial siting philosophy adopted. In a town or city these siting rules often differ from those employed on long range point-to-point links, primarily because conventional techniques are impracticable, notably in that the mobile terminal, in order to be mobile, must have its aerial fixed to the vehicle. The simplest, and thus cheapest and most popular, form of aerial is a quarter wavelength whip employing some portion of the vehicle's body as a ground plane. The base of the aerial is therefore rarely more than 3 m above the ground level and is consequently well below the level of the buildings.

The low aerial height associated with the mobile unit implies that an obstructed transmission path will exist within a city when the two terminals are separated by typically more than 1 km. The signal must therefore propagate between the transmitter and the receiver by way of reflection, scattering and diffraction mechanisms,[1.2-1.4] giving rise to an interference situation at the receiving aerial. As a result of this multipath propagation the receiver experiences a standing wave type of pattern with both the amplitude and phase of the resulting signal, measured with respect to some arbitrary but fixed reference, fluctuating rapidly when the mobile unit traverses small distances.[1.4-1.6] Examples of the signal magnitude variations are given in Figs.1.1, 1.2 and 1.3 for a location in Birmingham measured using radiated frequencies of 85.875, 167.2 and 441.025 MHz respectively.

Receiving systems employing coherent demodulation techniques will experience severe problems in maintaining the angular synchronism between the local oscillator and the received carrier necessary for undistorted demodulation. Even in the case of narrow band non-coherent demodulation systems, e.g. envelope detection of a voice modulated carrier, the rapid variations in the signal amplitude cause problems, usually in the form of brief signal "drop outs" which mar the intelligibility of the transmitted message. The severity of these rapid fading effects can to a large extent be overcome by the use of diversity techniques;[1.7] a subject which has received much attention in recent years.[1.1, 1.8-1.10]

While diversity systems are of use in reducing the depths of the closely spaced nulls in the spatially distributed interference pattern, they are generally impracticable against large area signal variations caused by such factors as terrain obstacles. These large scale effects tend to be evidenced when the mobile terminal travels distances greater than approximately 200 m [1.6,1.11] and cannot be combatted using space diversity (the aerial separation required would be many hundreds of metres), time diversity (the mobile unit can be within the affected area for many minutes) or polarisation diversity (the same problems exist with both horizontal and vertical polarisation in the VHF and UHF bands).

Regions can therefore be established within the desired coverage area about a fixed base station site where the propagation path loss is sufficiently high to prevent radio communications. These regions are termed radio "black spots" and are often located in the diffraction shadows of hills or other prominent terrain features.[1.12,1.13] A solution frequently adopted in order to ensure that the radio link will operate satisfactorily within the planned coverage area is to increase the effective radiated power of the transmitter. This, however, has the undesirable effect of increasing the coverage area beyond that required by the user, thereby adding to the problem of spectrum congestion by making that carrier frequency unallocatable to other users for a larger distance than is absolutely necessary. A more satisfactory solution to the problem would be to select that base station aerial site which provides reliable service (say 98% of all locations within the desired coverage area) while requiring the minimum

effective radiated transmitter power. To achieve this optimum siting many measurements of the propagation path loss must be made using all the base station sites of interest, thus making the determination of the grade of service prohibitively expensive when many base station locations are considered. Accordingly, there can be seen to be a definite need for a mathematical model which will permit the transmission loss to be predicted in terms of the large area characteristics of the terrain at VHF and UHF in urban and suburban areas. Formulation of such a model will facilitate the production of coverage diagrams using digital computer methods[1.14] at a fraction of the cost required for the execution of a complete measurement programme.

1.1 REFERENCES

1.1 IERE
"Civil Land Mobile Radio"
IERE Conference Proceedings No.33
November 1975

1.2 Ossanna J.F.
"A Model for Mobile Radio Fading due to Building Reflections: Theoretical and Experimental Power Spectra"
B.S.T.J., Vol.48, No.6, November 1964

1.3 Gans M.J.
"A Power Spectral Theory of Propagation in the Mobile-Radio Environment"
IEEE Trans. Vehic. Tech., Vol.VT-21, February 1972

1.4 Clarke R.H.

"A Statistical Theory of Mobile Radio Reception"

B.S.T.J., Vol.47, No.6, July/August 1968

1.5 Nylund H.W.

"Characteristics of Small Area Signal Fading on a Mobile Circuit in the 150 MHz Band"

IEEE Trans. Vehic. Tech., Vol.VT-17, October 1968

1.6 Young W.R. Jr.

"Comparison of Mobile Radio Transmissions at 150, 450, 900 and 3700 Mc"

B.S.T.J., Vol.31, November 1952

1.7 Brennan D.G.

"Linear Diversity Combining Techniques"

Proc. IRE, 47, June 1959

1.8 Parsons J.D. and Ratliff P.A.

"Diversity Reception for VHF Mobile Radio"

The Radio and Electronic Engineer, Vol.43, No.5, May 1973

1.9 Ratliff P.A.

"VHF Mobile Radio Communications - A Study of Multipath Fading and Diversity Reception"

Ph.D. Thesis, University of Birmingham, Dept. of Elec. and Elec Eng., September 1973

1.10 Henze M.

"A Diversity System for UHF Mobile Radio Reception"

Ph.D. Thesis, University of Birmingham, Dept. of Elec. and Elec. Eng., June 1975

1.11 Allsebrook K.

"VHF Propagation in an Urban Environment"

M.Sc. Thesis, University of Birmingham, Dept. of Elec. and Elec. Eng., October 1972

1.12 Sofaer E. and Bell C.P.

"Factors Affecting the Propagation and Reception of Broadcasting Signals in the UHF Bands"

Proc. IEE, Vol.113, No.7, July 1966

1.13 Kirby R.S. and Capps F.M.

"Correlation in VHF Propagation over Irregular Terrain"

IRE Trans. Ant. and Prop., AP-4, January 1956

1.14 Barsis A.P.

"Determination of Service Area for VHF/UHF Land Mobile and Broadcast Operations over Irregular Terrain"

IEEE Trans. Vehic. Tech., Vol.VT-22, No.2, May 1973

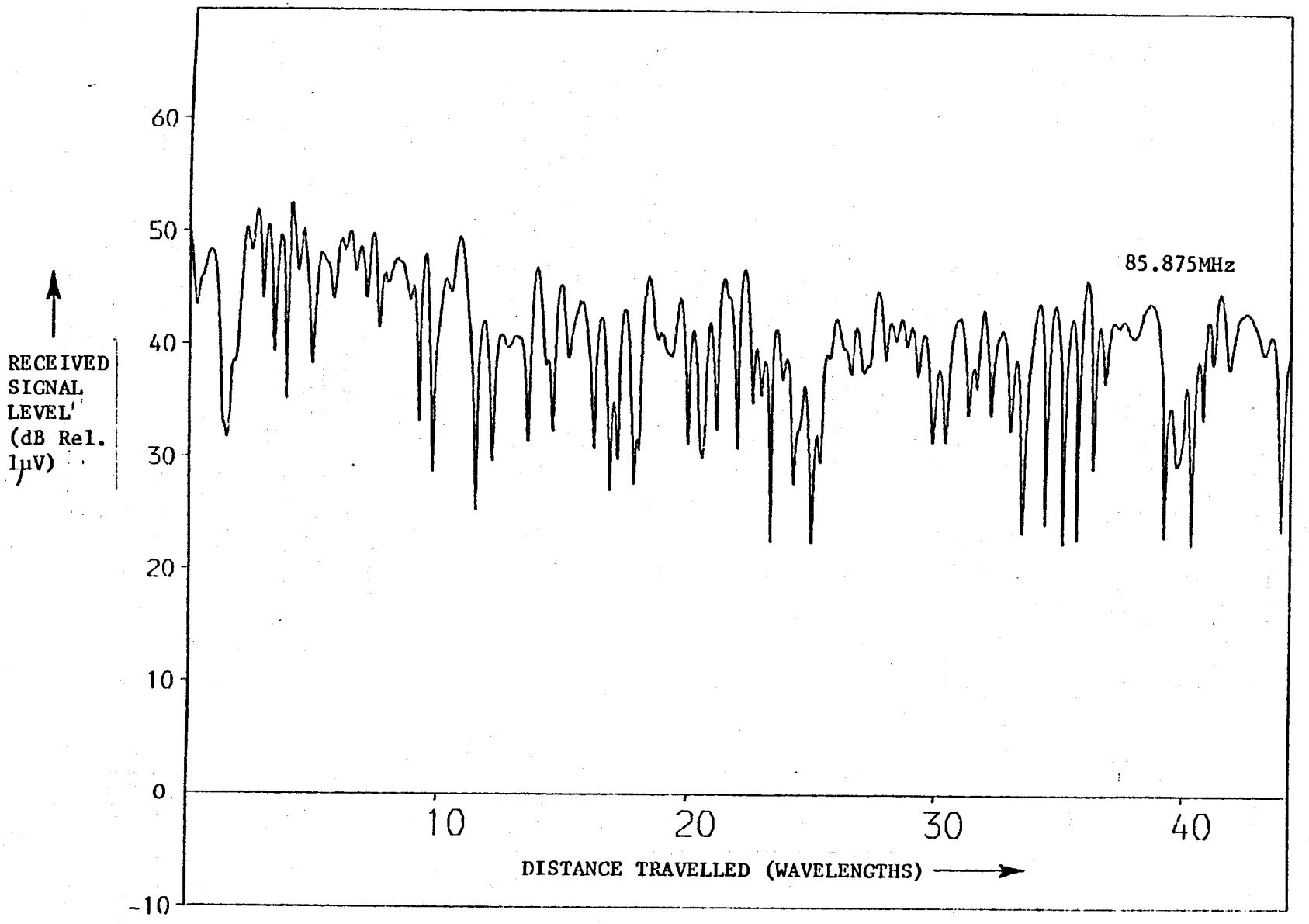

A MEASURED SIGNAL ENVELOPE

FIG. 1.1

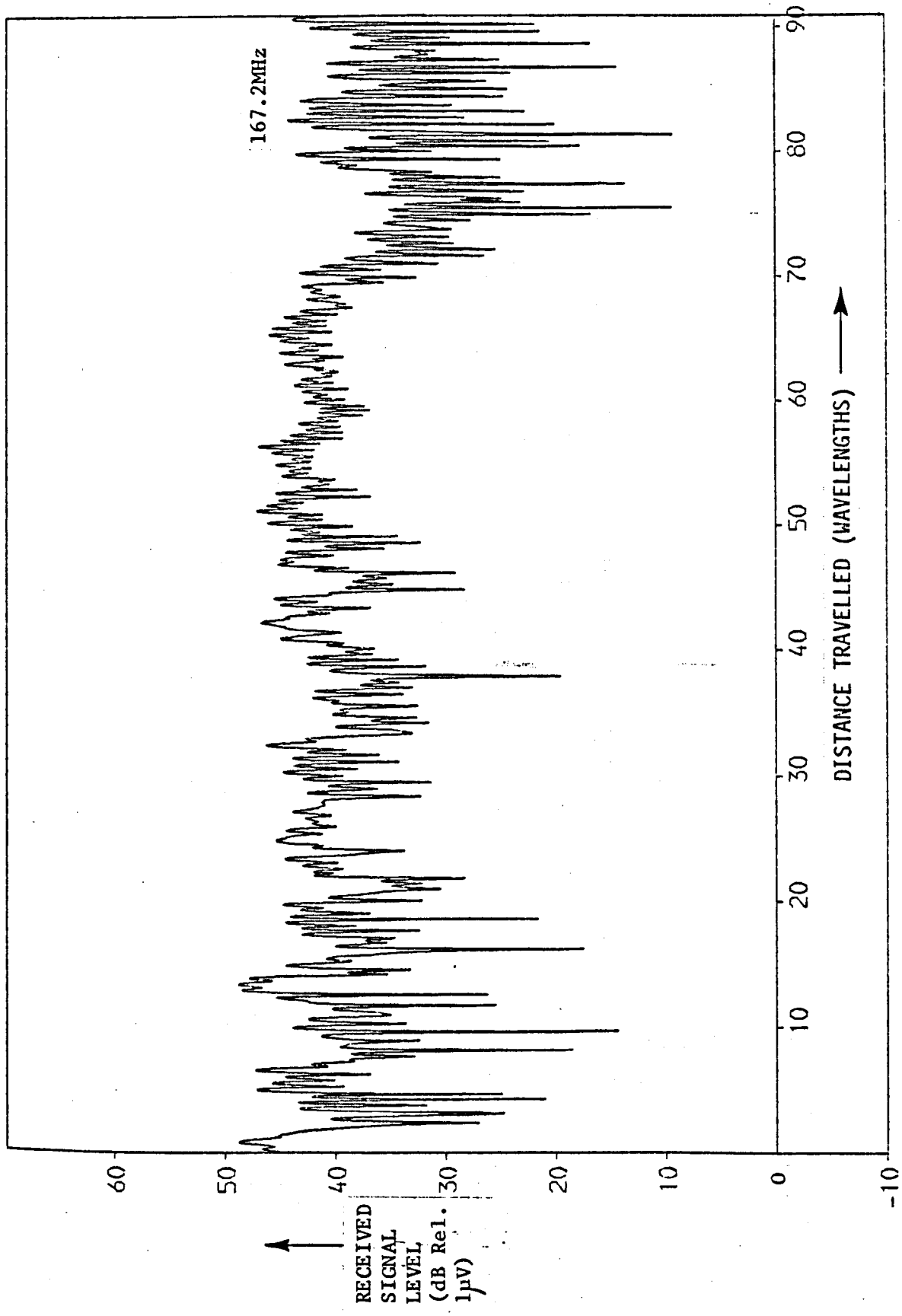

A MEASURED SIGNAL ENVELOPE

FIG. 12

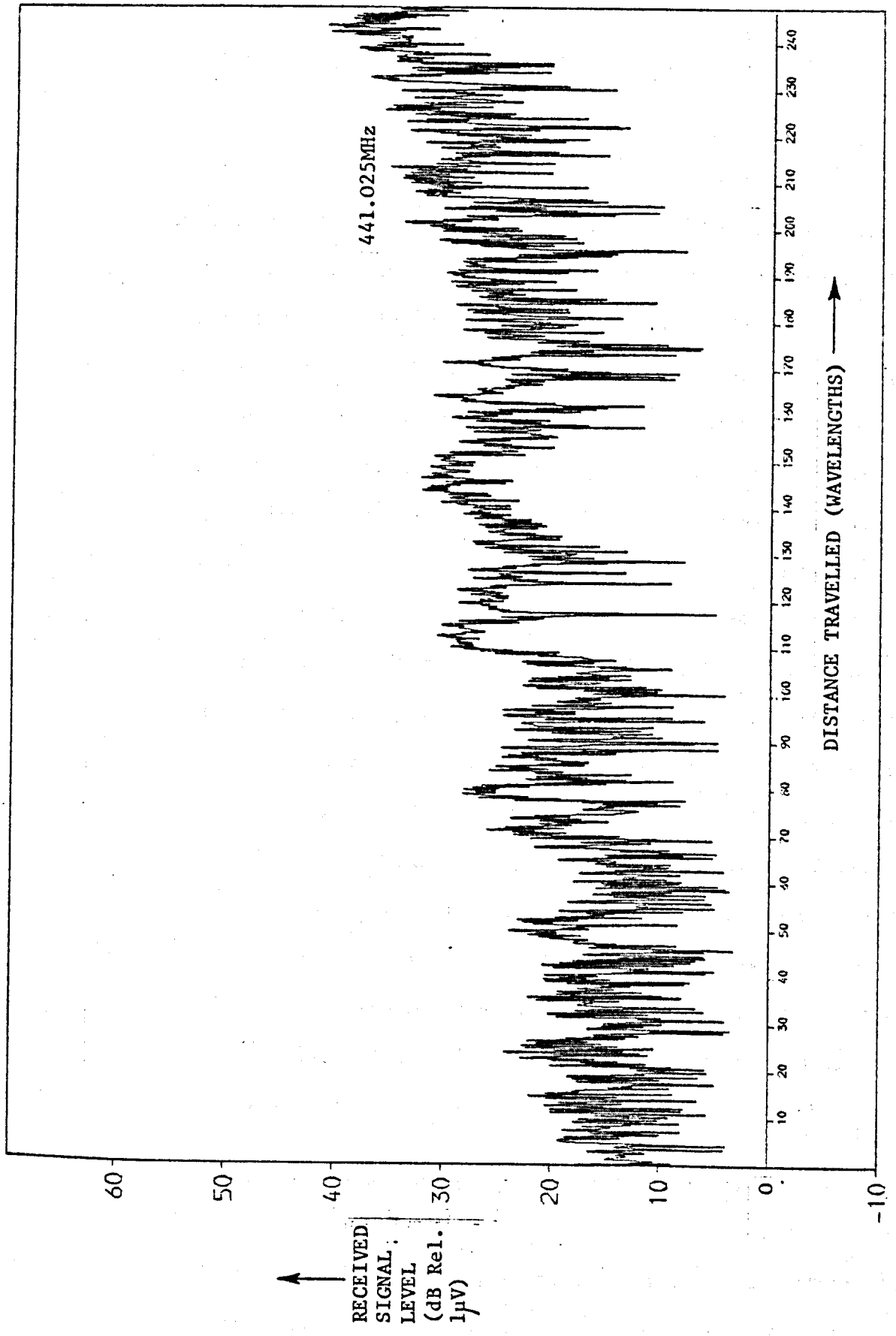

A MEASURED SIGNAL ENVELOPE

FIG. 13

CHAPTER 2

FAST FADING PROPERTIES OF THE RECEIVED SIGNAL ENVELOPE

The low aerial height associated with a mobile terminal results in the line-of-sight path between a transmitter and a vehicle-mounted receiver operating in a town or city being frequently obstructed by buildings and trees. It is intuitively reasonable, therefore, to describe the signal received by an aerial fixed to a vehicle as the sum of a number of components which have been diffracted and reflected by the various obstacles found in cities.[2.1,2.2,2.3] These obstructions are normally fabricated from an unknown inhomogeneous mixture of brick, concrete, glass, steel and wood, and frequently have large surface irregularities. The reflection coefficient and phase change on reflection will, in the absence of an exact description of the reflecting surface, be a seemingly random quantity. The incident r.f. energy will therefore be better described as being incoherently scattered at the surface rather than being coherently reflected. Under these circumstances the signal, x(t), at a point in space may be considered[2.2] to be the sum of 'N' components having random amplitudes, X, with phase angles, ϕ, uniformly distributed in the range 0 to 2π, and arriving at the aerial from random directions, ψ (Fig.2.1), in the horizontal plane, thus:

$$x(t) = \sum_{i=1}^{N} X_i \cos(\{\omega_c + \frac{2\pi}{\lambda} u \cos\psi_i\}t + \phi_i)$$

The resultant signal, x(t), is itself a random quantity[2.4,2.5] and varies rapidly when the receiving point moves distances of

only a few wavelengths, as demonstrated by the measured signal envelope records shown in Figs. 1.1, 1.2 and 1.3. The closely spaced noise-like signal fluctuations are colloquially termed "fast fades" as a result of their observation in time series by a moving receiver, or as "multipath fades" because of the multi-ray interference situation which created them.

2.1 THE ENVELOPE DISTRIBUTION OF THE FAST FADING FIELD

The vector sum of a large number of sinusoids (greater than approximately 6) with random amplitudes and phase angles has been demonstrated,[2.4,2.5] by recourse to the central limit theorem, to be a Gaussian random variable. The envelope of a Gaussian random process has also been shown[2.4,2.5] to be Rayleigh distributed (Fig.2.2):

$$p(x) = \begin{cases} \frac{x}{b^2} \exp\left(-\frac{x^2}{2b^2}\right) & , \quad x \geq 0 \\ 0 & , \quad x < 0 \end{cases}$$

The corresponding cumulative probability distribution, $P(x \leq X)$, is given by:

$$P(x \leq X) = \int_{-\infty}^{X} p(x)dx = 1 - \exp\left(-\frac{X^2}{2b^2}\right)$$

Table 2.1 lists some of the more important values on the Rayleigh probability distribution and indicates that only the mode "b" of the distribution is required to uniquely classify it.

Parameter	Value
Mode	b
Variance	$(2 - \pi/2)b^2$
R.M.S. Value	$\sqrt{2}$ b
Mean	$\sqrt{\pi/2}$ b
10 percentile	0.459 b
Median (50 percentile)	1.1774 b
90 percentile	2.146 b

Table 2.1

Important Points on the Rayleigh Distribution

Many authors[2.6,2.7,2.11,2.12] have reported the existence of a Rayleigh distributed signal envelope when the distance travelled by the measuring receiver was small, typically less than 200 m.[2.6] Investigations in Birmingham at 85.875, 167.2 and 441.025 MHz have indicated, however, that a Rayleigh distribution is rarely to be found at all frequencies over the same measurement path for the 250 m measurement interval employed. In a practical situation a slight change in the position of the receiver can result in a variation of the dominant low-frequency (slow fading) signal level but, as the vehicle must necessarily travel a finite and often large distance to cover sufficient fades (i.e. minima in the spatial interference pattern) to provide a statistically valid signal estimate, the probability of observing this "ideal" fading pattern is small.

Consider the transmission situation depicted in Fig.2.3 where the dominant component signal arrives at the receiver by way of diffraction over an obstacle. The signal strength received in

this example will be proportional to $\sqrt{\lambda d_2}^{2.8}$, suggesting that small variations will be more relevant at UHF than at VHF.

Figs. 2.4, 2.5 and 2.6 show data measured over the same path at each of the three frequencies of interest and demonstrate the practical existence of the Rayleigh distribution. Figs. 2.7, 2.8 and 2.9, however, show a path where the signal appears Rayleigh distributed at the VHF frequencies but describes an indeterminate distribution at the UHF frequency.

2.2 ENVELOPE POWER SPECTRA OF THE FIELD COMPONENTS

The baseband power spectrum of the electric field component of the received signal envelope is given by:[2.2,2.9]

$$S_{E_z}(f) = \frac{E_o^2}{8\omega_m} K\left(\sqrt{1 - \left(\frac{f}{2f_m}\right)^2}\right)$$

This power spectrum is depicted in Fig.2.10 and shows that a sharp cut-off frequency exists at twice the maximum doppler frequency, implying that the maximum doppler frequency, and therefore the vehicle's velocity, is a constant. However, observations taken over a large distance in a city must be made at variable velocity and therefore with a varying value of f_m. The resulting spectrum will appear smeared and will not exhibit a clearly defined cut-off frequency.

The magnetic field components of the received signal envelope, for a rms magnetic field strength of H_o, are given by:[2.9]

$$S_{H_x}(f) = \frac{2H_o^2}{3\omega_m}\left\{\left(1 + \left(\frac{f}{2f_m}\right)^2\right) E\left(\sqrt{1 - \left(\frac{f}{2f_m}\right)^2}\right) - 2\left(\frac{f}{2f_m}\right)^2 K\left(\sqrt{1 - \left(\frac{f}{2f_m}\right)^2}\right)\right\}$$

$$S_{H_y}(f) = \frac{H_o^2}{2\omega_m}\left\{\left(1 + \frac{1}{3}\left(\frac{f}{f_m}\right)^2\right) K\left(\sqrt{1 - \left(\frac{f}{2f_m}\right)^2}\right) - \frac{1}{3}\left(8 - \left(\frac{f}{f_m}\right)^2\right) E\left(\sqrt{1 - \left(\frac{f}{2f_m}\right)^2}\right)\right\}$$

2.3 LEVEL CROSSING RATES OF THE FIELD ENVELOPE COMPONENTS

The rate at which the signal envelope crosses a specified signal level, X, in a positive direction is given by the level crossing rate, N_X:

$$N_X = \int_o^\infty \frac{dx}{dt} \cdot p\left(X, \frac{dx}{dt}\right) \cdot d\left(\frac{dx}{dt}\right)$$

Assuming a Gaussian random process this expression, for the three field components, reduces to:[2.9(p.31)]

$$N_{X_{E_z}} = \sqrt{2\pi}\, f_m\, \eta\, e^{-\eta^2}$$

$$N_{X_{H_x}} = \sqrt{\pi}\, f_m\, \eta\, e^{-\eta^2}$$

$$N_{X_{H_y}} = \sqrt{3\pi}\, f_m\, \eta\, e^{-\eta^2}$$

where η is a normalised variable given by:

$$\eta = \frac{X}{X_{rms}}$$

These crossing rates are plotted as functions of η in Fig.2.11.

2.4 AVERAGE DURATION OF A FAST FADE

The position and depth of a fast fade have been found to be representable as random quantities.[2.7,2.10] An estimate of the average fade depth will be of interest, therefore, in the absence of an exact field description.

The probability that the signal envelope magnitude, x, will be below a specified level, X, is given by:[2.9]

$$P(x \leq X) = \frac{1}{T} \sum_{i=1}^{N} \tau_i$$

where τ_i is the duration of the i^{th} fade, there being a total of N fades in the total observation period, T.

The three field components have average fade durations of:[2.9]

$$\bar{\tau}_{E_z} = \frac{e^{\eta^2} - 1}{\eta f_m \sqrt{2\pi}}$$

$$\bar{\tau}_{H_x} = \frac{e^{\eta^2} - 1}{\eta f_m \sqrt{\pi}}$$

$$\bar{\tau}_{H_y} = \frac{e^{\eta^2} - 1}{\eta f_m \sqrt{3\pi}}$$

The average fade durations are shown in Fig.2.12 as functions of the normalised variable, η.

2.5 THE ENVELOPE COVARIANCE FUNCTIONS

The magnitudes of the autocovariance functions of the three field components have been demonstrated to be:[2.9]

$$V_{E_z}(\tau) = \frac{\pi}{16} E_o^2 J_o^2 (\omega_m \tau)$$

$$V_{H_x}(\tau) = \frac{\pi}{16} H_o^2 \left(J_o (\omega_m \tau) + J_2 (\omega_m \tau)\right)^2$$

$$V_{H_y}(\tau) = \frac{\pi}{16} H_o^2 \left(J_o (\omega_m \tau) - J_2 (\omega_m \tau)\right)^2$$

The magnitudes of the cross-covariance functions are given as:

$$V_{E_z H_x}(\tau) = 0$$

$$V_{H_x H_y}(\tau) = 0$$

These relationships hold for all τ, provided that the probability of the phase distribution of the individual signal components, $p(\phi)$, is an even function. If ϕ can be assumed to be uniformly distributed in the range 0 to 2π, i.e. $p(\phi) = 1/2\pi$, the remaining cross-covariance function magnitude approximates to:[2.9]

$$V_{E_z H_y}(\tau) = \frac{\pi}{8} E_o H_o J_1^2 (\omega_m \tau)$$

The forms of these covariances are depicted in Fig.2.13 as functions of $(f_m \tau)$.

2.6 REFERENCES

2.1 Ossanna J.F.

"A Model for Mobile Radio Fading due to Building Reflections: Theoretical and Experimental Power Spectra"

B.S.T.J., Vol.48, No.6, November 1964

2.2 Clarke R.H.

"A Statistical Theory of Mobile Radio Reception"

B.S.T.J., Vol.47, No.6, July/August 1968

2.3 Gans M.J.

"A Power Spectral Theory of Propagation in the Mobile Radio Environment"

IEEE Trans. Vehic. Tech., Vol.VT-21, February 1972

2.4 Slack M.

"The Probability of Sinusoidal Oscillations Combined in Random Phase"

J. IEEE, 93 Part III, 1946

2.5 Bennett W.R.

"Distribution of the Sum of Randomly Phased Components"

Quart. Appl. Math., 5, January 1948

2.6 Young W.R. Jr.

"Comparison of Mobile Radio Transmission at 150, 450, 900 and 3700 Mc"

B.S.T.J., Vol.31, November 1952

2.7 Nylund H.W.

"Characteristics of Small Area Signal Fading on Mobile Circuits in the 150 MHz Band"

IEEE Trans. Vehic. Tech., Vol.VT-17, No.1, October 1968

2.8 Rice P.L., Longley A.G., Norton K.A. and Barsis A.P.
"Transmission Loss Predictions for Tropospheric Communications Circuits"
NBS Tech Note 101, 1967

2.9 Jakes W.C. Jr.
"Microwave Mobile Communications"
John Wiley & Sons - London

2.10 Lee W.C.Y.
"Statistical Analysis of the Level Crossings and Duration of Fades of the Signal from an Energy Density Mobile Radio Antenna"
B.S.T.J., February 1967

2.11 Ratliff P.A.
"VHF Mobile Radio Communications - A Study of Multipath Fading and Diversity Reception"
Ph.D. Thesis, University of Birmingham, Dept. of Elec. and Elec. Eng., September 1973

2.12 Henze M.
"A Diversity System for UHF Mobile Radio Reception"
Ph.D. Thesis, University of Birmingham, Dept. of Elec. and Elec. Eng., June 1975

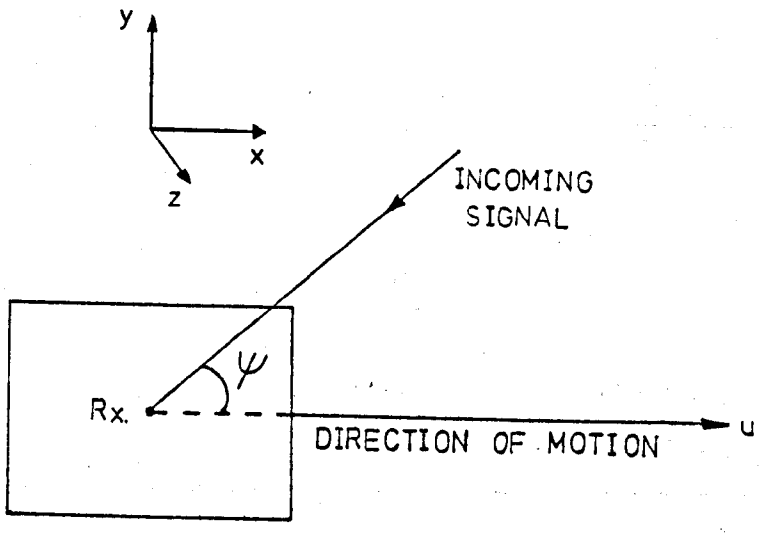

THE ANGLE OF ARRIVAL OF AN INCOMING SIGNAL FIG 2.1

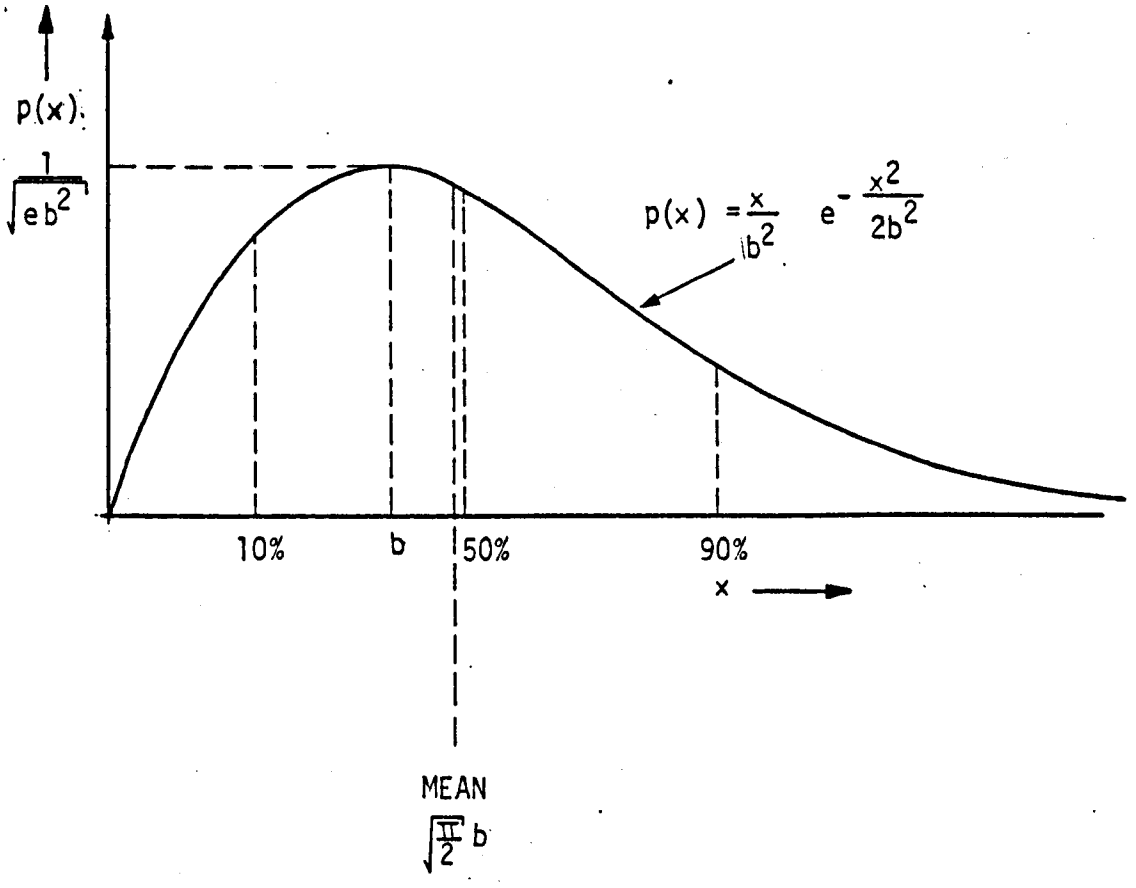

THE RAYLEIGH PROBABILITY DENSITY FUNCTION

FIG. 2.2

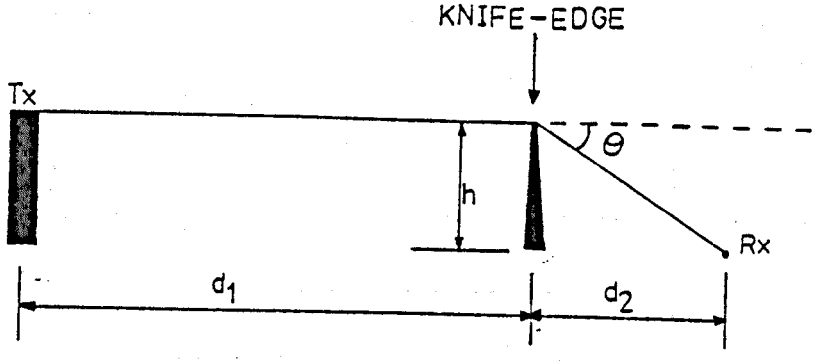

$$v = \sqrt{\frac{2 d_1 d_2}{\lambda (d_1 + d_2)}}\ \theta$$

if $d_1 \gg d_2$; $\quad v \doteq \sqrt{\frac{2}{\lambda d_2}}\ h$

IDEAL KNIFE-EDGE DIFFRACTION GEOMETRY

FIG. 2.3

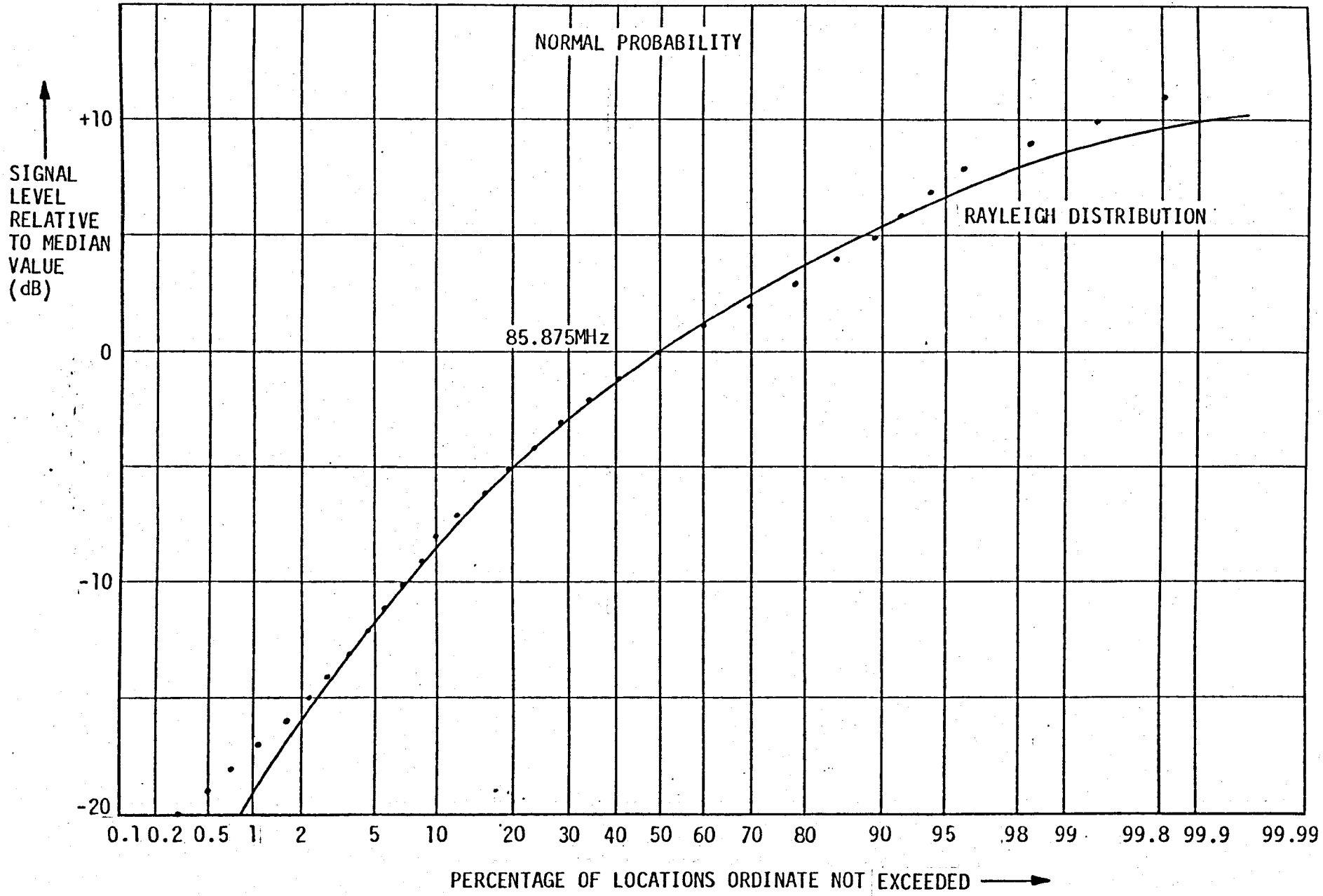

PROBABILITY DISTRIBUTION OF A MEASURED SIGNAL ENVELOPE (UMBERSLADE ROAD - BIRMINGHAM)

FIG. 2.4

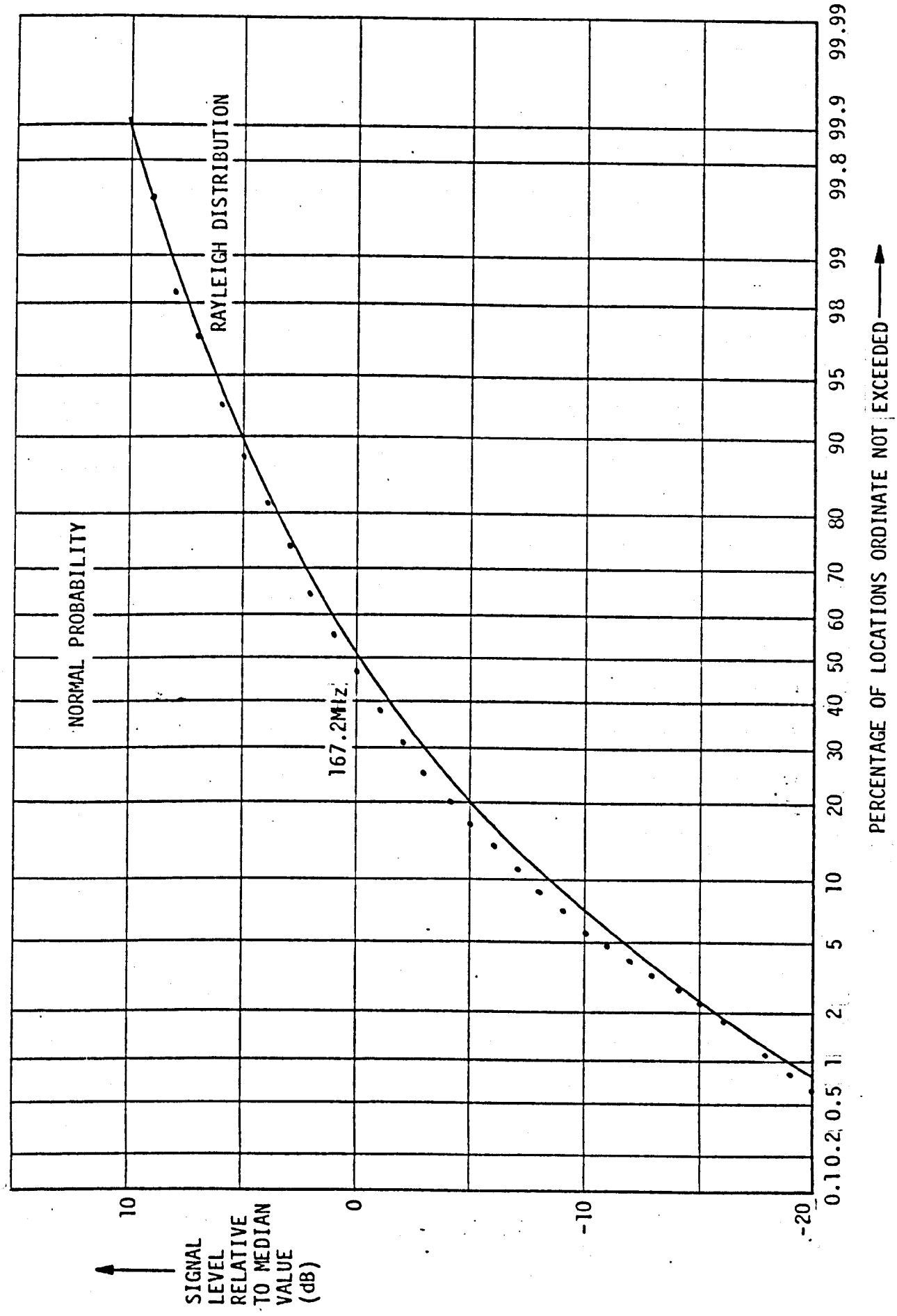

PROBABILITY DISTRIBUTION OF A MEASURED SIGNAL ENVELOPE (UMBERSLADE ROAD - BIRMINGHAM)

FIG. 2.5

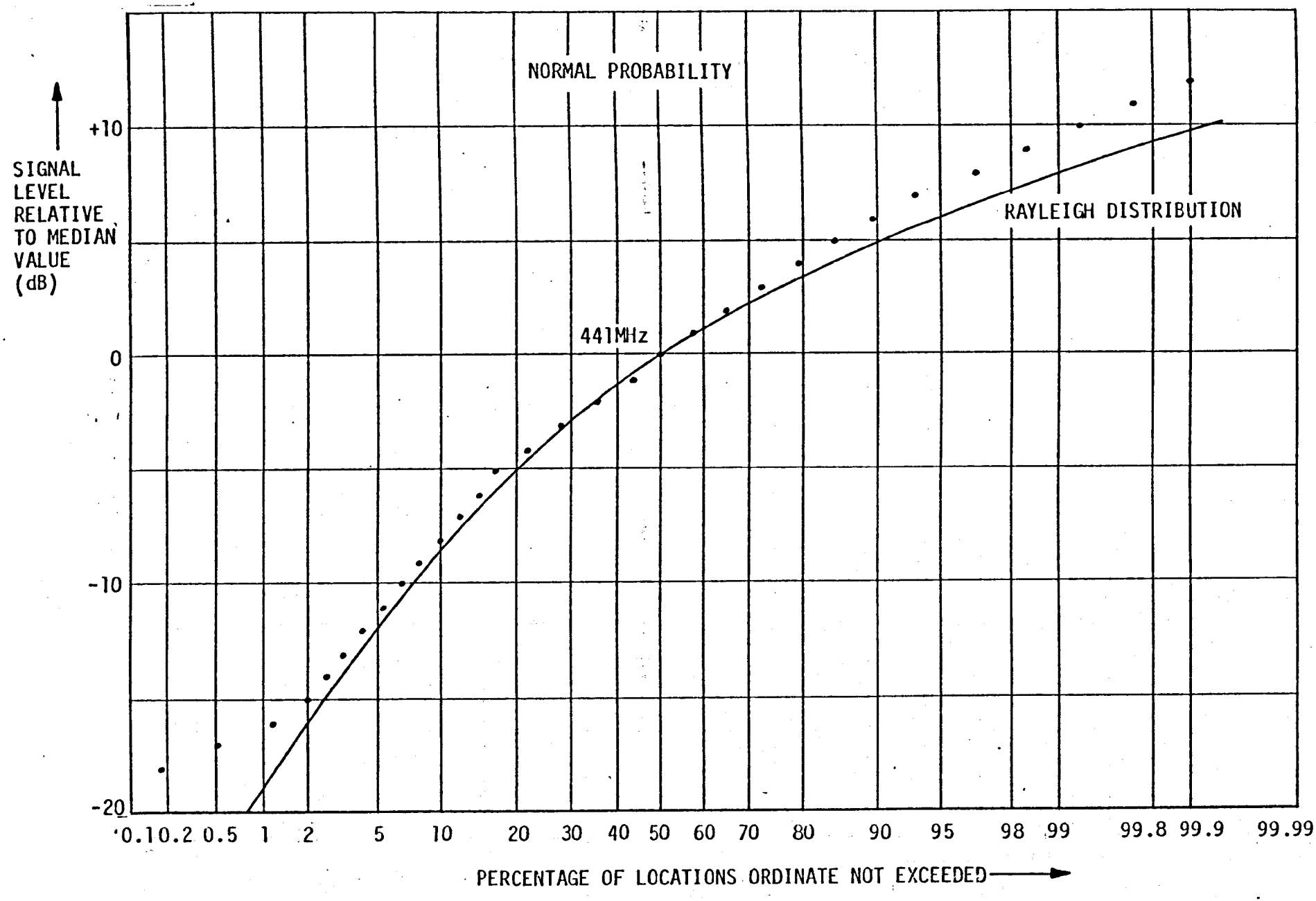

PROBABILITY DISTRIBUTION OF A MEASURED SIGNAL ENVELOPE (UMBERSLADE ROAD - BIRMINGHAM)

FIG. 2.6

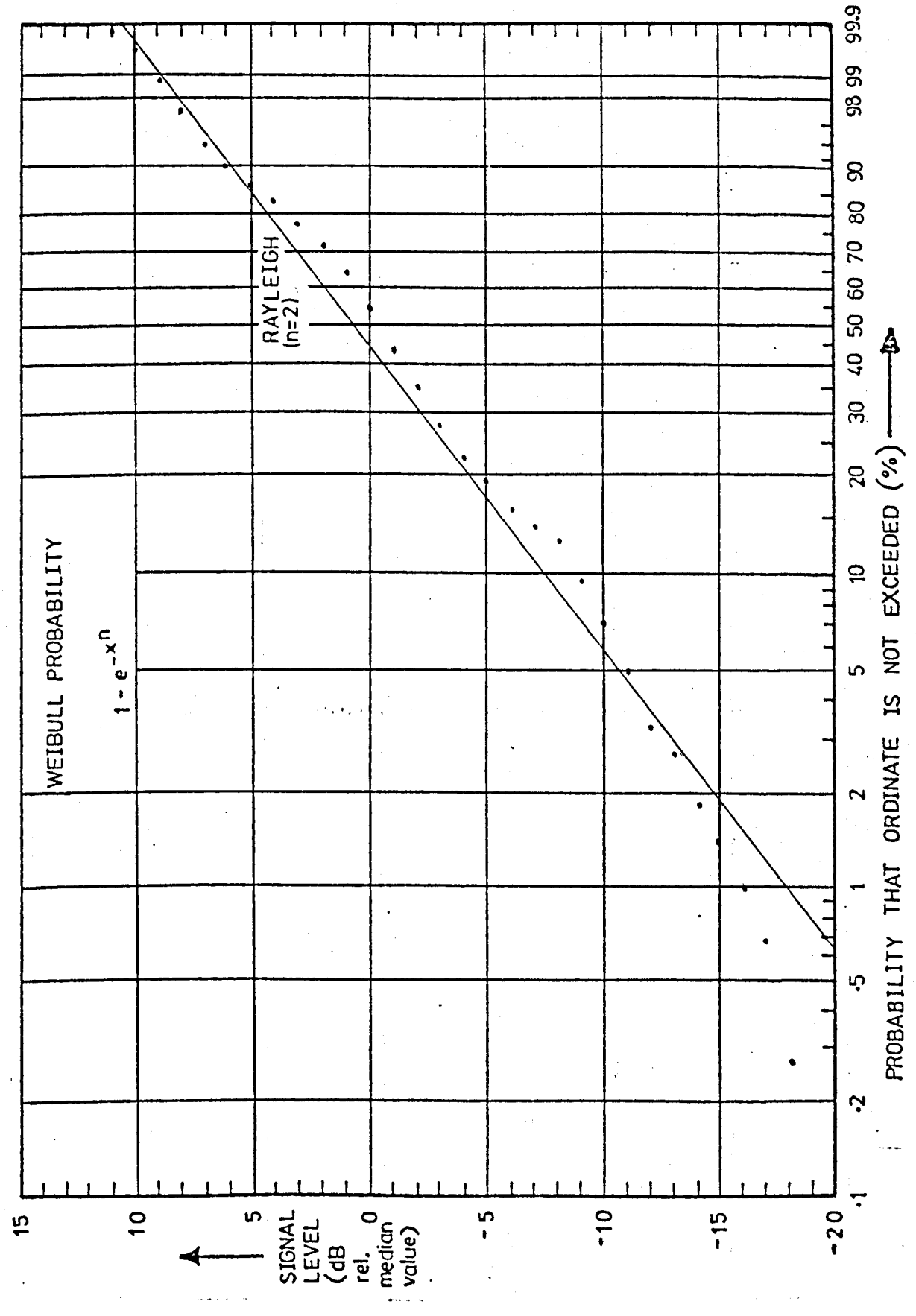

A MEASURED SIGNAL ENVELOPE DISTRIBUTION AT 85.875MHz
(NURSERY ROAD - BIRMINGHAM)

FIG. 2.7

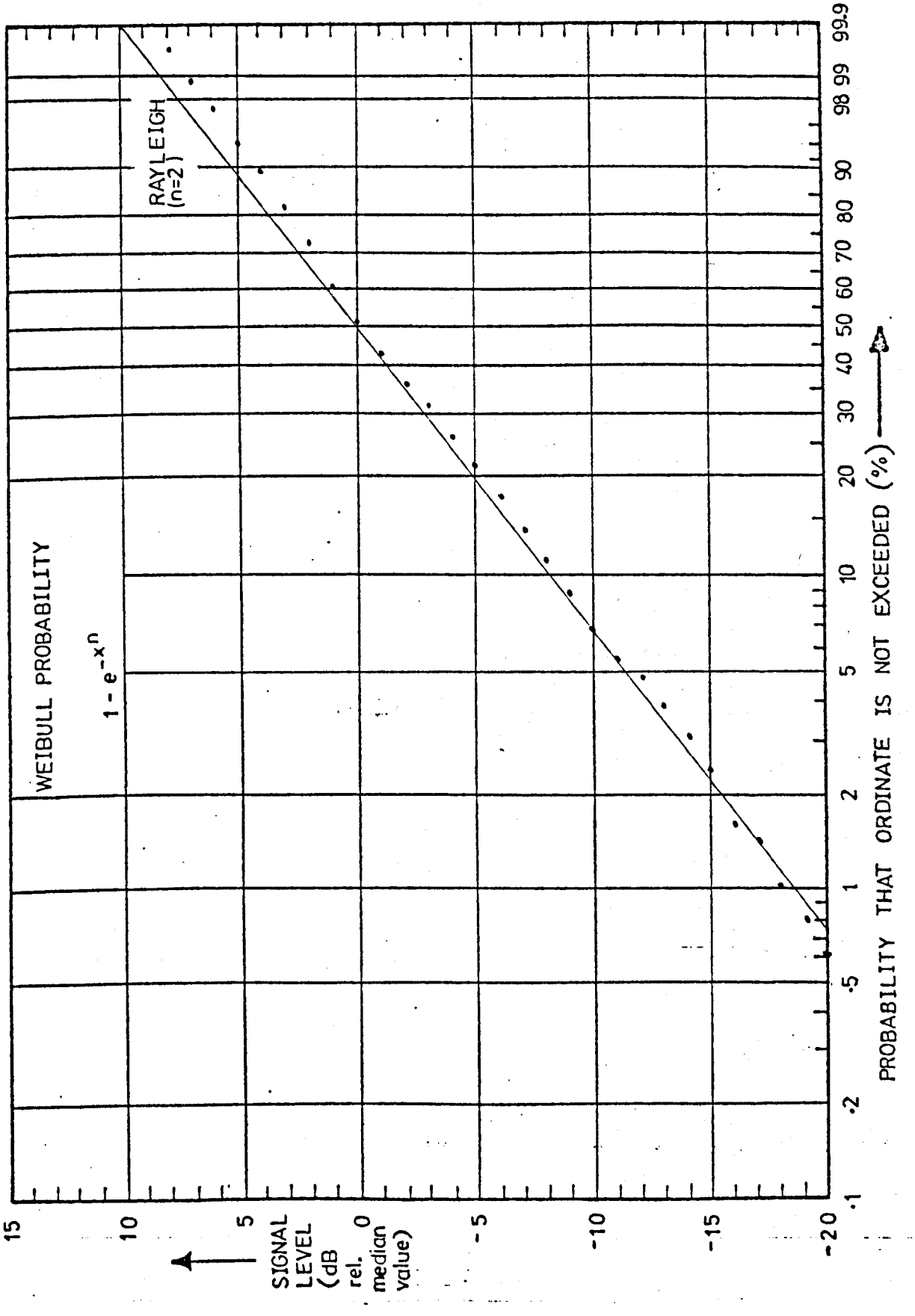

A MEASURED SIGNAL ENVELOPE DISTRIBUTION AT 167.2MHz
(NURSERY ROAD - BIRMINGHAM)

FIG. 2.8

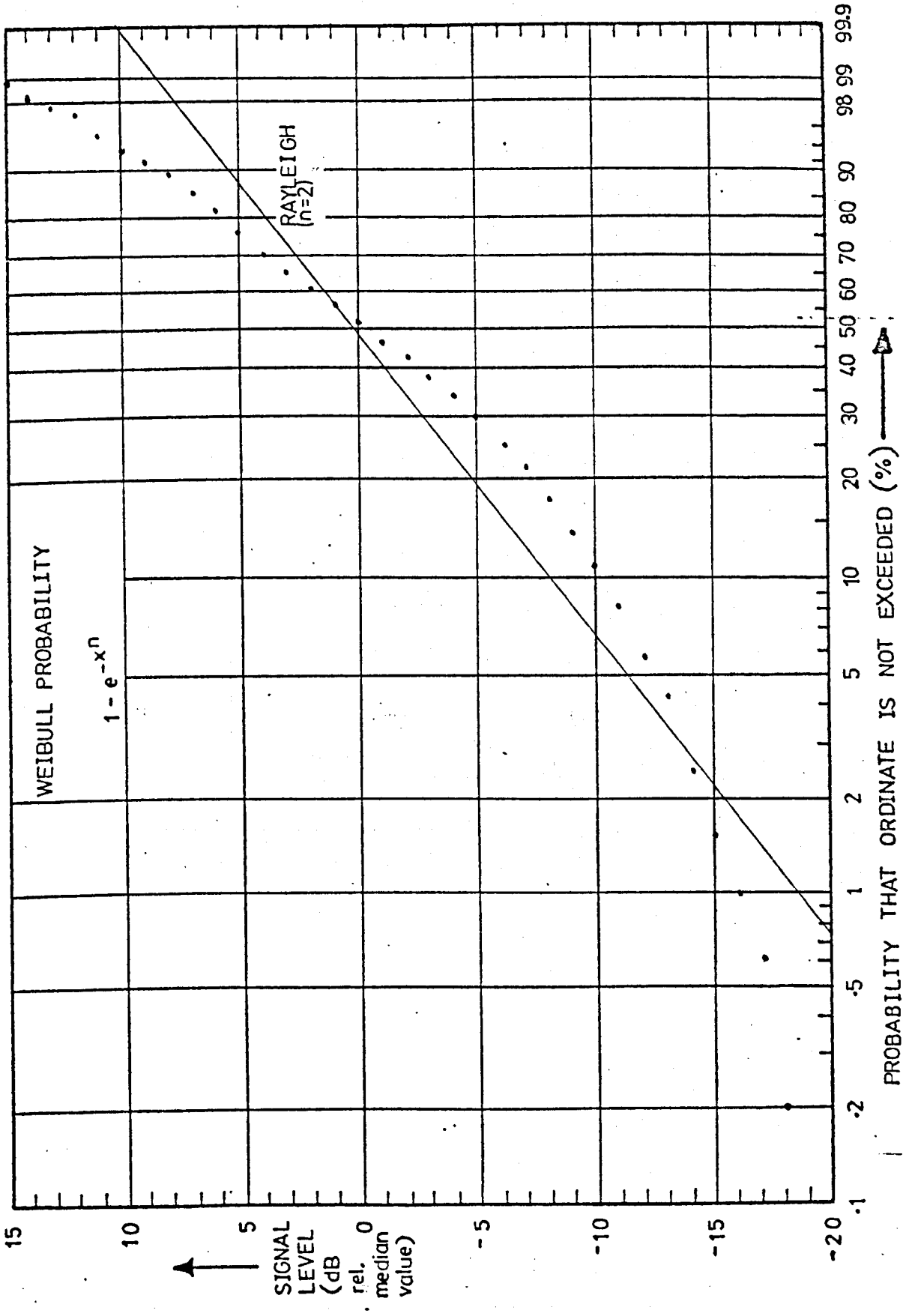

A MEASURED SIGNAL ENVELOPE DISTRIBUTION AT 441MHz
(NURSERY ROAD - BIRMINGHAM)

FIG. 2.9

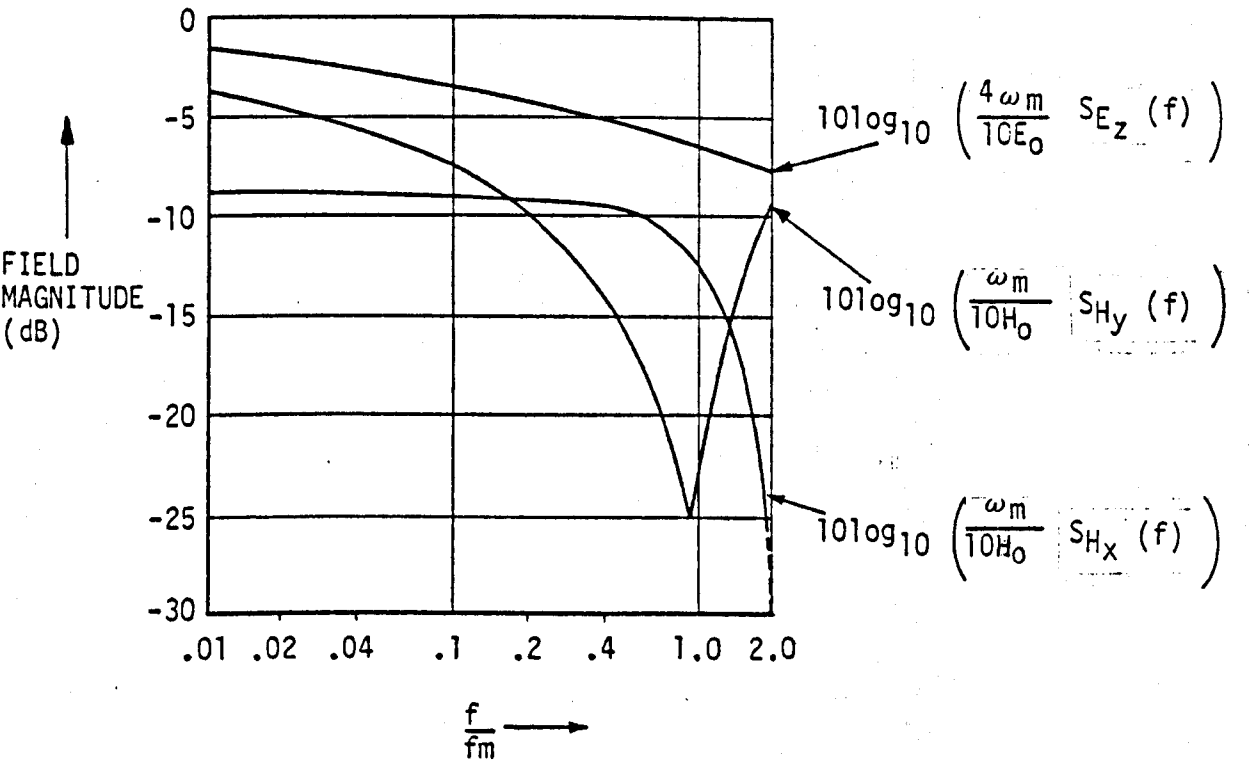

BASEBAND SPECTRA OF THE FIELD ENVELOPES

FIG. 2.10

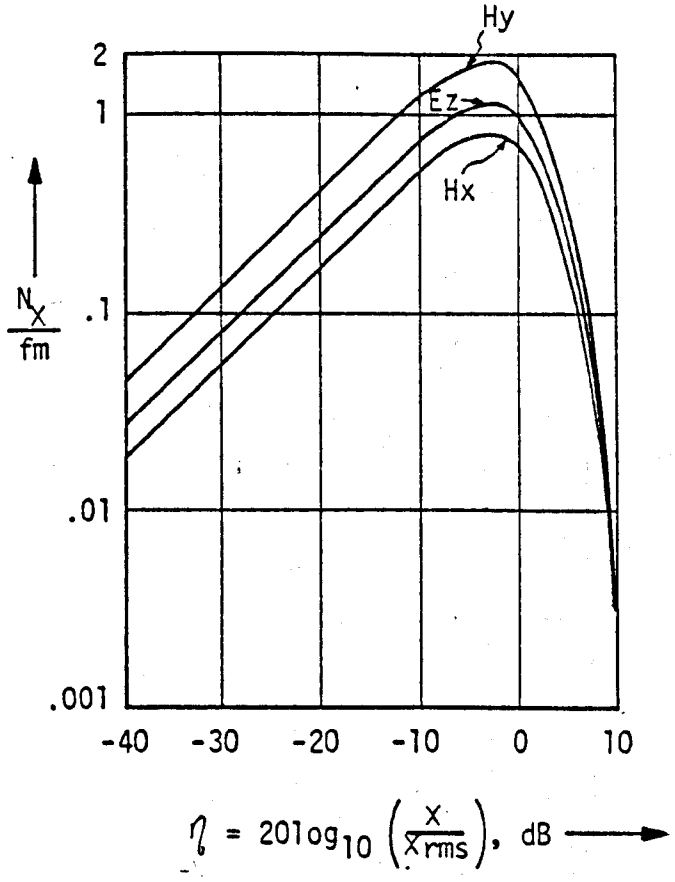

NORMALISED LEVEL CROSSING RATES OF THE ENVELOPES OF THE THREE FIELD COMPONENTS

FIG. 2.11

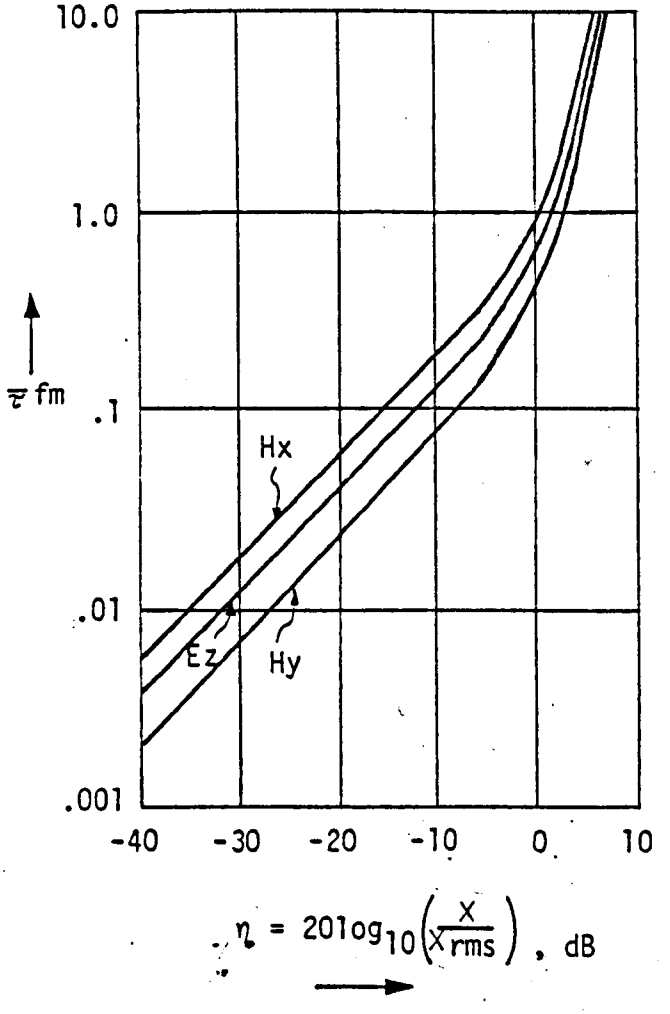

NORMALISED AVERAGE DURATIONS OF FADE OF THE ENVELOPES OF THE THREE FIELD COMPONENTS

FIG. 2.12

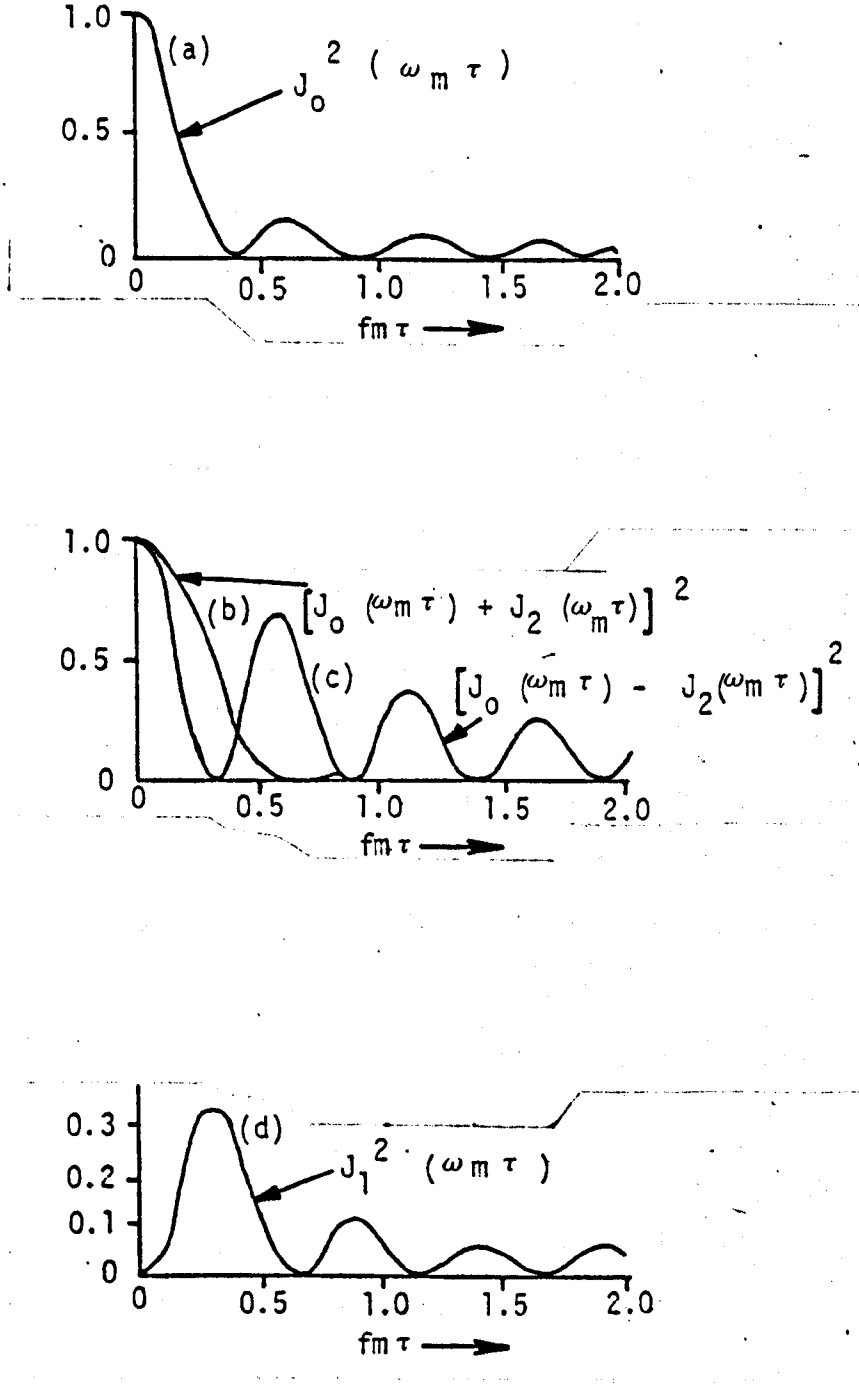

COVARIANCE FUNCTIONS OF
THE THREE FIELD ENVELOPES

(a) $|E_z|$, (b) $|H_x|$, (C) $|Hy|$,
(d) CROSS - COVARIANCE OF $|E_z|$ AND $|Hy|$

FIG. 2.13

CHAPTER 3

SEPARATION OF THE SLOW AND FAST FADING COMPONENTS OF THE RECEIVED SIGNAL ENVELOPE

It has been stated previously that the amplitude of the signal experienced by a radio receiver moving through the spatial field pattern existing in urban and suburban areas has been found to be well described as a Rayleigh distributed variable when the distance over which the observations are made is small (typically less than 200 m).[3.1] The envelope magnitude, however, has more frequently been experimentally demonstrated to be better described as log-normally[3.13] distributed, especially when the observation distance is greater than approximately 1 km.[3.2,3.3 3.4,3.14] Examples of measured signal envelopes are given in Figs. 3.1, 3.2 and 3.3 for a transmission frequency of 75.375 MHz; the corresponding probability distributions are shown in Figs. 3.4, 3.5 and 3.6 respectively. It should be noted that while the envelope more often appears to be log-normally distributed than Rayleigh, it is frequently neither if an intermediate measurement distance is considered. In these cases the signal envelope has some indeterminate distribution as indicated by Fig.3.7.

Close examination of the received signal envelope over large distances suggests the presence of two distinct phenomena. The more noticeable is the high frequency noise-like waveform, readily associated with the fast fading pattern. The other phenomenon is a large scale variation extending over many tens of wavelengths and is commonly termed "slow fading". Waveforms having this type

of characteristic, i.e. exhibiting changes in the "local mean" value over small sections of a stochastic waveform, have been analysed by many authors[3.5,3.6] as non-stationary random signals. The slow fading patterns of Figs. 3.1, 3.2 and 3.3 are given, for comparison, in Figs. 3.8, 3.9 and 3.10.

The parameters of the filter required to separate the slow and fast fading patterns must be determined before a full analysis of the field pattern may proceed. An investigation of the influences of the filter variables is documented in the following sections.

3.1 DETERMINATION OF THE FILTER REQUIRED TO ISOLATE THE SLOW FADING FIELD

The separation of the low frequency spatially distributed spectral components comprising the slow fading field from the noise-like fast fading requires the use of a low-pass filter. This operation is, classically,[3.7] the multiplication of the measured frequency spectrum, $X(\omega)$, with the filter frequency response, $W(\omega)$, to produce the output spectrum, $Y(\omega)$:

$$Y(\omega) = X(\omega) \cdot W(\omega)$$

This may be re-expressed in terms of the time domain variables as a convolution integral:[3.7]

$$y(t) = \int_{-\infty}^{\infty} x(\tau)\, w(t - \tau)\, d\tau$$

where $w(\tau)$ represents the filter's impulse response and:

$x(t), X(\omega)$

$y(t), Y(\omega)$

and $w(t), W(\omega)$

are Fourier Transform pairs[3.7] defined as:

$$F(\omega) = \int_{-\infty}^{\infty} f(t)\, e^{-j\omega t}\, dt$$

and $$f(t) = \frac{1}{2\pi} \int_{-\infty}^{\infty} F(\omega)\, e^{-j\omega t}\, d\omega$$

The waveform to be filtered has been measured as a time series and it is required that examinations of the filtered waveform are made in the time domain. Application of the multiplicative process will therefore necessitate two Fourier transformations but, even with the use of the Fast Fourier Transform algorithm [3.8], the length of this technique makes the convolution of the time series with a weighting function preferable. This latter method was employed where necessary.

3.1.1 DETERMINATION OF THE FILTER SHAPE

The rectangular, triangular and raised cosine window functions are shown, along with their associated power spectra, in Fig. 3.11. The spectra demonstrate that the rectangular window in Fig.3.11(a) has the highest sidelobe levels while the raised cosine weighting function in Fig.3.11(c) correspondingly has the lowest. The raised cosine shape therefore appears to be the most favourable of the three forms considered for the task in hand.

To facilitate a visual comparison of the performance of each filter type, the unprocessed waveform shown in Fig.3.12 was convolved with three weighting functions of the forms shown in Fig.3.11. The slow fading patterns produced using a rectangular window 256 data points wide (16λ), a triangular window 257 points wide and a raised cosine function 257 points wide are given in Figs. 3.13, 3.14 and 3.15 respectively. A close examination reveals that the differences in the performances of the raised cosine and triangular windows are negligible and that these filters perform only slightly better than the simple rectangular window.

Examination of Fig.3.11 shows that the first null in the frequency spectrum of the rectangular weighting function occurs at half the frequency of that for a triangular or raised cosine window of the same overall width. If a valid comparison between the various window types is to be made, the widths of the main lobes of the respective spectra must be equal. The slow fading pattern in Fig.3.16 was accordingly produced using a rectangular window 128 data points (8λ) wide.

A comparison of Figs. 3.16, 3.13 and 3.15 indicates that the improved filtering performance gained by doubling the filter width, or by employing a raised cosine rather than the equivalent rectangular window, is considerable. The difference between the slow fading waveforms obtained using rectangular and raised cosine windows of equal data width, however, is negligible. The computation of the convolution integral for the raised cosine

filter does not therefore appear to be justifiable while comparable performance can be obtained by recourse to a rectangular function, thereby requiring greatly reduced effort.

3.1.2 DETERMINATION OF THE FILTER WIDTH

A comparison of the slow fading patterns produced using the 16λ and 8λ rectangular weighting functions shown in Figs 3.13 and 3.16 respectively illustrates that the window width is an important factor in the selection of the filter parameters.

Consider the idealised situation depicted in Fig.3.17(a) where a sine wave impinges upon a reflecting surface and produces the classical standing wave pattern indicated in Fig.3.17(b). The spacing between adjacent nulls in the interference pattern is λ/2. Inclusion of more waves into the simple picture arriving from different directions, e.g. from randomly positioned reflectors or scatterers, in general causes the depths of the deep interference minima to be reduced while the total number of these fades increases. If the field pattern is to remain sensibly constant over many tens of wavelengths, therefore, one dominant transmission path must exist. This is the slow fading signal and must, with the exception of a line-of-sight situation, result from either diffraction over the obstacles or reflection around, or even through, them. This latter effect has been shown[3.9] to predominate at microwave frequencies in large North American cities where the obstacles are extremely tall sky-scraper blocks bordering relatively narrow streets.

Low pass filtering by a rectangular weighting function which encompasses more than 10 of the interference minima has been demonstrated[3.10] to produce negligible error in the determination of the mean signal level. A window was accordingly chosen which would satisfy this criterion while remaining sufficiently narrow to have a noticeable filtering effect. This window was fixed at 64 m, equivalent to 32 fades assuming a half wavelength spacing at the 75 MHz frequency. The autocovariance functions of three measured slow fading signals determined using this window are shown in Figs. 3.18, 3.19 and 3.20. The position at which the first zero in the autocovariance occurs may be seen to be greater than 75 m from the origin. Over displacements of less than 75 m it appears reasonable to assume that the variations in the slow fading signal are negligibly small and that the signal envelope will accordingly be Rayleigh distributed. The optimum window is therefore concluded to be narrower than 75 m, but must encompass sufficient data points to provide a statistically valid estimate of the signal's statistics.

The autocovariance plots of Figs. 3.18, 3.19 and 3.20 demonstrate the rate at which the slow fading signal fluctuations are evidenced. The behaviour of the overall slow fading waveform, inclusive of the mean level, is derived form the autocorrelation function. A typical autocorrelation plot is given in Fig.3.21 and demonstrates that the magnitudes of the slow fading variations, while being highly relevant, are very much smaller than the mean value.

3.2 HIGH PASS FILTERING OF THE RECEIVED SIGNAL ENVELOPE

Variations in the mean and median values of a Rayleigh distributed variable may be represented by changes in the mode "b" of that distribution (Table 2.1). Division of the measured signal at a point in space by the "local mean" of the signal at that point will consequently eliminate the effects of the mean variation on the distribution.[3.11] If the variable arose from a Rayleigh process, the resultant will subsequently exhibit Rayleigh properties.[3.11]

The slow fading pattern of a given data record was determined using one of the weighting functions under consideration. The filtered data was then divided into the "raw" data record at the appropriate displacement necessary to compensate for the window width and the probability distribution of this high pass filtered record determined. The probability functions created in this way were compared with the theoretical Rayleigh distribution and an assessment of the filtering performance made.

Cumulative probability distributions produced using rectangular, triangular and raised cosine weighting functions are shown in Figs. 3.22, 3.23 and 3.24 respectively. These are compared with the Rayleigh curve on both normal and Weibull probability[3.13] graph paper. It is immediately evident from a comparison of Figs. 3.22, 3.23 and 3.24 that there is little difference between the high pass filtered waveforms produced using the various window widths and types under consideration.

A comparison of the experimentally produced distributions with the Rayleigh distribution on normal probability paper apparently indicates that a good approximation has been obtained. This conclusion has also been reached by other workers[3.12] who have performed the identical analysis. Further comparion between the experimental and the theoretical Rayleigh distributions on the Weibull probability paper, however, reveals that the agreement is poor and that the conclusion drawn previously is ill founded, the distributions being better approximated as Weibull of the form:

$$P(x \leq X) = 1 - e^{-X^{2.5}} \quad ; \quad X \geq 0$$

The explanation of this property could be derived from the base-band frequency spectrum of the fast fading signal shown in Fig. 2.10. The large spectral content of the low frequency components signifies that the fast fading spectrum will overlap the low frequency spectrum of the slow fading signal. The slow and fast fading fields will therefore be inherently inseparable by simple filtering techniques and references to slow and fast fading signals as separate entities will only be approximations of the true state. It is more reasonable under these circumstances to define the median value over a suitably small interval, the "small sector" distance, and to categorise the fading properties of the signal about this level over that interval.

3.3 REFERENCES

3.1 Young W.R. Jr.

"Comparison of Mobile Radio Transmissions at 150, 450, 900 and 3700 Mc"

B.S.T.J., Vol.31, November 1952

3.2 Black D.M. and Reudink D.O.
"Some Characteristics of Radio Propagation at 800 MHz in the Philadelphia Area"
IEEE Trans. Vehic. Tech., Vol.VT-21, May 1972

3.3 Okumura Y., Ohmori E., Kawano T. and Fukuda K.
"Field Strength and its Variability in VHF and UHF Land Mobile Service"
Rev. Elec. Comm. Lab., 16, September-October 1968

3.4 Allsebrook K.
"VHF Propagation in an Urban Environment"
M.Sc. Degree Thesis, University of Birmingham, Dept. of Elec. and Elec. Eng., October 1972

3.5 Bendat J.S. and Piersol A.G.
"Random Data: Analysis and Measurement Procedures"
Wiley - Interscience, 1971

3.6 Papoulis A.
"Probability, Random Variables and Stochastic Processes"
McGraw-Hill, New York, 1965

3.7 Lathi B.P.
"An Introduction to Random Signals and Communication Theory"
ITC Intertext Series, 1970

3.8 Fotiades L.

"The Fast Fourier Transform in Signal Processing, Theory and Practice"

Dept. Elec. and Elec. Eng., University of Birmingham, Deptl. Memo. No.454, May 1974

3.9 Jakes W.C. Jr.

"Microwave Mobile Communications"

John Wiley and Sons, London

3.10 Ratliff P.A.

"VHF Mobile Radio Communications - A Study of Multipath Fading and Diversity Reception"

Ph.D. Thesis, University of Birmingham, Dept. of Elec. and Elec. Eng., September 1973

3.11 Clarke R.H.

"A Statistical Theory of Mobile Radio Reception"

B.S.T.J., Vol.47, No.6, July/August 1968

3.12 Parker R.E. and Roper G.B.

"Vehicular Radio Communication in London"

Report SDE/X/B70/1, AWRE, Aldermaston

3.13 Johnson N.L. and Kotz S.

"Distributions in Statistics"

Houghton Mifflin, 1970

3.14 Reudink D.O.

"Comparison of Radio Transmission at X-Band Frequencies in Suburban and Urban Areas"

IEEE Trans. Ant. and Prop., AP-20, July 1972

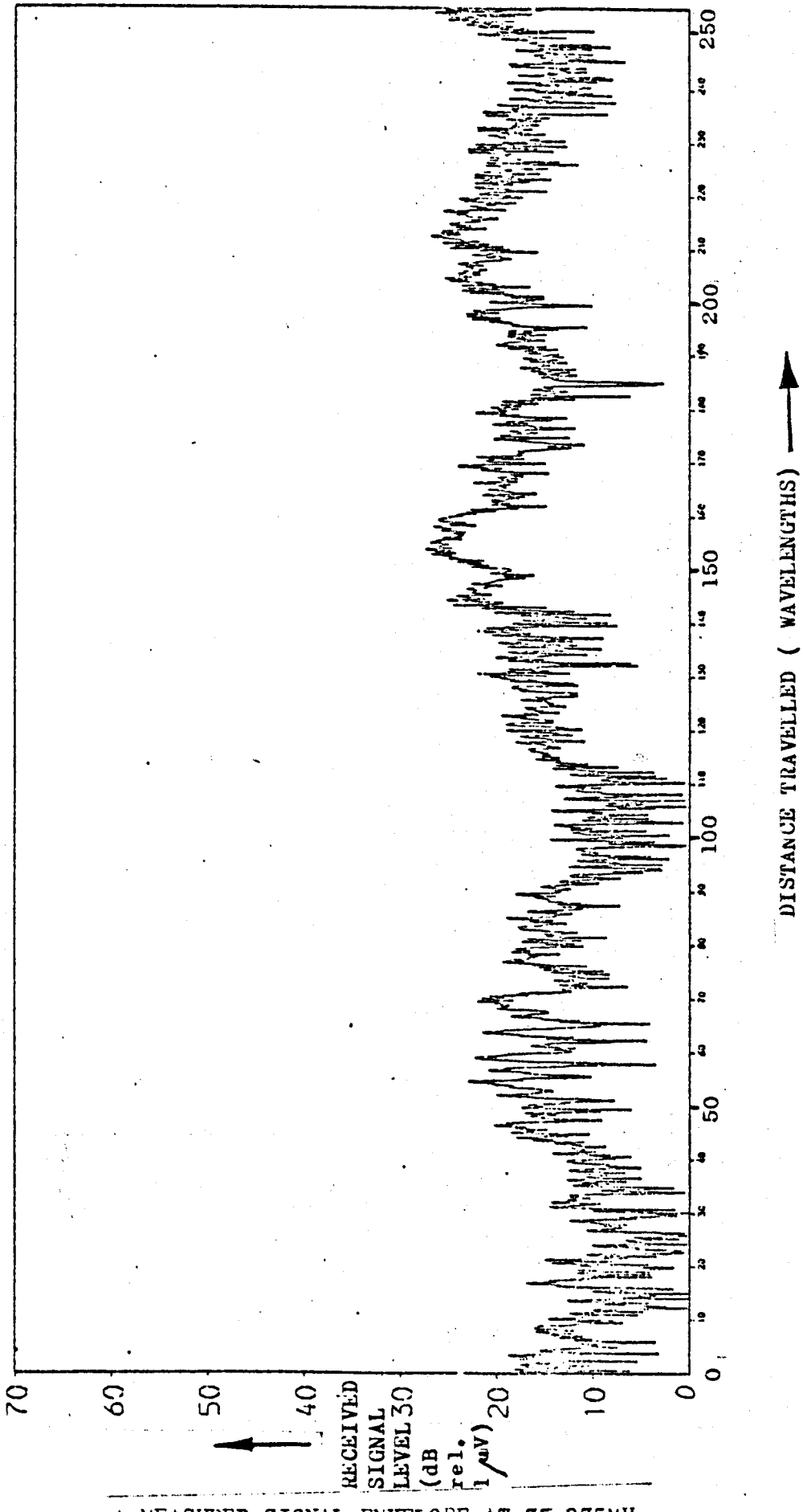

A MEASURED SIGNAL ENVELOPE AT 75.375MHz
(WITTON ROAD - BIRMINGHAM)

FIG. 3.1

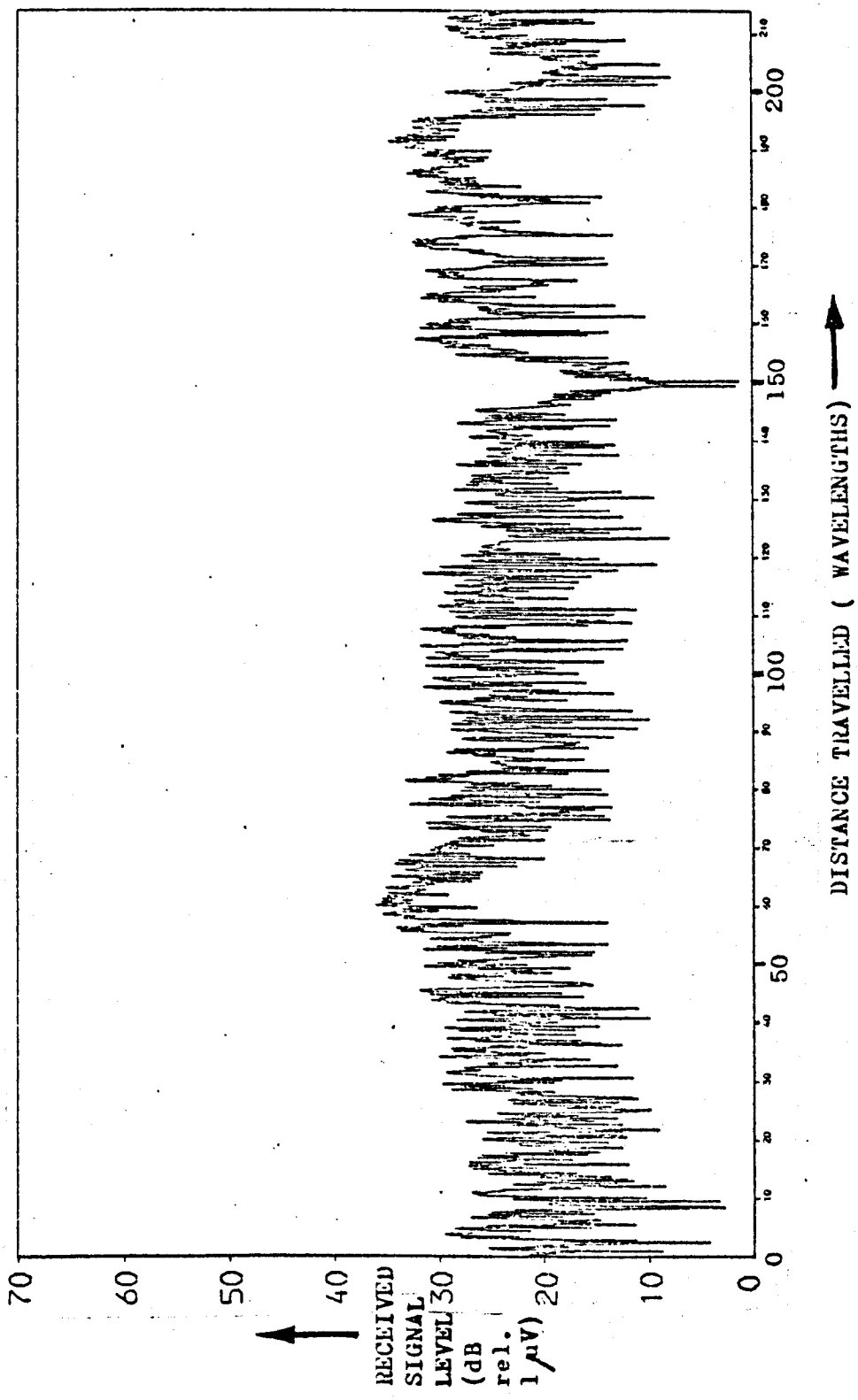

A MEASURED SIGNAL ENVELOPE AT 75.375MHz
(CITY CENTRE - BIRMINGHAM)

FIG. 3.2

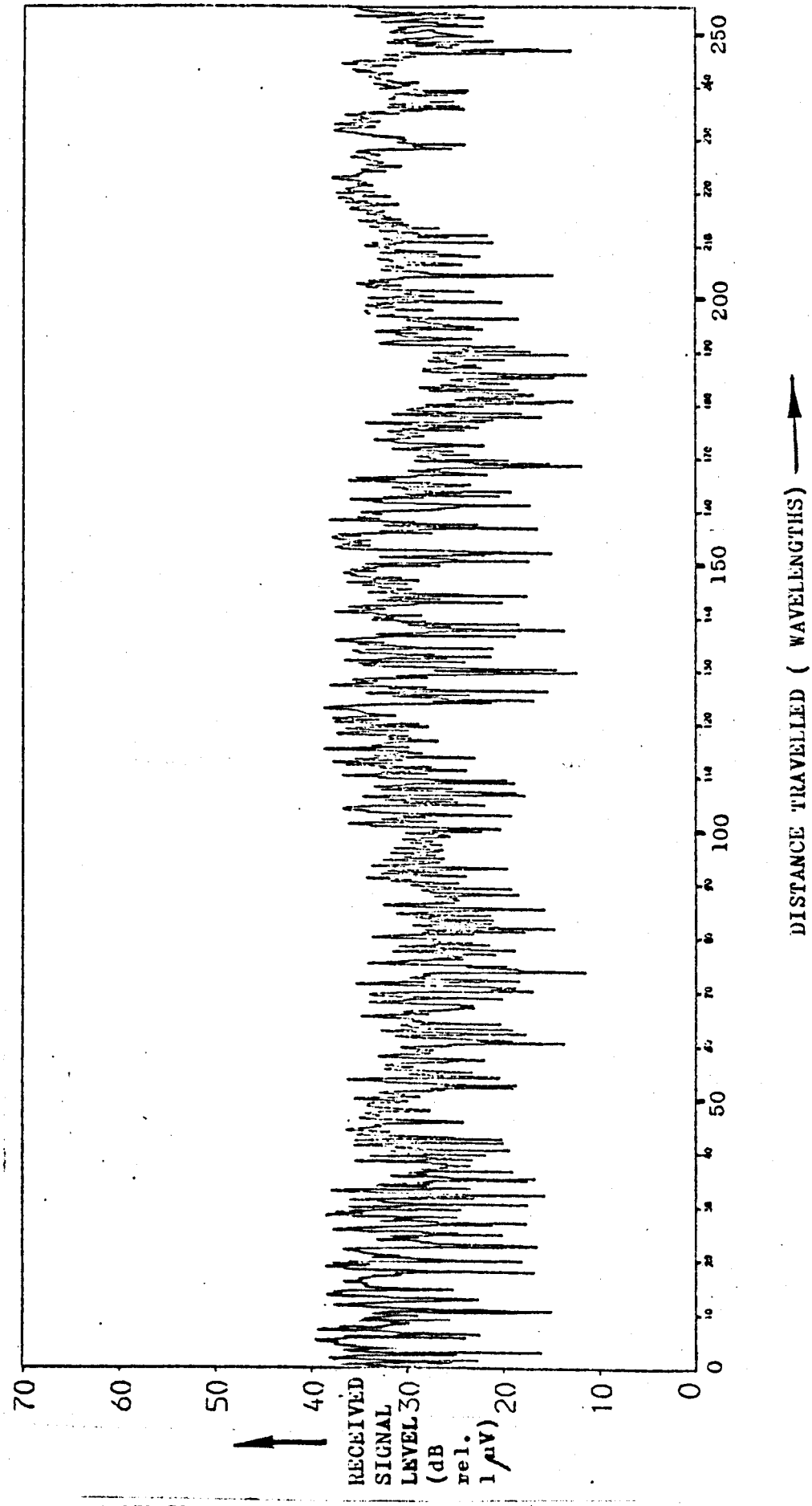

A MEASURED SIGNAL ENVELOPE AT 75.375MHz
(EDGBASTON ROAD - BIRMINGHAM)

FIG. 3.3

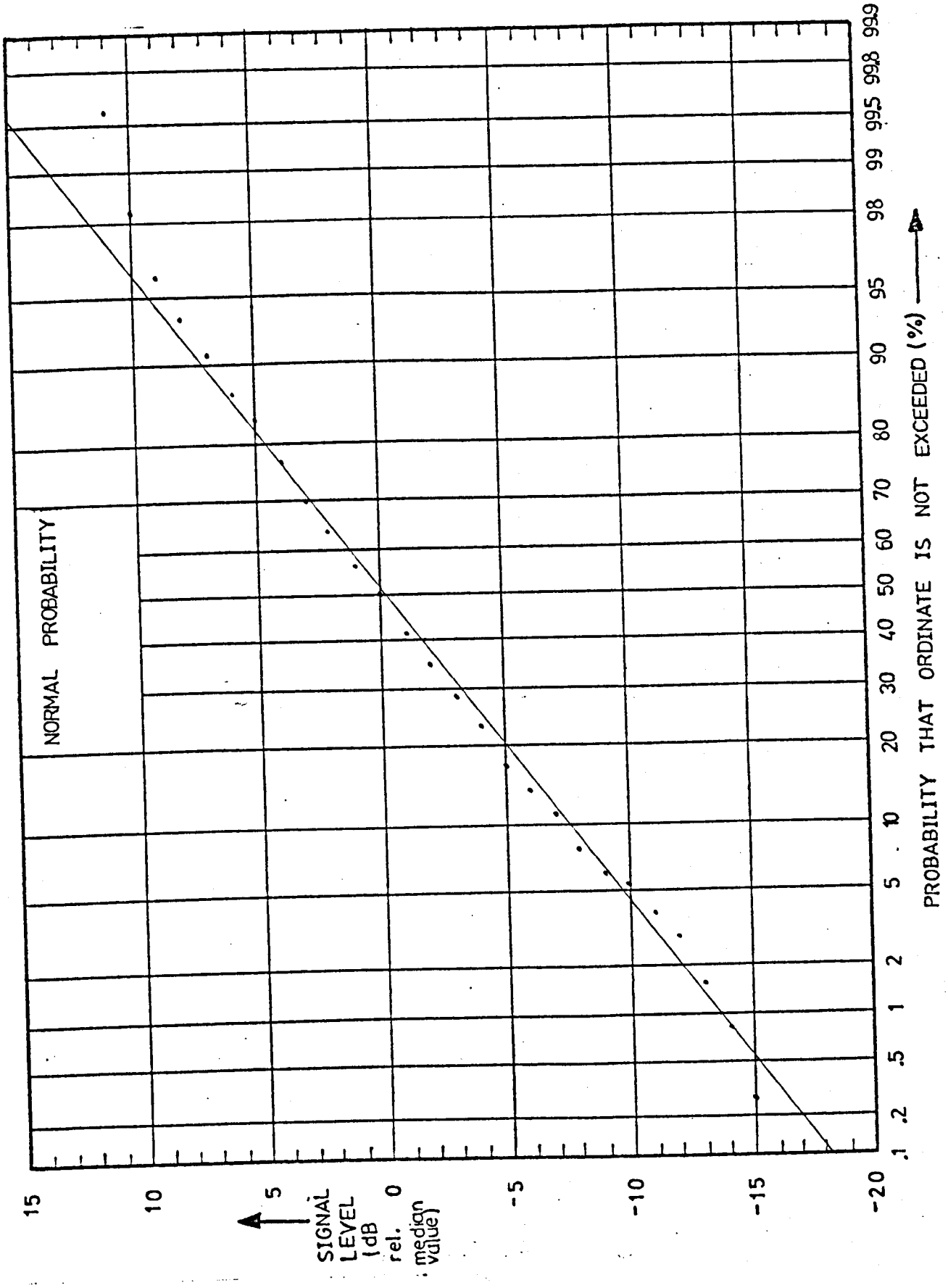

A MEASURED SIGNAL ENVELOPE DISTRIBUTION AT 75.375MHz
(WITTON ROAD - BIRMINGHAM)

FIG. 3.4

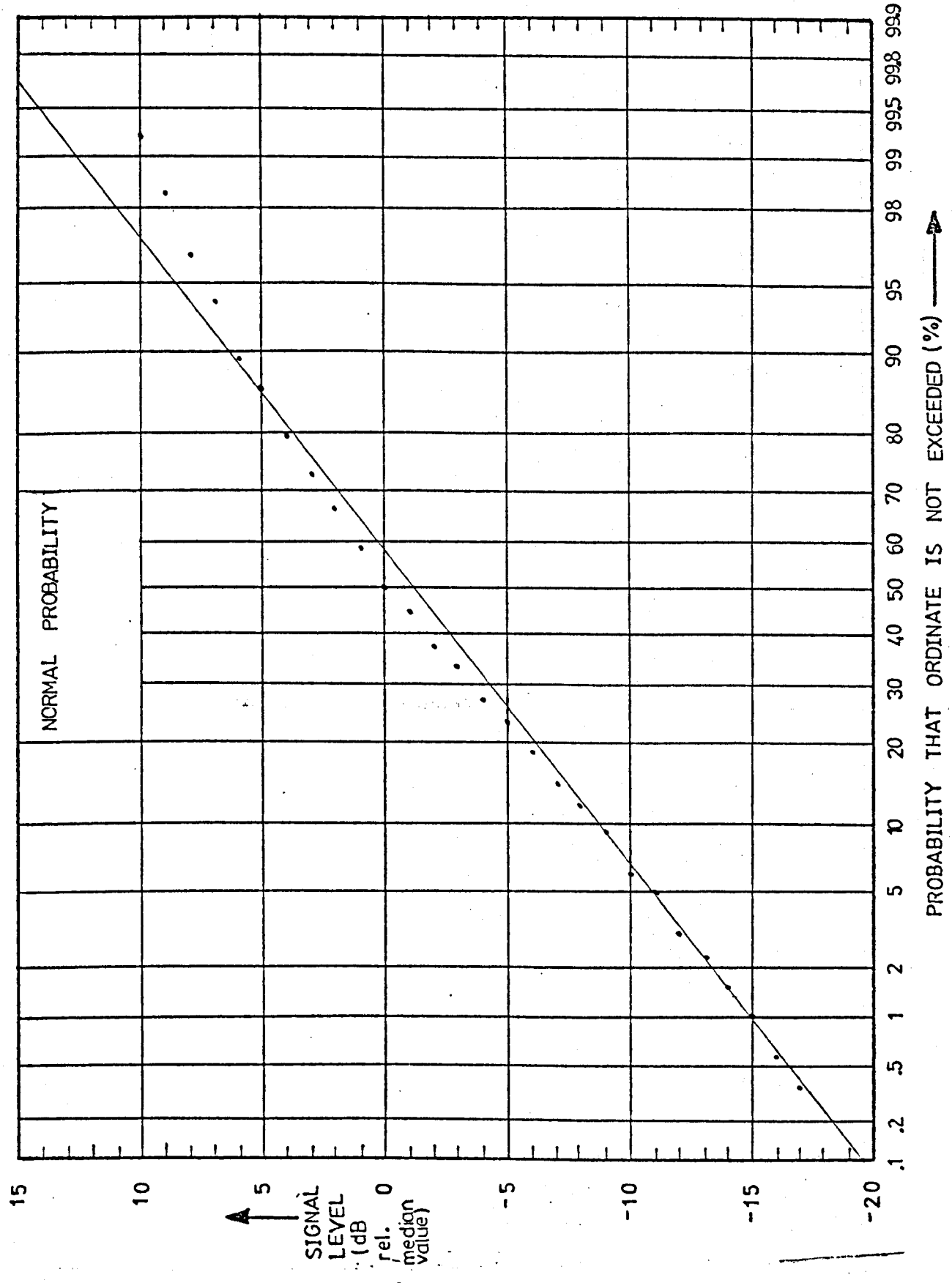

A MEASURED SIGNAL ENVELOPE DISTRIBUTION AT 75.375MHz
(CITY CENTRE - BIRMINGHAM)

FIG. 3.5

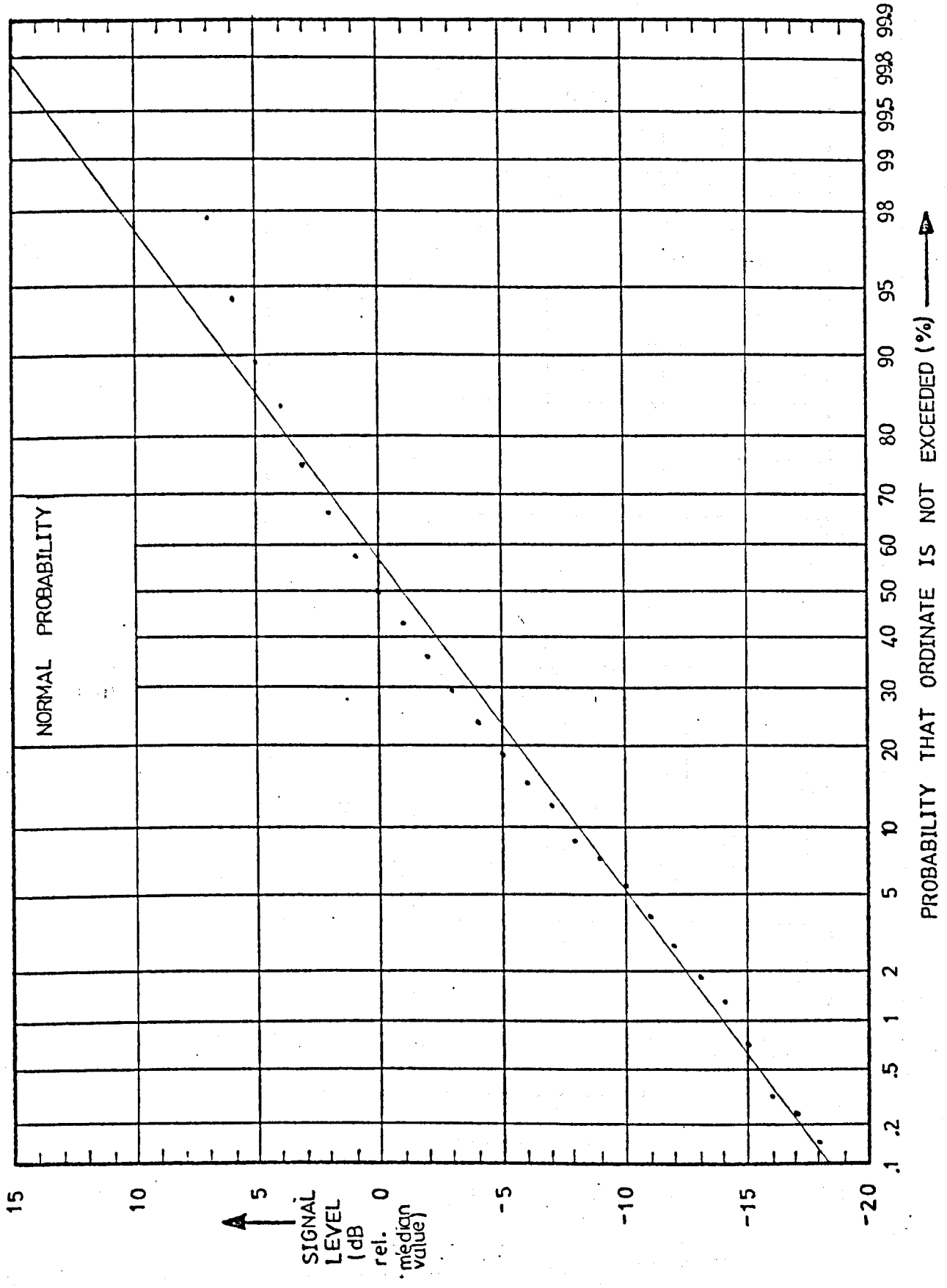

A MEASURED SIGNAL ENVELOPE DISTRIBUTION AT 75.375MHz
(EDGBASTON ROAD - BIRMINGHAM)

- FIG. 3.6

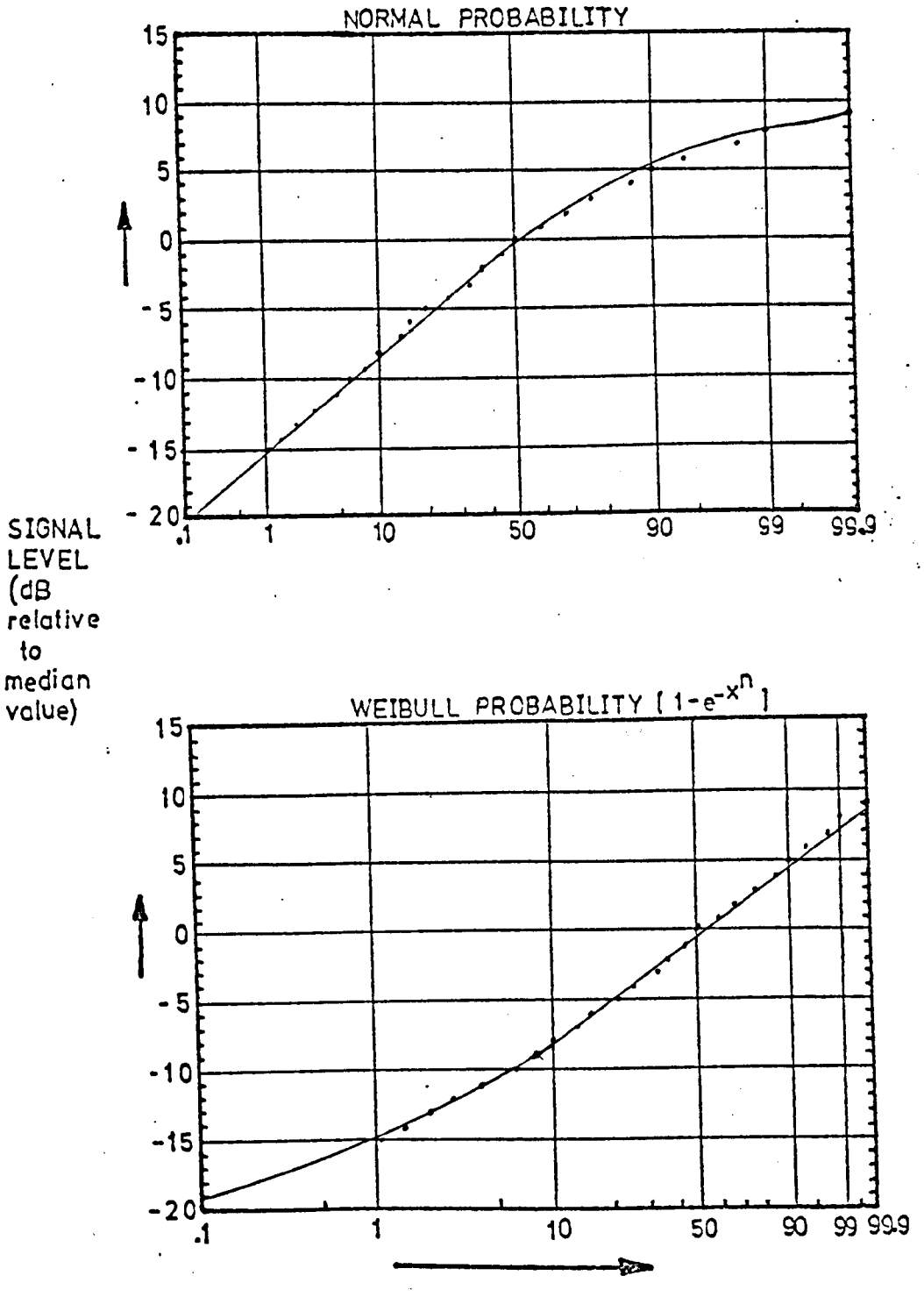

A MEASURED SIGNAL ENVELOPE DISTRIBUTION AT 75.375MHz
(NORFOLK ROAD - BIRMINGHAM)

FIG. 3.7

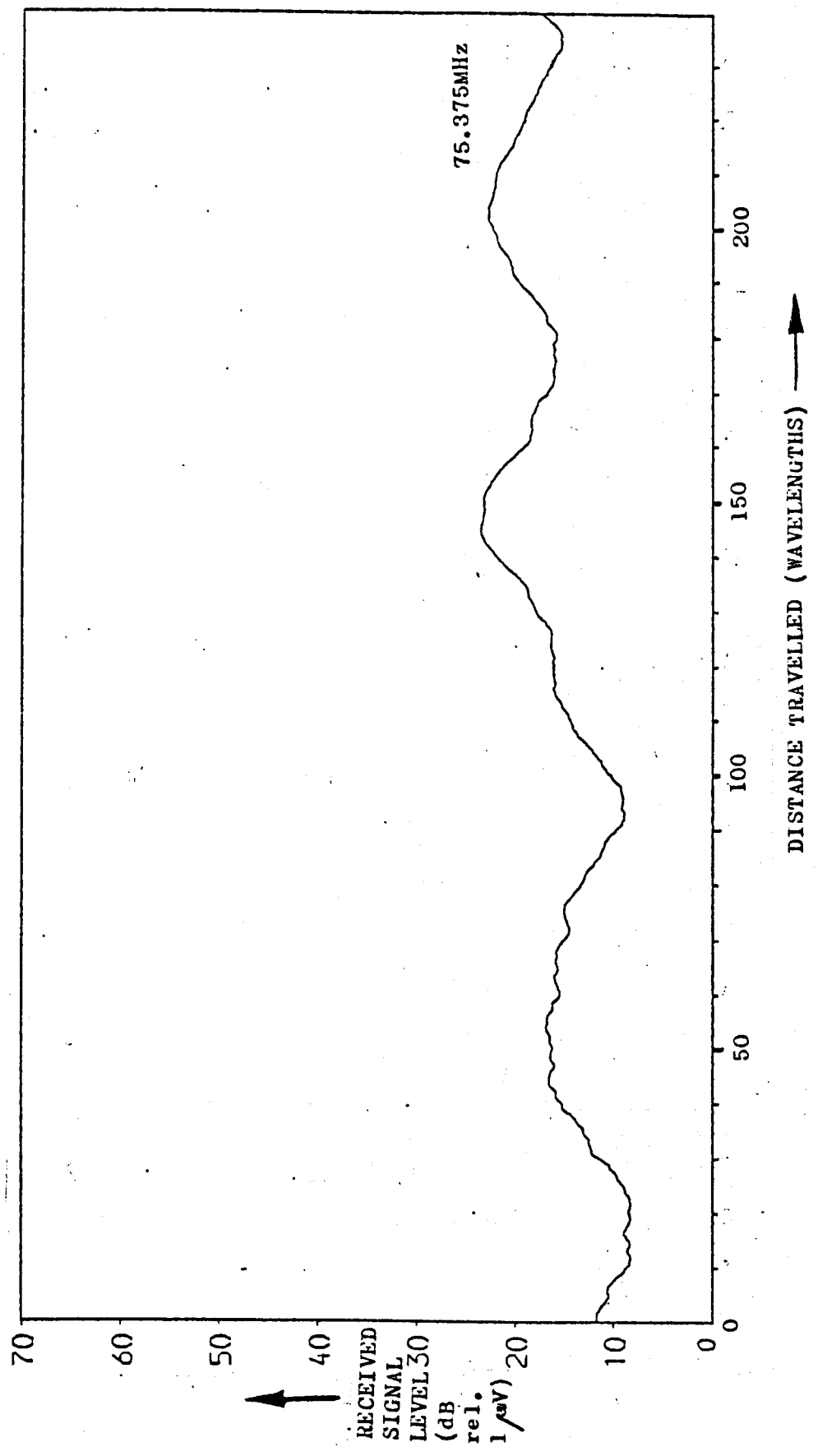

A MEASURED SLOW-FADING PATTERN
(WITTON ROAD - BIRMINGHAM)

FIG. 3.8

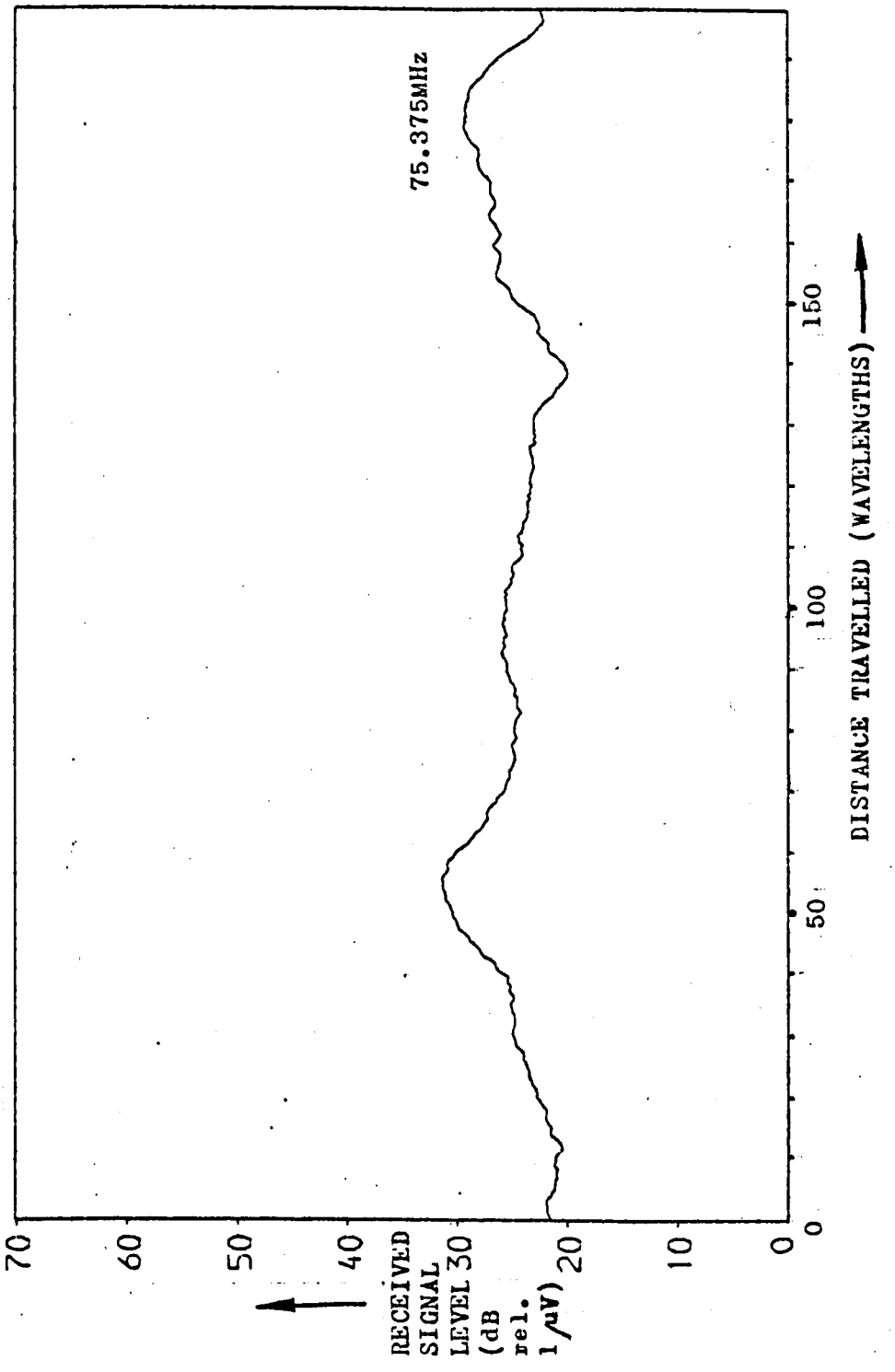

A MEASURED SLOW-FADING PATTERN
(CITY CENTRE - BIRMINGHAM)

FIG. 3.9

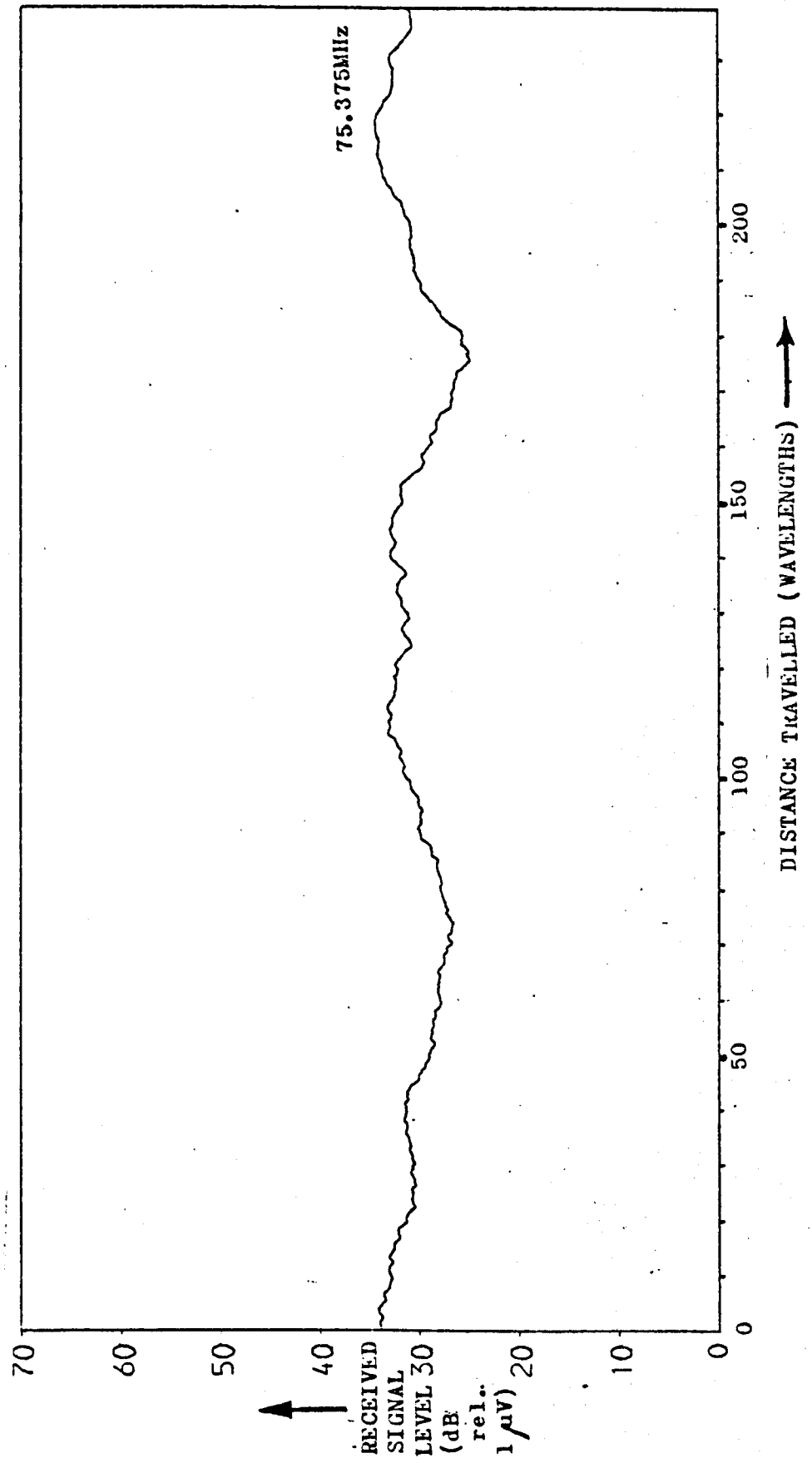

A MEASURED SLOW-FADING PATTERN
(EDGBASTON ROAD - BIRMINGHAM)

FIG. 3.10

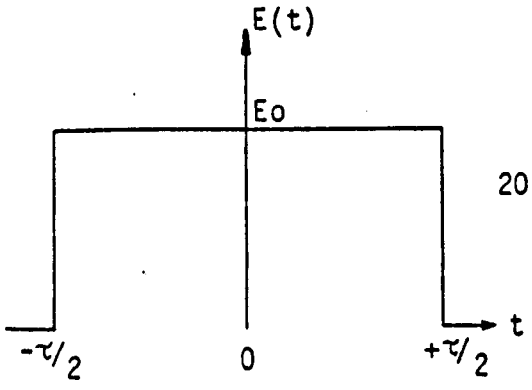

$$E(t) = \begin{cases} 0 & ,|t| \geq \tau/2 \\ Eo & ,|t| < \tau/2 \end{cases}$$

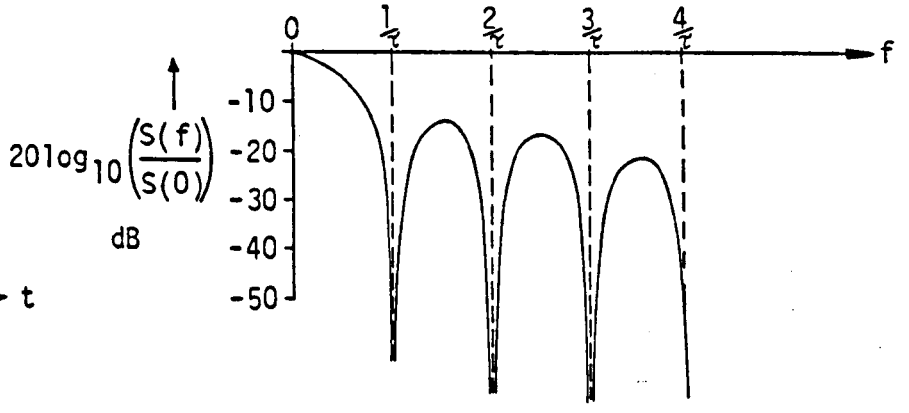

$$S(f) = 2Eo\tau \frac{\sin(\pi f \tau)}{(\pi f \tau)}$$

(a)

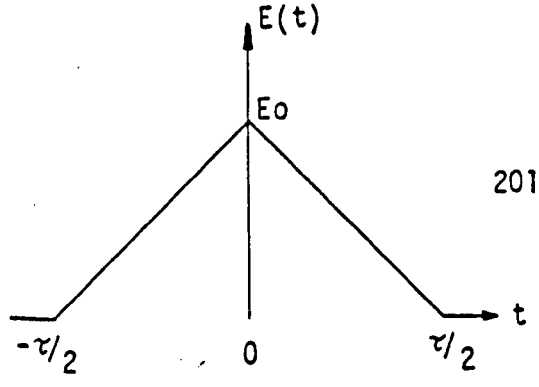

$$E(t) = \begin{cases} (1-\frac{2|t|}{\tau}) & ,|t| < \tau/2 \\ 0 & ,|t| \geq \tau/2 \end{cases}$$

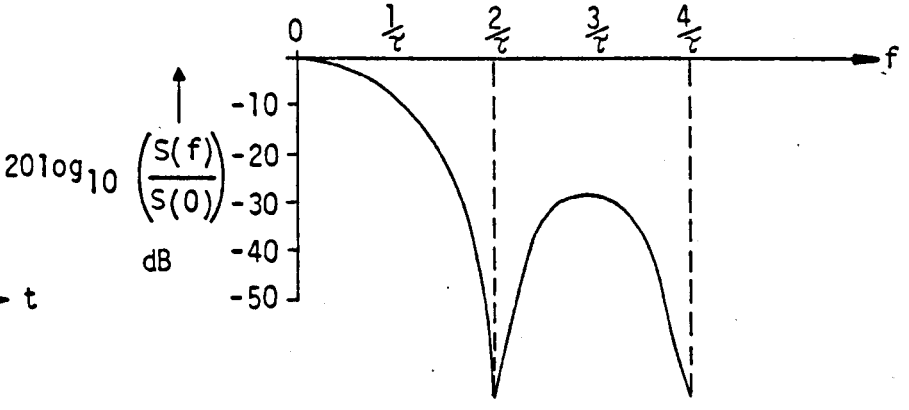

$$S(f) = Eo\tau \left\{ \frac{\sin(\frac{\pi f \tau}{2})}{(\frac{\pi f \tau}{2})} \right\}^2$$

(b)

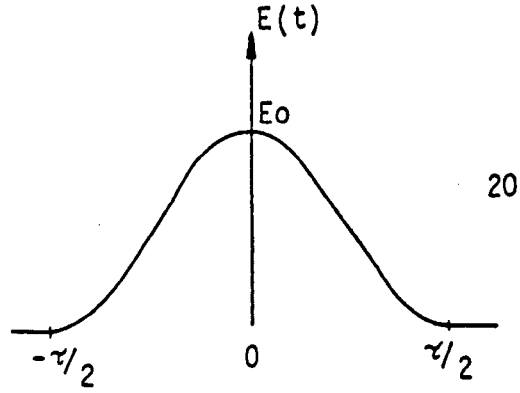

$$E(t) = \begin{cases} \frac{Eo}{2}(1+\cos(2\pi t/\tau)) & ,|t| < \tau/2 \\ 0 & ,|t| \geq \tau/2 \end{cases}$$

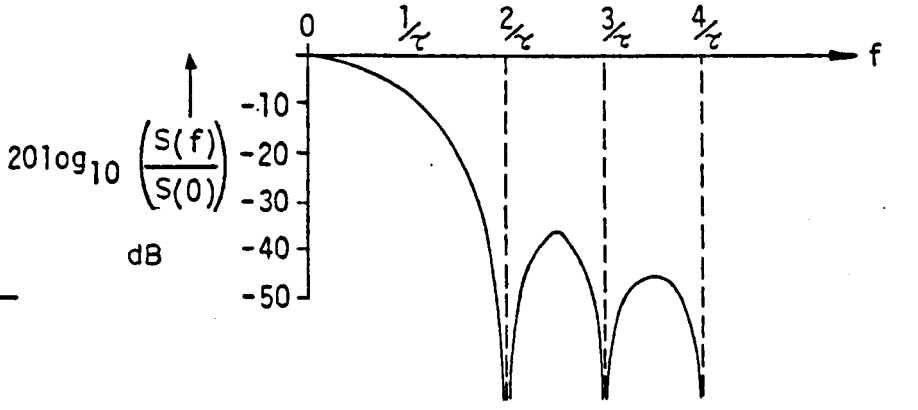

$$S(f) = Eo\tau \frac{\sin(\frac{\pi f \tau}{2})}{(\frac{\pi f \tau}{2})} \left\{ \frac{\cos(\pi f \tau/2)}{1-(f\tau)^2} \right\}$$

(c)

FREQUENCY SPECTRA OF (a) RECTANGULAR, (b) TRIANGULAR
(c) RAISED COSINE WEIGHTING FUNCTIONS

-FIG. 3.11

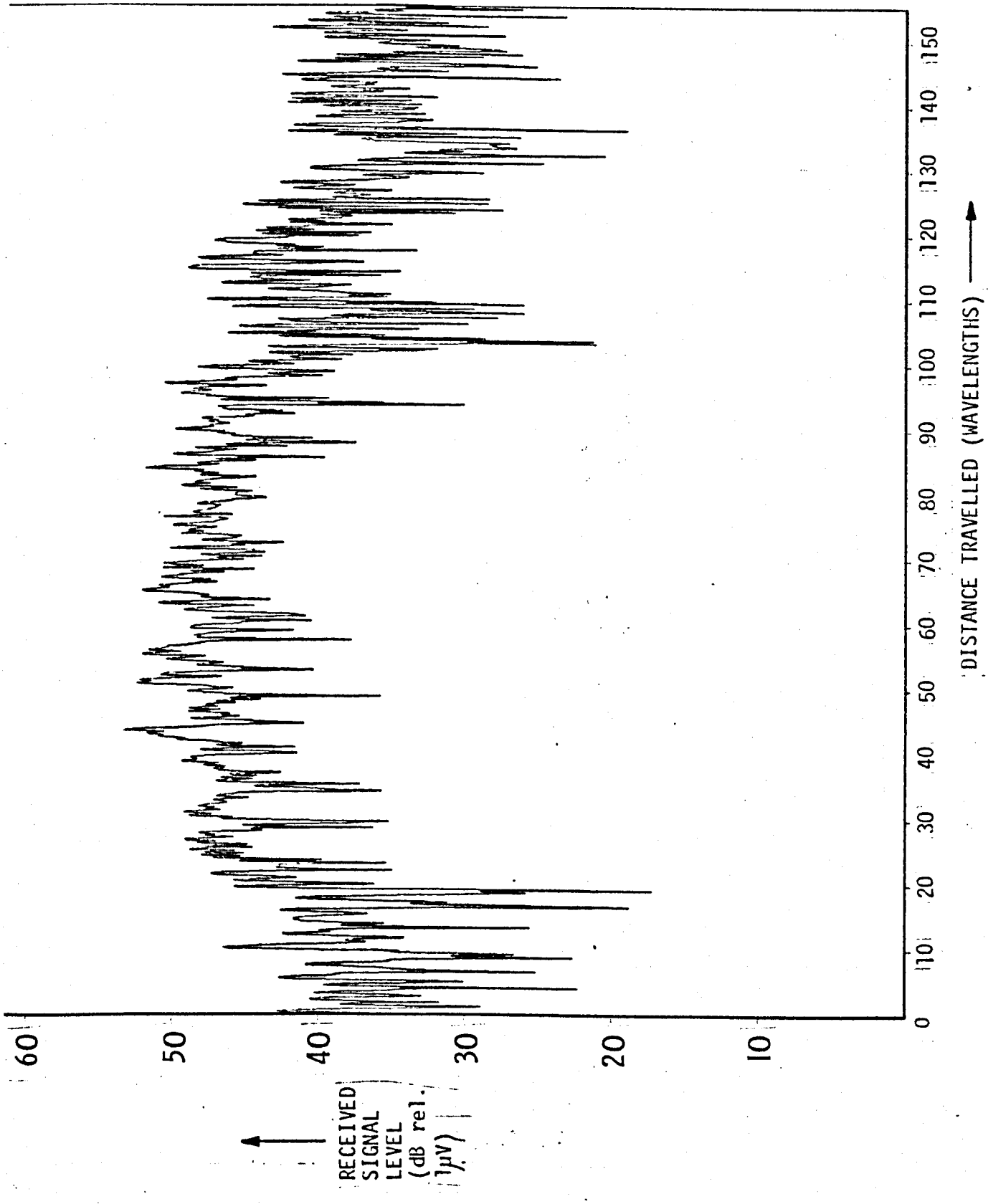

A MEASURED SIGNAL ENVELOPE AT 75.375MHz
(BARLOWS ROAD - BIRMINGHAM)

FIG. 3.12

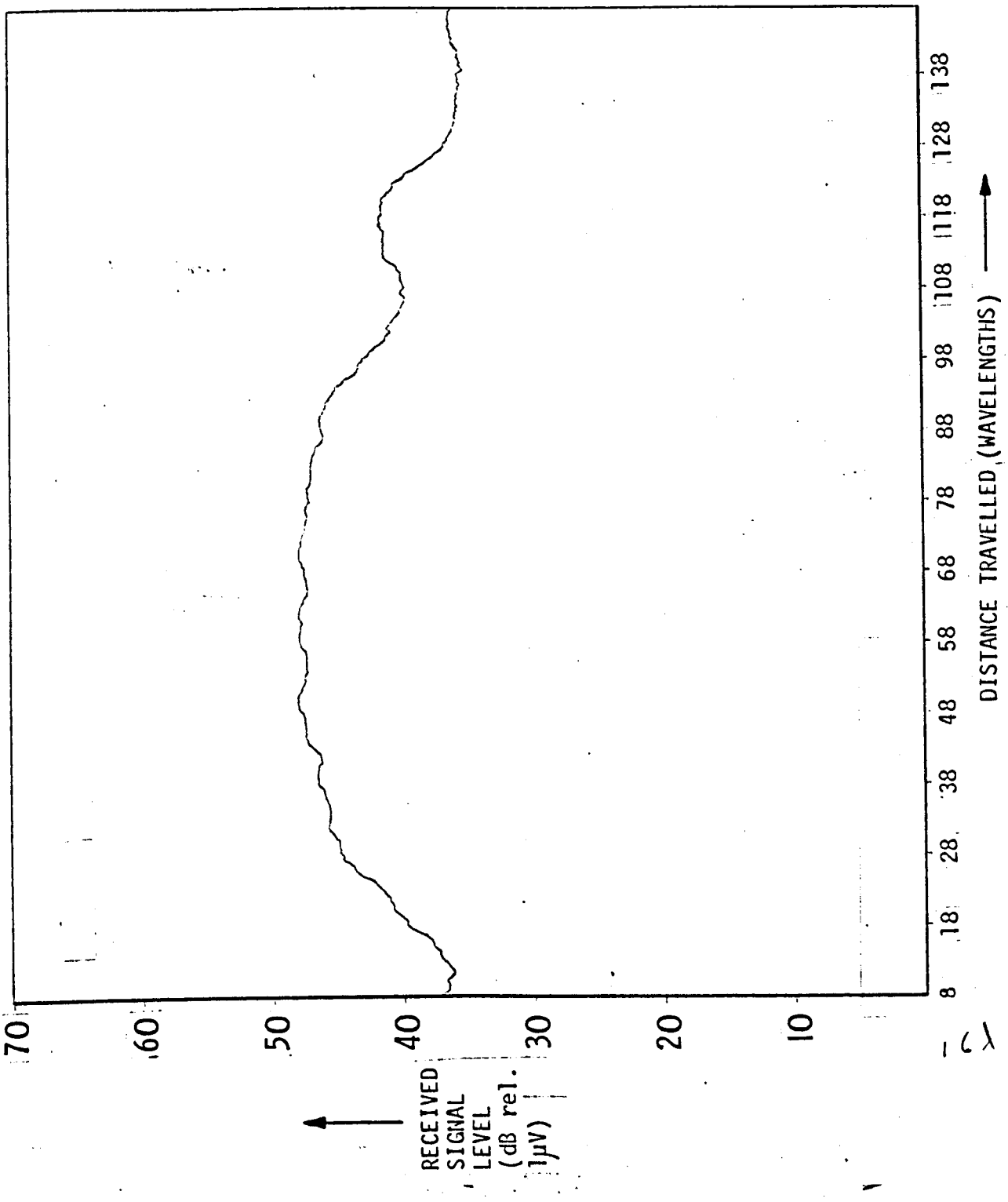

A MEASURED SIGNAL ENVELOPE AFTER FILTERING
WITH A RECTANGULAR WINDOW 256 POINTS WIDE
(BARLOWS ROAD - BIRMINGHAM)

FIG. 3.13

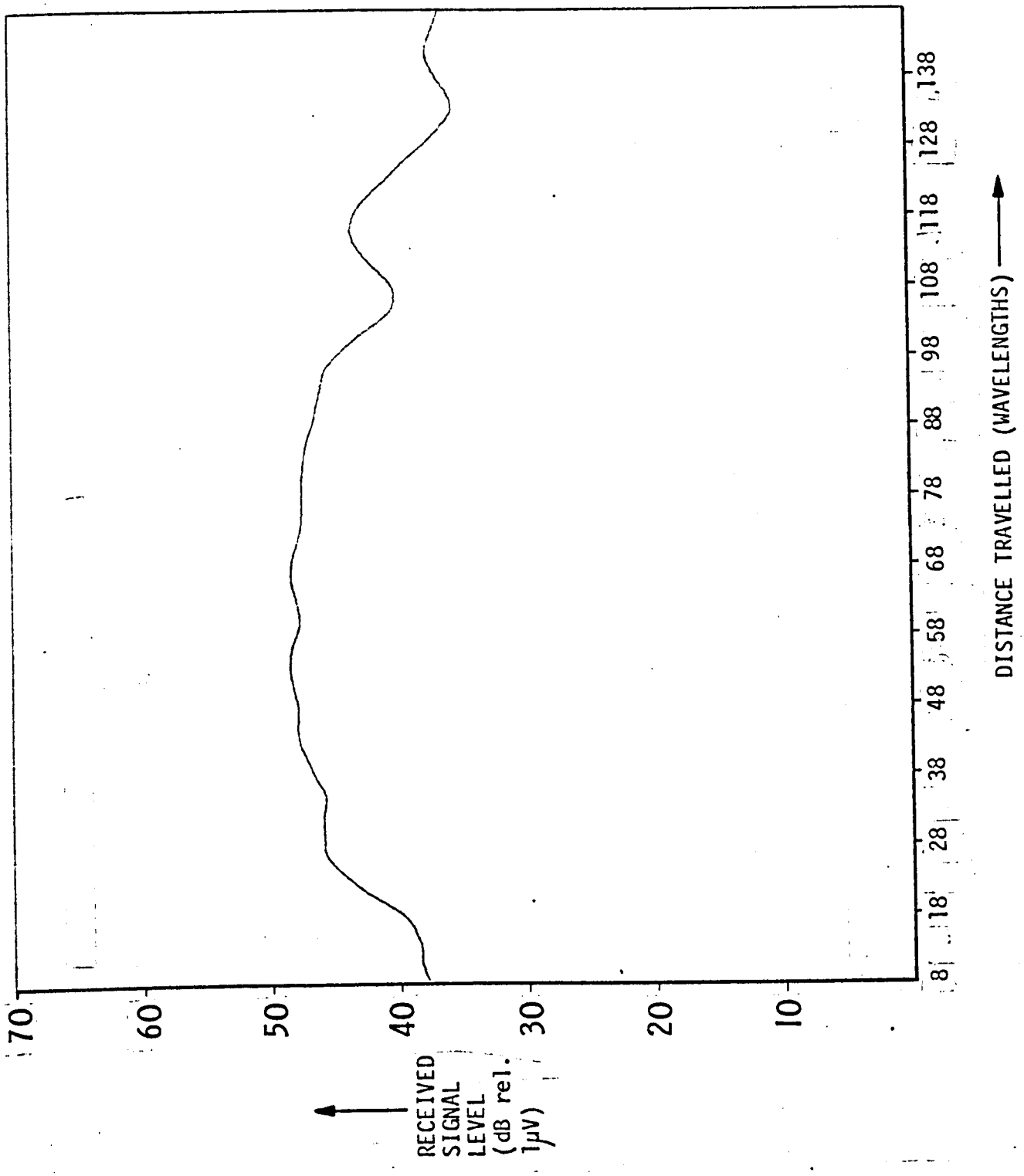

A MEASURED SIGNAL ENVELOPE AFTER FILTERING WITH A TRIANGULAR WINDOW 257 POINTS WIDE (BARLOWS ROAD - BIRMINGHAM)

FIG. 3.14

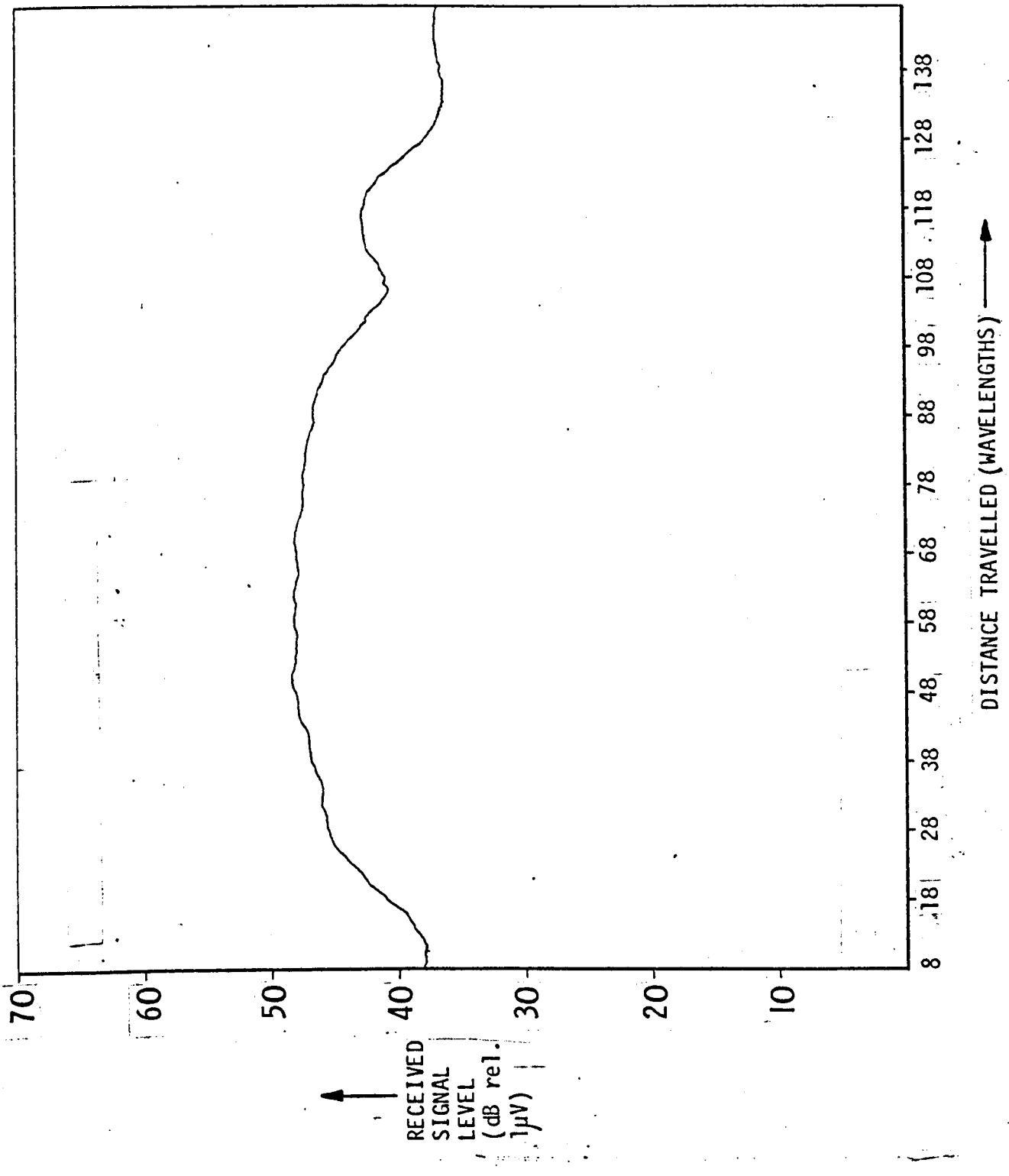

A MEASURED SIGNAL ENVELOPE AFTER FILTERING WITH A RAISED COSINE WINDOW 257 POINTS WIDE (BARLOWS ROAD - BIRMINGHAM)

FIG.3.15

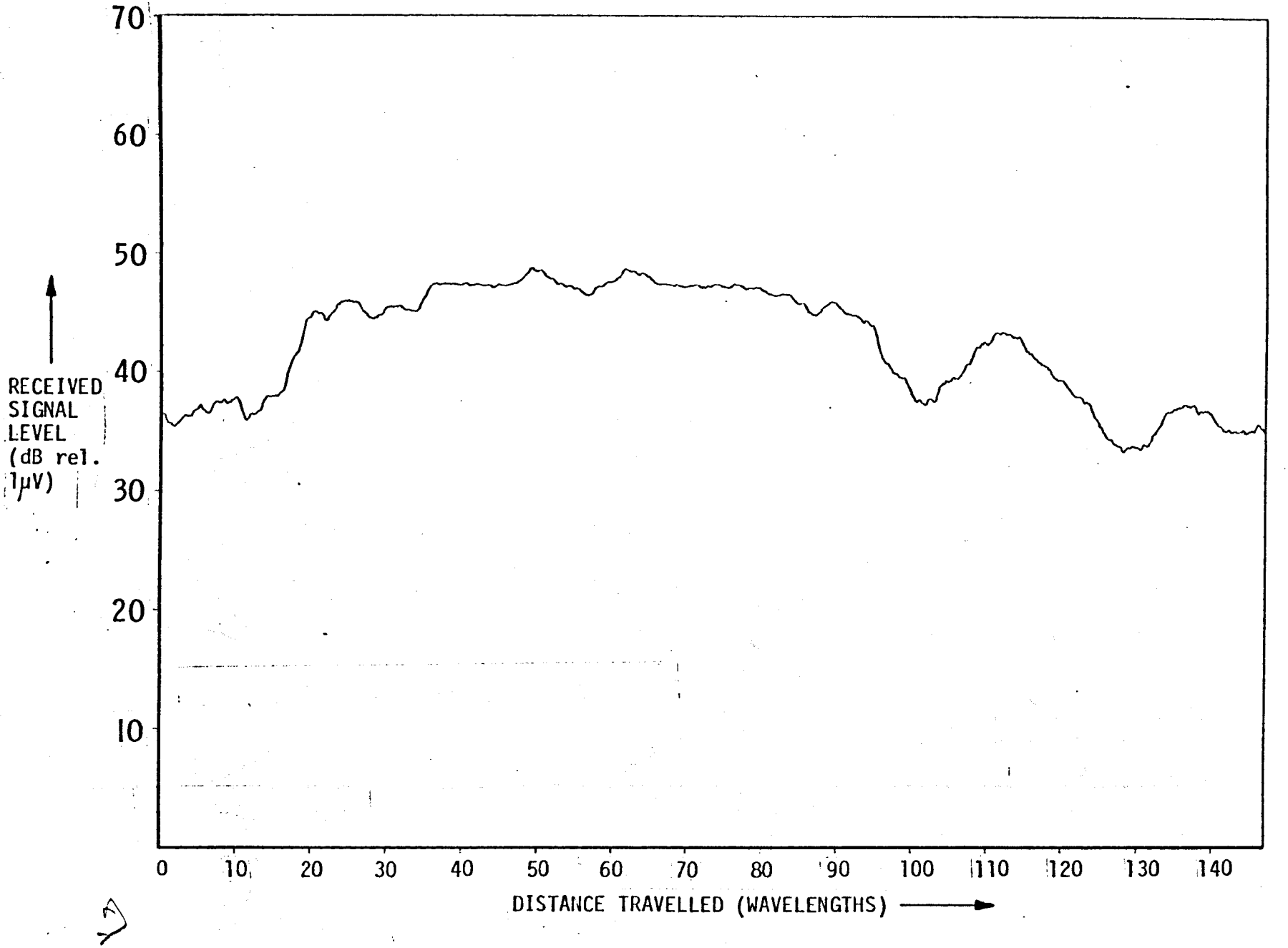

A MEASURED SIGNAL ENVELOPE AFTER FILTERING WITH A RECTANGULAR WINDOW 128 POINTS WIDE (BARLOWS ROAD - BIRMINGHAM)

FIG. 3.16

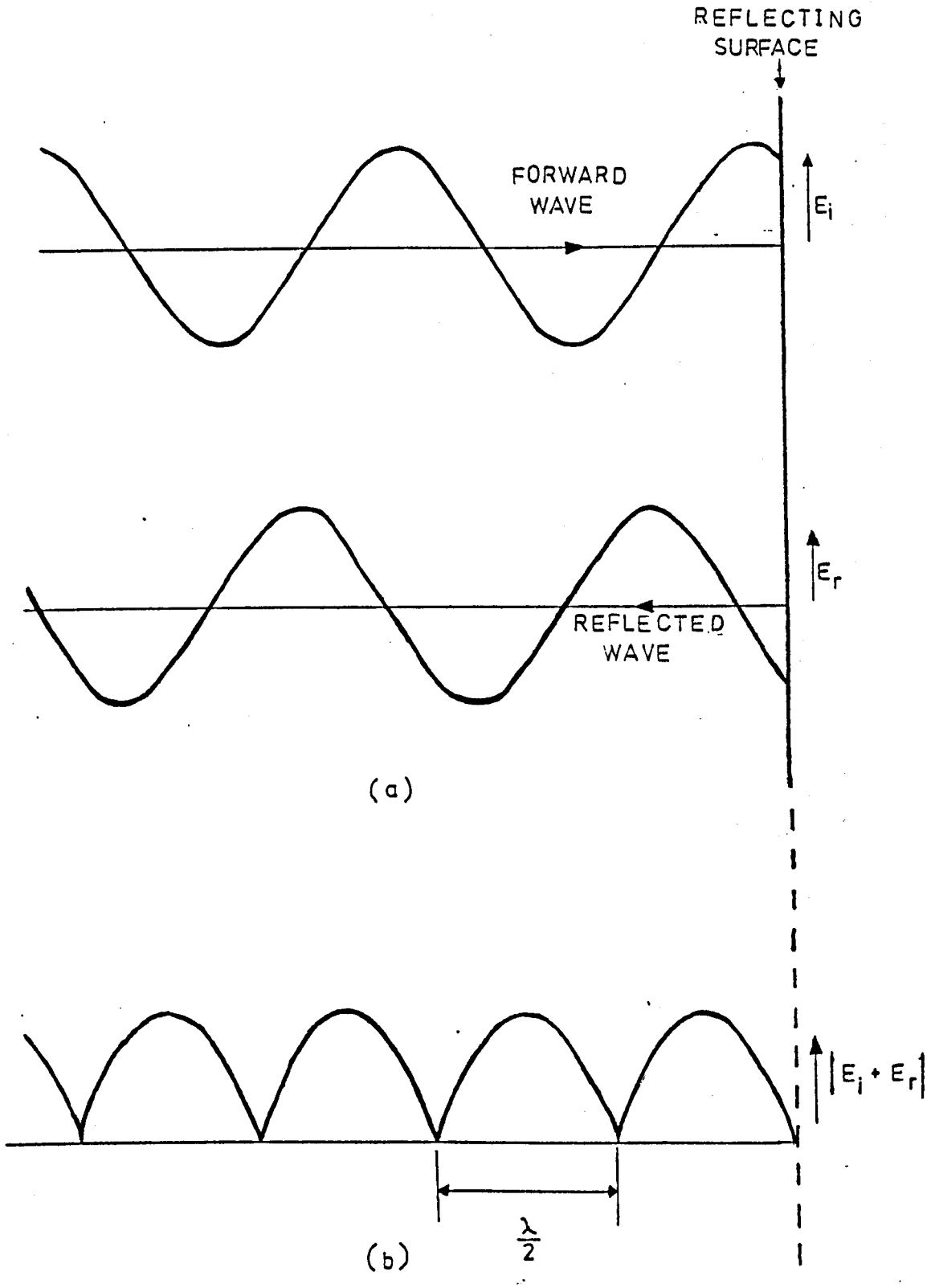

REFLECTION FROM A CONDUCTING SURFACE
(a) The Wave Structure
(b) The Standing Wave Pattern

FIG. 3.17

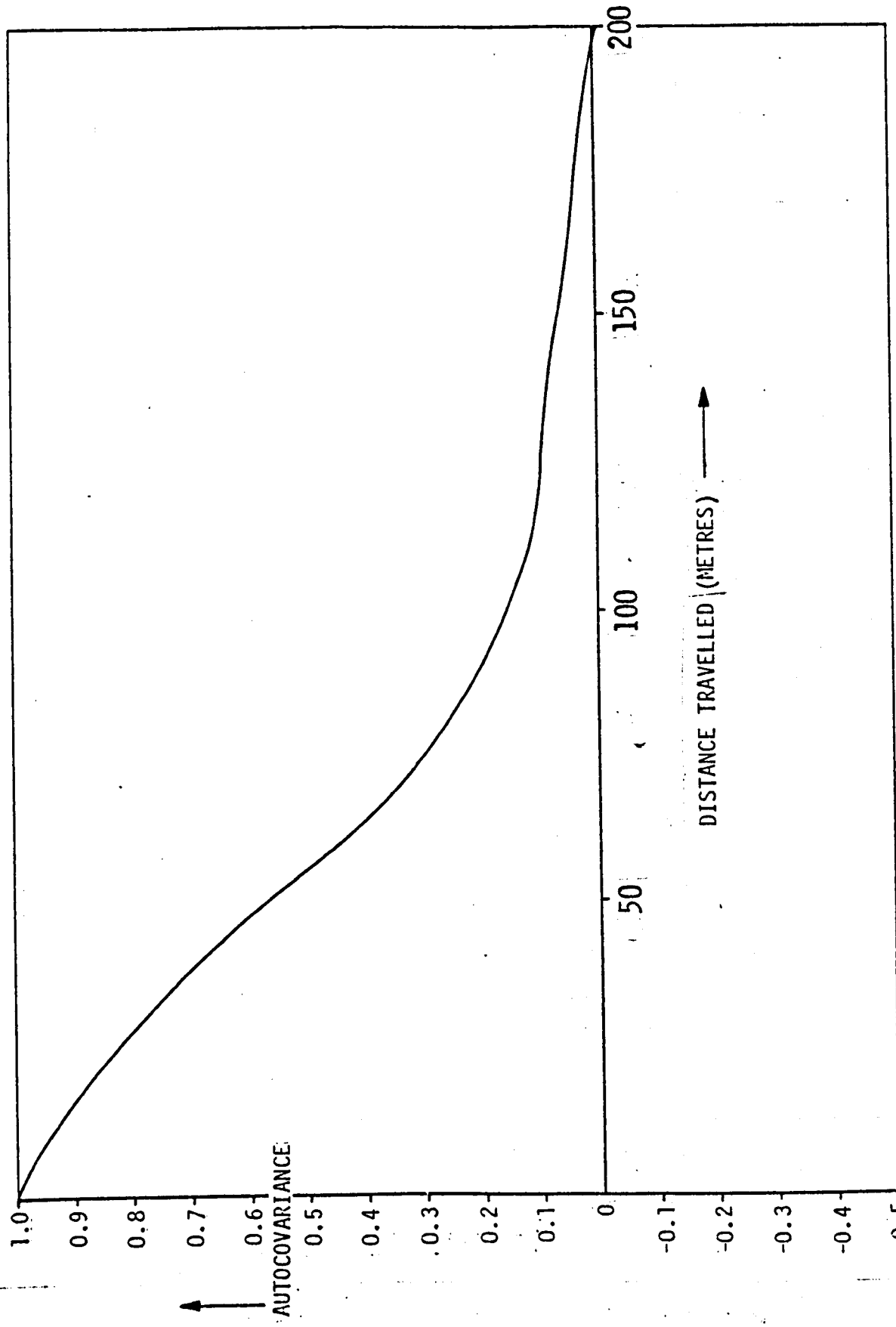

NORMALISED AUTOCOVARIANCE FUNCTION OF A MEASURED SLOW-FADING SIGNAL ENVELOPE AT 75MHz (ROTTON PARK ROAD - BIRMINGHAM)

FIG. 3.18

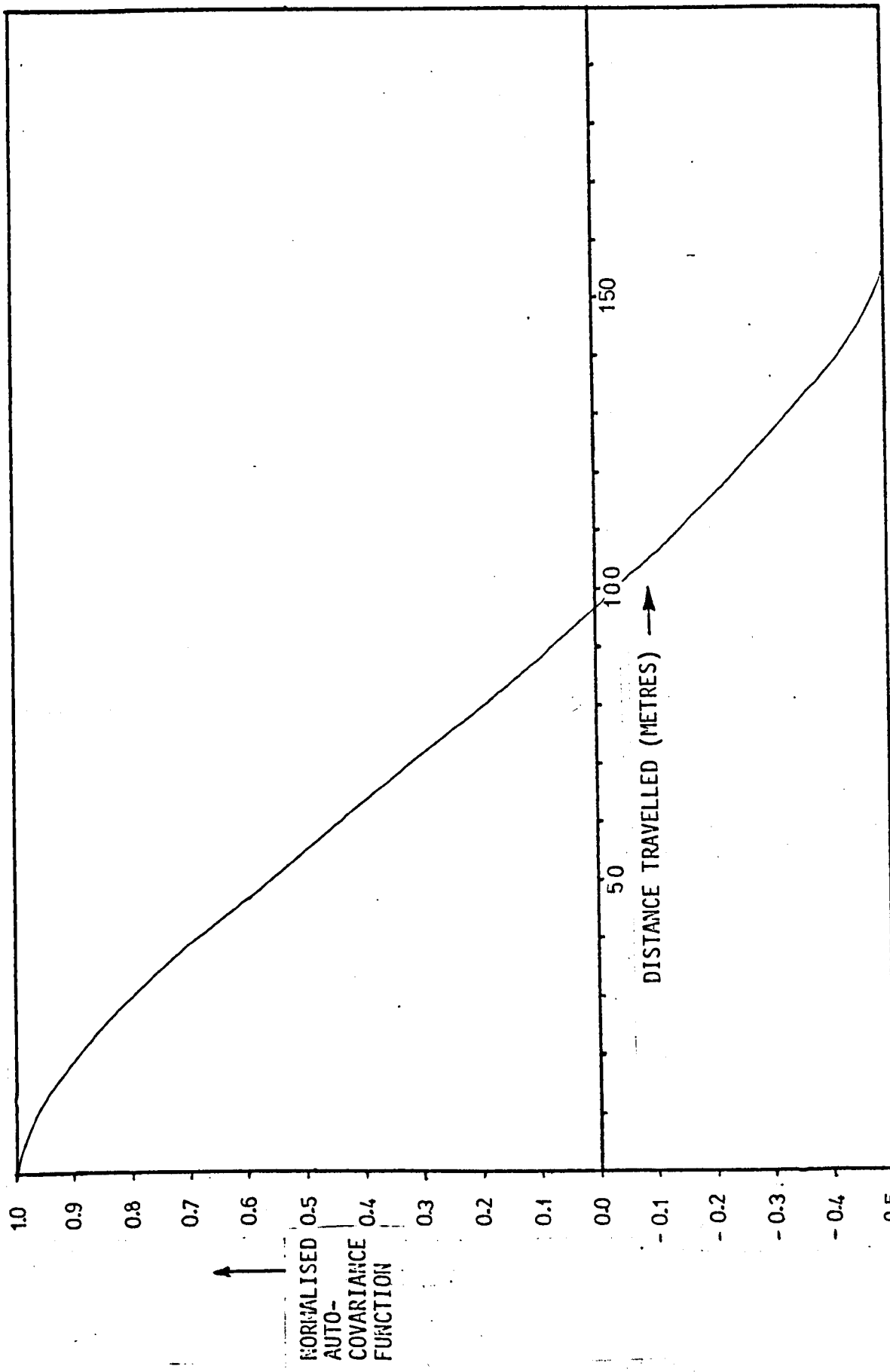

NORMALISED AUTOCOVARIANCE FUNCTION OF A MEASURED SLOW-FADING SIGNAL ENVELOPE AT 75MHz (EDGEBASTON ROAD -BIRMINGHAM)

FIG.3.19

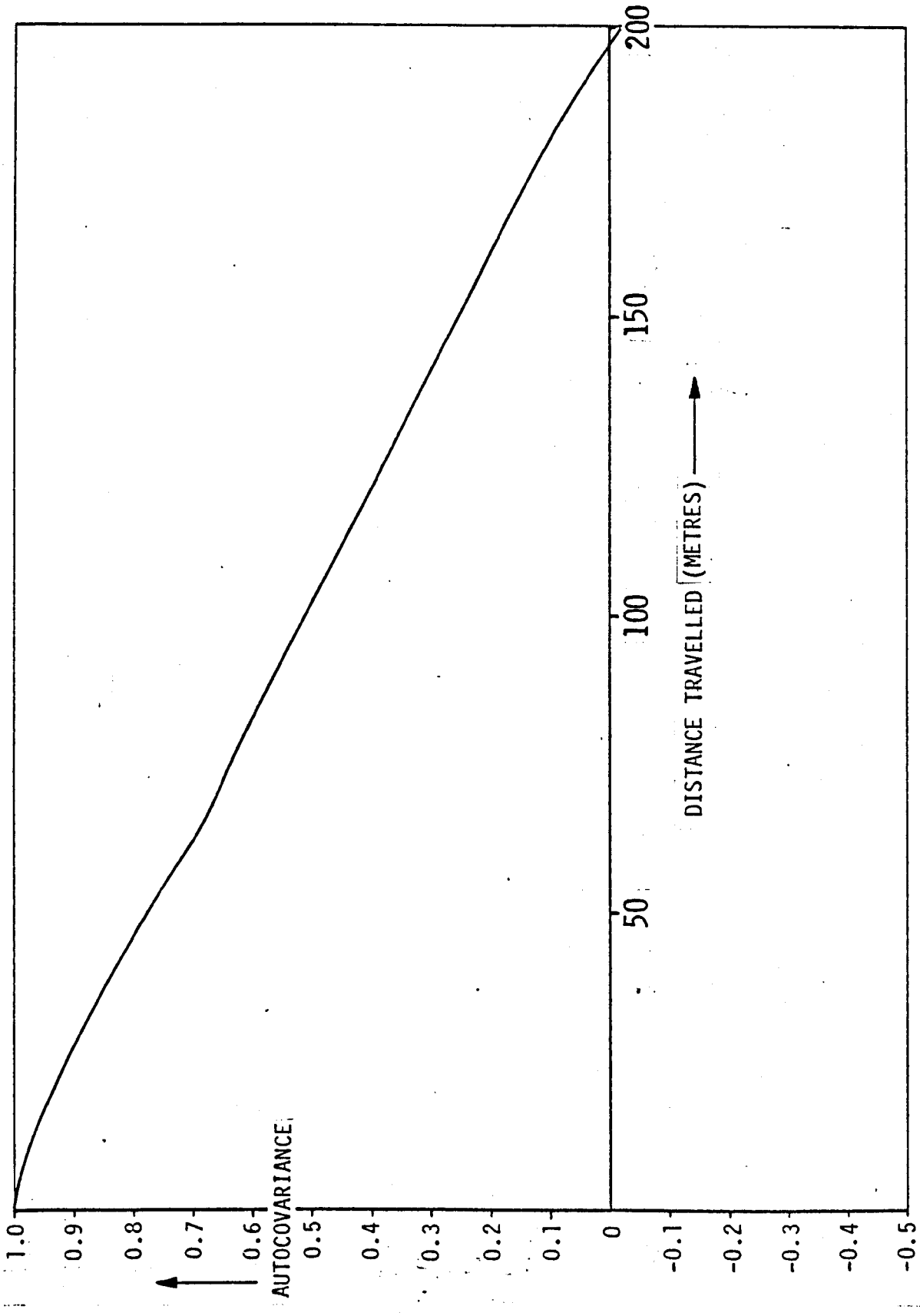

NORMALISED AUTOCOVARIANCE FUNCTION OF A MEASURED SLOW-FADING SIGNAL ENVELOPE AT 75MHz (BIRMINGHAM CITY CENTRE)

FIG. 3.20

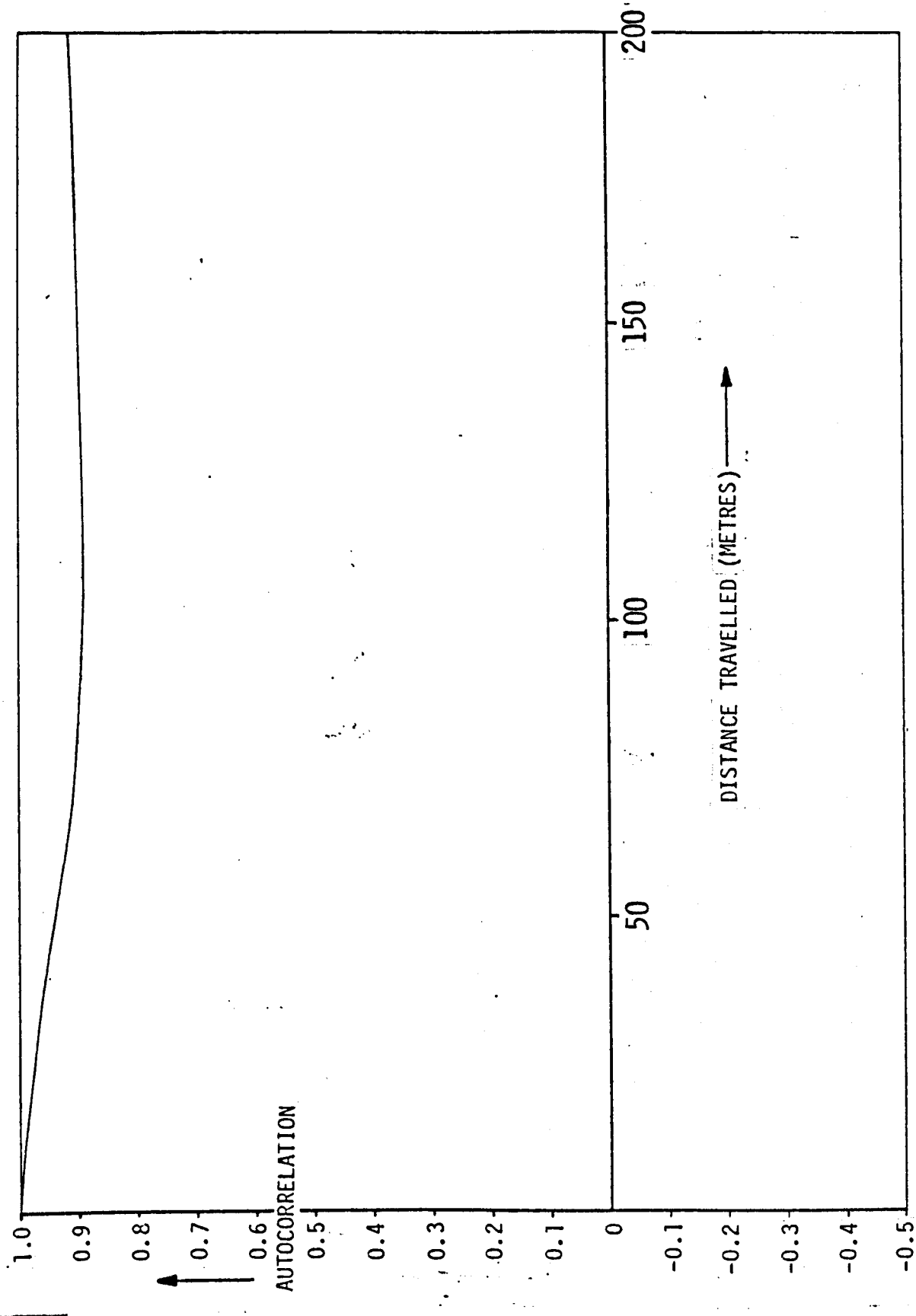

NORMALISED AUTOCORRELATION FUNCTION OF A MEASURED SLOW-FADING SIGNAL ENVELOPE AT 75MHz
(ROTTON PARK ROAD - BIRMINGHAM)

FIG. 3.21

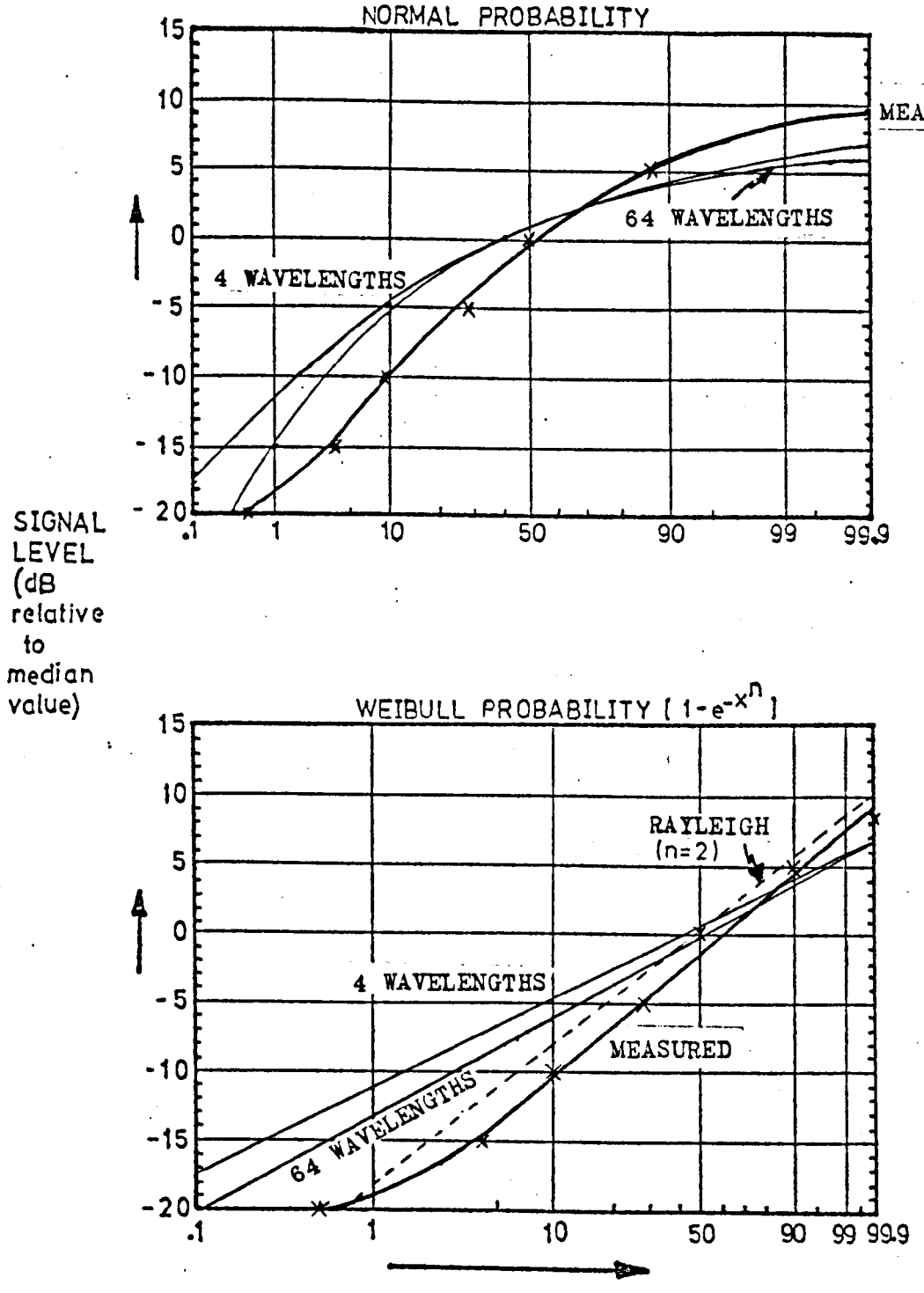

CUMULATIVE PROBABILITY DISTRIBUTIONS OF A MEASURED SIGNAL ENVELOPE AT 75.375MHz AFTER FILTERING USING A RECTANGULAR WINDOW OF VARIOUS WIDTHS

(BARLOWS ROAD - BIRMINGHAM)

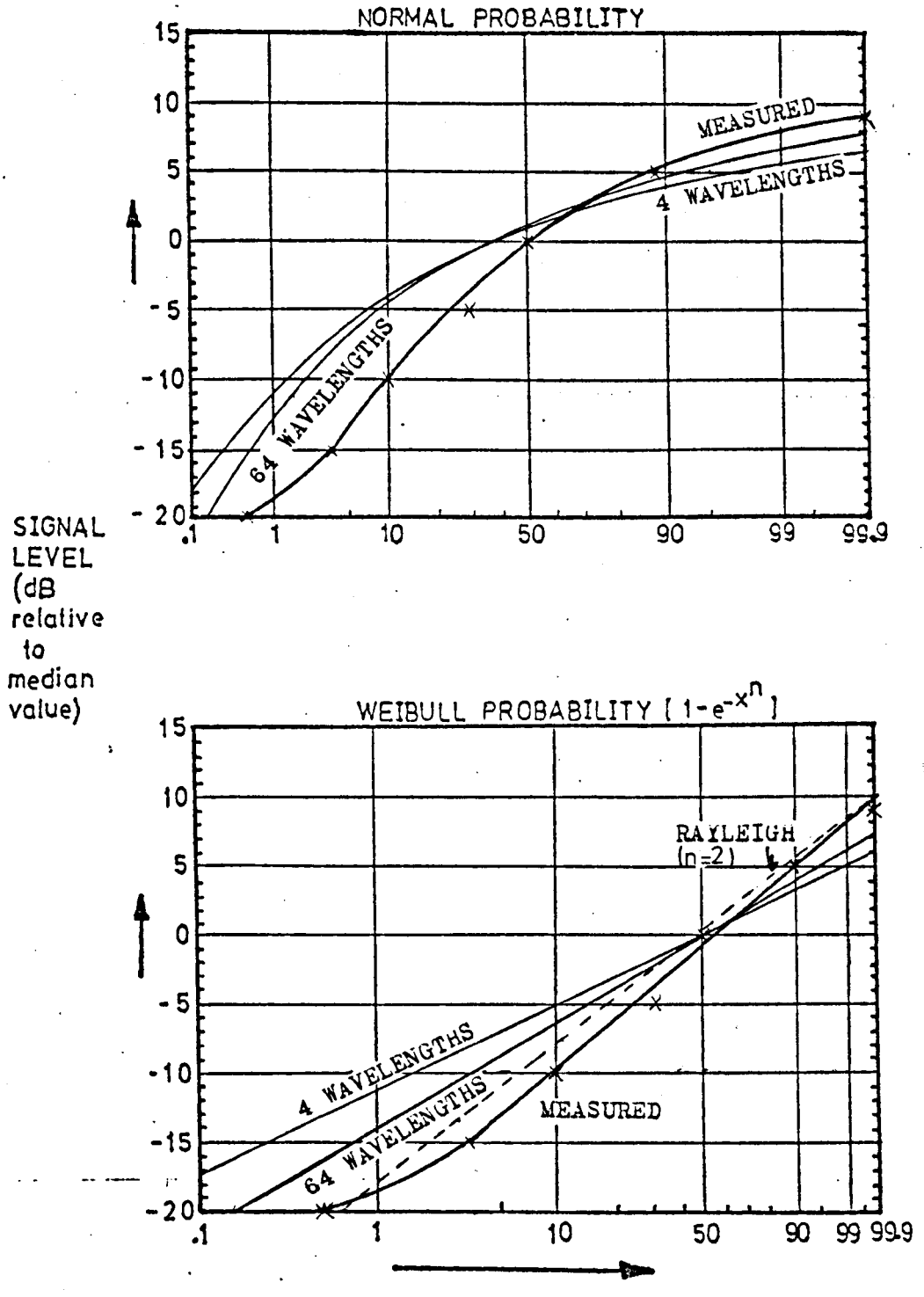

CUMULATIVE PROBABILITY DISTRIBUTIONS OF A MEASURED SIGNAL ENVELOPE AT 75.375MHz AFTER FILTERING USING A TRIANGULAR WINDOW OF VARIOUS WIDTHS
(BARLOWS ROAD - BIRMINGHAM)

FIG.3.23

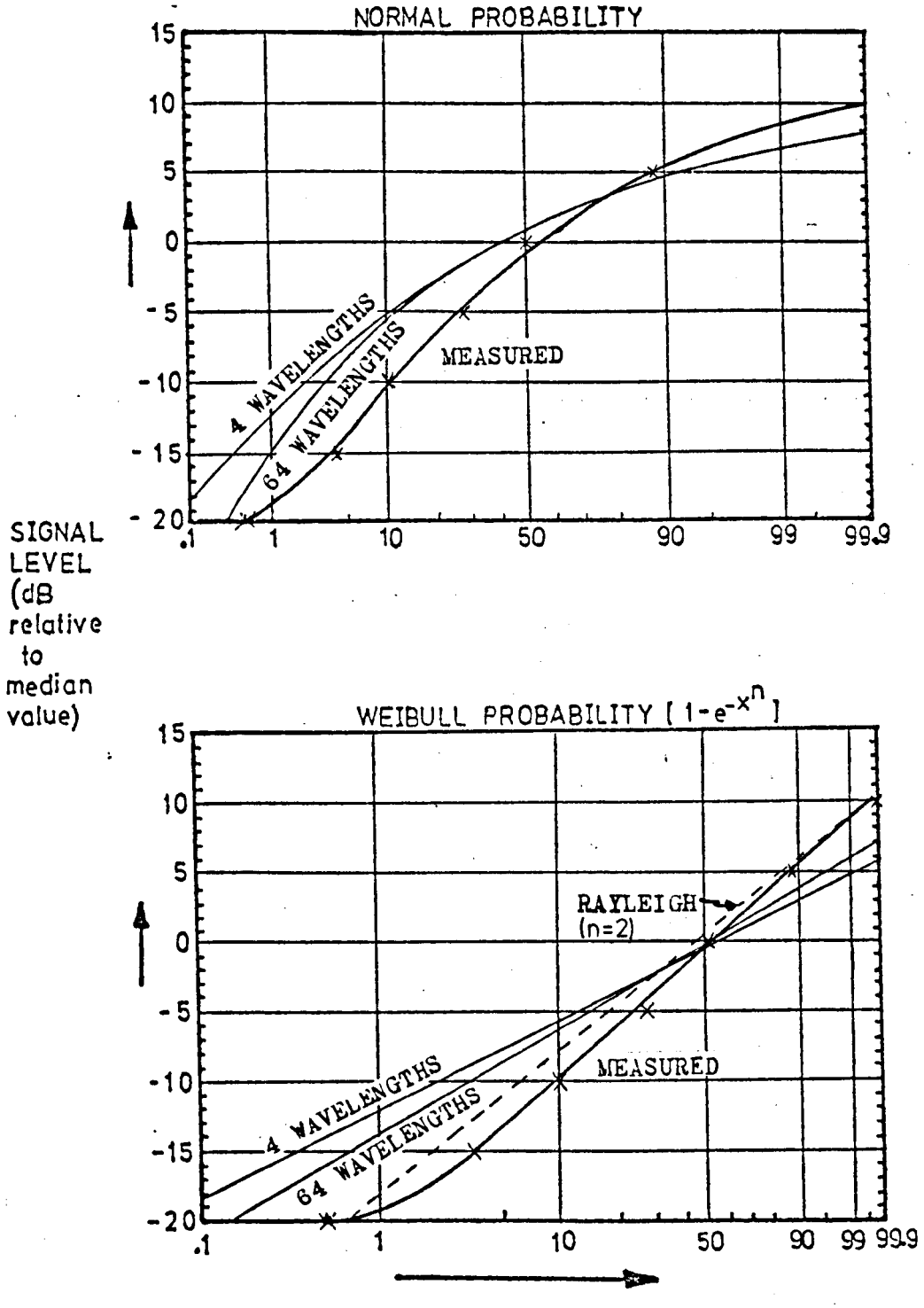

CUMULATIVE PROBABILITY DISTRIBUTIONS OF A MEASURED SIGNAL ENVELOPE AT 75.375MHz AFTER FILTERING USING A RAISED COSINE WINDOW OF VARIOUS WIDTHS
(BARLOWS ROAD - BIRMINGHAM)

FIG. 3.24

CHAPTER 4

A REVIEW OF MEDIAN SIGNAL PREDICTION TECHNIQUES

Before proceeding with the analysis of the measured data it is prudent to examine the factors which, according to the literature, are relevant in determining the transmission loss. This review commences by considering the basic propagation situation occurring in "free space" and progresses, in stages, to the case of propagation over a smooth, spherical homogeneous earth. Real terrain effects are included in this investigation by considering the diffraction losses over an isolated knife-edge, a smooth infinite cylinder and multiple knife-edge obstacles. Finally, propagation path loss prediction models are examined and, where possible, useful factors are isolated.

4.1 PROPAGATION THROUGH FREE SPACE

Radio propagation between aerials situated in a perfect, lossless transmission medium, e.g. a vacuum, when both aerials and the line connecting them are remote from any reflecting or absorbing surfaces, is governed by the "free space" or Friis transmission equation:[4.1]

$$P_r = \frac{P_t G_t G_r \lambda^2}{16 \pi^2 d^2}$$

For isotropic radiators this expression reduces to the basic transmission loss formula:

$$L_b = 32.45 + 20 \log_{10} f_{MHz} + 20 \log_{10} d_{km}, \quad dB$$

The loss may thus be seen to increase as f^2 and d^2 (6 dB/octave).

4.2 PROPAGATION THROUGH THE EARTH'S ATMOSPHERE

The change in the refractive index of the earth's atmosphere with altitude causes the radio waves to propagate along curved paths. This ray bending may be represented, within the first kilometer above the surface, by the use of an effective earth's radius (a) empirically determined as:[4.2,4.3,4.4]

$$a = a_o\left(1 - 0.04665 \exp(0.005577\, N_s)\right)^{-1}, \quad \text{km}$$

where a_o is the true earth's radius (6370 km) and N_s is the surface refractivity of the atmosphere.

The factor N_s can be expressed as a function of the refractive index, n_s, as:

$$N_s = (n_s - 1) \times 10^6$$

An average value of N_s is approximately 301, resulting in a ratio of the effective earth's radius to the true radius of 4/3. The effect of this curvature correction, however, is negligible for ranges below 10 km, the height differential being less than 6 m.

(1)

Other effects such as ducting[4.3] and ionospheric reflection[4.3] have not been reported in the literature for the low powers typically radiated by mobile systems in the VHF and UHF frequency bands.

(2)

4.3 PROPAGATION OVER A REFLECTING SURFACE

A situation where two aerials are mutually visible over a spherical earth of effective radius 'a' is depicted in Fig.4.1. The aerial heights measured above the earth's surface are h_1 and h_2, their heights above the tangent plane at the point of reflection on the sphere are h_1' and h_2' respectively. Assuming that these heights are small compared with the earth's radius, the reflection point on the sphere can be located as:

$$d_1 = d\left(1 + \frac{h_2'}{h_1'}\right)^{-1}$$

Substitution for h_1' and h_2' in the above expression results in a cubic equation, a root of which is approximately:

$$d_1 \simeq d\left(1 + \frac{h_2}{h_1}\right)^{-1}$$

The path length difference, Δr, between the direct and ground reflected rays, when h_1' and h_2' are very much less than the total range, d, is:

$$\Delta r = r_1 + r_2 - r_o$$
$$\simeq \frac{2h_1'h_2'}{d}$$

and the signal strength at the receiver is given by:[4.5]

$$\sqrt{1 + R_e^2 - 2R_e \cos\left(\frac{2\pi\Delta r}{\lambda} - C\right)} \quad \text{x Free Space Field Strength}$$

Here R_e is the effective value of the reflection coefficient[4.4] defined as the ratio of the magnitudes of the reflected and incident waves. The reflected wave will lag the direct wave by an angle of $\frac{2\pi}{\lambda}\Delta r + (\pi - C)$, where $(\pi - C)$ is the phase change on reflection from the surface.

4.3.1 PROPAGATION OVER PLANE EARTH

(2)

For a perfectly conducting surface ($R_e = 1$, $C = 0$), the received signal will be given, for vertical polarisation, by:

$$\sqrt{2\left(1 - \cos\left(\frac{2\pi}{\lambda}\Delta r\right)\right)} \quad \text{x} \quad \text{Free Space Signal Strength}$$

Substitution for Δr, assuming the aerial heights are small when compared with their separation, yields the "plane earth" transmission equation.[4.6]

$$P_r = \left(\frac{4\pi}{\lambda} \cdot \frac{h_1' h_2'}{d}\right)^2 \cdot \left(\frac{P_t G_t G_r \lambda^2}{16 \pi^2 d^2}\right)$$

$$= P_t G_t G_r \left(\frac{h_1' h_2'}{d^2}\right)^2$$

Note that the loss associated with this expression (P_t/P_r) is independent of frequency but is a function of d^4 (12 dB/octave).

4.3.2 PROPAGATION OVER A SMOOTH CURVED EARTH

When a beam of radio waves is reflected from a smooth, plane surface, the beam continues to diverge after reflection at the same rate as the incident beam. Only the phase, magnitude and direction of propagation are modified. The reflection of a radio beam from a curved surface, however, results in the alteration of the divergence, convex surfaces serving to diverge the beam at a greater rate than the plane reflector and concave having a focussing influence. To account for this change in the divergence of the incident energy, a "divergence factor" (Q) may be calculated.[4.3]

The divergence factor for the smooth sphere depicted in Fig.4.1 can be expressed[4.3] as:

$$Q \simeq \left(1 + \frac{2\, d_1\, d_2}{a\, d\, \tan\Phi}\right)^{-\frac{1}{2}}$$

where the assumption that $\sin\Phi = \tan\Phi$ is implicit.

The effective reflection coefficient can then be defined:[4.3]

$$R_e = R\, Q \left(\frac{G_{r1}\, G_{r2}}{G_{o1}\, G_{o2}}\right)^{\frac{1}{2}}$$

G_{o1} and G_{o2} are the gains of the aerials in the direction of each other, G_{r1} and G_{r2} are their gains in the direction if the ground reflection point.

4.3.3 PROPAGATION OVER A ROUGH SURFACE

The application of simple geometric ray theory becomes questionable when the reflecting surface is roughened. In this case the reflection is no longer a coherent divergence of energy but is an incoherent scatter of the incident field occurring over a large area of the surface. The signal at a point in space above the plane will therefore be the vector sum of component rays having seemingly random amplitudes, by virtue of the scattering mechanism, and random phase angles, as a result of the differing path lengths travelled (Fig.4.2). The treatment of this type of situation must, in the absence of an accurate surface profile description, be statistical.

If the surface undulations are such that a single curve fit to the mean level appears reasonable (Fig.4.3), an empirical estimate of the effective reflection coefficient may be used:[4.4]

$$R_e = R\,Q\left(\frac{G_{r1}G_{r2}}{G_{o1}G_{o2}}\right)^{\frac{1}{2}} \exp\left(\frac{-0.6\ s_h \sin\Phi}{\lambda}\right)$$

on condition that

$$Q\,R \exp\left(\frac{-0.6\ s_h \sin\Phi}{\lambda}\right) \text{ is greater than either } \sqrt{\sin\Phi} \text{ or } 0.5.$$

In the situation where the above condition is invalid, the following approximation has been suggested:[4.4]

$$R_e = \left(\frac{G_{r1}G_{r2}}{G_{o1}G_{o2}}\right)^{\frac{1}{2}} \sqrt{\sin\Phi}$$

s_h is the rms deviation of the terrain values from the smooth curve fit, $\frac{s_h \sin\Phi}{\lambda}$ is the Rayleigh Criterion of roughness.

4.3.4 LIMITATIONS OF THE SMOOTH EARTH AND ROUGH EARTH MODELS

4.3.4.1 Line-Of-Sight Propagation Over Smooth Earth

The calculations performed in section 4.3.2 involved the use of geometric ray theory and consequently have the following limitations on their validity:[4.7]

(a) The operating region must be within the radio horizon.

(b) The aerials must be sufficiently high for the surface wave to be neglected.

(c) The grazing angle has the following restriction:

$$\tan\Phi > \left(\frac{c}{2\pi a f}\right)^{\frac{1}{3}}$$

For the case of propagation over a smooth homogeneous spherical earth when the surface wave may be neglected, recourse to the rigorous mathematical solution is required.[4.7] Nevertheless,

significant simplifications are available if some degree of error is tolerable and the range of the parameters is restricted.[4.5, 4.8, 4.9]

The assumption that the earth is an homogeneous sphere of uniform dielectric constant is generally untrue for terminal separations greater than approximately 10 km. The presence of water or minerals in the surface layers will produce a locationally variable surface conductivity, and the existence of water on the surface will greatly modify the magnitude of the reflection coefficient.[4.4]

At frequencies above approximately 1 GHz the treatment of the earth as a smooth sphere is generally untrue. Consequently the theory will only be strictly applicable to such surfaces as tide-washed sand, tarmac or calm water[4.10] and most practical surfaces would be more reasonably treated as rough reflecting planes.

4.3.4.2 Line-Of-Sight Propagation Over Rough Earth

The method described in section 4.3.3 employs a single curve fit to the terrain profile. In a situation where two effective reflecting areas are possible (Fig.4.4) the method will be inapplicable. Furthermore, the equations given for the effective reflection coefficient will be wholly inappropriate when a high degree of shadowing of the reflecting area results from the predominance of a large irregularity. In this case diffraction effects should be incorporated.

4.4 DIFFRACTION

When the line-of-sight path between the two terminals of a radio link is obstructed by, say, a mountain ridge, the propagation path loss measured is much greater than that predicted using the free space propagation equation (section 4.1), even if it may be assumed that, ignoring the obstacle itself, the transmission medium is indeed free space. The excess loss experienced may be attributed to a diffraction mechanism, i.e. the means by which radio waves bend around obstacles to partially illuminate the "shadow" cast by the obstruction.

4.4.1 DIFFRACTION OVER ISOLATED OBSTACLES

4.4.1.1 Diffraction Over A Perfect Knife-Edge

The signal strength at a point P behind a perfectly absorbing infinite half-plane (Fig.4.5), or knife-edge, placed orthogonal to the direction of propagation is determined as the vector sum of all contributions from the secondary Huygen's sources in the half-plane above the knife-edge (Fig.4.6). The solution yields a Fresnel integral of the form:[4.17]

$$F(v) = \left(\frac{1 - j}{2}\right) \int_{v}^{\infty} \exp\{j\tfrac{1}{2}\pi t^2\} dt$$

where v is the Fresnel parameter defined as (Fig.4.5):

$$v = \sqrt{\frac{2}{\lambda} \cdot \left(\frac{d_1 d_2}{d_1 + d_2}\right)}\ \theta$$

Evaluation of the Fresnel integral requires numerical techniques and is shown graphically in Fig.4.7 as a function of v. If the v parameter is greater than approximately 2.4 the integral may be determined using a series expansion of the integrand. Subsequent

integration by series yields:[4.4]

$$|F(v)| \simeq \frac{1}{\sqrt{2}\,\pi\, v}$$

Approximations to the value of the integral are available[4.4] for $v < 2.4$ as:

$$A(v) = -10 \log_{10}|F(v)| = 6.02 + 9.11\, v - 1.27\, v^2 \quad \text{for } 0 < v \leq 2.4$$

$$A(v) = -10 \log_{10}|F(v)| = 6.02 + 9.0\, v + 1.65\, v^2 \quad \text{for } -0.8 \leq v \leq 0$$

4.4.1.2 Diffraction Over A Perfect Knife-Edge Situated On Conducting Ground

The placement of an absorbing knife-edge on a conductiong ground plane will permit four possible paths to exist by which radio waves may travel between a transmitter and receiver located on opposite sides of the obstacle. For this reason the geometrical construction is termed the "four ray" method.[4.11]

(3)

The four rays shown in Fig.4.8 have travelled along different paths and accordingly have different phase angles and amplitudes, the latter being a consequence of the diffraction losses incurred by propagation over the obstruction. The resulting signal must therefore be obtained by the vector addition of the individual rays.

4.4.1.3 Diffraction Over Rounded Obstacles

The assumption that obstacles may be regarded as knife-edges for the purpose of diffraction calculations is often invalid when

physical obstructions are being considered, especially at UHF frequencies and above when the wavelength is shorter than 1 m. In these cases the influence of the diffractor's profile on the loss must be incorporated into the calculation.

Fig.4.9 depicts a semi-infinite cylinder placed normal to the direction of propagation. The cylinder can support reflections from its surface which subsequently modify the Huygen's wave-front above it in a manner similar to that of the four ray theory[4.12] described in section 4.4.1.2.

An alternative approximate solution[4.13,4.14] may be obtained by defining a dimensionless parameter ρ as (Fig.4.10):

$$\rho = \left(\frac{\lambda}{\pi}\right)^{\frac{1}{6}} R^{\frac{1}{3}} \left(\frac{d}{d_1 d_2}\right)^{\frac{1}{2}}$$

where R is the radius of curvature of the obstacle's crest.

The diffraction loss can then be represented by a two dimensional quantity $A(v,\rho)$ which, in turn, can be related to the one dimensional ideal knife-edge attenuation, $A(v,0)$, and a "curvature loss", $A(0,\rho)$, by:

$$A(v,\rho) = A(v,0) + A(0,\rho) + U(v\rho) \quad , \text{dB}$$

where the factor $U(v\rho)$ is a correction term.

The function $A(v,0)$ has been given in Fig.4.7 for the case of a perfect knife-edge. The functions $A(0,\rho)$ and $U(v\rho)$ are shown in Figs. 4.11 and 4.12 respectively.

A series of approximations for the term A(v,0) have been given in section 4.4.1.1. The functions A(0,ρ) and U(vρ) may be calculated by:[4.15]

$$A(0,\rho) = 6 + 7.19\,\rho - 2.02\,\rho^2 + 3.63\,\rho^3 - 0.75\,\rho^4 \quad \text{for } \rho < 1.4$$

$$U(v\rho) = (43.6 + 23.5\,v\rho)\log_{10}(1 + v\rho) - 6 - 6.7\,v\rho \quad \text{for } v\rho < 2$$

$$U(v\rho) = 22\,v\rho - 20\log_{10}(v\rho) - 14.13 \quad \text{for } v\rho \geq 2$$

The curves of Figs. 4.11 and 4.12 are strictly valid for horizontal polarisation only, but a series of documented measurements has shown that they may be employed for vertical polarisation at VHF and UHF frequencies in the diffraction shadow region with negligible error.[4.12]

The effective radius of curvature of a hill crest (Fig.4.13) has been suggested[4.4] as:

$$R = \frac{2D_s\, d_{st}\, d_{sr}}{\theta(d_{st}^2 + d_{sr}^2)}$$

where $D_s = d - d_{Lt} - d_{Lr}$ is the distance between the transmitter and receiver horizons.

Irregularities on the surface of the cylinder have been found to incoherently scatter the incident radio energy.[4.12] The resulting diffraction process then tends to agree with results obtained by recourse to knife-edge theory.

4.4.2 MULTIPLE KNIFE-EDGE DIFFRACTION

The application of single knife-edge diffraction concepts to the problem of a two obstacle transmission path involves the evaluation of a double Fresnel integral over the planes above the knife-edges as indicated in Fig.4.14. The full solution[4.16,4.17] results in such considerable mathematical complexity that it cannot easily be extended to cases involving three or more diffractors. Consequently the trend has been for the continued use of simple models, the most notable of which are outlined in the following sections.

4.4.2.1 The Bullington Equivalent Knife-Edge Construction

Bullington[4.18] suggested that the diffraction loss over a terrain path containing multiple obstructions could be evaluated using a single equivalent knife-edge placed at the point of intersection of the transmitter and receiver horizon rays as shown in Fig.4.15. The diffraction loss over the original terrain situation is then taken as that over the virtual knife-edge.

Because the equivalent knife-edge construction reduces a fundamentally complex propagation situation to a simple problem it has obvious advantages. On the other hand, terrain paths having more than two significant obstructions are oversimplified, only two of these ever being relevant in the construction of the equivalent knife-edge. The situation of Fig.4.16, by way of an example, has two obstacles which are completely ignored and will probably result in the final loss being under-estimated.

4.4.2.2 The Epstein-Peterson Method

The method of determining the diffraction loss for a multiply obstructed path proposed by Epstein and Peterson[4.19] sums the attenuations produced by the individual obstacles taken in cascade. The diffraction loss for each edge is computed over the path joining the crest of the previous obstacle (or transmitter if the first edge in the chain is being considered) to the crest of the knife-edge under investigation and then to the crest of the following obstacle (or receiver if the last edge in the chain is being considered). The total loss for the case of Fig.4.17 will be given as:

$$A(T - O1 - O2) + A(O1 - O2 - R) \ , \ dB$$

where A(x - y - z) denotes the diffraction loss, in dB, evaluated for the general path connecting points x, y and z.

Comparisons of the results obtained using this approximate construction with those from the rigorous solution[4.16] for a two knife-edge case have shown that large errors are produced when the obstacles are closely spaced. A correction factor has been derived[4.16] for the situation where the Fresnel v parameters of both edges are much greater than unity as:

$$10\log_{10} (\text{cosec}\delta) \ , \ dB$$

where

$$\text{cosec}\ \delta = \sqrt{\frac{(d_1 + d_2)(d_2 + d_3)}{(d_1 + d_2 + d_3)\ d_2}}$$

Accurate results from the Epstein-Peterson method have been demonstrated[4.20] to exist only when $\delta > 80^{\circ}$.

4.4.2.3 The Japanese Method

Inclusion of the previously specified correction factor into the Epstein-Peterson method has been shown[4.22] to be equivalent to a method originally attributable to the Japanese postal service.[4.21] The difference between the geometric constructions used by the Epstein-Peterson and Japanese methods lies in the positioning of the hypothetical transmitter. For the Epstein-Peterson model this conceptual radiator is placed at the summit of the previous obstacle while the Japanese construction places it at the point where the projected horizon ray meets the plane of the true transmitter. The total diffraction loss for the two obstacle case shown in Fig.4.18 is given by:

$$A(T - O1 - O2) + A(T' - O2 - R) \ , \quad dB$$

The comments regarding the accuracy of the Epstein-Peterson model are also true for the Japanese method.[4.15]

4.4.2.4 The Deygout Method

Deygout[4.23] has proposed that the diffraction loss over a multiply obstructed path be evaluated as the loss over each edge in order of decreasing influence. This is a complicated procedure and is best explained by way of an example. Consider the two obstacle path shown in Fig.4.19. The Fresnel v parameter of each edge is calculated in the absence of the other, v_1 and v_2 say. The obstacle with the larger value is termed the "main edge" and produces the greater diffraction loss. For the situation of Fig.4.19 this is the edge labelled O1 and the associated loss

is given as A(T -O1 - R). The diffraction loss resulting from the remaining obstruction is evaluated between the "main edge" and the obstructed terminal, in this case the receiver, A(O1 - O2 - R). The total loss is therefore given as:

$$A(T - O1 - R) + A(O1 - O2 - R) \text{ , dB}$$

The process subdivides the path into sections on either side of the main edge. If many edges are present the number of sub-divisions created each time the problem is sectioned about firstly the main edge, then a sub-main edge, and so on, are numerous. Consequently a path containing more than four obstacles results in a lengthy solution which is not easily programmed on a digital computer.

In a double knife-edge situation where one edge is largely dominant ($v_1/v_2 >> 1$), good agreement with the exact solution[4.16] is obtained. When the magnitudes of the Fresnel v parameters are comparable, however, the method is found to overestimate the total diffraction loss.[4.15] A correction factor for this case has been derived as:

(a) when $v_1 \geq v_2$ and v_1, v_2, $(v_2 \operatorname{cosec} \delta - v_1 \cot \delta) > 1$

$$\text{correction} = 20 \log_{10}\{\operatorname{cosec}^2\delta - \frac{v_2}{v_1} \operatorname{cosec} \delta \cot \delta\} \text{ , dB}$$

(b) when $v_2 \geq v_1$ and v_1, v_2, $(v_1 \operatorname{cosec} \delta - v_2 \cot \delta) > 1$

$$\text{correction} = 20 \log_{10}\{\operatorname{cosec}^2\delta - \frac{v_1}{v_2} \operatorname{cosec} \delta \cot \delta\} \text{ , dB}$$

where

$$\text{cosec } \delta = \sqrt{\frac{(d_1 + d_2)(d_2 + d_3)}{(d_1 + d_2 + d_3)\, d_2}}$$

and

$$\cot \delta = \sqrt{\frac{d_1 d_3}{(d_1 + d_2 + d_3)\, d_2}}$$

This correction factor reaches a minimum of 6 dB for $v_1 = v_2$ and $\delta = 0^\circ$.

4.4.2.5 Comparison Of Diffraction Models

The Bullington, Epstein-Peterson and Japanese models, together with some simple variants have been compared with the exact solution for two knife-edges over many practical paths by Wilkerson.[4.24] Each model was found to have specific regions over which it produced the minimum error.

(a) Unobstructed links with both obstacles below the line-of-sight path (Fig.4.20).

The minimum overall error in this region was obtained by summing the diffraction losses over each edge in the absence of the other:

$$A(T - O1 - R) + A(T - O2 - R) \text{ , dB}$$

(b) One Edge Predominant (Fig.4.21)

Here the Bullington equivalent knife-edge model was found to consistently produce the lowest errors although the errors obtained from all the methods were small.

(c) Lightly obstructed paths where both v parameters are slightly greater than unity.

The Epstein-Peterson model proved the most accurate in this region.

(d) Heavily obstructed paths where both v parameters are much greater than unity.

The Japanese method was found to be superior in this case.

Consideration of the models' performances in all the classes resulted in the Epstein-Peterson model being recommended[4.21] for general use.

A comparison[4.23] of the Epstein-Peterson and Deygout models with measured values obtained over a limited number of highly obstructed paths has shown that the Deygout method produced the lowest errors while the Epstein-Peterson consistently underestimated the loss. It is doubted, however, whether the improvement gained by recourse to the Deygout model justifies the increased procedural complexity entailed.

4.5 PROPAGATION PREDICTION MODELS

Many methods of predicting the transmission loss over practical terrain situations have been advanced in the literature. The techniques employed fall basically in two classes: empirical and semi-theoretical. Models in the former category result from large quantities of measurements and are, as such, formulated to be applicable without recourse to anything except the most

fundamental of formulae or other methods. The latter series of models combine the principles outlined in the preceding sections in different manners to produce techniques which may be interpreted to provide some indication of the modes of propagation.

4.5.1 THE EGLI MODEL

This method[4.25] was advanced in 1957 following an extensive series of path loss measurements at frequencies above 40 MHz over irregular terrain paths. The model forces agreement between the measured values and predictions made using the plane earth transmission approximation by utilising a correction factor (ξ):

$$P_r = P_t G_t G_r \left(\frac{h_t h_r}{d^2}\right)^2 . \xi$$

The correction factor is presented in the original publication[4.25] as a function of the aerial heights, polarisation, terrain roughness and transmission frequency. The standard deviation of the predictions has also been related to the terrain undulations, these being presumed to be a log-normally distributed random quantity.

It should be noted that while the plane earth propagation equation forms the basis of the prediction model, this is for convenience only and is not intended to signify the propagation mechanisms existing along the path.

4.5.2 THE EDWARDS AND DURKIN MODEL

A method of predicting the signal level which will be received over a communications link working in the VHF band has been

proposed by Edwards and Durkin.[4.26] The model requires the terrain diffraction loss to be calculated as a parameter and recommends that all the necessary terrain profile analysis be performed using a digital computer. The diffraction loss is subsequently added to the larger of the free space or plane earth transmission losses to provide the estimate of the total propagation path loss.

In the region close to the transmitter the direct and ground reflected rays interfere to form a signal fading pattern about the free space loss value. As the range increases, however, the path difference between the two rays decreases until, at differences of less than approximately $\lambda/6$, the signal level follows that predicted using the plane earth transmission expression. The resulting complex interference waveform[4.33] (Fig.4.22) is therefore simply modelled as free space propagation out to that range from the transmitter where the path difference is $\lambda/6$, and plane earth propagation beyond.

4.5.3 THE BLOMQUIST AND LADELL METHOD

Blomquist and Ladell[4.27] have advanced a model in an attempt to describe the propagation path loss over irregular terrain. This is essentially given by:

$$\text{Total Loss} = L_F + \left(L_D^2 + (L_p - L_F)^2\right)^{\frac{1}{2}} \quad , \text{dB}$$

The path loss over flat land ($L_D = 0$) reduces to the plane earth transmission equation whereas a highly obstructed link $\{L_D >> (L_p - L_F)\}$ gives a total path loss equal to the sum of the

free space and diffraction losses ($L_F + L_D$). While the limiting conditions appear intuitively reasonable, it is worth noting that no justification, either mathematical or conceptual, has been given in support of the model. The advantage of this technique over, say, the Edwards and Durkin method is that it is continuous in all space and for all terrain types.

4.5.4 THE ARMY SCHOOL OF SIGNALS METHOD

The method[4.28] employed by the British Armed Forces in planning their point-to-point radio relay links at frequencies above 2 MHz depends largely on hand calculations made using information obtained from maps, 4/3 earth charts and nomograms. The basic technique requires that the terrain profile of the transmission path be compared with a series of reference profiles and a decision made to determine which is the closest to the true situation. The series of instructions accompanying the reference profile must then be obeyed to calculate the propagation path loss.

The technique is specifically intended for use with carefully engineered radio links having both aerials clear of any local obstructions (e.g. trees or buildings) and sited on high ground or aerial masts. The influence of buildings on the propagation loss is not included in the method but the attenuation resulting from diffraction over terrain obstacles is computed using the Bullington equivalent knife-edge construction.

The big disadvantage of this technique is that a decision must be made using human judgement in order to determine which reference profile is required. The method is therefore difficult to programme on a digital computer and will be inapplicable to paths which do not clearly fall into one of the defined categories.

4.5.5 THE B.B.C. METHOD

This model[4.29] has been formulated by the British Broadcasting Corporation (BBC) to facilitate the production of the area coverage diagrams for their UHF (approximately 500 MHz) television transmitters. The transmitting aerials are implicitly assumed to be sited well clear of any local obstructions and the receiving aerials are taken to be at roof-top height (10 m).

The total propagation loss is enumerated by summing, in dB's, the following three factors:

(1) The free space path loss

(2) The terrain diffraction loss

(3) An "absorption loss"

This last item, the absorption loss, is incorporated in the summation to account for the effects which buildings and trees in the vicinity of the receiving aerial have on the transmission loss. It is evaluated by considering the last mile of the propagation path, i.e. that closest to the receiver, in ten 0.1 mile steps and computing a loss factor for each increment as a function of the tree and building density within it. The ten

resulting loss values are then weighted in inverse proportion to their range from the receiver and summed. The section closest to the receiving aerial is therefore given the greatest significance while the section 1 mile away is apportioned the least influence. Factors are required in this prediction model which are not readily attainable from Ordnance Survey maps of the regions, therefore necessitating a specialised site survey and, ultimately, the formulation of an extremely detailed terrain data base. The commercial applicability of the model is consequently limited by the expense entailed in performing the survey.

The assumption that the transmitter is unobstructed and well sited limits the model's use to systems where the base station (i.e. the broadcasting aerial) is atop a prominent terrain feature. If the base station aerial becomes partially obstructed it appears reasonable to presume that an extra absorption loss term must be evaluated to account for the effects of the clutter around the fixed terminal.

All ground reflections have been ignored in computing the transmission loss, a reasonable assumption at UHF frequencies when the magnitudes of the terrain undulations are large with respect to the wavelengths. At VHF, however, the ground reflections should be included unless the terrain path can be shown to be extremely irregular.[4.29]

Modifications would also be necessary to enable the model to be used when the receiver is below roof-top level, as is typical of vehicle mounted equipment.

4.5.6 THE OKUMURA METHOD

A large set of measurements[4.31] obtained over various terrain paths in Japan has provided the basis for an empirical propagation prediction model.[4.31,4.32] The majority of these experimental data were derived in towns or cities and consequently the model is intended for use with radio links having the vehicular terminal in the vicinity of buildings. Suitable correction factors are recommended, however, for the cases when the mobile station is in suburban and open areas.

The parameters which must be evaluated in order to determine the various correction factors of the Okumura model are:

(a) The Effective Base Station Height (h_{te}):
The height of the base station aerial above the average ground level calculated over the range interval of 3 to 15 km (or less if the total range is below 15 km).

(b) The Interdecile Terrain Undulation Height (Δh):
The difference between the 90 and 10 percentiles of the "peak-to-peak" value of the terrain undulation height, computed over the 10 km of the path closest to the vehicular station.

(c) Average Ground Slope (θ_m):
The average ground slope is determined over the 5 to 10 km of the terrain path closest to the vehicular terminal.

The following corrections are given in graphical form within the bounds of the relevant variables as specified.

(1) Basic Median Attenuation (A_{mu}):

1 to 100 km link range

100 to 3000 MHz transmission frequency

(2) Base Station Height Gain (H_{tu}):

1 to 100 km link range

20 to 1000 m effective base station aerial height

(3) Vehicular Station Height Gain (H_{ru}):

1 to 10 m vehicular aerial height

100 to 1000 MHz for a large city

or 100 to 2000 MHz for a medium city

(4) Rolling Hilly Correction Factor (K_H):

10 to 500 m Interdecile terrain undulation height

450 to 1500 MHz transmission frequency

(5) Sloping Ground Correction Factor (K_{SP}):

-20 milliradians to +20 milliradians average ground slope

Further corrections are available for the situation where the vehicle is free from all obstructions for a range of 300 to 400 m (open ground) at frequencies in the range 100 to 2000 MHz and in a village or sparsely tree lined road (suburban area) at frequencies from 100 to 3000 MHz.

The total path loss is predicted as the free space loss plus (or minus depending upon the context) all the various correction factors.

Extrapolations of the curves and re-definition of the parameters will be required if the Okumura model is to be employed for radio links operating below 100 MHz and over ranges below 15 km.

4.6 REFERENCES

4.1 Friis H.T.
"A Note on a Simple Transmission Formula"
Proc. IRE, 34, May 1946

4.2 CCIR Study Groups
"Statistical Distribution of K Obtained by Measurements of the Angle of Incidence on a 70 km Line-of-Sight-Path in the Frequency Band about 500 MHz"
Doc. V/3-E, 11th January 1968

4.3 Reed H.R. and Russel C.M.
"Ultra High Frequency Propagation"
John Wiley and Sons, NY 1953

4.4 Rice P.L., Longley A.G., Norton K.A. and Barsis A.P.
"Transmission Loss Predictions for Tropospheric Communications Circuits"
NBS Tech. Note 101, 1967

4.5 Norton K.A.
"The Calculation of Groundwave Field Intensity over a Finitely Conducting Spherical Earth"
Proc. IRE, 29, December 1941

4.6 Jakes W.C. Jr.
"Microwave Mobile Communications"
John Wiley and Sons, London

4.7 Bremmer H.
"Terrestrial Radio Waves, Theory of Propagation"
Elsevier Publishing Co. 1949

4.8 Vogler L.E.
"Calculation of Groundwave Attenuation in the Far Diffracting Region"
Radio Science, Vol.68D, No.7, July 1964

4.9 Reed H.R.
"Propagation Data for Interference Analysis"
RADC-TDR-61-313, Vol.1, January 1962

4.10 Bachynski M.P.
"Microwave Propagation over Rough Surfaces"
RCA Review, June 1959

4.11 Anderson L.J. and Trolese L.G.
"Simplified Method for Computing Knife-Edge Diffraction in the Shadow Region"
IRE Trans. Ant. and Prop., July 1958

4.12 Hacking K.
"Propagation Over Rounded Hills"
BBC Research Report RA-21, 1968

4.13 Wait J.R. and Conda A.M.
"Diffraction of Electromagnetic Waves by Smooth Obstacles for Grazing Angles"
J. Res. N.B.S., 1958, 63D, 2.

4.14 Dougherty H.T. and Maloney L.J.
"Application of Diffractions by Convex Surfaces to Irregular Terrain Situations"
Radio Science Vol.68D, No.2, February 1964

4.15 Causebrook J.H. and Davies B.
"Tropospheric Radio Wave Propagation over Irregular Terrain: The Computation of Field Strength for UHF Broadcasting"
BBC Research Report 1971/43, 1971

4.16 Millington G., Hewitt R and Immirzi F.S.
"Double Knife-Edge Diffraction in Field Strength Predictions"
IEE Monograph 1962, No.507E

4.17 Millington G., Hewitt R and Immirzi F.S.
"The Fresnel Surface Integral"
IEE Monograph 1962, No.508E

4.18 Bullington K.
"Radio Propagation at Frequencies above 30 Megacycles"
Proc. IRE, October 1947

4.19 Epstein J. and Peterson D.W.
"An Experimental Study of Wave Propagation at 850 mc/s"
Trans. IRE Antennas and Propagation, April 1955

4.20 Haikonen T.
"The Accuracy of Practical Approximations of Double Knife-Edge Diffraction Loss"
Sahko - Electricity in Finland. July/August 1966

4.21 "Atlas of Radio Wave Propagation Curves for Frequencies between 30 and 10000 mc/s"
The Radio Research Labs., Ministry of Postal Services, Tokyo, Japan

4.22 Hacking K.
"Approximate Methods for Calculating Multiple Diffraction Loss"
Electronics Letters, May 1966, Vol.2, No.5

4.23 Deygout J.
"Multiple Knife-Edge Diffraction of Microwaves"
IEEE Trans., Vol.AP-14, No.4, July 1966

4.24 Wilkerson R.E.
"Approximations to the Double Knife-Edge Attenuation Coefficient"
Radio Science, Vol.1, No.12, December 1966

4.25 Egli J.J.
"Radio Propagation above 40 Mc over Irregular Terrain"
Proc. IRE, October 1957

4.26 Edwards R. and Durkin J.
"Computer Prediction of Service Area for VHF Mobile Radio Networks"
Proc. IEE, Vol.116, No.9, September 1969

4.27 Blomquist A. and Ladell L.
"Prediction and Calculation of Transmission Loss in Different Types of Terrain"
Research Institute of Nat. Defence, Dept.3, 5-104 50 Stockholm 80 Sweden, March 1974 - NATO AGARD Conference Publ. CP-144

4.28 Army School of Signals
"Path Profile Analysis"
Systems RP02, Army Code No.14427

4.29 Sofaer E. and Davies B.
"Computer Method of Service Area Prediction at UHF"
BBC Research Dept., Service Planning Section, Tech. Memo. No.RA-1010, August 1967

4.30 Causebrook J.H.
"Computer Prediction of UHF Broadcast Service Areas"
BBC Research Report RD 1974/4, January 1974

4.31 Okumura Y., Ohmori E., Kawano T. and Fukuda K.
"Field Strength and its Variability in VHF and UHF Land Mobile Service"
Rev. Elec. Comm., Lab.16, September-October 1968

4.32 Reudink D.O.

"Properties of Mobile Radio Propagation above 400 MHz"

IEEE Trans. Vehic. Tech., Vol.VT-23, No.4, November 1974

4.33 Felix C. and Allsebrook K.

"Low Level Microwave Propagation"

Tech. Memo. EM-14/76, Dept.890, Communications Systems Analysis, BAC (Bristol), 1976

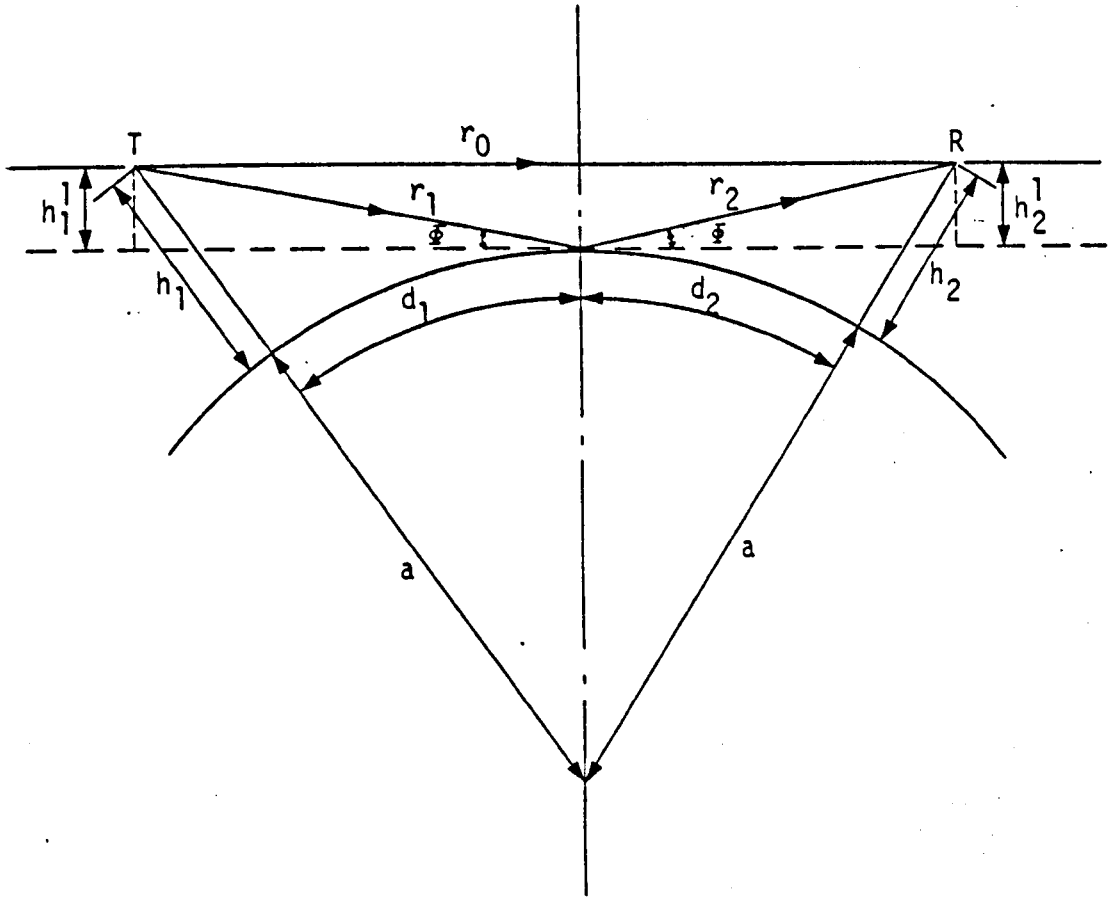

a = EFFECTIVE EARTHS RADIUS

$$\tan \Phi = \frac{h_1'}{d_1} = \frac{h_2'}{d_2}$$

range = $d = d_1 + d_2$

LINE-OF-SIGHT PROPAGATION OVER A SPHERICAL EARTH

FIG.4.1

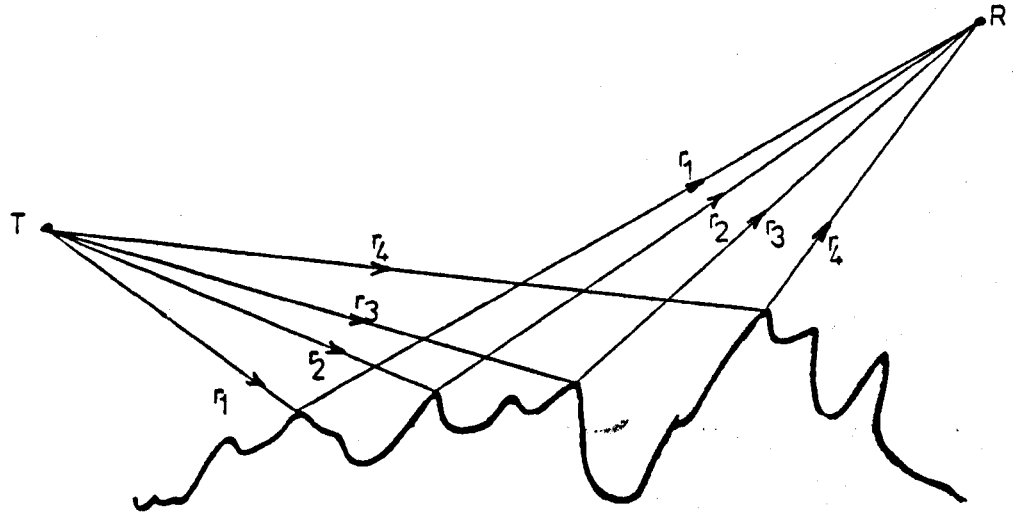

REFLECTION FROM A ROUGH SURFACE

FIG. 4.2

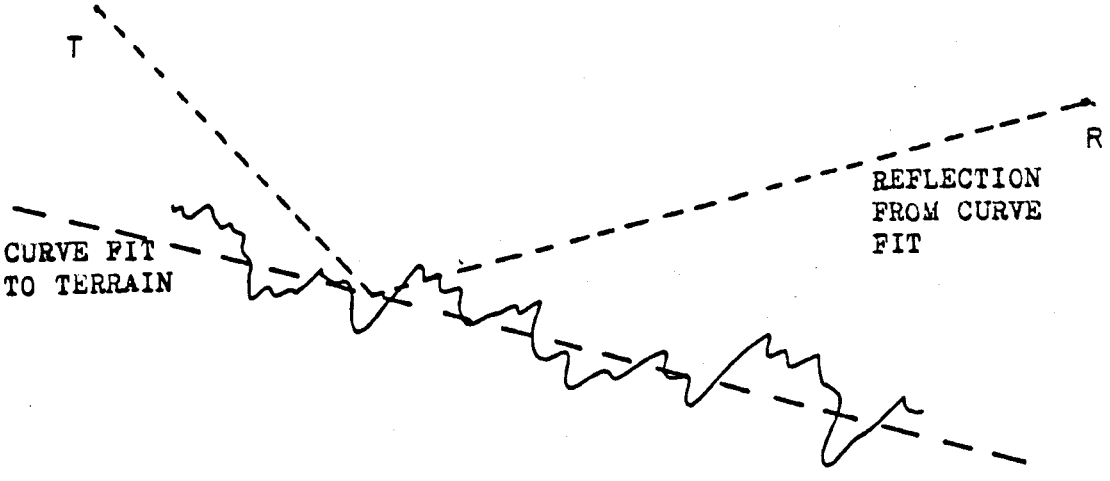

SINGLE CURVE FIT TO A ROUGH SURFACE

FIG. 4.3

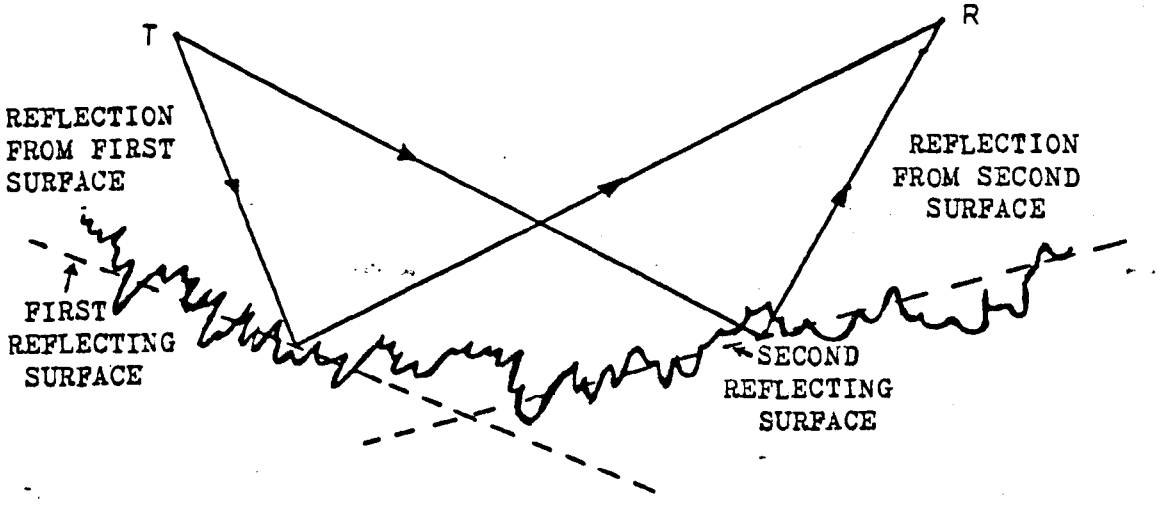

A ROUGH SURFACE YIELDING TWO REFLECTING AREAS

FIG. 4.4

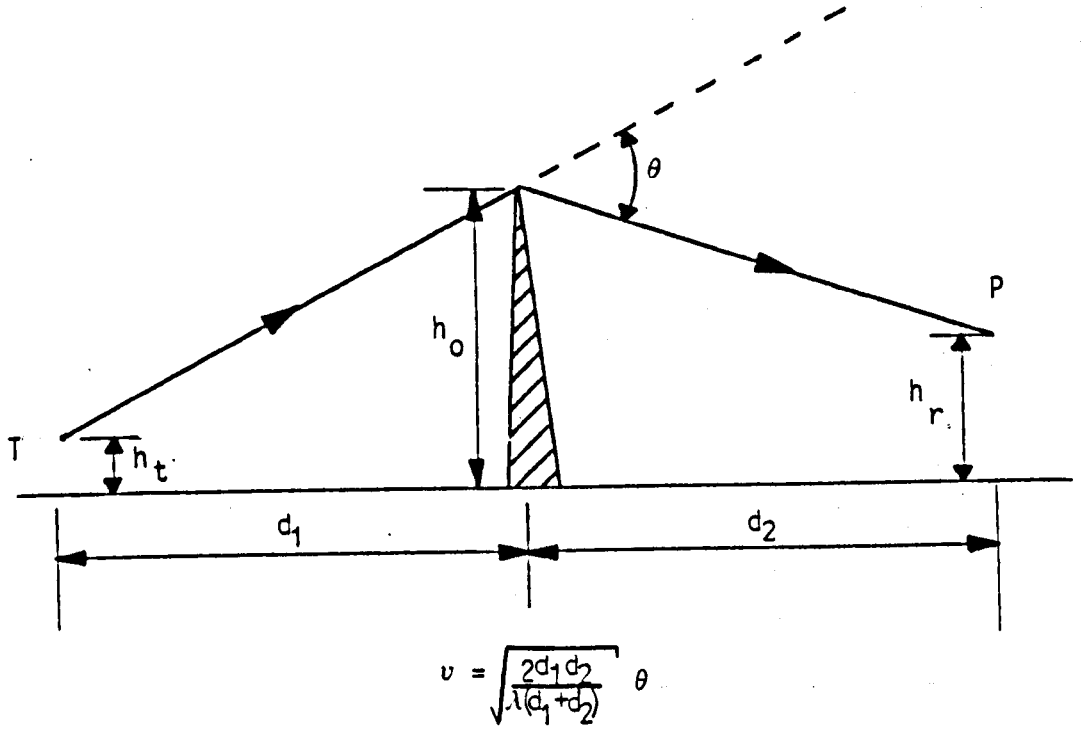

$$v = \sqrt{\frac{2d_1 d_2}{\lambda(d_1+d_2)}}\,\theta$$

KNIFE EDGE DIFFRACTION

FIG. 4.5

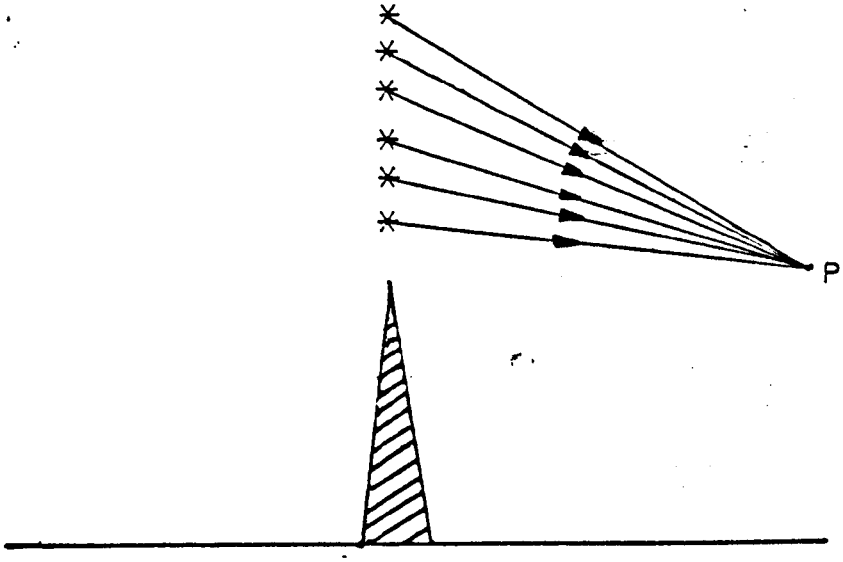

SUMMATION OF THE SECONDARY HUYGEN'S SOURCES

IN THE HALF-PLANE ABOVE A KNIFE-EDGE

FIG. 4.6

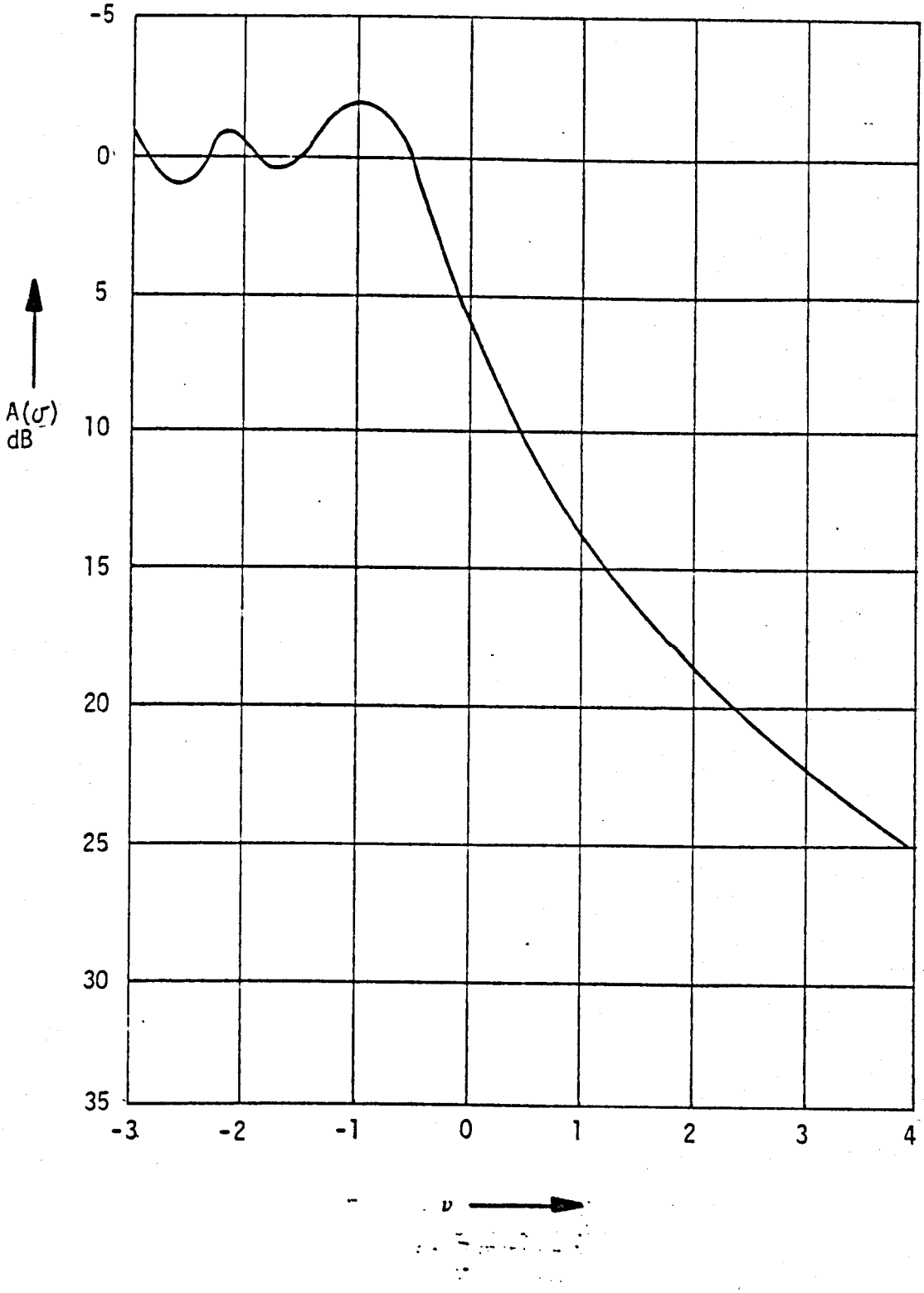

KNIFE EDGE DIFFRACTION LOSS

FIG.4.7

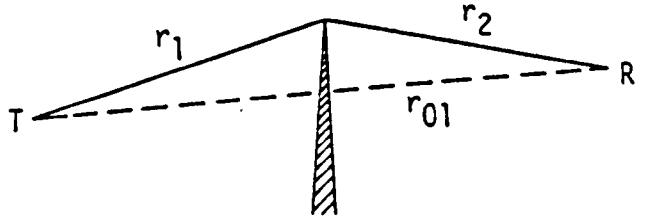

$$\Delta_1 = r_1 + r_2 - r_{01}$$

$$V_1 = 2\sqrt{\frac{\Delta_1}{\lambda}}$$

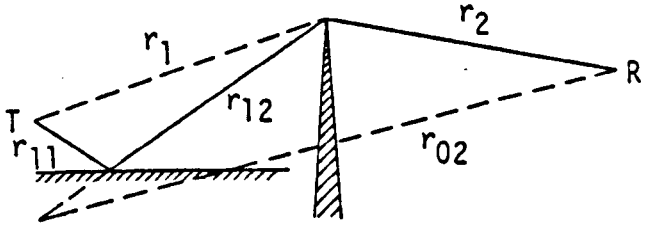

$$\Delta_2 = r_{11} + r_{12} + r_2 - r_{02}$$

$$\Delta_{2r} = r_{11} + r_{12} - r_1$$

$$V_2 = 2\sqrt{\frac{\Delta_2}{\lambda}}$$

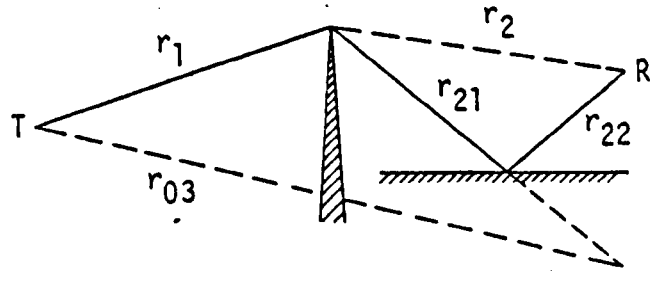

$$\Delta_3 = r_{22} + r_{21} + r_1 - r_{03}$$

$$V_3 = 2\sqrt{\frac{\Delta_3}{\lambda}}$$

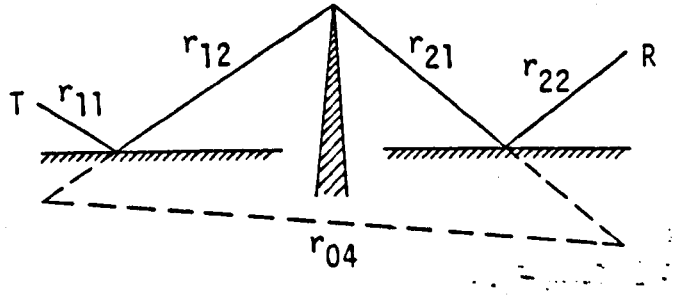

$$\Delta_4 = r_{11} + r_{12} + r_{21} + r_{22} - r_{04}$$

$$V_4 = 2\sqrt{\frac{\Delta_4}{\lambda}}$$

KNIFE EDGE DIFFRACTION WITH GROUND REFLECTIONS

FIG. 4.8

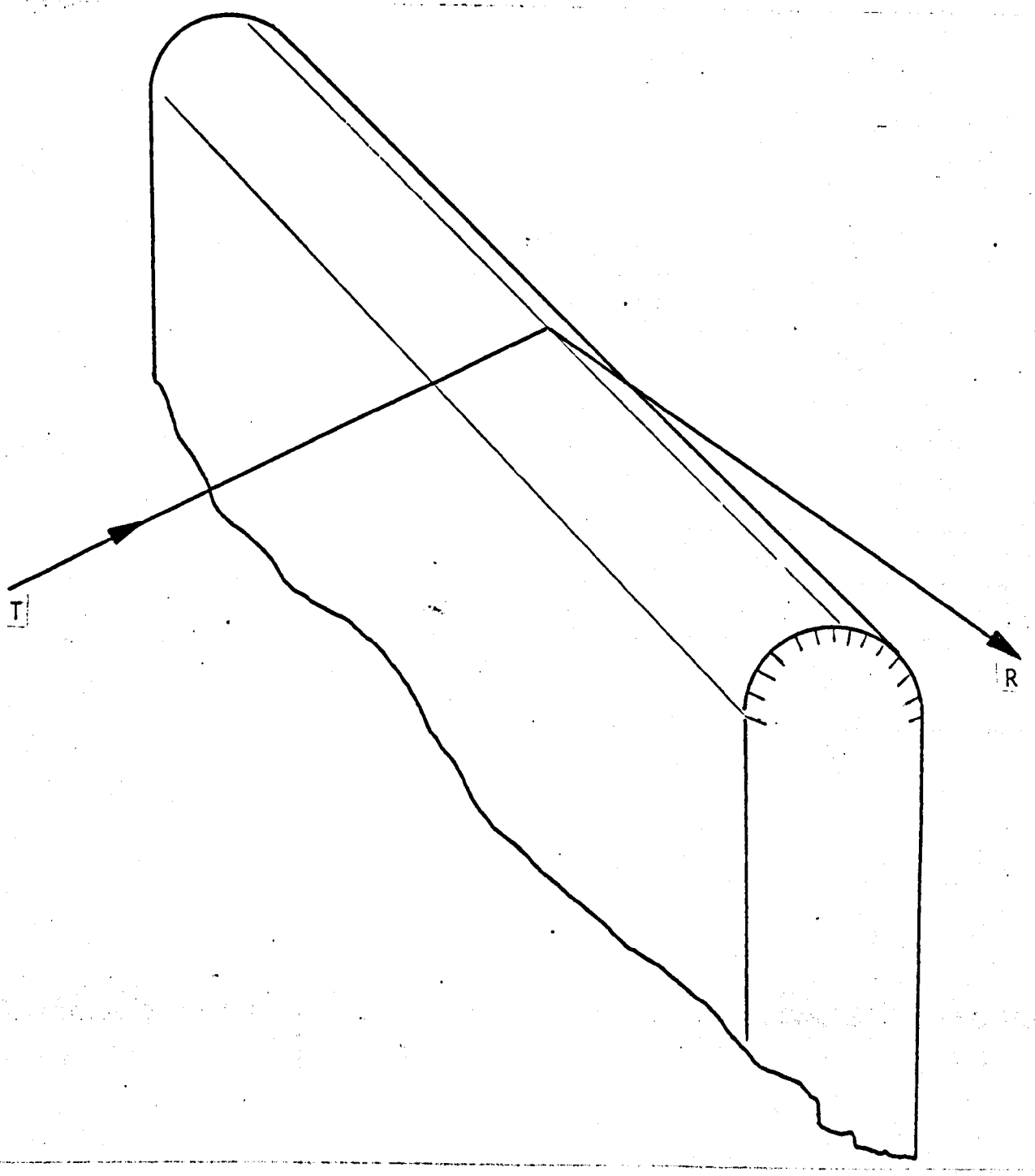

DIFFRACTION OVER A CYLINDER

FIG. 4.9

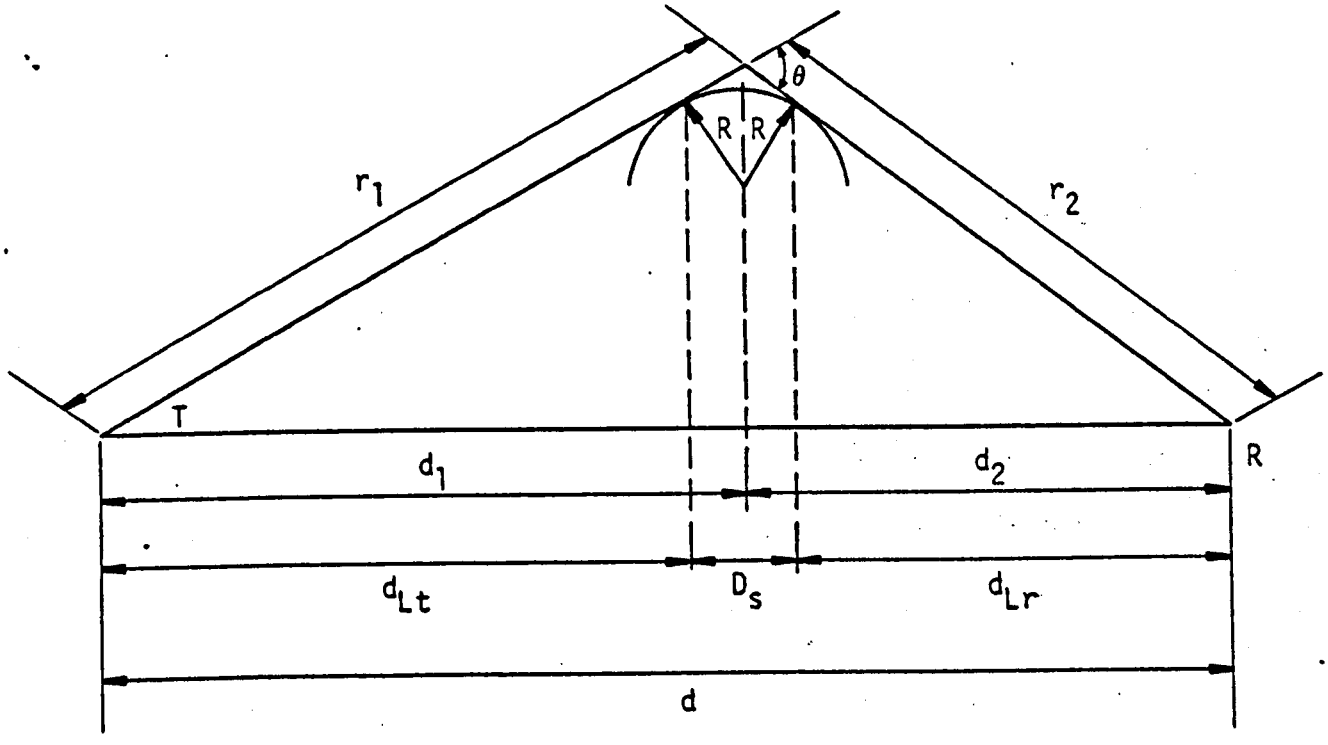

DIFFRACTION OVER A CYLINDER

FIG. 4.10

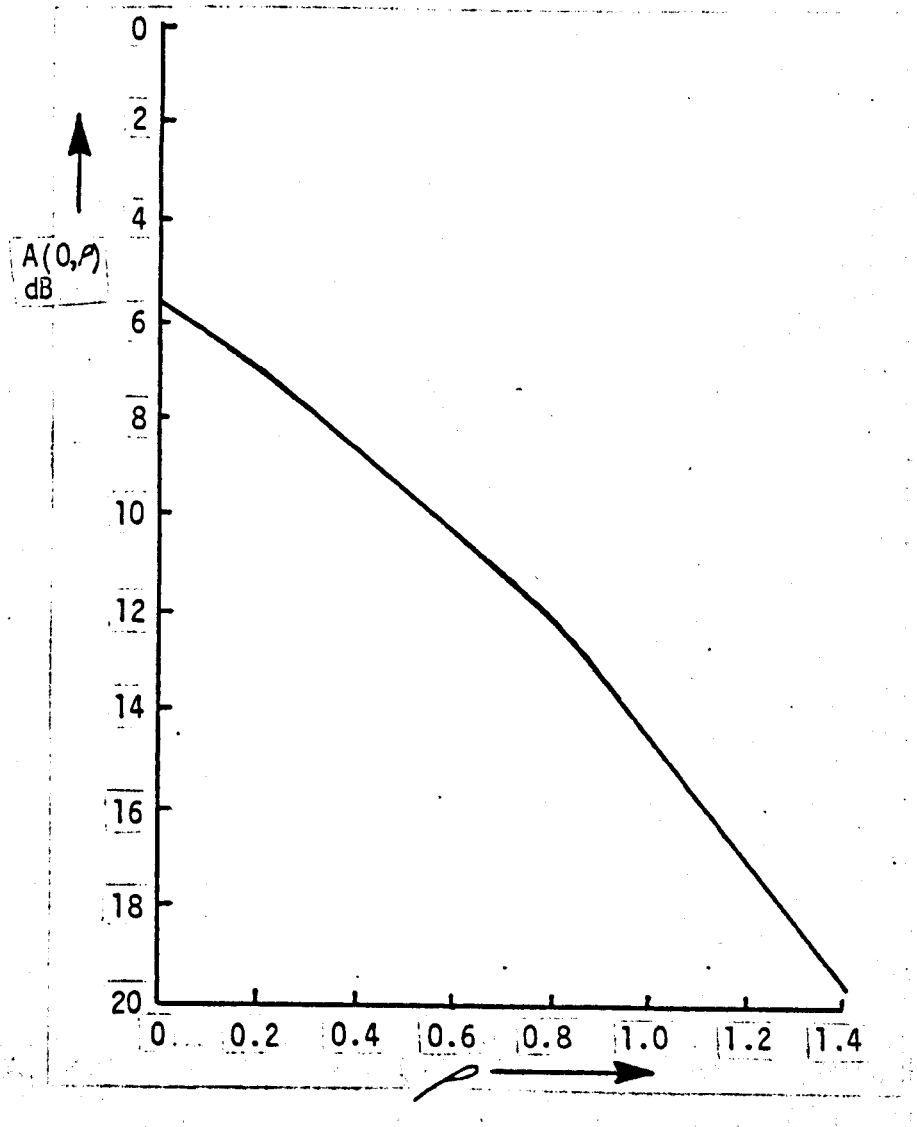

DIFFRACTION LOSS OVER A CYLINDER

FIG. 4.11

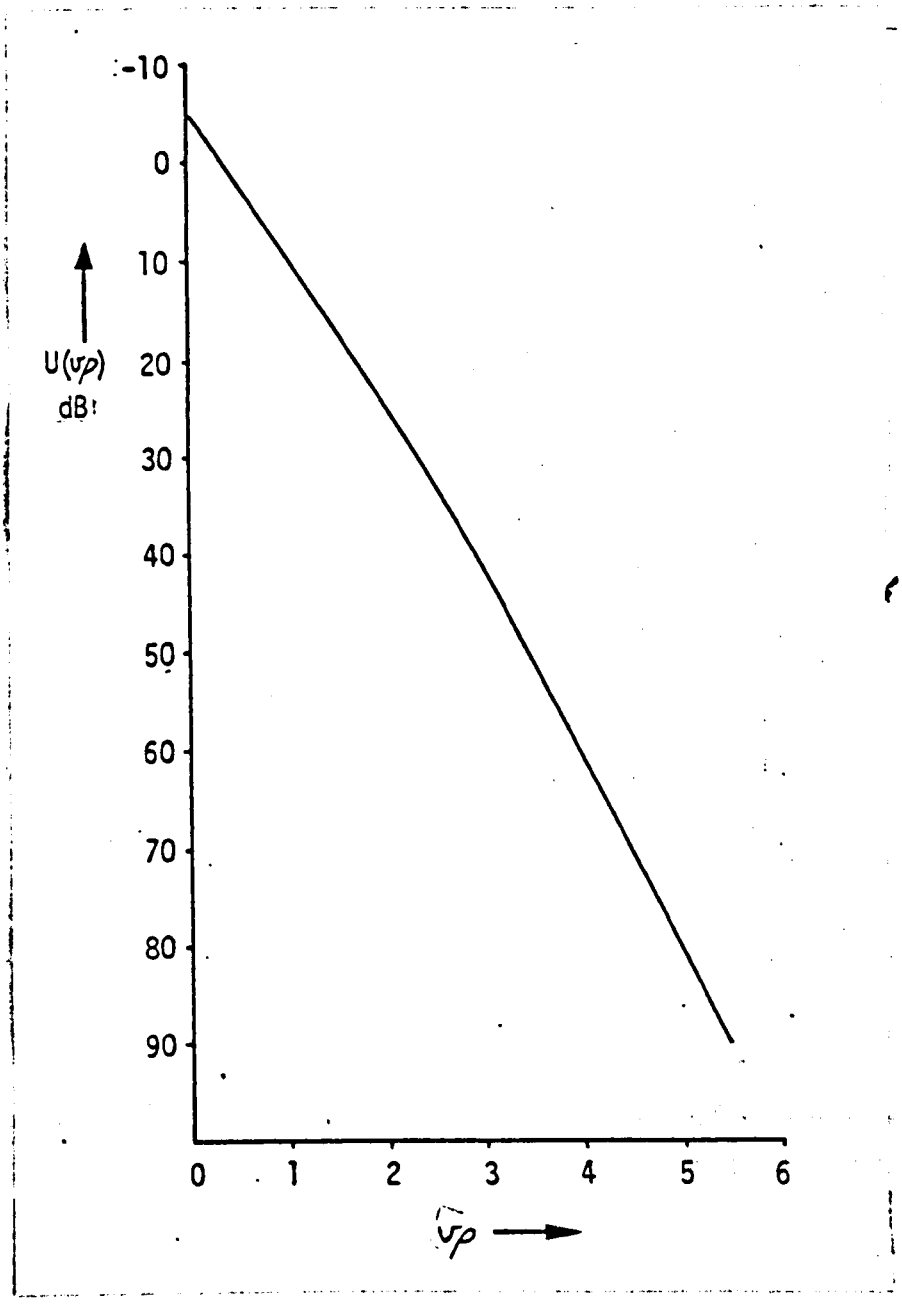

CORRECTION FACTOR U(υρ) FOR DIFFRACTION OVER A CYLINDER

FIG. 4.12

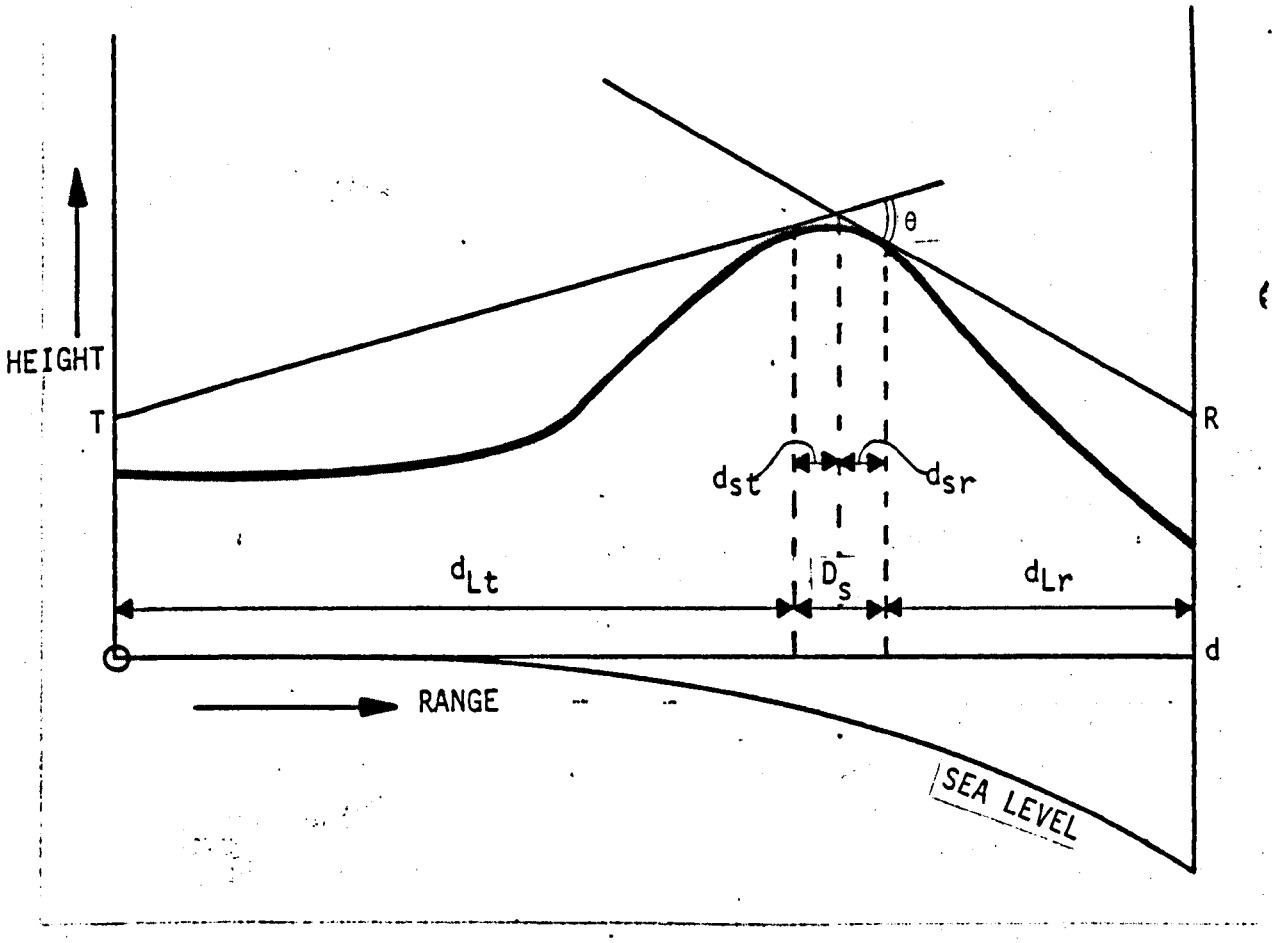

DIFFRACTION OVER A ROUNDED HILL CREST

FIG.4.13

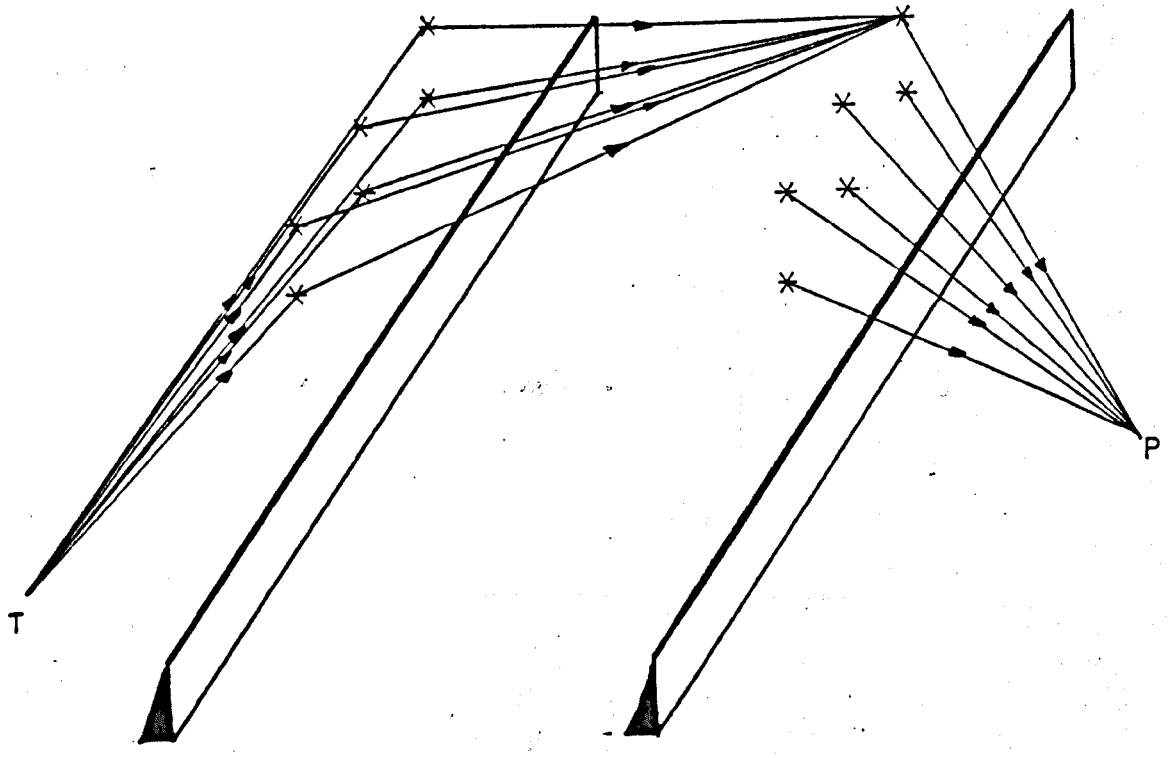

THE SUMMATIONS OF THE SECONDARY HUYGEN'S

SOURCES IN THE HALF-PLANES ABOVE TWO KNIFE-EDGES

FIG. 4.14

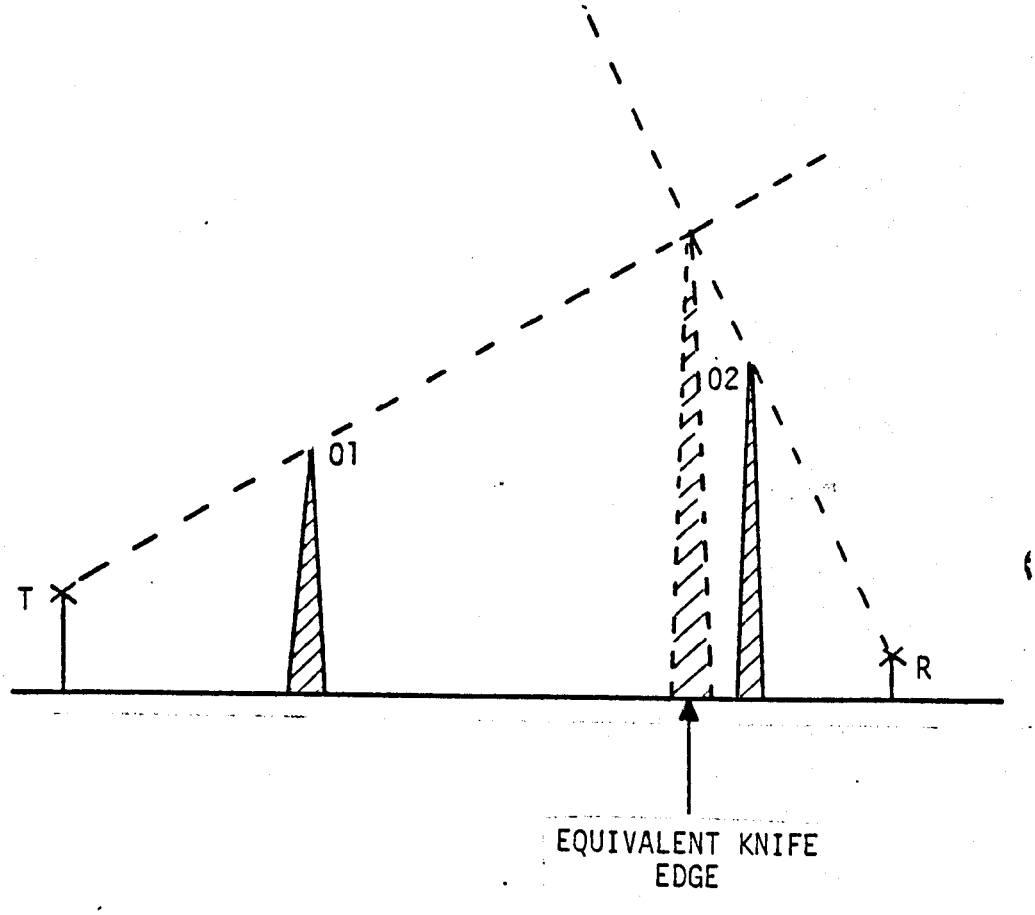

THE BULLINGTON EQUIVALENT KNIFE EDGE CONSTRUCTION

FIG. 4.15

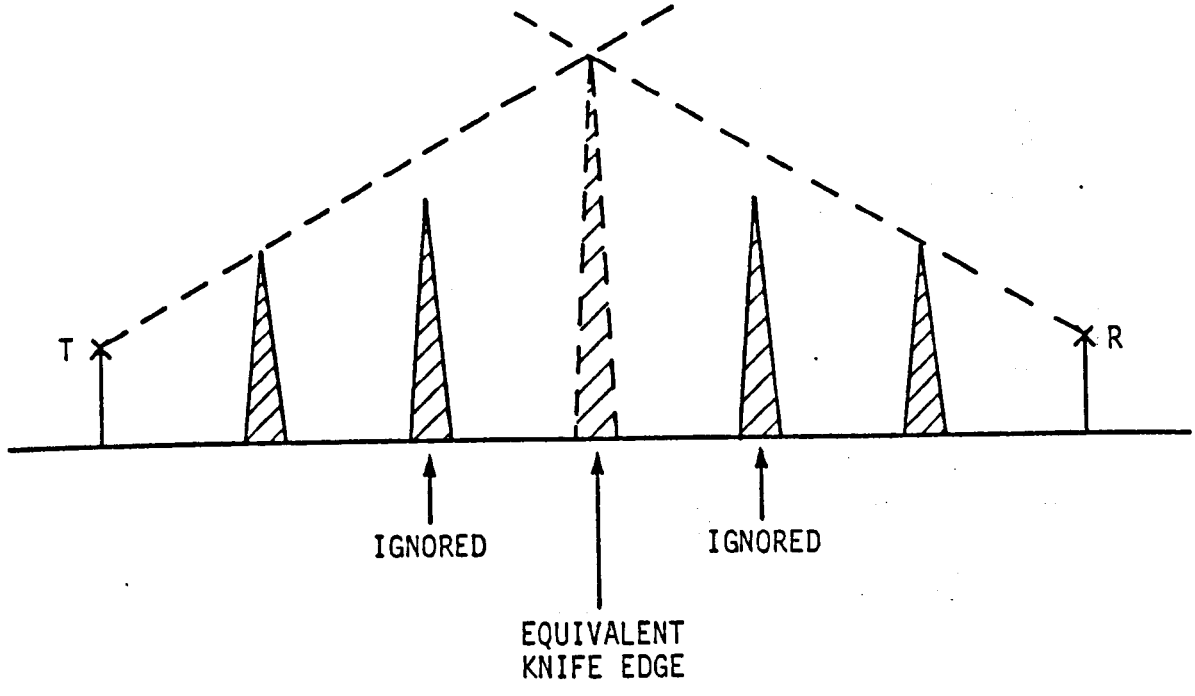

BULLINGTON EQUIVALENT KNIFE EDGE CONSTRUCTION
FOR FOUR OBSTACLES

FIG. 4.16

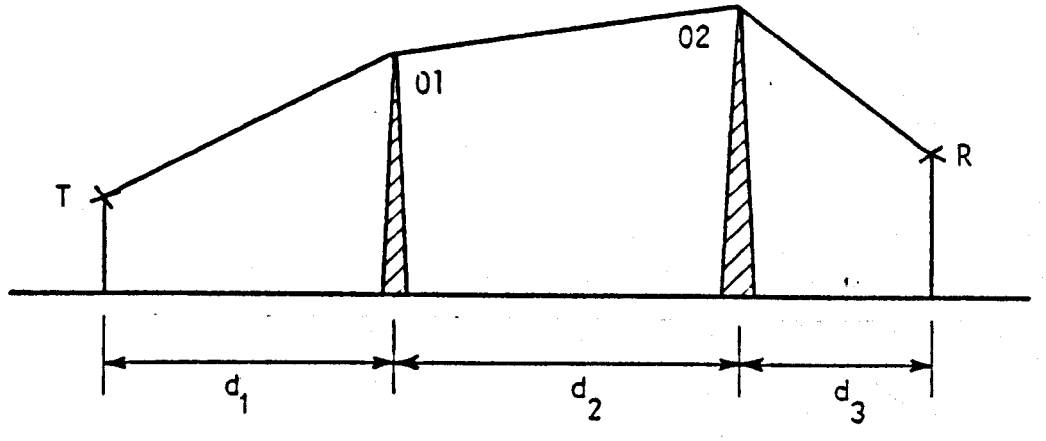

THE EPSTEIN-PETERSON DIFFRACTION CONSTRUCTION

FIG.4.17

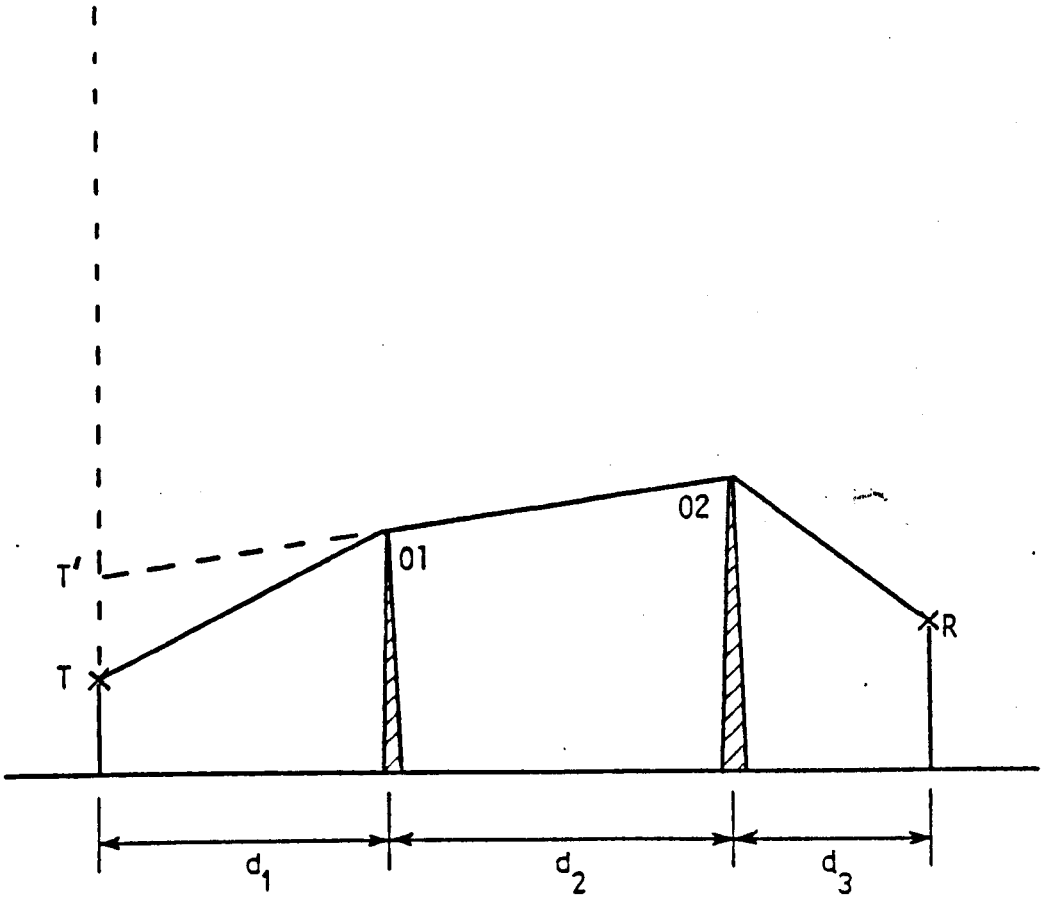

THE JAPANESE ATLAS DIFFRACTION CONSTRUCTION

FIG.4.18

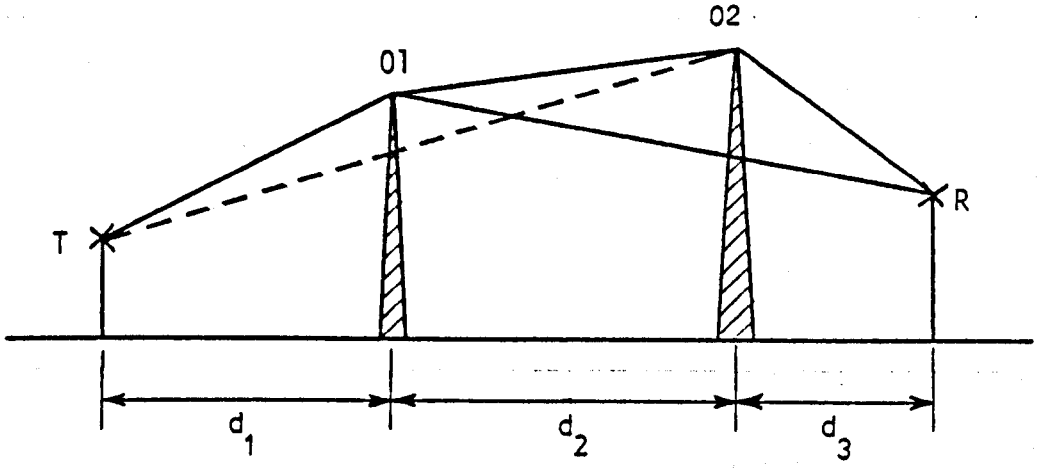

THE DEYGOUT DIFFRACTION CONSTRUCTION

FIG. 4.19

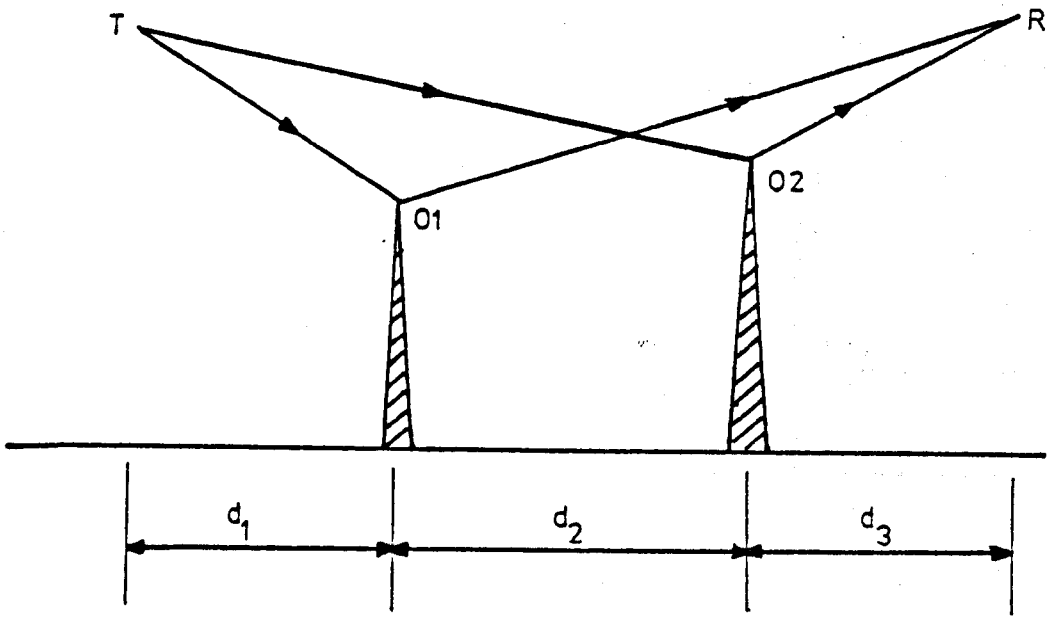

TWO KNIFE-EDGES BELOW LINE-OF-SIGHT

FIG. 4.20

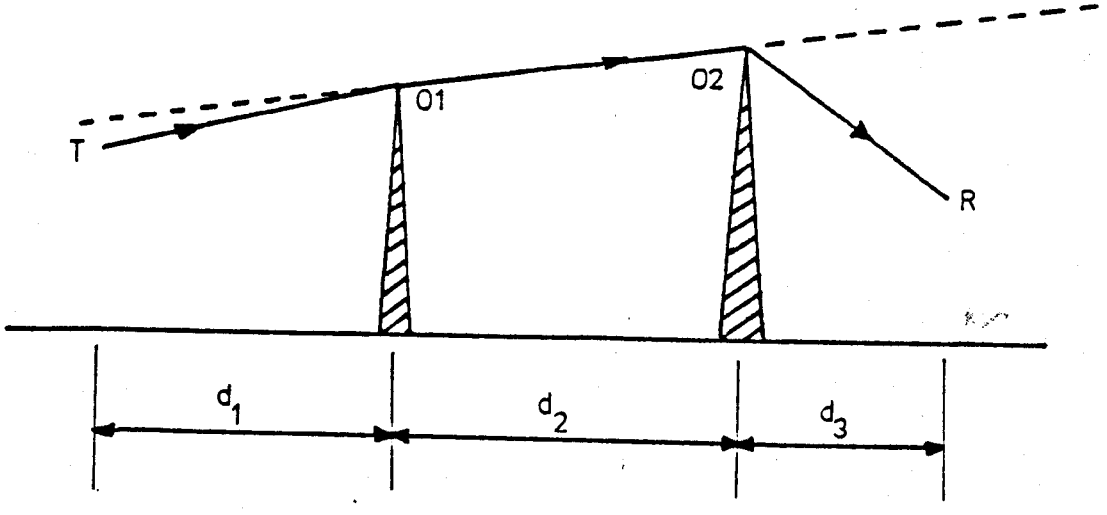

A DOUBLE KNIFE-EDGE PATH WITH ONE EDGE PREDOMINANT

FIG. 4.21

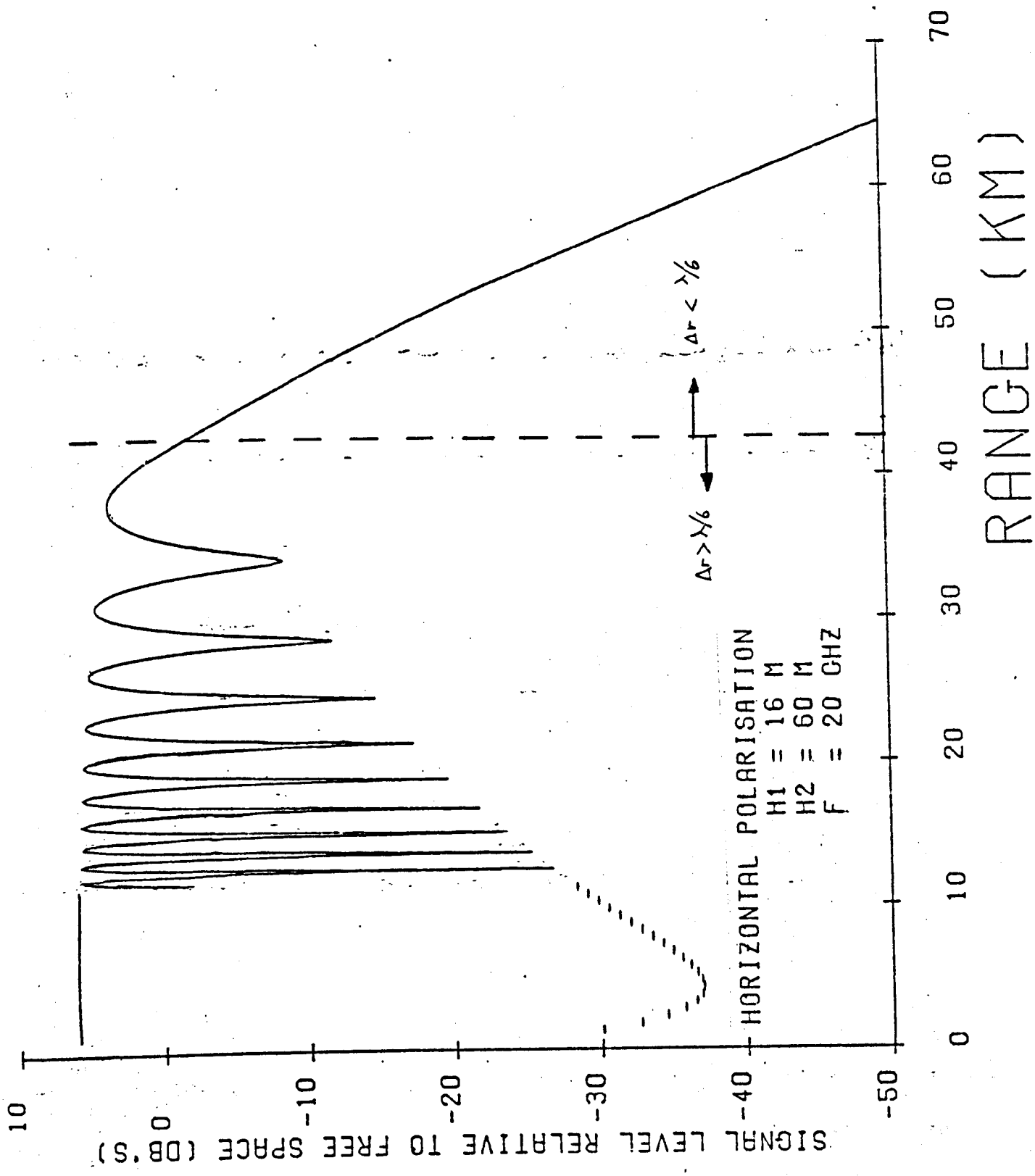

PROPAGATION OVER SMOOTH, HOMOGENEOUS, SPHERICAL EARTH

FIG. 4.22

CHAPTER 5

MEASUREMENT AND ANALYSIS OF THE RECEIVED SIGNAL ENVELOPE MAGNITUDE

A detailed investigation of the spatially distributed r.f. signal pattern created when the propagation path contains many obstructions necessitates the motion of either the transmitting or the receiving terminal. Furthermore, the complete characterisation of the properties of the signal envelope requires the precise knowledge of the mobile unit's position at every point on the received waveform.

Communication of the details relating to a remotely located, moving transmitter's instantaneous position can pose formidable problems, particularly when the distance to be travelled is large. If the instrumentation is to be usable anywhere within a city, it is preferable that the positional data be communicated to the receiver by means of a radio link, thereby obviating the need to trail cables behind the transporting vehicle. The behaviour of the radio link under investigation, however, normally has unknown properties and it would be unwise to utilise this channel as the data link unless it can be ensured that severe signal fading will not be in evidence at the receiver. For the data link to be reliably established over a large area, frequencies in the h.f. band (3 - 30 MHz) are occasionally used, higher frequencies being judged to produce intolerable fading patterns. The need for an h.f. aerial on, or in the immediate vicinity of, the vehicle can result in serious

E.M.C. problems being evidenced, notably in the deformation of the aerial polar diagrams.

The movement of the receiver, on the other hand, does not require a secondary communications channel, the positional information being directly accessible at the receiver. However, much more equipment must be transported in a receiving vehicle than in a transmitting vehicle.

The problems posed by conveying positional data from a mobile transmitter to a stationary receiver makes the moving receiver method highly preferable.

5.1 THE TRANSMITTING STATIONS

A qualitative determination of the properties of radio signals requires a radiator and a receptor of the r.f. energy.

Precise quantification of the propagation path loss between the two terminals further demands the exact knowledge of the power radiated and the use of a calibrated detector. A requirement is established, therefore, for a controlled, continuously monitored power source.

The investigations were largely conducted at frequencies in the civil land mobile radiotelephone bands at 85.875 MHz (Low-Band VHF), 167.2 MHz (High-Band VHF) and 441.025 MHz (UHF). Certain of the investigations were also performed at 75.375 MHz, notably during the period while the three main frequency allocations were being obtained and the transmitting equipment was being commissioned. In all cases the transmissions were radiated by

aerials atop prominent buildings in selected British cities and received at a mobile unit driving along the streets of the relevant city.

5.1.1 THE TRANSMITTING EQUIPMENT

The city being investigated was irradiated using the transmitting equipment outlined in Table 5.1. All transmissions were of unmodulated, frequency stable carriers. The lack of modulation over prolonged periods was, itself, found to be sufficient identification of the signal at the receiver.

Observation of the power output of the transmitters over many hours of continuous operation revealed that negligible fluctuations occurred.

FREQUENCY MHz	APPROX POWER AT AE. TERMINALS (W)	AERIAL TYPE	APPROX AERIAL GAIN (dB REL ½ WAVE DIPOLE)
75.375	10	CENTRE FED ½ WAVE DIPOLE	0
85.875	30	END-FED λ/4 MONOPOLES ABOVE GROUND PLANES	0
167.2	30		0
441.025	3.8	4 CO-LINEAR FOLDED DIPOLES SPACED 90° IN AZIMUTH	5.6.

TABLE 5.1

DETAILS OF THE TRANSMITTING EQUIPMENT

5.1.2 THE TRANSMITTING AERIAL SITES

The transmitting equipment outlined in Table 5.1 was transported between sites in the cities of Birmingham, Bath and Bradford. An indication of these sitings is given in Table 5.2.

CITY	MAP REFERENCE	APPROX HEIGHT ABOVE LOCAL TERRAIN (m)	OUTLOOK
BIRMINGHAM	SP 4050 2839	36	FLAT CITY
BATH	ST 3773 1646	18	ON THE SHOULDER OF A VALLEY. APPROX 10° DOWNHILL TO CITY CENTRE
BRADFORD	SE 4157 4329	50	TALLEST BUILDING IN THE VALLEY. COMPLETELY SURROUNDED BY HILLS

TABLE 5.2

THE TRANSMITTING SITES

5.1.2.1 The Birmingham Aerial Site

The transmitting aerials were mounted on the roof of the Department of Electronic and Electrical Engineering's building at the University of Birmingham. The installations for the 85.875, 167.2 and 441 MHz aerials, shown in Figures 5.1 and 5.2, provided an unobstructed view of the city centre (Fig 5.3) and many surrounding suburban areas. The 75.375 MHz half-wave dipole, however, was mounted at a different location on the roof of the building from that employed for the other three frequencies. While a clear siting was again achieved, care must be exercised in comparing the results at 75 MHz with those at the alternate frequencies.

5.1.2.2 The Bath Aerial Site

The investigation in the city of Bath was conducted with the aerials atop the Department of Electronic Engineering's building at the University of Bath. This building, while having a fairly low profile, is on the top of a large hill and affords a view of the city centre and its surrounding districts unobstructed by terrain obstacles. The positioning of the base station aerial on a prominent hill is a technique frequently employed in civil land mobile radiotelephony to achieve large coverage areas and is considered to be a useful case for the purposes of the research. The steep downhill slope into the city centre of approximately 10° is not anticipated to have caused significant modification of the aerial gains.

5.1.2.3 The Bradford Aerial Site

In the city of Bradford, the transmitting aerials were installed atop the main building at the University of Bradford. This is the tallest building in the valley and provides an excellent view of the city centre. The site is completely surrounded by hills at small ranges (approx 5 km) and afforded an opportunity to examine the effects of terrain obstacles on the propagation path loss.

5.2 THE RECEIVING STATION

Determination of the statistical parameters of the spatially distributed field requires that the received signal envelope is measured over a large distance of travel, typically many tens of wavelengths.

The necessary mobility was provided by mounting the receiving equipment in a vehicle and deriving the power supply from a towed, petrol fuelled mains generator. The resulting system constituted a semi-permanent mobile test station, usable in any town or city without major alteration.

5.2.1 THE FIELD STRENGTH MEASURING SYSTEM

Quarter wavelength whip aerials, cut for resonance at the frequencies of interest, were mounted in the centre of the vehicle's roof and employed as the signal receptors. The whip elements for each frequency were interchangable and all utilised the same physical mounting structure, the vehicle's roof acting as a ground plane. This aerial, being the only protrusion on the vehicle's roof, produced an omnidirectional radiation pattern in the azimuthal plane[5.1].

The received signal was fed along screened coaxial cable to a field strength measuring set having a large dynamic range (80 dB), a small IF bandwidth (25 kHz) and internal calibration facilities. This receiver was tunable between 25 and 600 MHz.

The envelope detected output of the receiver was recorded, with suitable buffering[5.2], on an analogue FM instrumentation tape recorder for analysis at a later time. The transfer characteristic of the receiving system measured between the r.f. input terminals of the receiver and the input terminals of the tape recorder is shown in Fig 5.4. In the absence of suitable low-noise standards the characteristic has been extrapolated from

5.2.1 (cont'd) 1 μV down to 0.3 μV r.f. input level, thereby extending the operating range of the system.

The receiving system was continuously monitored during its operation by listening to the audio output of the receiver and by observing the input to the tape recorder using an oscillo scope. By these means such faults as interfering transmissions and receiver drift were noticed immediately.

The field strength measuring system is shown in the upper half of Fig 5.5.

5.2.2 DERIVATION OF POSITIONAL INFORMATION

A complete description of the spatially distributed field envelope pattern requires that its physical location at every instant is known. This positional information was obtained using pulses derived at regular intervals of the vehicle's travel and by subsequently counting the total number of pulses produced since a known reference point along the route, e.g. a street intersection. These distance markers were generated by photoelectrically sensing the rotation of a wheel towed behind the measuring vehicle. The electronic system[5.2] created short duration pulses at intervals equivalent to approximately 2.8 cm of the vehicle's travel for the 85.875, 167.2 and 441.025 MHz data and, using a slightly different configuration, 25 cm for the 75.375 MHz measurements. The markers were recorded on the tape recorder co-instantaneously with the field strength information as shown in the lower half of Fig 5.5.

5.2.3 THE MEASUREMENT PROCEDURE

The desired distance marker separation was achieved by inflating the pneumatic tyre of the towed wheel to a pressure of approximately 16 psi and by providing a spring loading on the wheel of approximately 20 lb. This latter adjustment ensured that the wheel would remain in contact with the road surface at a speed of 9 m/sec (20 mph) even on quite rough roads.[5.3] The time invariance of these parameters was such that the checks only needed to be made at the start of each day's recording.

The appropriate quarter wavelength whip aerial for the frequency of the investigation was installed on the mount in the centre of the vehicle's roof, ensuring that any other aerials were removed. The field strength measuring receiver was set for AM detection and 25 kHz IF bandwidth, tuned for a maximum deflection on the field strength meter at the transmission frequency being used and the rf input attenuator adjusted such that the internal meter indicated approximately mid-range. The input attenuator setting was found to affect the loading on the receiver's input stages and was accordingly held constant at its operational value while the receiver was calibrated using the internal oscillators.

The tape recorder was started and the vehicle driven along the measurement route at approximately 9 m/sec (20 miles/hr). Continuous recordings of the signal envelope magnitude, the distance marker pulses and a voice commentary of geographical details for future use were made.

5.2.3 (cont'd) The calibrations were checked at the end of each series of measurements to ensure that no equipment malfunctions or receiver drift had occurred.

5.2.4 THE AREAS UNDER INVESTIGATION

Propagation path loss values have been measured in three British cities over differing, but frequently encountered, geographical situations. The most comprehensive set of measurements was obtained over the ostensibly flat terrain of Birmingham, permitting the influence of the buildings on transmission to be determined largely in isolation from terrain effects. The remaining two measurement sets were obtained over the sloping ground of Bath and the hilly terrain of Bradford.

5.2.4.1 The Birmingham Measurements

Terrain profiles drawn along radials from the Birmingham transmitter site to locations in the outlying districts of the city are shown in Figures 5.6, 5.7, 5.8 and 5.9. The magnitudes of the ground undulations can be seen to be typically less than approximately 20m, sufficiently small to suggest that the influences of the terrain on the propagation may be ostensibly neglected. The urban case to be considered in Birmingham, therefore, is one of a city constructed on sensibly flat ground with suburbs comprising two or three storey buildings extending for a range of approximately 10km around a heavily built-up centre.

The propagation situation to be investigated is one where the trans-

5.2.4.1 (cont'd) mitter is mounted atop a large building and radiates to outlying districts in the manner shown, in idealised form, in Fig.5.10. In these circumstances the presence of the urban obstacles (eg buildings) may be considered to be responsible for the departure of the measured values from simple theoretical predictions. The measurements were accordingly tailored to enable the influences of physical urban parameters to be isolated.

The vehicle containing the field strength measuring system was driven along routes selected to provide a representative sample of street widths and street orientations on all compass bearings around the transmitter at ranges from 1 to 10 km. The lower of these range limits was imposed by the unavailability of suitable roads at smaller ranges, and the upper limit by the maximum tolerable path loss which, as indicated in Chapter 4, is a function of the transmission frequency.

Where possible the measurements were taken as a continuous series. This action greatly reduced the time "wasted" in moving from one location to another and correspondingly increased the amount of data collected. Routes were thus devised by which the vehicle might traverse all the preselected individual streets within an area in sequence. This process often resulted in the vehicle being compelled to travel along meandering paths. The quantity of data eventually collected in this manner was equivalent to approximately 50 km of the vehicle's travel at each of the frequencies used.

5.2.4.2 The Bath Measurements

The city of Bath is situated in a river valley and is composed of taller buildings than are generally found in suburban Birmingham along narrower streets. These buildings, while being taller than in the suburbs of Birmingham, are much smaller than in central Birmingham. The suburbs of Bath, however, are largely similar to those of Birmingham except that their extent is substantially less.

A terrain profile drawn from the transmitter, through the city centre and out to one of the suburbs investigated is presented in Fig. 5.11. The topography, in so much as the central region is concerned, may be regarded as downward sloping but otherwise flat (Fig. 5.12)

5.2.4.3 The Bradford Measurements

The city centre of Bradford is situated in a river valley and is very similar in building type and density to central Birmingham. Transmission to the outlying suburbs and villages, however, is obstructed by gross geographical features. An estimate of the effect of terrain obstacles on propagation can therefore be gained from measurements made in the outskirts. Terrain profiles to the measured regions are shown in Fig. 5.13.

5.3 DIGITISATION OF THE MEASURED SIGNAL ENVELOPE

The quantity of measurements needed to average the effects of any uncontrolled parameters and consequently derive a valid statistical estimate of the influence of known factors is large. The storage and

5.3 (cont'd) manipulation of this bulk data calls for the use of digital computers, both for the mass storage media available and for the high processing speeds attainable on such machines. These benefits are most readily attained on large computer installations such as the University of Birmingham's central ICL 1906A.

A problem is encountered, however, in the conversion of the analogue record into binary form prior to the mathematical manipulations by digital computer. Here the computer in command of the digitisations must be exclusively occupied in monitoring the conversion process if none of the digitisations are to be overlooked, a facility not generally available on large machines because of the large running costs incurred by the inefficient operation. A system was accordingly developed which enabled analogue-to-digital conversions to be performed on a PDP-11 minicomputer and transferred to a 1906A installation by the various means described.

5.3.1 ANALOGUE-TO-DIGITAL CONVERSION OF THE RECEIVED SIGNAL ENVELOPE RECORD

The analogue record of received signal strength stored on magnetic tape as part of the measurement process was digitised on a PDP-11 minicomputer using the system described in detail in Appendix A. Each analogue-to-digital conversion was performed when commanded by the existence of a distance marker pulse. The points on the resulting digitised signal envelope were thus effectively spaced by approximately 2.8cm of the receiver's travel, giving equivalent average detectable fade depths of 34, 28 and 20 dB at 85, 167 and 441 MHz respectively.

The 25cm distance marker spacing used

5.3.1 (cont'd) at 75 MHz provided an equivalent average detectable fade depth of 18 dB.

The interconnection of the equipment for the conversion process is shown in Figure 5.14. The x10 temperature compensated amplifiers were incorporated to ensure that the full ±10V dynamic range of the converter was utilised when working from the ±1V output of the tape recorder. A simple passive R-C low-pass filter was included to reduce the effects of impulsive noise. This filter's cut-off frequency (30 Hz) was selected to be slightly greater than the maximum baseband spectral component of the waveform. Reference to Figure 2.10 reveals this to be twice the maximum doppler frequency which, for a 440 MHz receiver travelling at 9 m/sec, is approximately 25 Hz. The analogue signal envelope record was monitored continuously at conversion time using a storage oscilloscope operating with a slow scan rate. By this means the presence of interferers could be instantly recognised and appropriate allowances made in the subsequent analyses.

The distance marker pulses also recorded on the magnetic tape were amplified on playback to attain TTL logic circuitry compatibility and checked using the pulse verification network shown in Figure 5.15. This network examines both the amplitude and duration of an incoming pulse and produces an output pulse only if these were within permissible limits. Any spurious pulses originating from such vagaries as power supply fluctuation or magnetic tape vibration across the ferrite heads were therefore eliminated.

5.3.1 (cont'd) The signal envelope record was digitised in sections over which the parameters of street width and orientation remained sensibly constant. Close scrutinisation of a town plan reveals this interval to have a maximum value of approximately 250m . The route was accordingly plotted on a street map and subdivided at easily locatable positions, eg street intersections, which were specified on the voice commentary of the tape record.

5.3.2 DATA TRANSFER TO THE ICL 1906A COMPUTER

The data samples created by the analogue-to-digital conversion process were written in unformatted binary mode onto the magnetic disc store. This enabled the converter system to operate at maximum speed by using the most compact data format available. Before analysis may proceed, however, it needed to be transferred to the central ICL 1906A computer from the PDP-11 minicomputer. The two methods of transfer employed, namely magnetic tape and direct data link, are described.

5.3.2.1 Data Transfer by Magnetic Tape

During the period while a data link to the 1906A was being commissioned, a system involving 7-track magnetic computer tape was developed as an interim measure. This system is operable with all forms of frequently encountered PDP-11 files and is described in detail in Appendix B.

5.3.2.2 Data Transfer by Data Link

The operation of the data link connecting the PDP-11 and 1906A computers is described in detail in Appendix C. The PDP-11 is interfaced to the link to appear as a remote card reader on the 1906A

5.3.2.2 (cont'd) and, as such, must transmit card image records in formatted ASCII (GRAPHIC) mode. The data is written to the PDP-11 magnetic disc store in unformatted binary mode for maximum efficiency of the analogue-to-digital conversion process and maximum packing density on the disc store. Consequently the data must be reformatted before being sent along the link.

5.4 ANALYSIS OF THE SIGNAL ENVELOPE

The received signal envelope records were analysed on the University of Birmingham's central ICL 1906A digital computer using FORTRAN IV programmes. These analysis programmes, documented in Appendix D, calculate the mean and median signal levels of the 250m small sector segments, the signal envelope probability distributions, produce visual signal presentations on the incremental graph plotter, auto-correlation analyses,etc.

5.5 REFERENCES

5.1 Ratliff P.A.
"VHF Mobile Radio Communications - A study of Multipath Fading and Diversity Reception"
Ph.D Degree Thesis,
University of Birmingham, Dept of Elec and Elec Eng, Sept 1973.

5.2 Henze M.
"A Diversity System for UHF Mobile Radio Reception"
Ph.D Degree Thesis,
University of Birmingham, Dept of Elec and Elec Eng, June 1975.

5.3 Lister R.D.

"A Fifth Wheel for Measuring Speed and Braking Distance"

Road Research Labs.

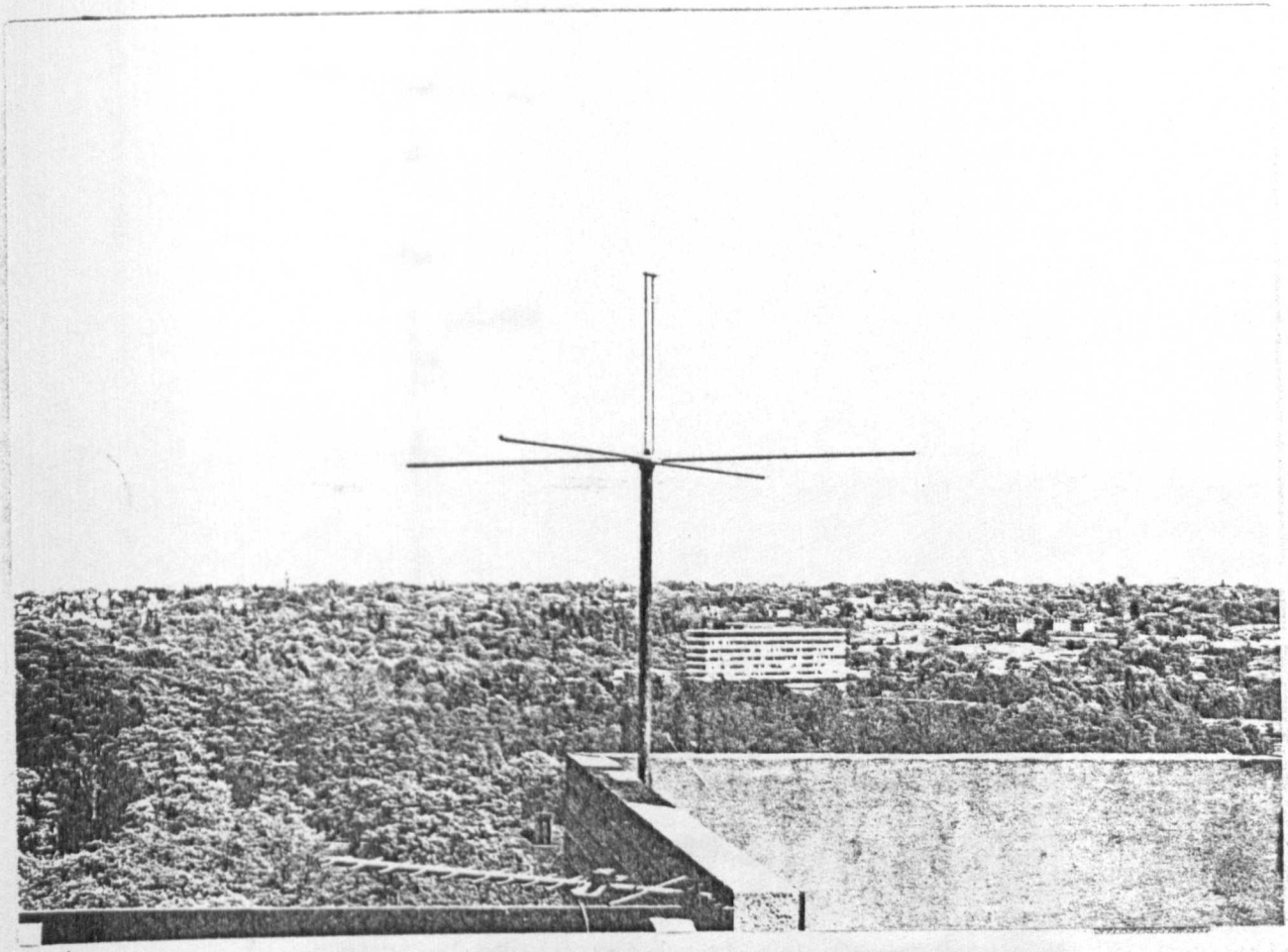

THE 85MHz BIRMINGHAM BASE STATION AERIAL

FIG. 5.1

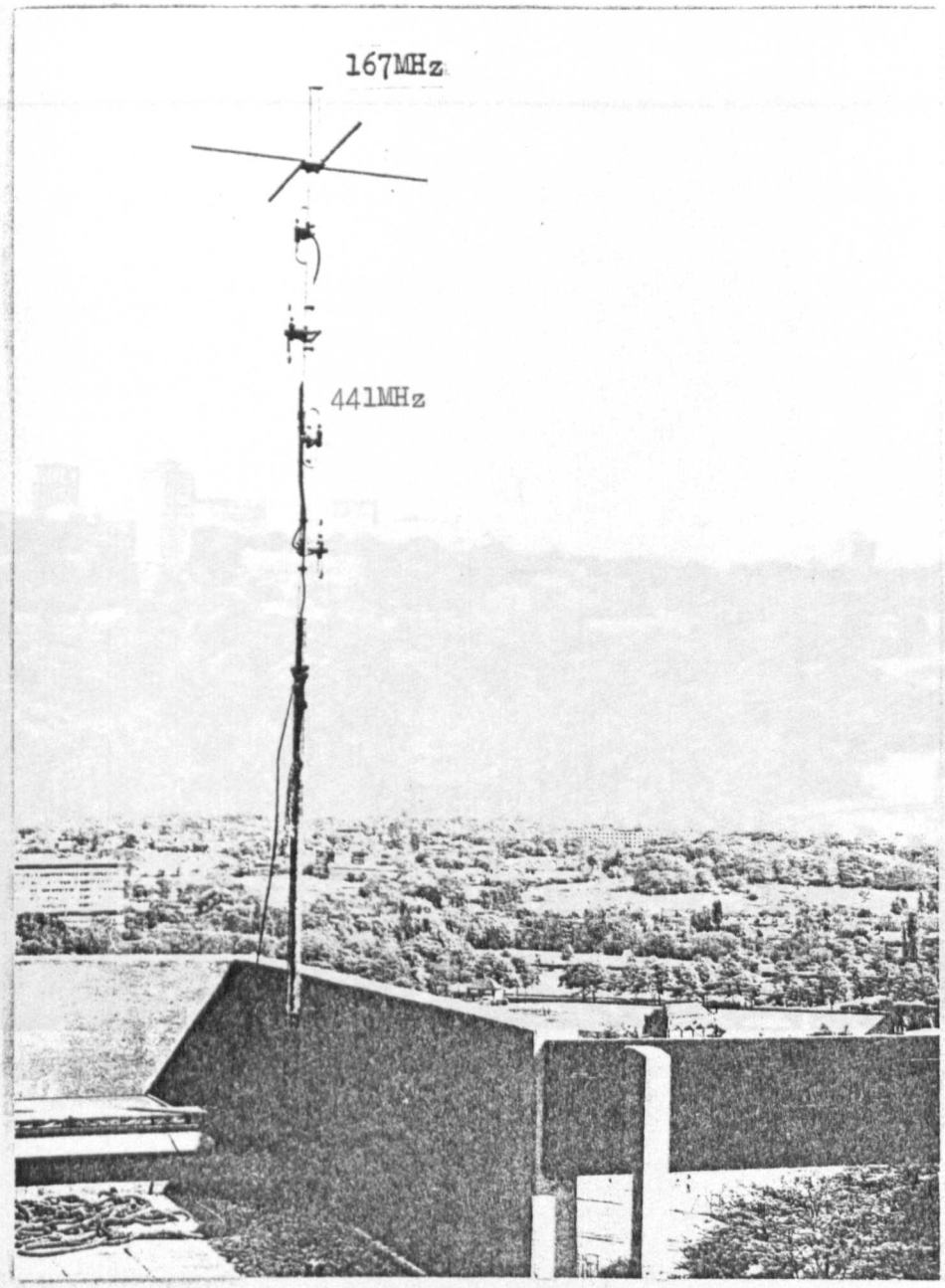

THE 167MHz (UPPER) AND 441MHz (LOWER) BIRMINGHAM BASE STATION AERIALS

FIG. 5.2

VIEW INTO BIRMINGHAM CITY CENTRE FROM THE BASE STATION SITE

FIG. 5.3

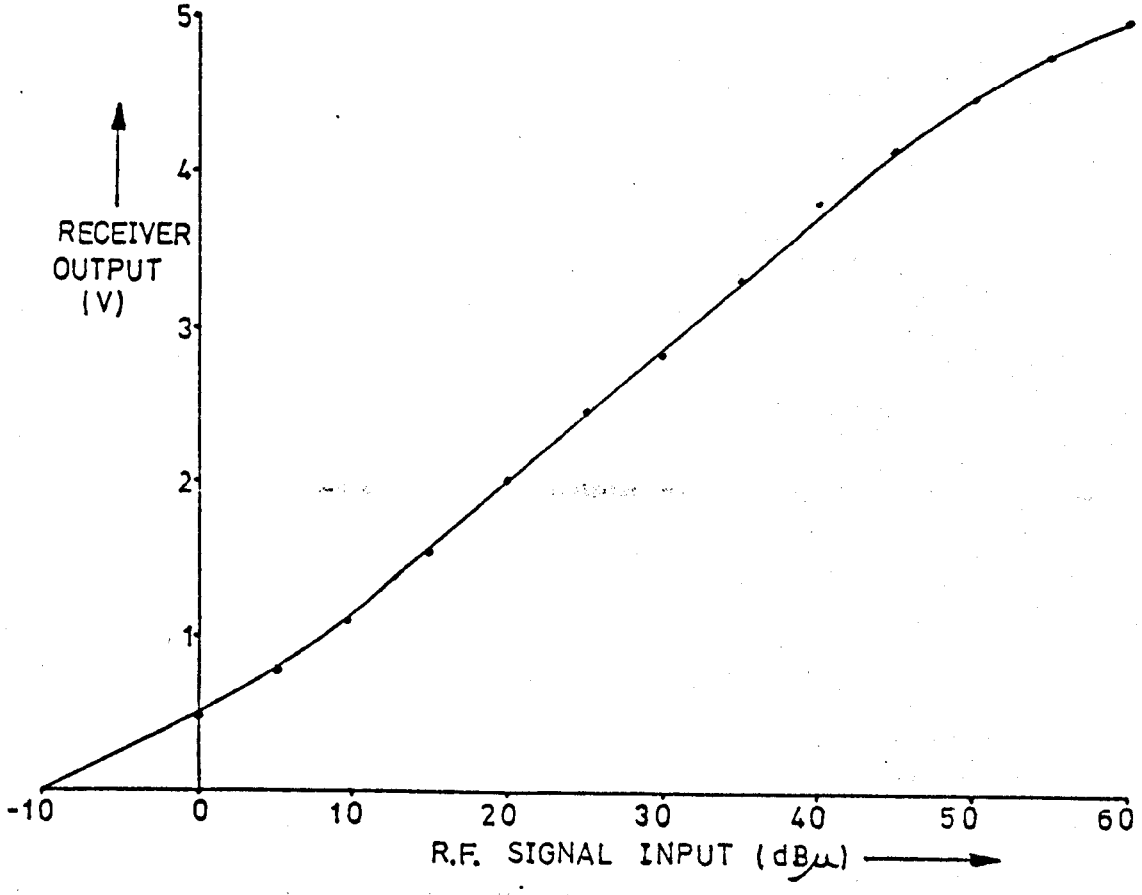

TRANSFER FUNCTION OF THE RECEIVING SYSTEM

FIG. 5.4

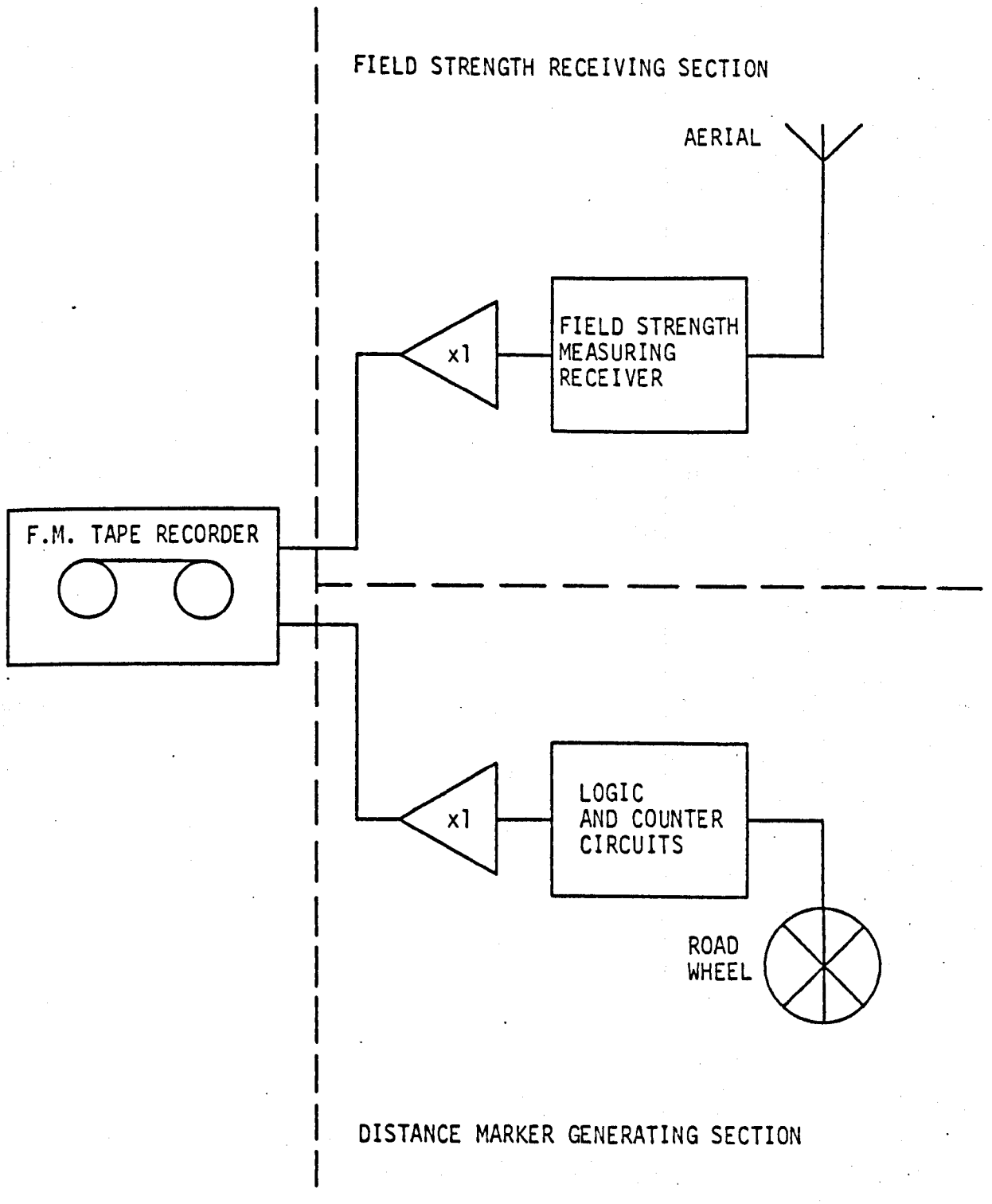

THE RECEIVING SYSTEM

FIG. 5.5

BIRMINGHAM PROFILE

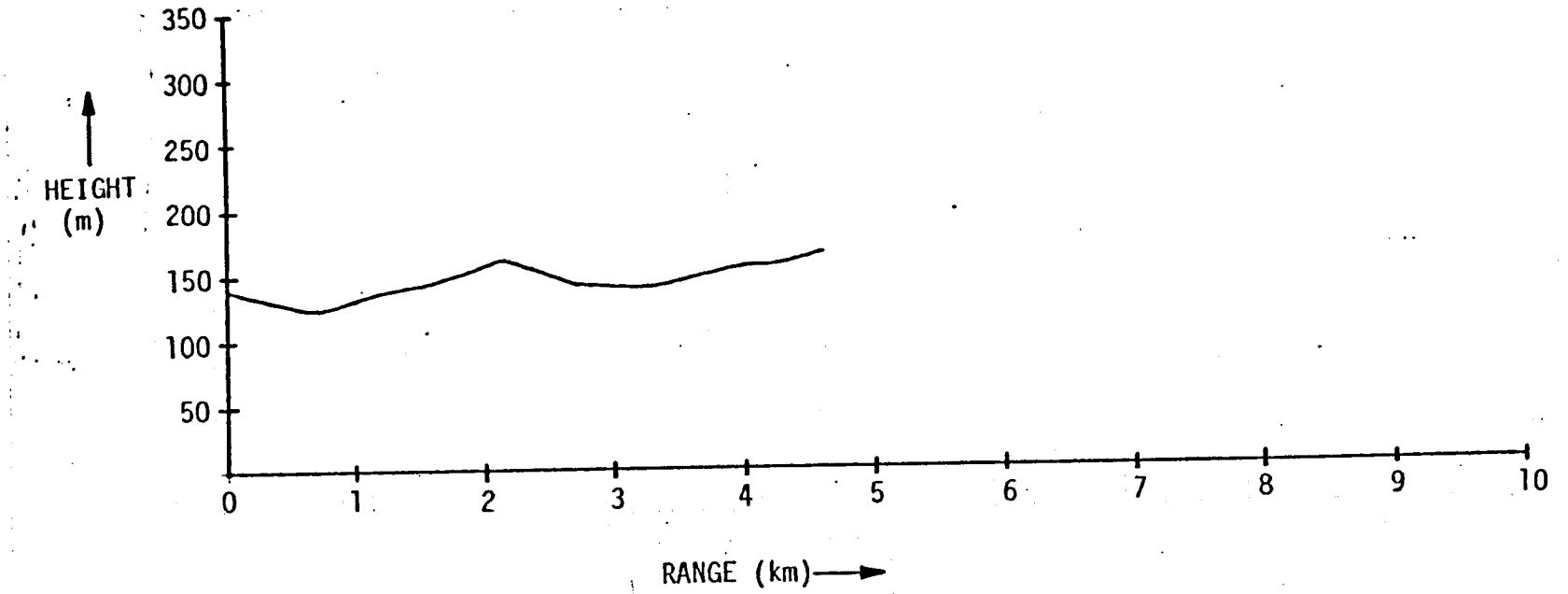

FIG. 5.6

PATH PROFILE FROM 405.00 283.90
TO 412.30 288.30

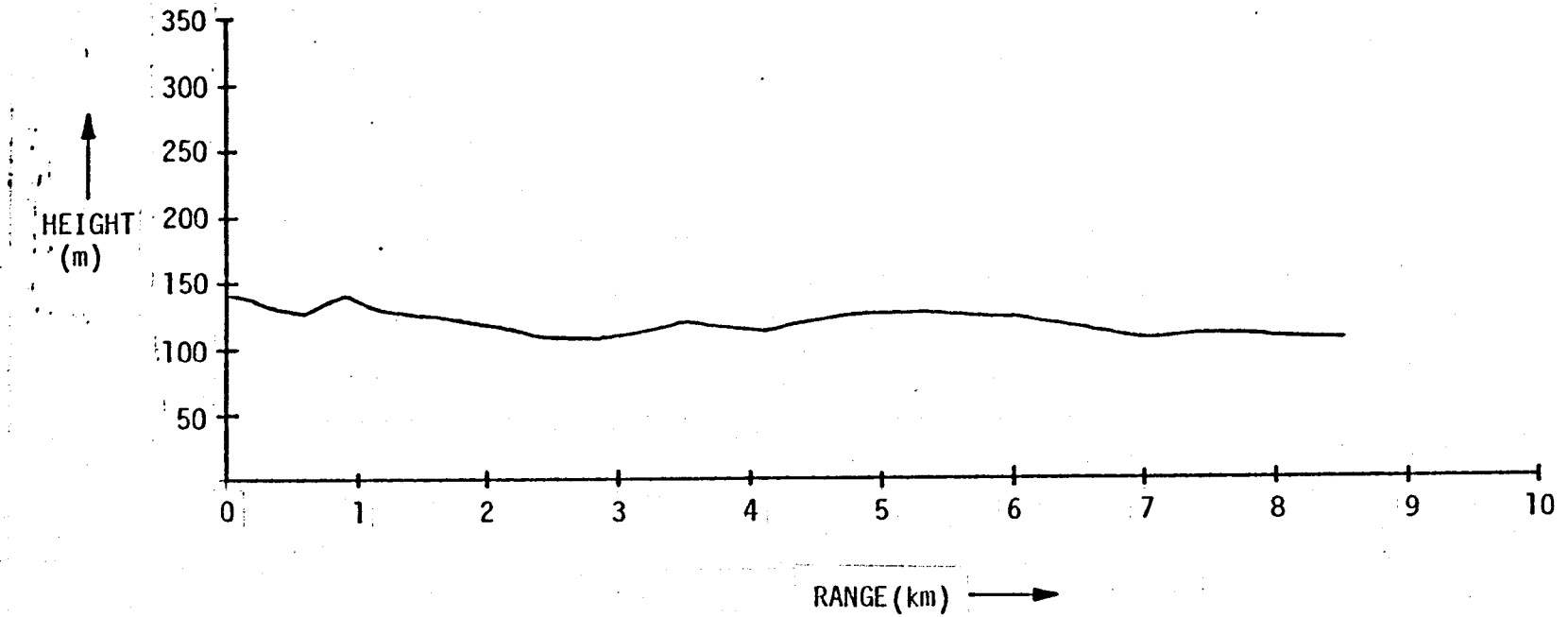

BIRMINGHAM PROFILE

FIG.5.7

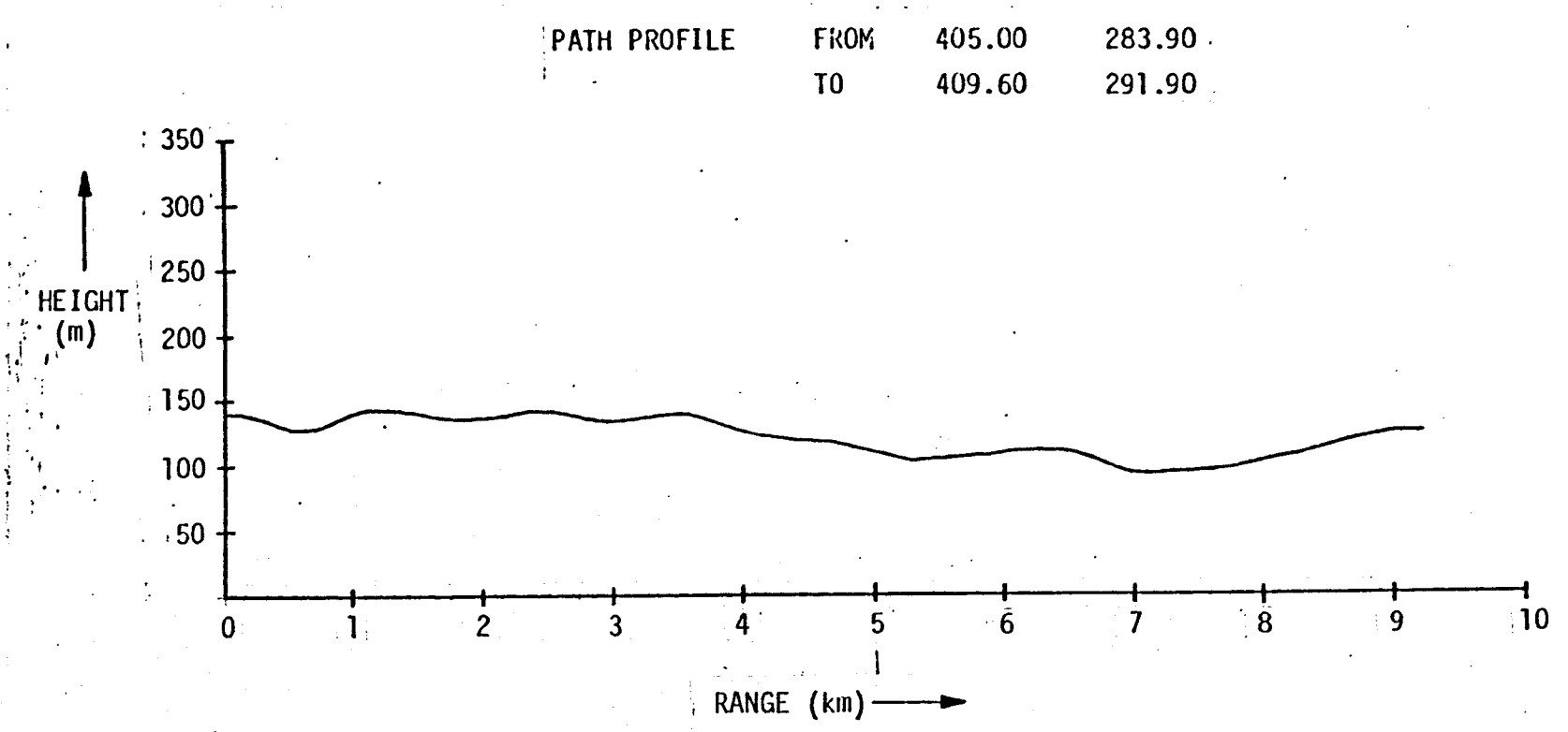

BIRMINGHAM PROFILE

FIG.5.8

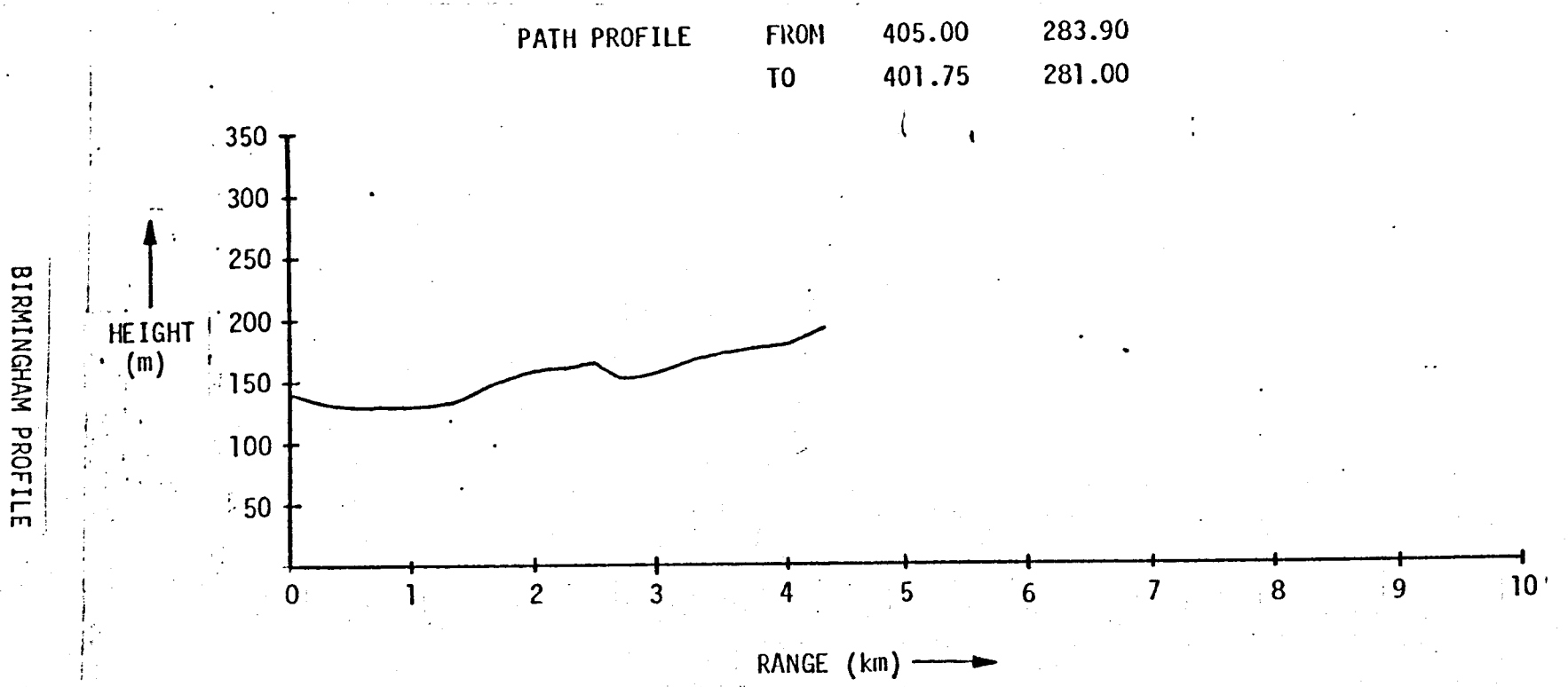

BIRMINGHAM PROFILE

FIG.5.9

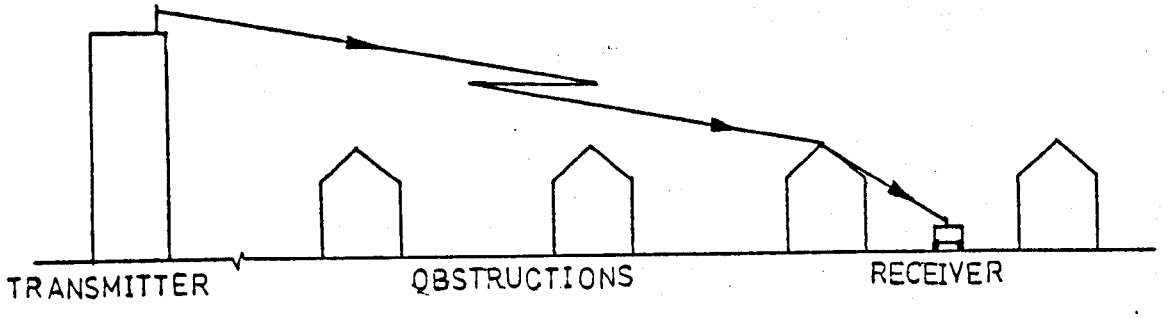

IDEALISED REPRESENTATION OF THE BIRMINGHAM TRANSMISSION PATH

FIG. 5.10

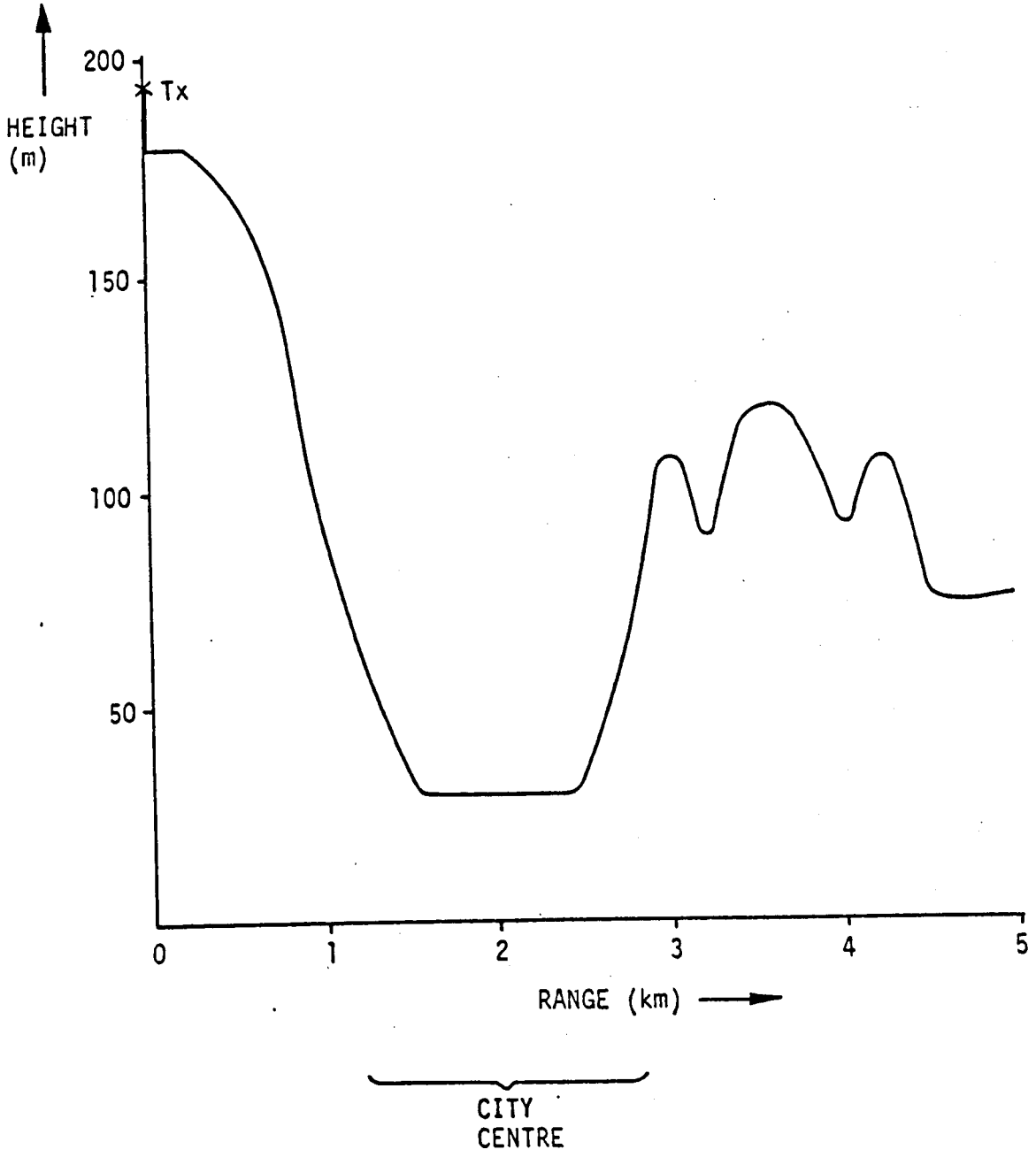

TERRAIN PROFILE OF BATH

FIG.5.11

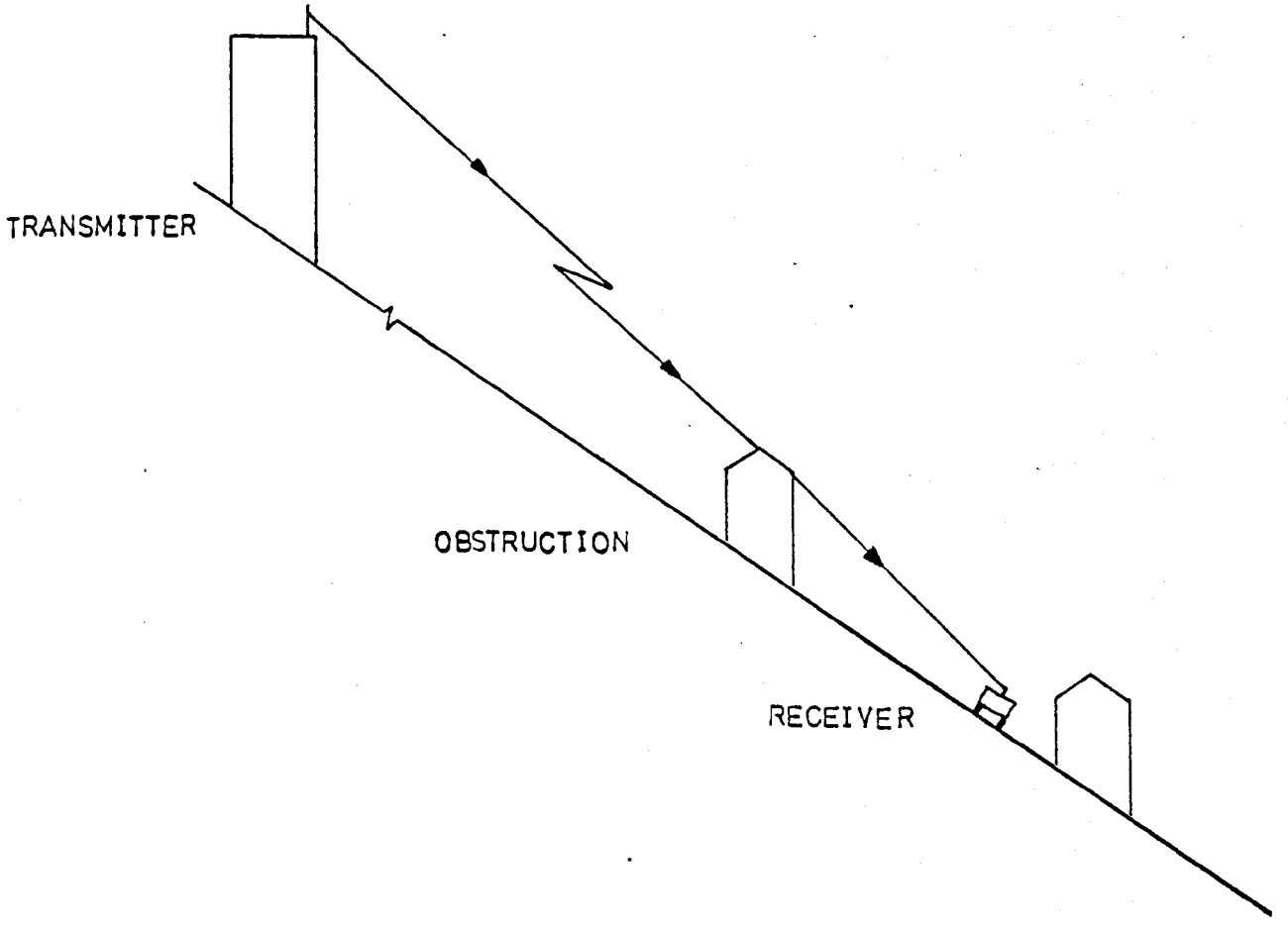

IDEALISED REPRESENTATION OF THE BATH TRANSMISSION PATH

FIG. 5.12

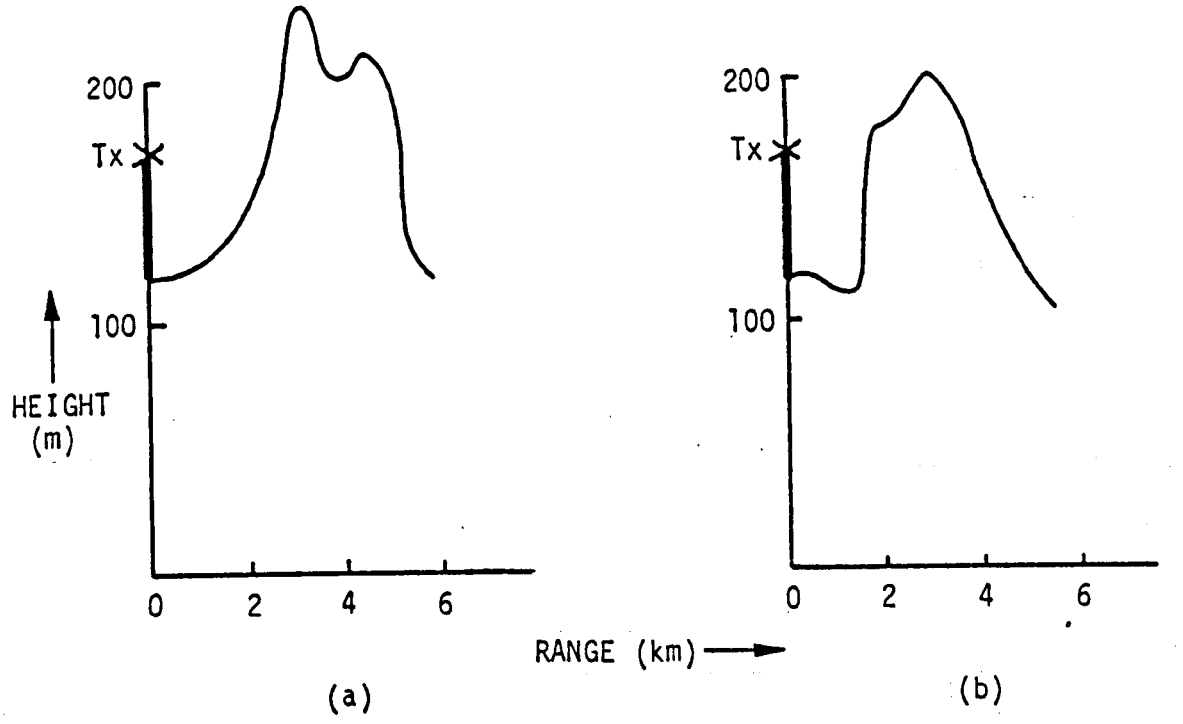

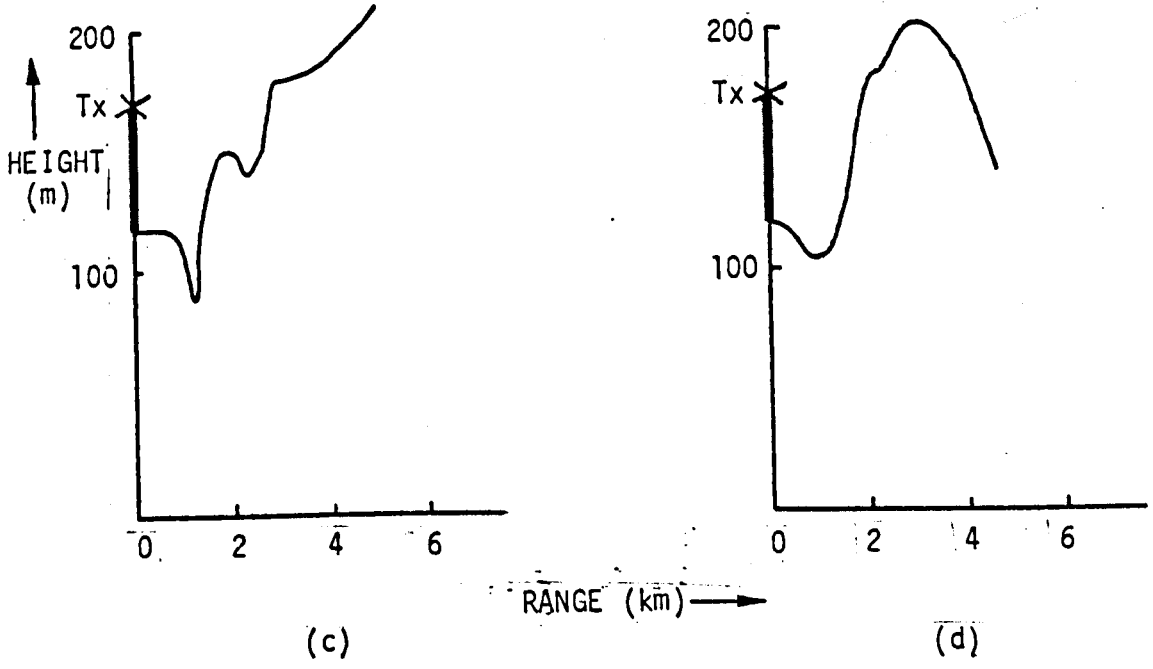

TERRAIN PROFILES OF BRADFORD

(a) COTTINGLEY (b) GREENGATES

(c) ECCLESHILL (d) UNDERCLIFFE

FIG. 5.13
Page 1 of 2

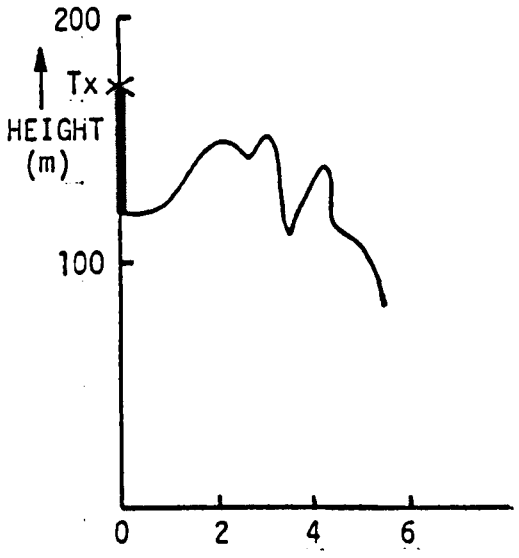

(e)

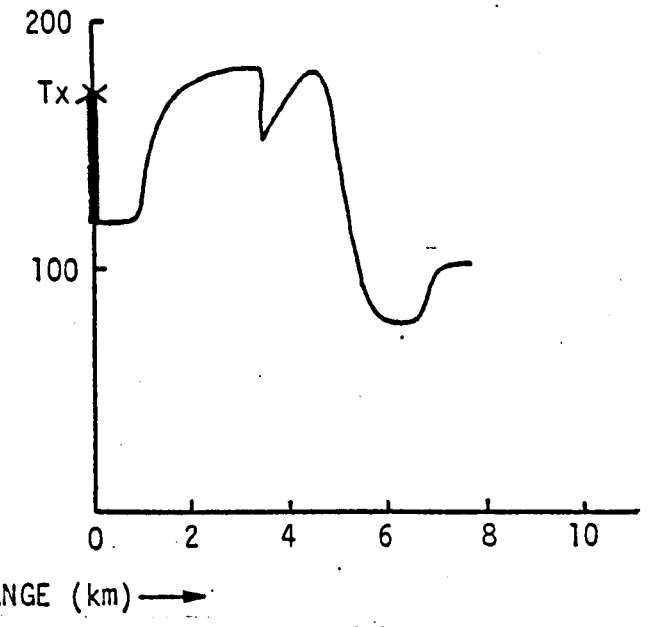

(f)

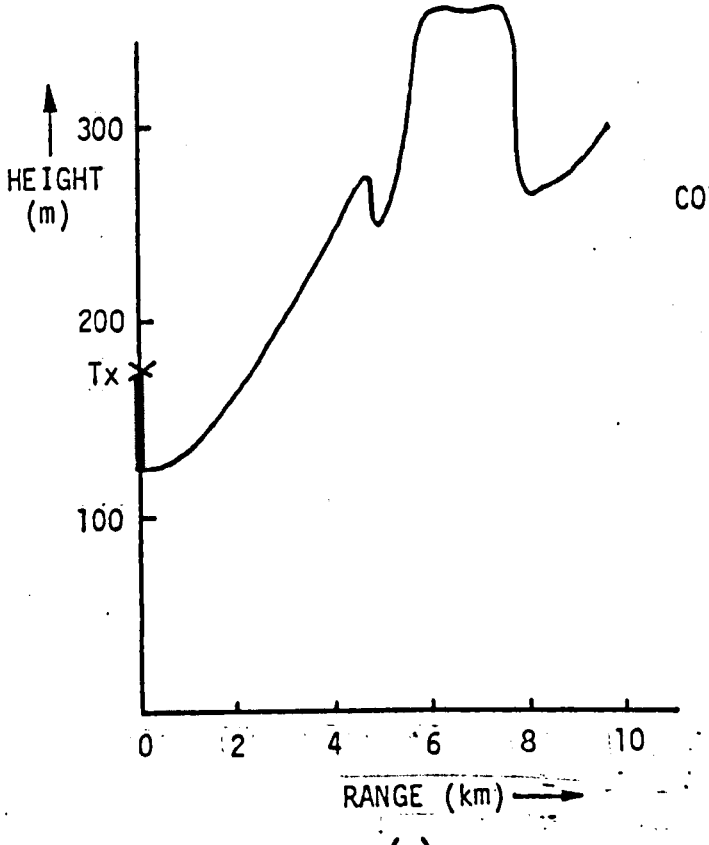

(g)

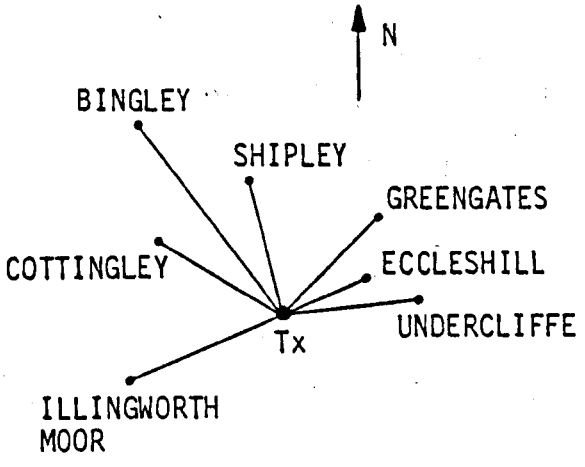

(h)

TERRAIN PROFILES OF BRADFORD

(e) SHIPLEY (f) BINGLEY (g) ILLINGWORTH MOOR

(h) BRADFORD REGIONAL PLAN

FIG. 5.13
Page 2 of 2

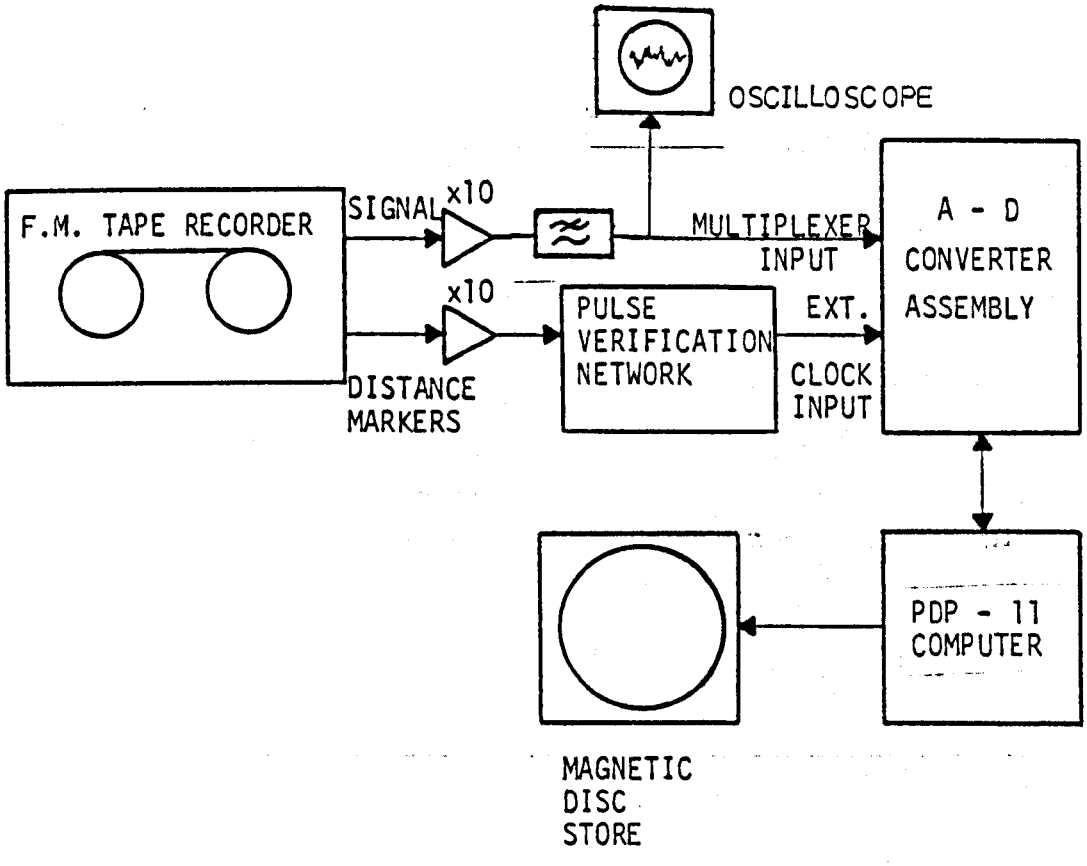

DIGITISATION OF MEASURED SIGNAL

FIG.5.14

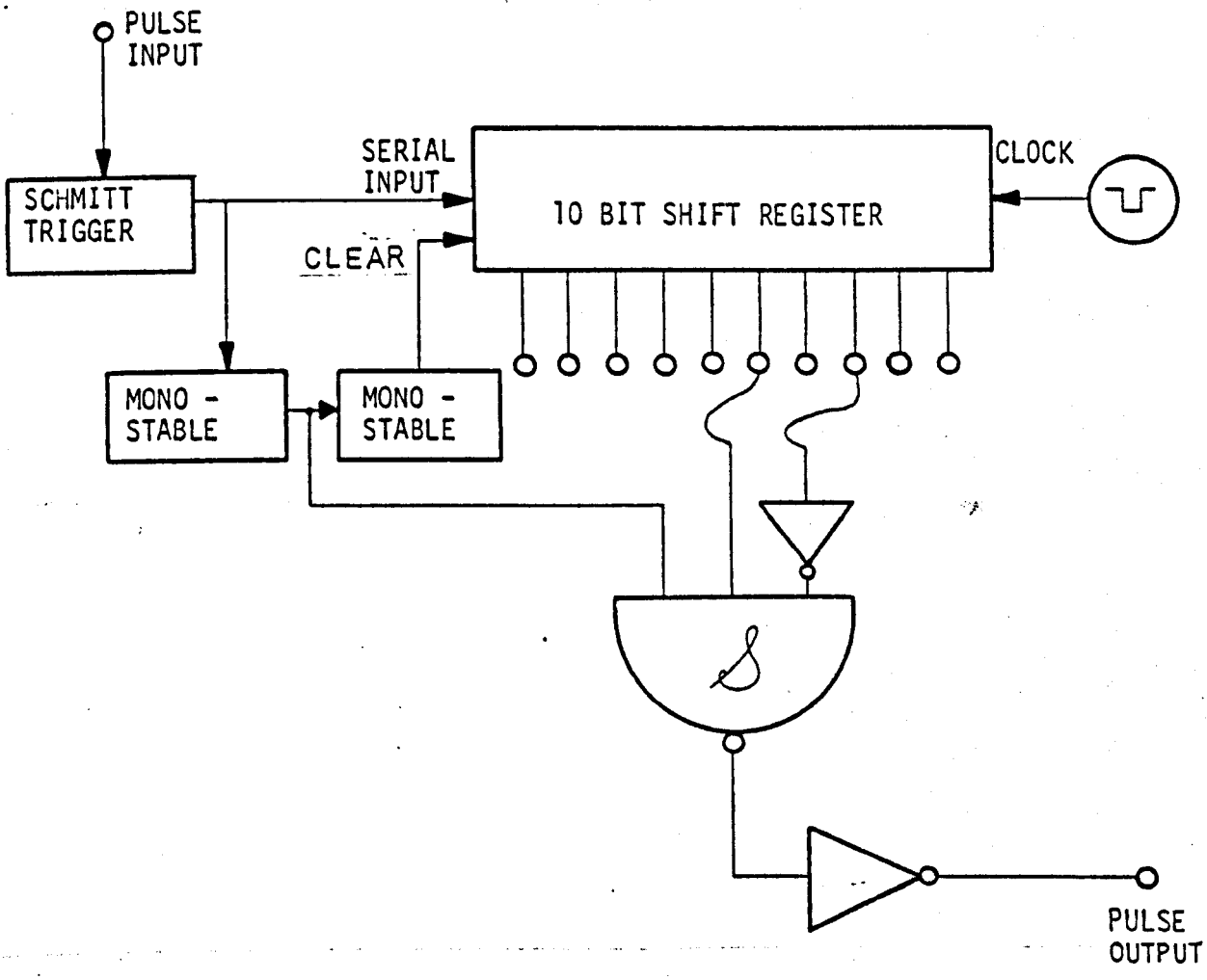

PULSE VERIFICATION NETWORK

FIG.5.15

CHAPTER 6

FACTORS INFLUENCING THE SMALL SECTOR MEDIAN PATH LOSS

The investigation of the filtering processes detailed in Chapter 3 demonstrated that the magnitude of the signal experienced by a moving receiver must be described in terms of its "small sector" statistics. The characteristics of the spatially distributed field pattern existing within these small sector cells have been documented in Chapter 2 as those of the fast fading field. The factors influencing the small sector median received signal level are now examined with a view to the formulation of a prediction model based on the measurements obtained in the largely flat city of Birmingham.

Before commencing the analysis of the experimental data it should be noted that the broadcasts at 75.375 MHz were detected using a receiver which travelled along routes of up to 1 km and that the resulting signal records were digitised at displacements equivalent to 25 cm of the vehicle's movement. The total number of routes investigated by these means was less than 100. Furthermore, the base station aerial was sited at a different position on the building's roof from those at the alternate three frequencies. For these reasons, the results obtained at 75.375 MHz will not be directly compared with those at 85.875, 167.2 and 441.025 MHz, but trends will be examined where possible.

6.1 RANGE DEPENDENCE

A significant factor in the quantification of the propagation path loss incurred by a radio link is the distance (d) by which the transmitting and receiving aerials are spatially separated (Chapter 4). In order to establish the precise nature of this range dependence the measured small sector median transmission loss values have been regressed against a curve of the form $P_r \alpha d^{-n}$ applied by the least squares error method to the experimental data. The results shown in Table 6.1 indicate that an inverse fourth power range law may be used to describe the path loss measurements at the two VHF frequencies with reasonable accuracy. No such conclusion is evident for the 441 MHz values.

Frequency	Exponent n	Mean Error	Standard Deviation of Error
MHz		dB	dB
85.875	3.8	0.004	7.4
167.2	3.9	0.005	6.2
441.025	2.4	0.002	7.8

TABLE 6.1

REGRESSION AGAINST A CURVE OF THE FORM $P_r \alpha$ (TOTAL LINK RANGE)$^{-n}$

As a further test the measured data has been regressed against a curve of the form $P_r \alpha d^{-4}$. The results are given in Table 6.2.

6.1 (cont'd)

Frequency	Mean Error	Standard Deviation of Error
MHz	dB	dB
85.875	0.005	7.5
167.2	0.005	6.2
441.025	0.004	8.3

TABLE 6.2

REGRESSION AGAINST A CURVE OF THE FORM $P_r \alpha$ (TOTAL LINK RANGE)$^{-4}$

Examination of the error statistics of the UHF measurements shown in Tables 6.1 and 6.2 reveals that recourse to an inverse fourth power range dependence, rather than that of the optimum exponent value, only results in a small degradation of the statistical parameters. It is reasonable to suggest, therefore, that the small sector median path loss can be satisfactorily predicted using a model of the form proposed by Egli [6.1] :

$$P_r = P_t G_t G_r \left(\frac{h_t h_r}{d^2}\right)^2 \beta$$

Here the factor "β" is incorporated to correct the plane earth propagation expression (Section 4.3.1) for the influences which buildings and trees have on the propagation path loss and in no way attempts to physically describe the propagation mechanisms which exist (Section 7.1). Accordingly "β" is termed the "urban clutter factor".

Figures 6.1, 6.2, 6.3 and 6.4 depict the variation of the measured small sector median transmission loss values at 75.375, 85.875, 167.2

6.1 (cont'd) and 441.025 MHz respectively against the total link range. Fourth power range laws describing the propagation path losses are drawn through the measured points and are compared with the plane earth propagation curves computed utilising the aerial heights measured above local ground. Table 6.3 shows the results of a statistical comparison between the measured data and their equivalent Egli predictions.

Frequency	β	Mean Error	Standard Deviation of Error
MHz	dB	dB	dB
85.875	16	0.8	7.5
167.2	19	0.2	6.2
441.025	36	0.8	8.3

TABLE 6.3

STATISTICAL COMPARISON OF MEASURED DATA WITH EGLI PREDICTIONS

6.2 FREQUENCY DEPENDENCE

The departures of the small sector median path loss measurements from their corresponding plane earth values are plotted against frequency in Figure 6.5. For ease of comparison only the spread of the points and the mean value at each frequency are shown.

The curve sketched through the measured data in Figure 6.5 has the same general shape as results reported by other workers [6.2, 6.3, 6.4] inasmuch as the loss (expressed in dB) is not linearly related to the logarithm of the frequency. The precise form of this dependence will

6.2 (cont'd) be discussed in more detail in later sections.

6.3 THE INFLUENCE OF PHYSICAL URBAN PARAMETERS

The knowledge of the manner in which the urban clutter factor (β) varies with frequency (Figure 6.5) permits the measured values to be normalised against both range and frequency to form a secondary data set which will be referred to as the "frequency corrected urban clutter factors" (β'). This correction process will facilitate a direct comparison of the measured small sector median path loss data at all the frequencies (some 900 values in all) with relevant physical parameters.

6.3.1 VARIATION WITH STREET ORIENTATION

For the purposes of this investigation the street orientation (α) is defined as the angle subtended between the longitudinal axis of the road and the line joining the transmitting and receiving aerials. To enable the influences which uncontrolled variables have on the propagation path loss to be minimised, large quantities of measurements needed to be analysed at each of the street orientation angles considered. For this reason a quantisation interval of 5^{o} has been employed, thereby providing approximately 50 values at each of the angular steps.

Figure 6.6 shows the spread of the measurements and their mean value at each angular interval. Although street orientation is undoubtedly an important factor [6.3, 6.5], a simple relationship cannot be immediately discerned.

6.3.2 VARIATION WITH STREET WIDTH

If the street width is measured as the distance between the buildings on opposite sides of the road, open spaces such as gardens, footpaths and cycle tracks are then included in the value obtained. In most practical situations this action places the vehicle very close to the centre of the street and therefore obviates the need to know the precise position of the receiver at every measured location. Localities where buildings only exist along a single side of the street will have an indeterminate width and consequently the measurements pertaining to these cases must be examined with care.

The spreads of the frequency corrected urban clutter factors and their mean values are shown in Figure 6.7 at 3m intervals of street width. The form of this relationship will be examined in detail in the following sections.

6.3.3 VARIATION WITH EFFECTIVE STREET WIDTH

Figure 6.7 demonstrates that the width of the street in which the mobile terminal is situated is closely related to the small sector median path loss. A more relevant factor, however, will be the distance between the mobile unit and the buildings measured along the line-of-sight path between the transmitting and receiving aerials, as shown in Figure 6.8. This distance will be termed the "effective street width" (W^1) and may be seen to directly incorporate the variable of street orientation and width, possibly making it a useful physical parameter.

6.3.3 (cont'd) The mean values of the frequency corrected urban clutter factors at 3m intervals of the effective street width variable are shown in Figure 6.9. The general trend indicates that higher path losses are experienced in narrow streets than in wide, a not altogether unexpected conclusion. [6.5]

6.3.4 RELATIONSHIP OF PATH LOSS TO DIFFRACTION LOSS*

The single knife-edge diffraction situation depicted in Figure 4.5 has a Fresnel-Kirchoff v parameter given by (Section 4.4.1.1):

$$v = \sqrt{\frac{2}{\lambda} \cdot \frac{d_1 d_2}{(d_1+d_2)}}\,\theta$$

The case under consideration normally has the mobile terminal located close to the diffractor, assumed to be a building, and remote from the fixed station. The assumption may therefore be made that $d_1 >> d_2$, in which case the v parameter simplifies to:

$$v \approx \sqrt{\frac{2}{\lambda d_2}}\,(h_o - h_r)$$

The resulting diffraction loss, if $v > 1$, may be approximated [6.8] by:

$$A(v) = -20 \log_{10}\sqrt{d_2} + \text{constant} \quad , \text{dB}$$

A curve of the form "$-10 \log d_2 + k$" is compared with the measured values in Figure 6.9 and can be seen to closely describe the overall trend of the excess clutter factor (β'). This observation leads to the hypothesis that the diffraction loss over the buildings adjacent to the mobile terminal and obstructing the line-of-sight transmission path is an important factor in determining the small sector median

---

* Please see over.

Footnote to page 80

Here the diffractor is positioned at a distance W' from the mobile terminal and is taken to be orthogonal to the line-of-sight path between the transmitter and the receiver. However, the influence of an inclined diffractor may be assessed using techniques developed in the Geometrical Theory of Diffraction.[6.9]

The field strength existing behind a diffractor inclined at an angle α to the direct ray (Fig.6.8) can be shown to be inversely proportional to $\sin(\alpha)$. The assumption of an orthogonal knife-edge therefore holds to within approximately 1dB for inclinations greater than 60° and to 3dB for inclinations greater than 45°.

6.3.4 path loss[6.6, 6.7, 6.4]

(cont'd)

If it is assumed that the buildings are 12 m tall, that the vehicle's aerial is 2m above local ground and that the mobile unit is located 30m away from the obstructing buildings, diffraction loss values of 16, 19 and 23 dB are obtained at frequencies of 85, 167 and 441 MHz respectively. These values are compared with the measured data in the frequency dependency of Figure 6.5 and demonstrate that a good estimate of the urban clutter factor (β) may be derived at VHF from the use of the simple knife-edge diffraction approximation. The departure of the measured values from the theoretical knife-edge model at 441 MHz however, suggests that the buildings must be treated as diffracting wedges having finite thicknesses when compared with the 60 cm wavelength.

6.3.5 VARIATION WITH AERIAL HEIGHTS

The plane earth propagation equation (Section 4.3.1) has, for convenience only, been used throughout the preceding analysis to describe the manner in which parameters such as the overall link range and the heights of the aerials influence the transmission loss. While the range dependence has been demonstrated to be largely in accordance with this expression, verification of the effects which the aerial heights have on the propagation loss has yet to be given. An investigation to this end has, regrettably, not been performed, primarily as a result of the unavailability of the specialised equipment required, eg a large aerial tower (up to around 50 m) for the base station height investigation and an extendable mast on the vehicle (up to 10 m). It is therefore necessary to draw upon suitable results

6.3.5 published by other authors.

(cont'd)

Okumura [6.3] has measured the height gain dependency of the transmission loss on both the base station and vehicular aerial heights. The base station aerial height, h_t, was found to satisfactorily describe a law of the form $P_r \alpha h_t^2$ for all aerial heights above 20 m when the link range was less than 20 km. The vehicular aerial height, hr, was found to obey the following:-

$$P_r \alpha h_r \quad \text{for} \quad h_r < 3m$$

$$P_r \alpha h_r^2 \quad \text{for} \quad h_r > 3m$$

The error in using the term $(h_t h_r)^2$ therefore appears to be relevant in the region where the vehicular aerial is below 3m. In this case the law would be better described as $h_t^2 h_r$. However, when h_r attains its maximum value of 3m in this region the error betwewn the two forms is only 5 dB, insufficient to cause any serious problems. At the 2m vehicular aerial height used, this error is 3dB.

6.4 REFERENCES

6.1 Egli J.J.
"Radio Propagation above 40Mc over Irregular Terrain"
Proc IRE, October 1957.

6.2 Young W.R. Jr
"Comparison of Radio Transmissions at 150, 450, 900 and 3700 Mc"
B.S.T.J., Vol 31, November 1952.

6.3 Okumura Y., Ohmori E., Kawano T and Fukuda K.
"Field Strength and its Variability in VHF and UHF Land Mobile Service"
Rev Elec Comm Lab, 16 , September - October 1968.

6.4 Parker R.E. and Roper G.B.
"Vehicular Radio Communications in London"
Report SDE/X/B70/1
AWRE Aldermaston.

6.5 Black D.M. and Reudink D.O.
"Some Characteristics of Radio Propagation at 800 MHz in the Philadelphia Area"
IEEE Trans Vehic Tech, Vol VT-21, May 1972.

6.6 Bell C.P.
"The Effects of Buildings and Trees upon the Propagation of Waves in the UHF and VHF bands"
BBC Research Report K-162, 1963/39, 1963

6.7 Kinase A.

"Influences of Terrain Irregularities and Environmental Clutter Surroundings on the Propagation of Broadcasting Waves in the UHF and VHF Bands"

NHK Tech Monograph No 14, March 1969.

6.8 Hacking K.

"Approximate Methods for Calculating Multiple Diffraction Loss"

Electronics Letters, May 1966, Vol 2, No 5.

6.9 Keller J.B.

"Geometrical Theory of Diffraction"

Journ. Opt. Soc. America,Vol. 52,No. 2,Feb. 1962

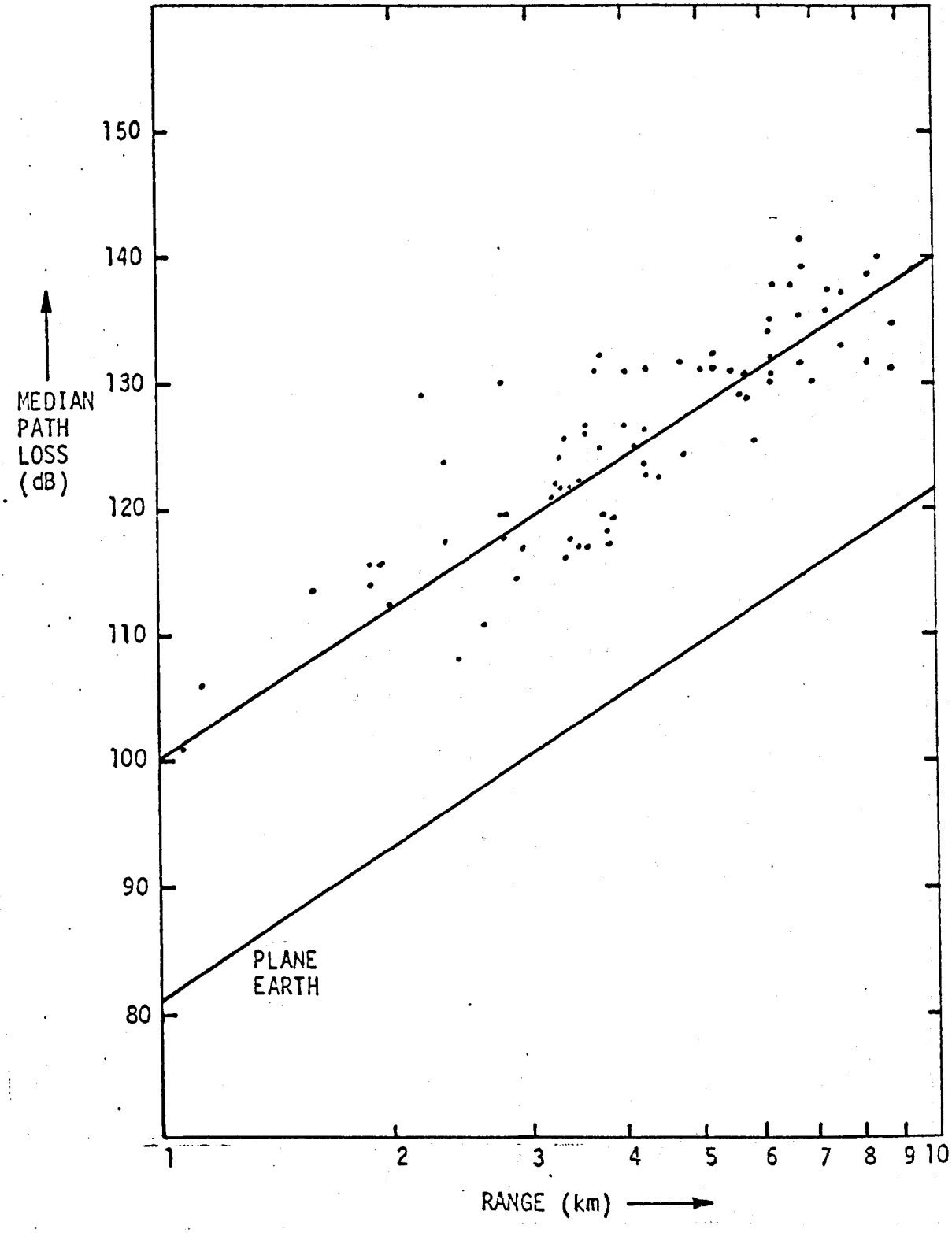

MEDIAN PATH LOSS BETWEEN ISOTROPIC AERIALS Vs. RANGE
75.375MHz

FIG 6.1

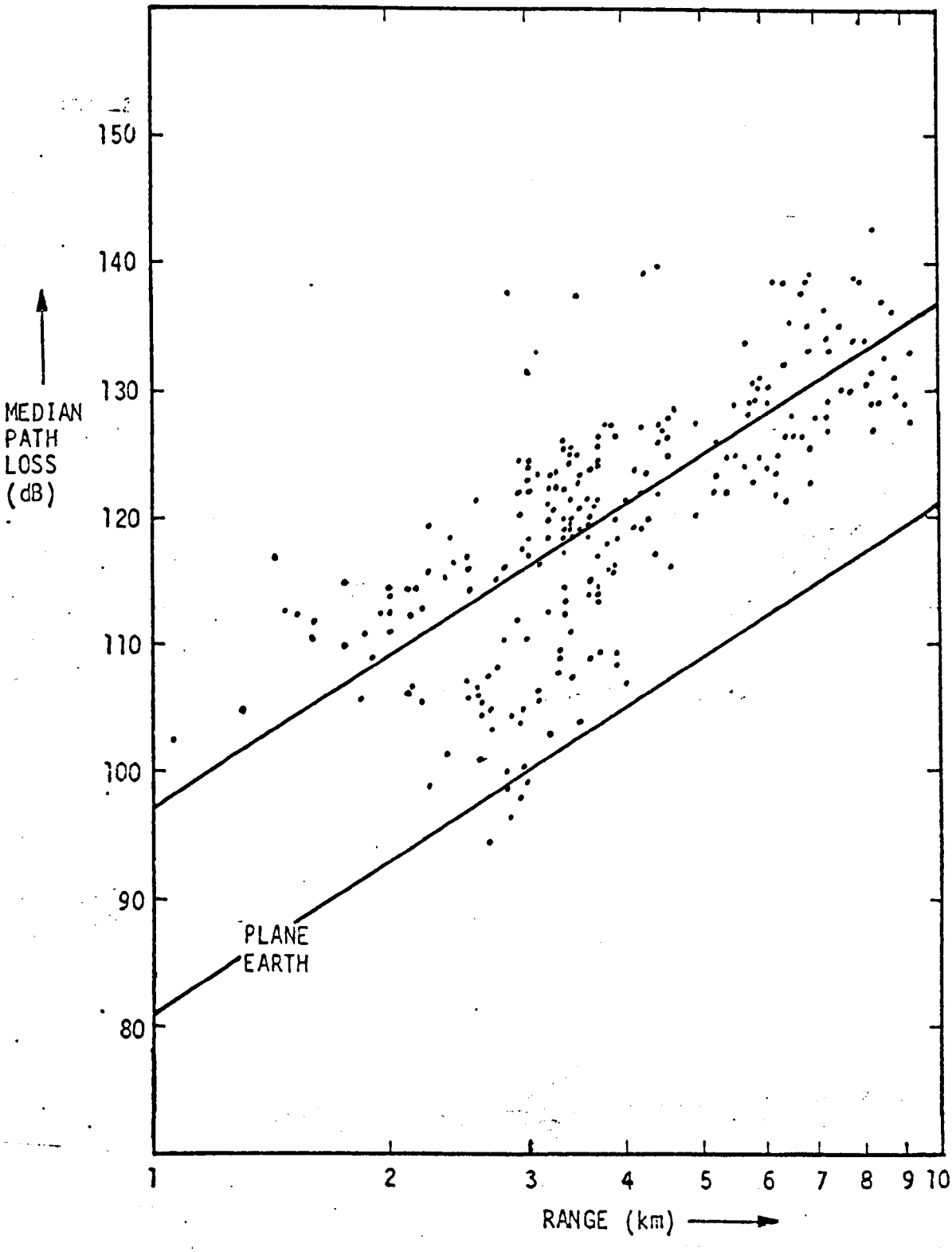

MEDIAN PATH LOSS BETWEEN ISOTROPIC AERIALS Vs. RANGE
85.875MHz

FIG 6.2

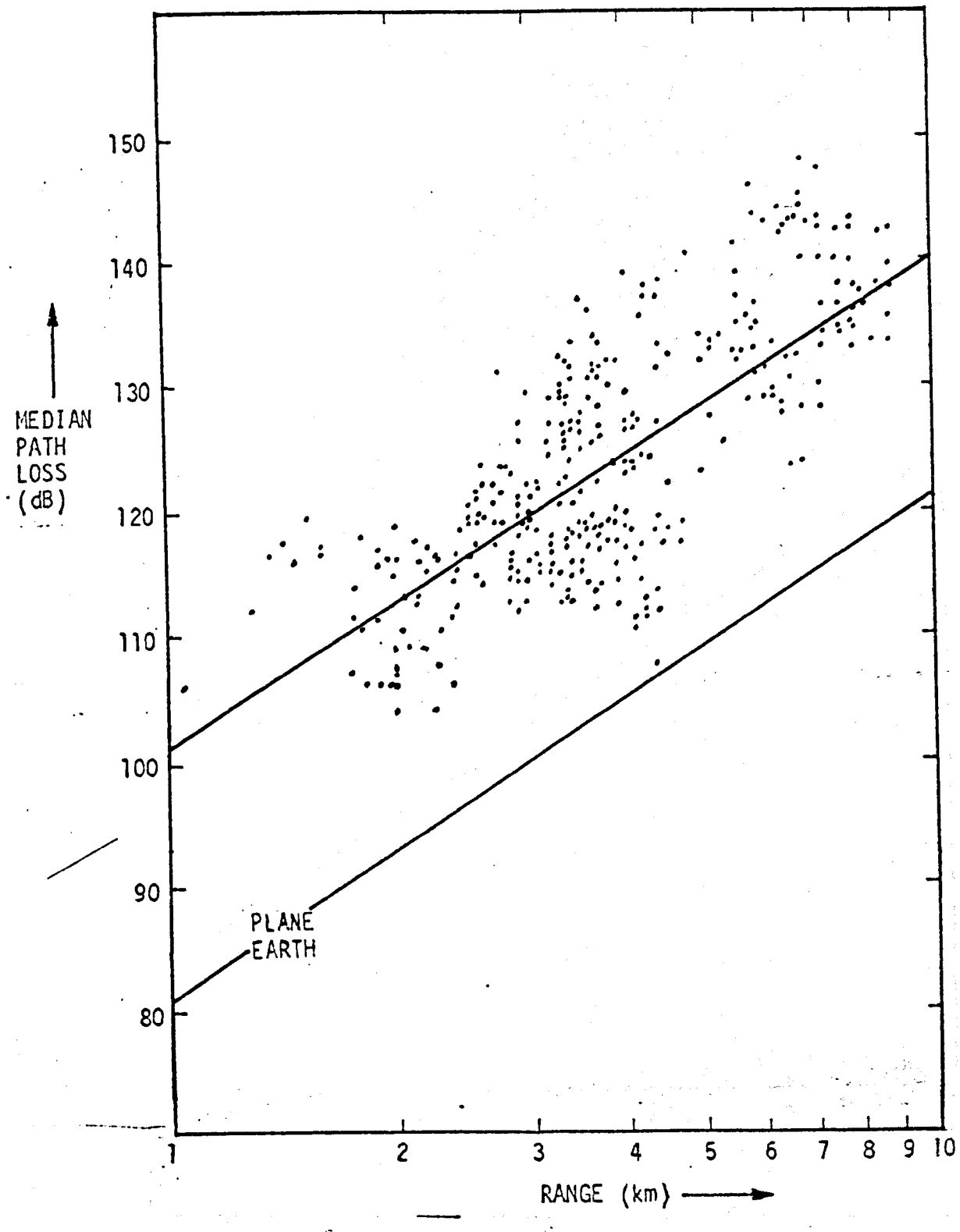

MEDIAN PATH LOSS BETWEEN ISOTROPIC AERIALS Vs. RANGE
167.2MHz

FIG 6.3

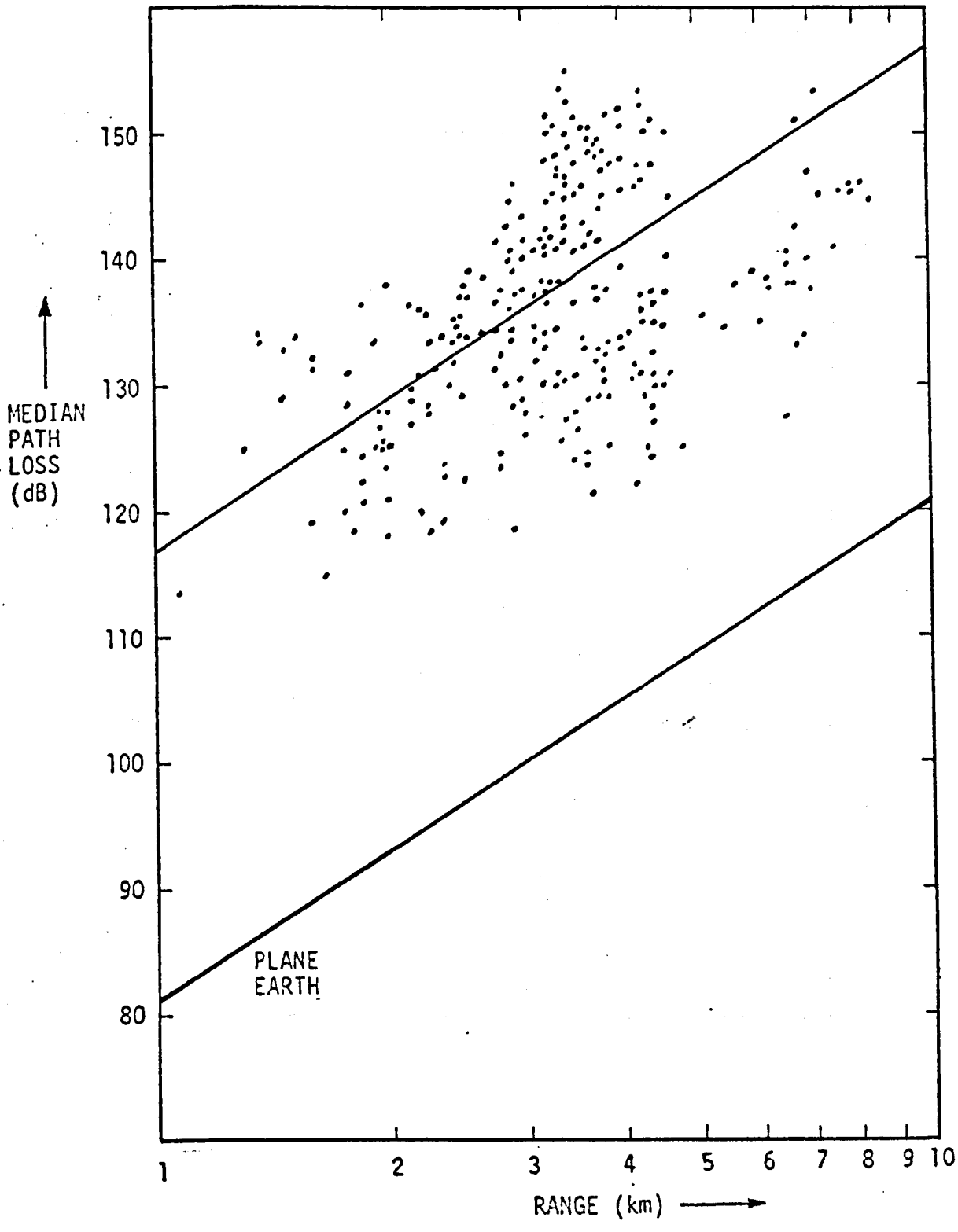

MEDIAN PATH LOSS BETWEEN ISOTROPIC AERIALS Vs. RANGE
441.025MHz

FIG 6.4

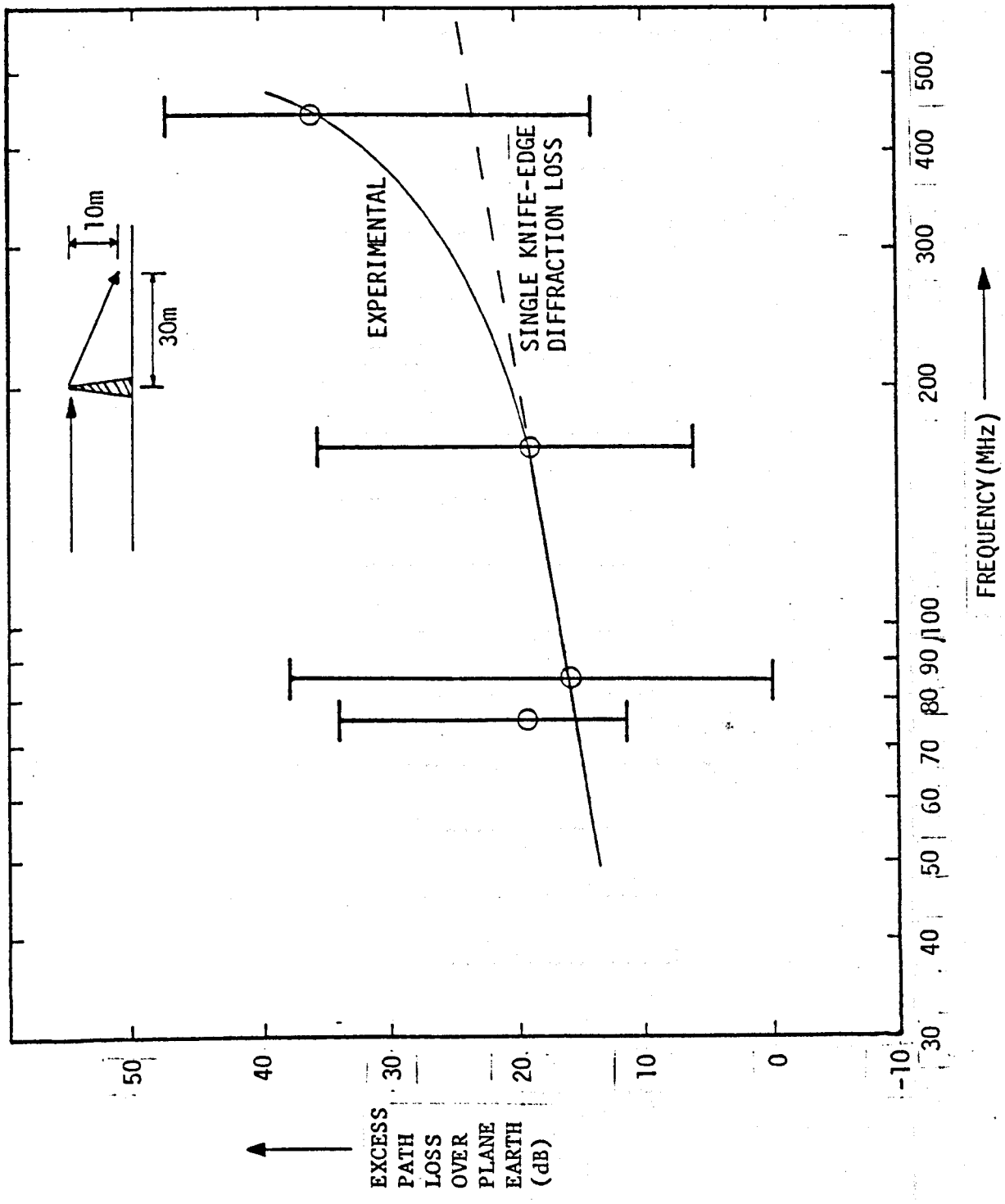

FREQUENCY DEPENDENCE OF URBAN CLUTTER FACTOR(β)

FIG. 6.5

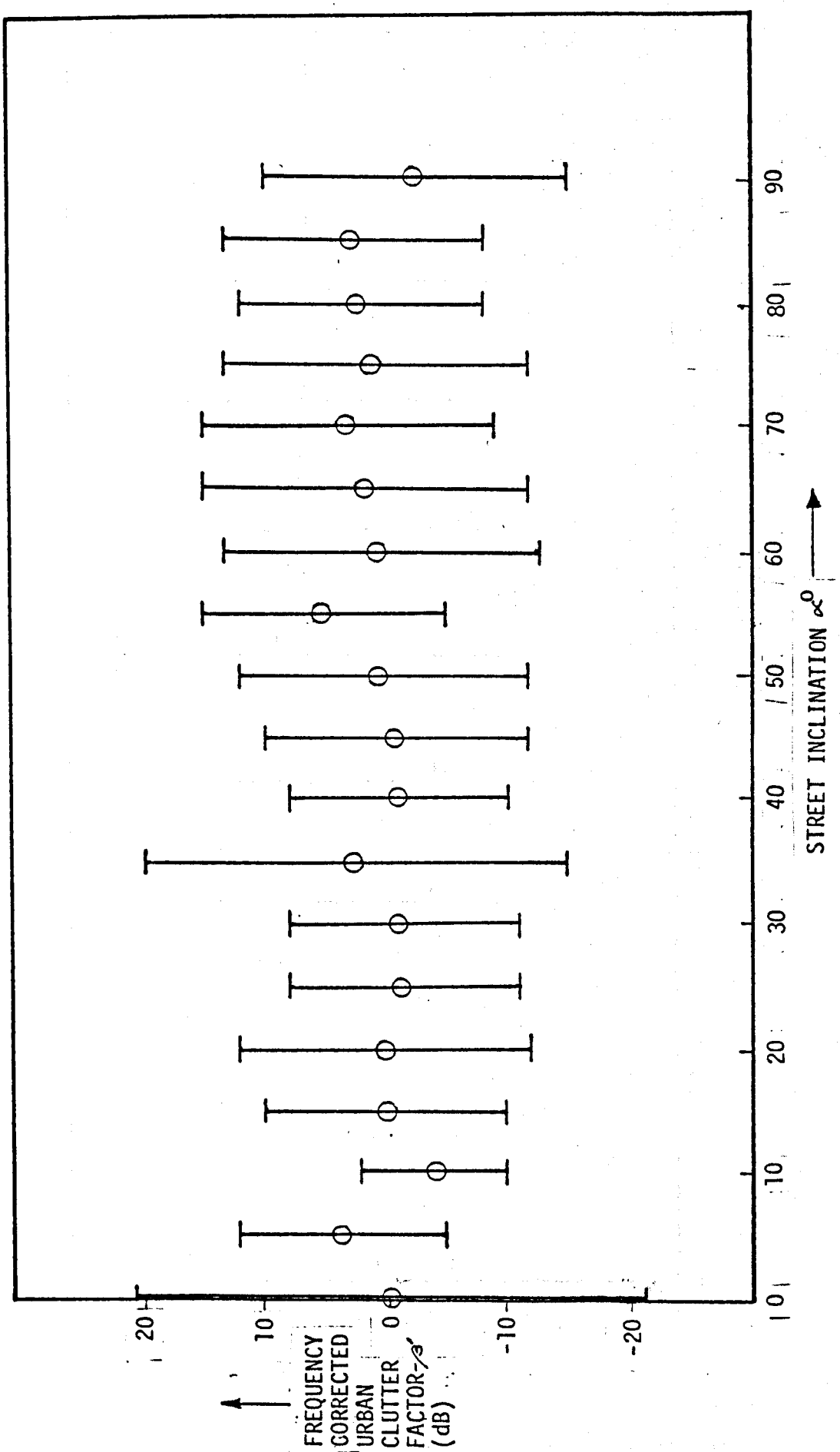

VARIATION OF FREQUENCY CORRECTED URBAN CLUTTER FACTOR(β') WITH STREET INCLINATION(α)

FIG.6.6

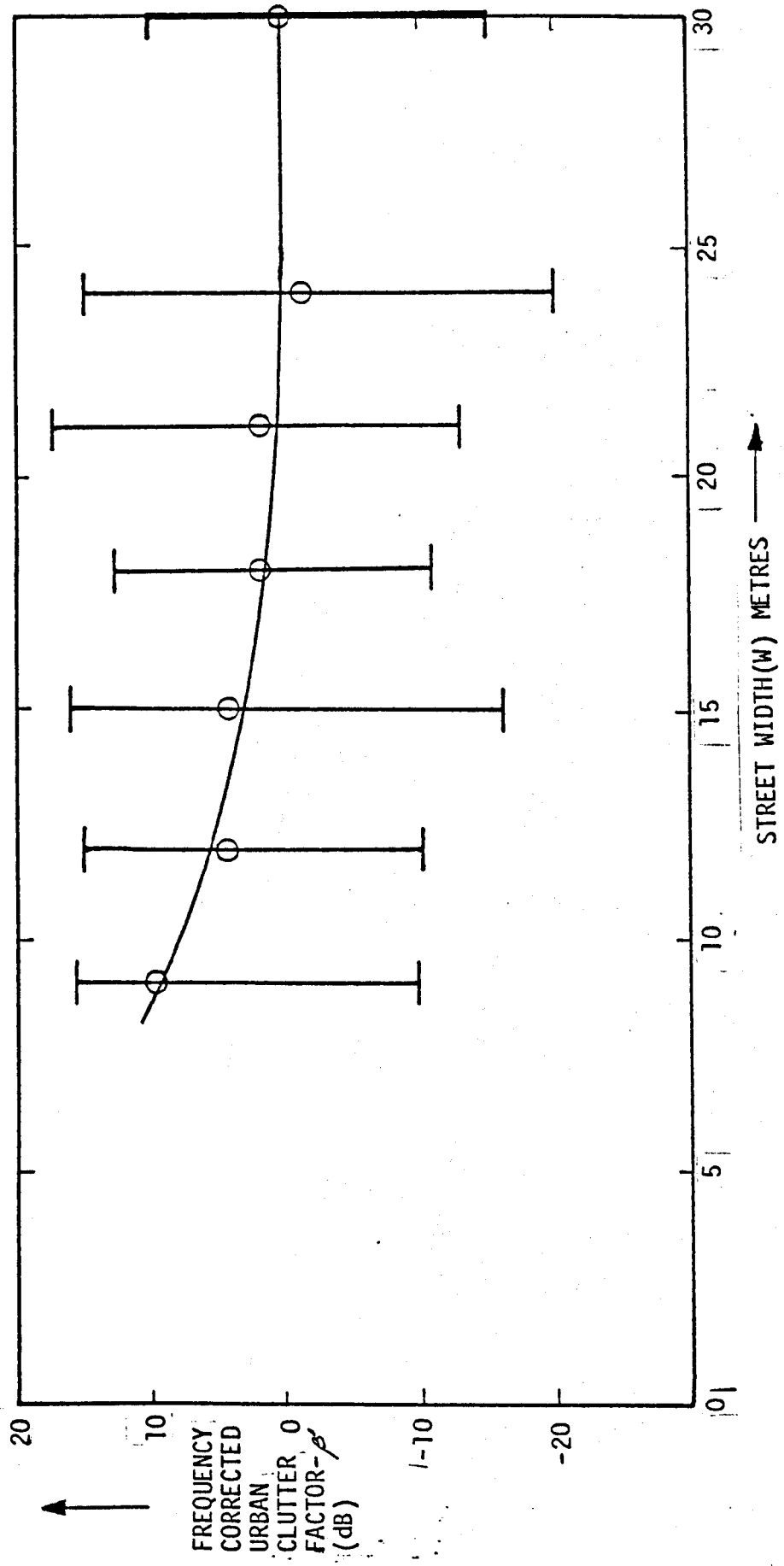

VARIATION OF FREQUENCY CORRECTED URBAN CLUTTER FACTOR(β) WITH STREET WIDTH(W)

FIG.6.7

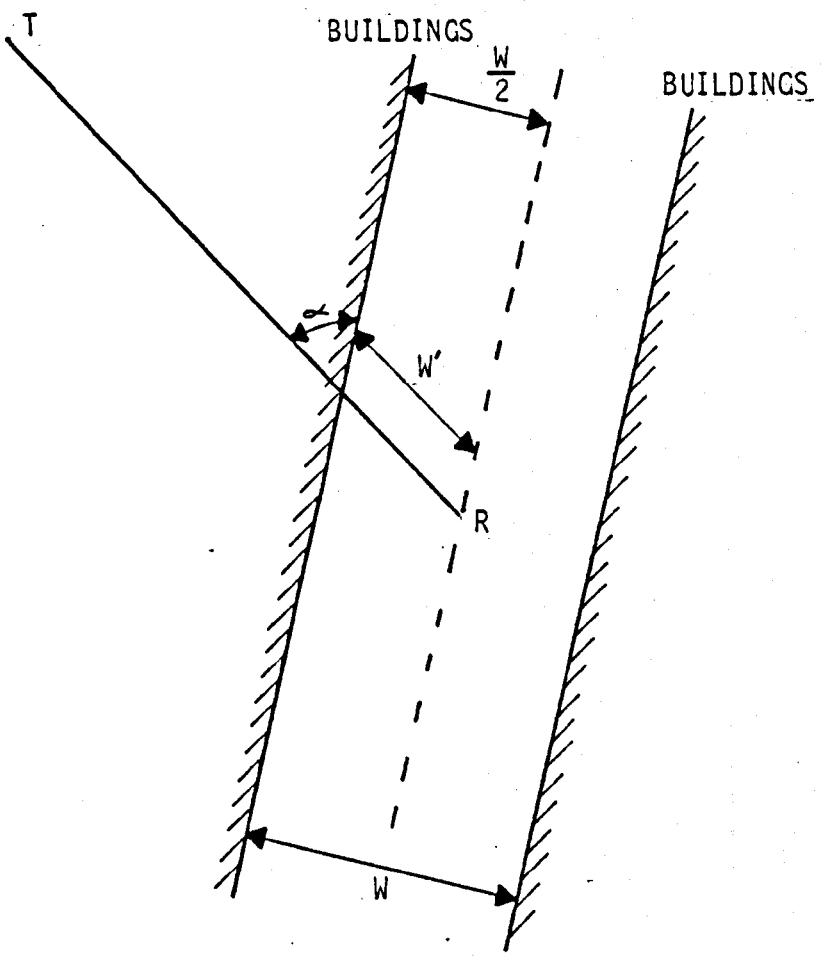

$$W' = \frac{W}{2\sin\alpha}$$

DEFINITION OF EFFECTIVE STREET WIDTH W'

FIG.6.8

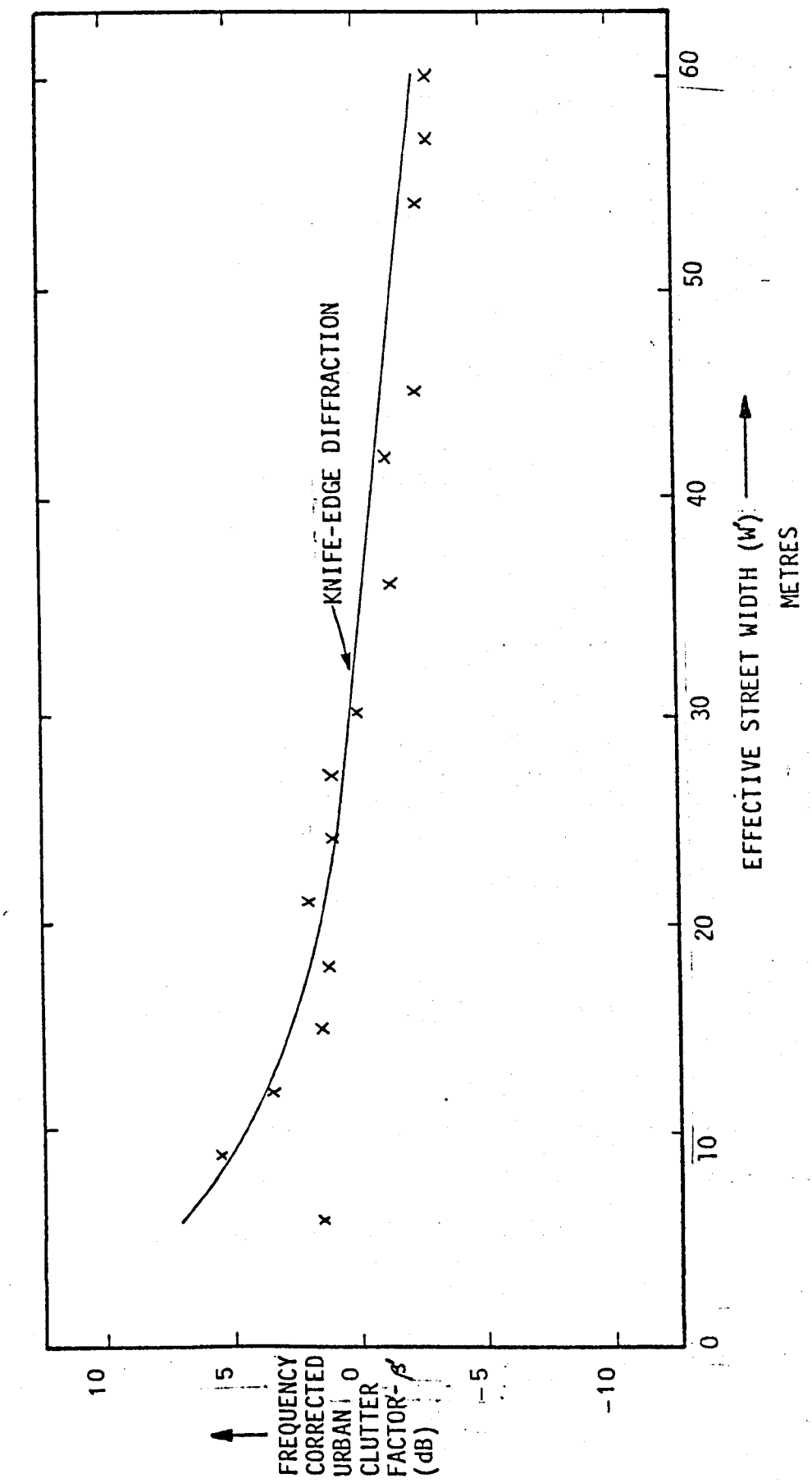

VARIATION OF FREQUENCY CORRECTED URBAN CLUTTER FACTOR (β') WITH EFFECTIVE STREET WIDTH (W')

FIG 6.9

CHAPTER 7

THE SMALL SECTOR MEDIAN PATH LOSS PREDICTION MODELS

7.1 COMPARISON OF POSSIBLE PREDICTION TECHNIQUES

The propagation situation depicted in Figure 7.1 is an idealised representation of a path chosen at random from amongst those encountered in Birmingham. The small sector median transmission loss over this path was measured as 127dB at 85.875MHz. Path loss predictions calculated using various techniques are compared in Table 7.1. These methods are:

(1) Edwards and Durkin (Section 4.5.2).

   (a) Free Space Path Loss + Diffraction Loss , dB

   (b) Plane Earth Path Loss + DiffractionLoss , dB

(2) Blomquist and Ladell (Section 4.5.3).

(3) Multi-Ray Analyses (Section 4.4.1.2).

   (a) All four rays indicated in Figure 7.2.

   (b) Rays 1 and 2 in Figure 7.2.

   (c) Rays 1 and 3 in Figure 7.2

7.1 (cont'd)

Model	Method	Predicted Path Loss dB
Edwards and Durkin	Free Space + Diffraction	99.4
Edwards and Durkin	Plane Earth + Diffraction	124.4
Blomquist and Ladell	Section 4.5.3	113.7
Multi-Ray Analysis	Rays 1,2,3 and 4 in Fig 7.2	131.6
Multi-Ray Analysis	Rays 1 and 2 in Fig 7.2	120.8
Multi-Ray Analysis	Rays 1 and 3 in Fig 7.2	96.2

TABLE 7.1

COMPARISON OF VARIOUS PREDICTION TECHNIQUES

Of those models employed, the Edwards and Durkin method of combining the plane earth and diffraction losses can be seen from Table 7.1 to provide the closest estimate of the measured value, the error in this case being less than 3 dB. Also giving a good measure of agreement is the multi-ray analysis utilising all the four rays shown in Fig 7.2, the error produced being 4.6 dB when a perfect reflection is assumed. However, a number of points are worth noting before any conclusions about this latter method are drawn.

The grazing angle of the ray which is reflected from the ground surface on the vehicle's side of the obstacle (Φ_2) has a value in the region of 0.4 radians for the parameters specified in Fig 7.1. This is very close to the pseudo-Brewster angle for vertically polarised signals over land [7.1] (of all forms) and, in reality, the magnitude of the theoretical reflection coefficient will be less than approximately 0.4 for frequencies above 30 MHz. [7.1] The presence of surface roughness and ground undulations will serve to further reduce the magnitudes

7.1 (cont'd) of the rays propagated in this manner [7.2] (Rays 3 and 4 in Fig 7.2). By comparison, the grazing angle of the ray reflected on the base station side of the obstacle (Φ_1) has a value of approximately 0.01 radians, giving rise to a reflection coefficient with a theoretical magnitude in excess of 0.9.[7.1] The value of 120.8 dB derived by summing rays 1 and 2 in Fig 7.2 is therefore more realistic than those obtained using the other multi-ray constructions.

If it may be assumed that $d_1 >> d_2, h_1$ and h_0 (Fig 7.3), the diffraction loss for ray paths r_1 and r_2 can be approximately expressed, for v greater than unity [7.3], as:

$$A(v) \simeq \frac{\sqrt{\lambda d_2}}{2\pi(h_0 - h_2)}$$

If isotropic radiators are used, the total path loss for the construction of Fig 7.3 approximates to:

$$20 \log_{10} \left(\frac{2\pi d_1^2}{\sqrt{\pi d_2}} \cdot \frac{(h_0 - h_2)}{h_0 h_1} \right) \quad , \quad \text{dB}$$

The Edwards and Durkin model utilises the same diffraction loss value as stated above but incorporates the plane earth expression to give:

$$20 \log_{10} \left(\frac{2\pi d_1^2}{\sqrt{\pi d_2}} \cdot \frac{(h_0 - h_2)}{h_1 h_2} \right) \quad , \quad \text{dB}$$

The error generated in the use of the Edwards and Durkin model is therefore:

$$20 \log \frac{h_0}{h_1} \quad , \quad \text{dB}$$

7.1 (cont'd) For the situation under consideration, h_0 = 10 m and h_2 = 2m, the magnitude of the error is 15 dB. It should be noted that the predicted values in Table 7.1 obtained using the multi-ray analysis assumed a unity reflection coefficient but did not resort to the approximate knife-edge diffraction computation. The final solution may accordingly be seen to be sensitive to the factors involved in the determination of the magnitudes of the rays. The application of the multi-ray constructions is therefore limited to transmission paths which have accurately defined parameters. The use of approximations becomes necessary, however, if the propagation path loss prediction is to be calculated quickly and easily.

A final point to note is that, in a practical situation, the location of the reflecting plane is a difficult task, especially in a town or city. Indeed, it is unlikely to be a simple, smooth plane but more probably a large irregular surface supporting reflections of the rf signal over a large area. The magnitudes of the various parameters are therefore difficult to define but will rarely be the true values measured with respect to the local ground level, as were used in the computations of the figures in Table 7.1. Nevertheless, the accuracy attained using the mast heights appears sufficient to warrant their continued utilisation.

7.2 THE "FLAT CITY" MODEL

The results of the analysis of the small sector median path loss measurements detailed in Chapter 6 and the comparison of the prediction techniques given in Table 7.1 indicate that the transmission loss may be satisfactorily estimated at VHF by summing, in dB, the plane earth path loss and the diffraction loss incurred by the propagation of the signal over the buildings adjacent to the mobile terminal. At UHF a further correction was found to be necessary, accordingly termed the "UHF Correction Factor" (γ). This correction factor, given in Fig. 7.4, is the departure of the measured and the predicted curves shown in Fig. 6.5.

The "flat city" prediction model, so called because it does not incorporate factors to account for effects attributable to terrain features, is similar in form to that proposed by Edwards and Durkin (Section 4.5.2) for propagation over irregular terrain. The difference is that the diffraction loss for the terrain features computed in the Edwards and Durkin model is replaced in the "flat city" model by the diffraction loss for the buildings plus the UHF correction.

$$\text{Path Loss} = L_P + L_B + \gamma \quad , \text{dB}$$

7.2.1 COMPARISON OF THE BIRMINGHAM MEASURMENTS WITH PREDICTED VALUES

Path loss predictions calculated using the "flat city" model have been compared with the equivalent small sector median transmission loss measurements made in Birmingham. A statistical analysis of the prediction errors (measured-predicted path loss values) obtained using all the 918 Birmingham measurements at 85.875, 167.2 and 441.025 MHz

7.2.1 (cont'd) revealed the mean prediction error to be 0.8 dB with a standard deviation of 8 dB. The performance of the model at each individual frequency is shown in Table 7.2.

Frequency	Mean Error	Standard Deviation of Error
MHz	dB	dB
85.875	1.8	7.5
167.2	2.3	6.5
441.025	-2.4	8.2

TABLE 7.2

PERFORMANCE OF THE "FLAT CITY" PREDICTION MODEL IN BIRMINGHAM

The standard deviations of the prediction errors at each of the frequencies shown in Table 7.2 are similar to those obtained using the range regressions (Tables 6.1 and 6.2). The performance of the proposed model is therefore comparable with that of a purely statistical approach tailored specifically to the measured data.

The mean prediction error derived using this "flat city" model can be seen to be sufficiently small to vindicate its use over level ground but the validity of its application to other types of ostensibly flat cities must be investigated further.

7.2.2 COMPARISON OF THE BATH MEASUREMENTS WITH PREDICTED VALUES

The elevated position of the transmitter site at the University of Bath (Figure 5.11) afforded an unobstructed view of a large part of the city centre. The Bath measurements will accordingly be assumed to have been obtained from a flat city situated on a sloping base as represented in Figure 5.12.

7.2.2 (cont'd) A statistical analysis of the prediction errors obtained using the "flat city" model revealed the following:

Mean Prediction Error	= 3.6 dB
Standard Deviation of the Prediction Errors	= 7.9 dB
Total Number of Measurements Analysed	= 98

The increase in the mean prediction error over that arising from the Birmingham analysis is a possible result of the partial intrusion by the shoulder of the valley into the first Fresnel zone ellipsoid having the transmitter and receiver as foci, therefore requiring that a correction should be included for the terrain diffraction loss produced. However, the magnitudes of the mean error and the standard deviation of the errors are sufficiently small to suggest that the "sloping-flat city" assumption has been largely verified and that the "flat city" model could become a viable prediction technique.

7.3 THE "HILLY CITY" PREDICTION MODEL

The influences of terrain irregularities on the propagation path loss have not been considered in the preceding analysis and consequently the "flat city" model is only applicable to cities built on sensibly level ground. Further investigations must therefore be conducted to establish an appropriate means of quantifying the effects of the various geographical parameters, i.e. the terrain diffraction losses, and to determine how these additional factors should be incorporated into a mathematical prediction model. The resulting "hilly city" model may ultimately be dissimilar from the "flat city" version as a result of

7.3 (cont'd) the existence of differing propagation mechanisms, notably in the inability of rough or mountainous terrain to support a coherent reflection from the ground surface. In this case the criteria governing the use of the two models must be defined. However, it would be preferable if a single model could be formulated for use in cities constructed on any type of terrain, this latter "continuous" model reducing to the "flat city" form as the terrain diffraction loss becomes negligible.

Values of terrain diffraction loss determined using the Bullington (Section 4.4.2.1), Epstein-Peterson (Section 4.4.2.2), Japanese atlas (Section 4.4.2.3) and Deygout (Section 4.4.2.4) approximate knife-edge models for the terrain profiles shown in Figure 5.13 are given in Table 7.3. As anticipated in Section 4.4.2.1 the Bullington Equivalent knife-edge construction underestimates the magnitude of the diffraction loss when it is compared with the remaining three methods. It is worth noting from Table 7.3 that the Epstein-Peterson, Japanese atlas and Deygout constructions produce similar values and that the additional compexity entailed in the application of the Deygout method does not therefore appear to be warranted. It is concluded from this cursory examination of the diffraction models that the Japanese atlas method is the most appropriate for the terrain profiles considered, having been shown [7.3] to be more accurate than the Epstein-Peterson model yet being easily calculable.

TABLE 7.3

COMPARISON OF DIFFRACTION LOSS MODELS OVER THE BRADFORD TERRAIN PATHS

Region	Profile Fig No	Diffraction Loss Models				Frequency	Number Of Obstacles
		Bullington	Epstein-Peterson	Japanese Atlas	Deygout		
		dB	dB	dB	dB	MHz	
Cottingley	5.13(a)	20.5 23.4 27.6	27.0 31.5 39.0	28.4 33.0 40.7	30.8 35.5 43.3	85.875 167.2 441.025	2
Greengates	5.13(b)	16.4 19.1 23.1	-	-	-	85.875 167.2 441.025	1
Eccleshill	5.13(c)	0.0 0.0 0.0	-	-	-	-	0
Undercliffe	5.13(d)	14.9 17.5 21.4	-	-	-	85.875 167.2 441.025	1
Shipley	5.13(e)	13.7 16.0 19.9	23.7 25.6 29.3	25.4 27.8 32.2	24.5 26.6 29.9	85.875 167.2 441.025	3
Bingley	5.13(f)	12.7 14.9 18.7	22.7 24.4 27.8	24.5 26.8 30.9	25.1 27.5 31.9	85.875 167.2 441.025	3
Illingworth Moor	5.13(g)	17.4 20.0 24.1	20.7 23.7 29.6	22.3 25.8 32.5	25.8 29.7 36.2	85.875 167.2 441.025	2

7.3 (cont'd) Three propagation prediction models are compared with measured path loss values in Table 7.4. These models, in detail, are:

(1) Edwards and Durkin Models (Section 4.5.2)

(a) Free space path loss + terrain diffraction loss
+ building diffraction loss
+ UHF correction

$$L_T = L_F + L_D + L_B + \gamma \quad , \text{dB}$$

(b) Plane earth path loss + terrain diffraction loss
+ building diffraction loss
+ UHF correction

$$L_T = L_P + L_D + L_B + \gamma \quad , \text{dB}$$

(2) Blomquist and Ladell Model (Section 4.5.3)

$$L_T = L_F + ((L_P - L_F)^2 + L_D^2)^{\frac{1}{2}} + L_B + \gamma \ , \quad \text{dB}$$

The limited data available appears to indicate that the Edwards and Durkin plane earth based model (1(b)) is the best of those examined for paths having an isolated obstacle while the Blomquist and Ladell model (2) gives the smallest prediction errors for paths having two or more obstructions. In the case involving an unobstructed path the Edwards and Durkin model (1(b)) and the Blomquist and Ladell model (2) agree. Even for the single obstacle situation the Blomquist and Ladell model produces a more accurate prediction than does the free space based Edwards and Durkin model (1(a)), and is within 10 dB of

7.3 (cont'd) prediction obtained using the plane earth Edwards and Durkin version (1(b)). The Blomquist and Ladell model therefore appears to be a reasonable compromise as the "hilly city" model and achieves compatability with the "flat city" case.

Region	Profile Fig No	Free Space Path Loss	Plane Earth Path Loss*	Edwards and Durkin Models		Blomquist & Ladell	Measured Path Loss	Frequency	No. of Obstacl
				1(a)	1(b)				
		dB	dB	dB	dB	dB	dB	MHz	
Cottingley	5.13(a)	86.7	110.0	126.5	140.8	133.0	135.5	85.875	2
		92.5		141.0	158.5	145.0	145.2	167.2	
		101.0		176.3	185.3	177.0	148.7	441.025	
Greengates	5.13(b)	85.4	107.6	113.7	135.9	125.0	145.0	85.875	1
		91.2		126.2	142.6	132.0	154.5	167.2	
		99.7		157.7	165.6	159.0	-	441.025	
Eccleshill	5.13(c)	83.2	103.0	92.2	112.0	112.0	114.8	85.875	0
		89.0		102.0	116.0	116.0	117.9	167.2	
		97.4		129.4	135.0	135.0	119.7	441.025	
Undercliffe	5.13(d)	84.5	105.6	116.3	137.4	127.0	140.0	85.875	1
		90.3		128.6	144.0	134.4	150.7	167.2	
		98.7		159.9	166.9	161.0	-	441.025	
Shipley	5.13(e)	86.0	108.5	119.5	142.0	128.0	136.8	85.875	3
		91.7		131.3	148.1	136.0	142.2	167.2	
		100.0		161.9	170.4	163.0	150.0	441.025	
Bingley	5.13(f)	89.2	115.0	123.3	149.0	134.0	141.0	85.875	3
		95.0		135.5	155.5	142.0	143.0	167.2	
		103.4		167.3	147.0	169.0	-	441.025	
Illingworth Moor	5.13(g)	90.9	118.4	125.7	153.2	137.6	136.0	85.875	2
		96.6		139.3	161.1	146.5	148.0	167.2	
		105.1		173.3	186.6	175.7	-	441.025	

* Aerial heights measured above local ground have been assumed

TABLE 7.4

COMPARISON OF PROPAGATION PREDICTION TECHNIQUES OVER THE BRADFORD TERRAIN PATHS

7.3.1 COMPARISON OF THE BRADFORD MEASUREMENTS WITH PREDICTED VALUES

A statistical comparison of path loss predictions calculated using the "hilly city" model and the corresponding small sector median transmission loss measurements obtained in Bradford has been performed. The statistical parameters were found to be:

Mean Prediction Error	= 5.5 dB
Standard Deviation of Error	= 10.7 dB
Total Number of Measurements Analysed	= 118

Insufficient experimental data have been collated over irregular terrain paths to enable any definite conclusions to be drawn but the error statistics derived from the Bradford measurements suggest that the "hilly city" prediction model may not be summarily dismissed.

7.4 THE OKUMURA EXTENDED MODEL

The Okumura prediction model has been applied by various authors [7.4, 7.5] to radio links operating in towns or cities and has given close agreement with measured values. This, coupled with the ability of the model to operate over all forms of terrain, with various building densities and at frequencies in the VHF and UHF bands, has led to the Okumura model being frequently quoted as a standard against which other prediction techniques are compared.

The Okumura model [7.6], described in detail in Section 4.5.6, was specifically formulated for use over the frequency range 100 to 3000 MHz. Extrapolation of the various curves to facilitate operation down in frequency to 75 MHz is a straightforward process and will not be reported.

7.4 (cont'd) Some of the correction curves given by Okumura are directly applicable in terms of the range between the two terminals and the transmission frequency, eg the basic median attenuation, while others are presented as functions of intermediate terrain factors, eg the base station height gain factor. The definitionsof these physical terrain parameters are only given in the literature for radio links having a total operating range greater than approximately 10 km, the precise range limit depending upon the factor to be calculated. The methods of calculating these parameters over paths of less than 10 km have not been clearly defined by Okumura [7.6].

If the Okumura propagation prediction model is to be employed for the 1 to 10 km urban radio link ranges under consideration a method must be devised whereby the terrain parameters may be calculated for any link greater than 1 km, thereby enabling all the various correction factors to be utilised. Suitable laws governing the computation of these terrain factors, produced largely by recourse to "engineering judgement", are presented. These are not necessarily the optimum choices and therefore a great deal of experimental validation of this "Okumura Extended" model is required before it may be freely employed.

7.4.1 BASE STATION AERIAL EFFECTIVE HEIGHT

For a radio link with the transmitter and receiver separated by a distance 'd', the base station effective aerial height is determined as the height of the base station aerial above the straight line curve fit to the terrain profile computed using the least squares error method over whichever of the following intervals is appropriate:

7.4.1 (cont'd)

$\frac{d}{4}$ to d	if 8 km $\geq$ d $\geq$ 1 km
3 km to d	if 15 km $\geq$ d > 8 km
3 km to 15 km	if d > 15 km

The base station is assumed to be located at zero range.

7.4.2 INTERDECILE TERRAIN UNDULATION HEIGHT

The interdecile terrain undulation height is calculated as the difference between 90% and 10% of the peak excursions of the terrain undulation height about the least squares regression line to the terrain profile over the following link range intervals:

(d - 10 km) to d	if d > 12 km
2 km to d	if 12 km $\geq$ d > 6 km
1 km to d	if 6 km $\geq$ d $\geq$1 km

7.4.3 AVERAGE VEHICULAR GROUND SLOPE

The average ground slope in the vicinity of the vehicular terminal is determined as the slope of the least squares regression line applied to the terrain profile over the following intervals:

1 km to d	if 4 km > d $\geq$ 1 km
2 km to d	if 7 km > d $\geq$ 4 km
(d - 5 km) to d	if 9 km > d $\geq$ 7 km

In the case where d $\geq$ 9 km, the larger of the computed slope values over the following intervals is taken:

7.4.3 (cont'd)

(d - 5 km) to d

and (d - 10 km) to d if d ≥ 12 km

or 2 km to d if d < 12 km

7.5 COMPARISON OF THE OKUMURA EXTENDED MODEL WITH MEASURED VALUES

Measured values of small sector median path loss have been selected from amongst the set of measurements made in Birmingham such that the corresponding locations of any two measurements were never closer than 1 km. A statistical evaluation of the errors obtained when predicting these transmission losses using the Okumura extended model and, for comparison, the "flat city" model is given in Table 7.5.

	Okumura Extended Model	"Flat City" Model
Mean Prediction Error (dB)	4.9	2.2
Standard Deviation of Error (dB)	7.7	6.75
Total Measurements	176	176

TABLE 7.5.

COMPARISON OF PREDICTION MODELS WITH THE BIRMINGHAM MEASUREMENTS

A similar comparison using the Bath measurements was found to be unfeasible because of the limited area (only a few square kilometers) over which the path loss values were obtained.

Predictions of the path loss for the terrain paths shown in Figure 5.13, calculated by both the Okumura Extended and the "hilly city"

7.5 (cont'd) models, are compared with the measured losses in Table 7.6. The two prediction techniques can be seen to produce very different estimates of the path loss at UHF, the Okumura model being the closer to the measurements. The UHF correction factor (Figure 7.4) incorporated into the "hilly city" model therefore appears to be inappropriate for highly obstructed terrain paths. However, insufficient data is available at UHF to enable a corrective procedure to be determined. At the 85.875 and 167.2 MHz frequencies the predictions calculated using both models can be seen to be similar to the measured values, thereby demonstrating that the models are adequate for general use. An important factor to note is that the number of computations required in the employment of the "hilly city" model is much less than in the Okumura Extended model.

TABLE 7.6

COMPARISON OF PREDICTION MODELS WITH THE BRADFORD MEASUREMENTS

Region	Profile Fig No	Predicted Path Loss		Measured Path Loss	Frequency	Number of Obstacles
		Hilly City Model	Okumura Extended Model			
		dB	dB	dB	MHz	
Cottingley	5.13(a)	133	130.6	135.5	85.875	2
		145	137.4	145.2	167.2	
		177	147.8	148.7	441.025	
Greengates	5.13(b)	125	128.4	145	85.875	1
		132	134.4	154.5	167.2	
		159	144.7	-	441.025	
Eccleshill	5.13(c)	112	111.5	114.8	85.875	0
		116	117.5	117.9	167.2	
		159	127.8	119.7	441.025	
Undercliffe	5.13(d)	127	123	140	85.875	1
		134.4	129	150.7	167.2	
		161	139.3	-	441.025	
Shipley	5.13(e)	128	123.2	136.8	85.875	3
		136	129.2	142.2	167.2	
		163	139.5	150	441.025	
Bingley	5.13(f)	134	130	141	85.875	3
		142	136	143	167.2	
		169	146.2	-	441.025	
Illingworth Moor	5.13(g)	137.6	139.5	136	85.875	2
		146.5	145.4	148	167.2	
		175.7	155.6	-	441.025	

7.6 REFERENCES

7.1 Rice P.L., Longley A.G., Norton K.A. and Barsis A.P.
"Transmission Loss Predictions for Tropospheric Communications Circuits"
N.B.S. Tech Note 101, 1967.

7.2 Beckmann P. and Spizzichino A.
"The Scattering of Electromagnetic Waves from Rough Surfaces"
International Series of Monographs on Electromagnetic Waves.
Pergamon Press

7.3 Hacking K.
"Approximate Methods for Calculating Multiple Diffraction Loss"
Electronics Letters, May 1966, Vol 2, No 5.

7.4 Jakes W.C. Jr
"Microwave Mobile Communications"
John Wiley and Sons, London.

7.5 Reudink D.O.
"Properties of Mobile Radio Propagation above 400 MHz"
IEEE Trans.Vehic.Tech.Vol VT-23, No 4, November 1974.

7.6 Okumura Y., Ohmori E., Kawano T. and Fukuda K.
"Field Strength and its Variability in VHF and UHF Land Mobile Service"
Rev.Elec.Comm.Lab.16, September - October 1968.

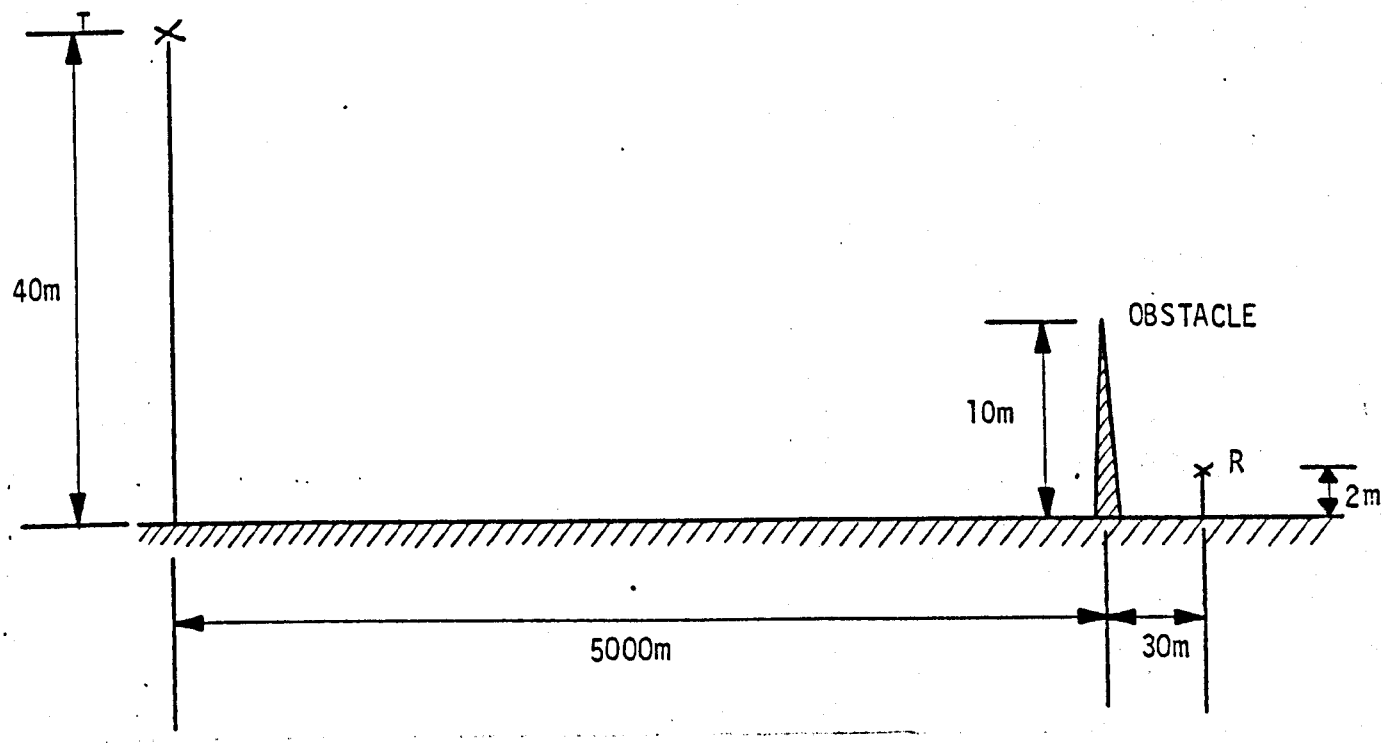

AN IDEALISED EXAMPLE OF A MEASURED TRANSMISSION PATH

FIG.7.1

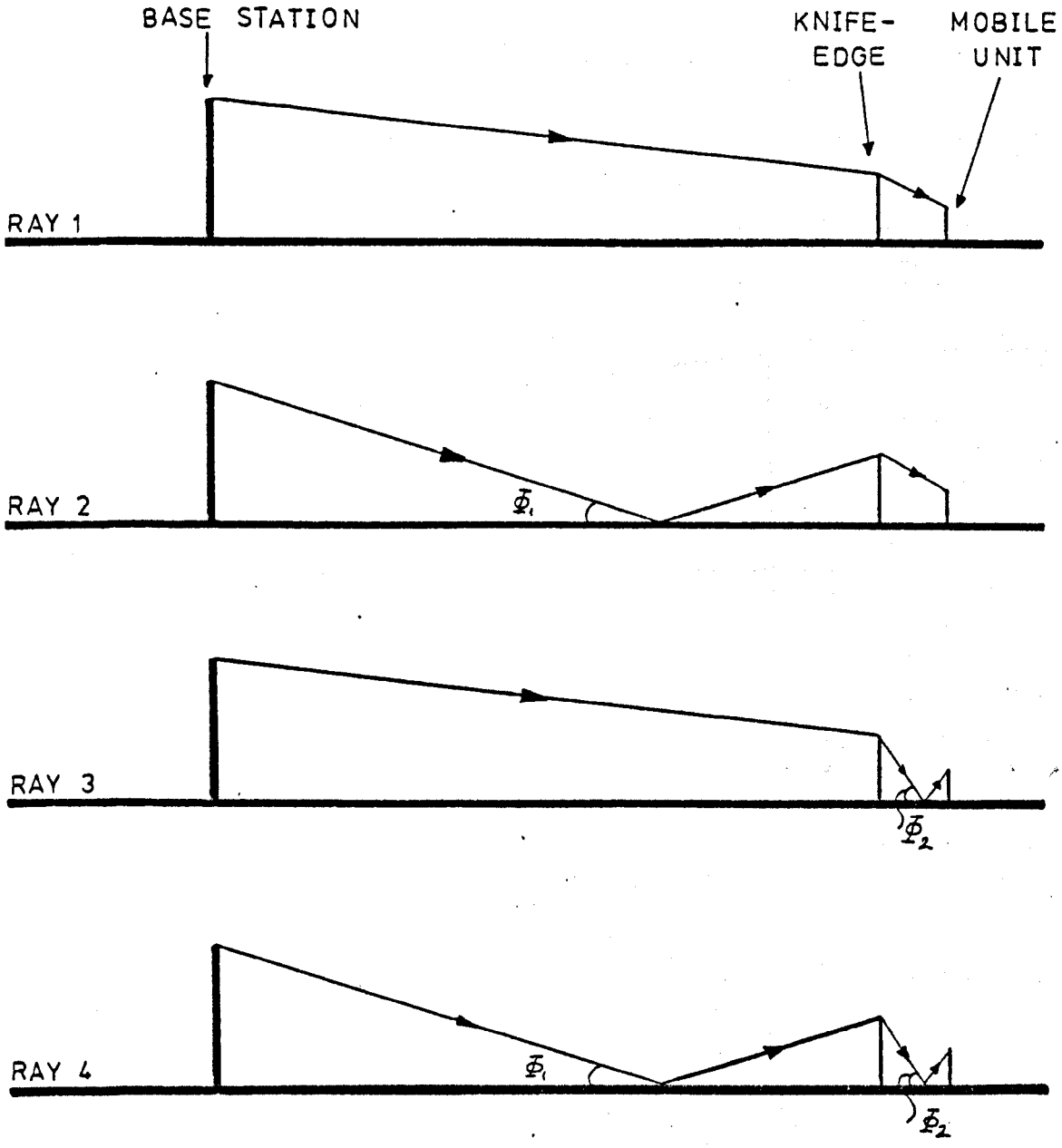

THE MULTI - RAY CONSTRUCTION

FIG. 7.2

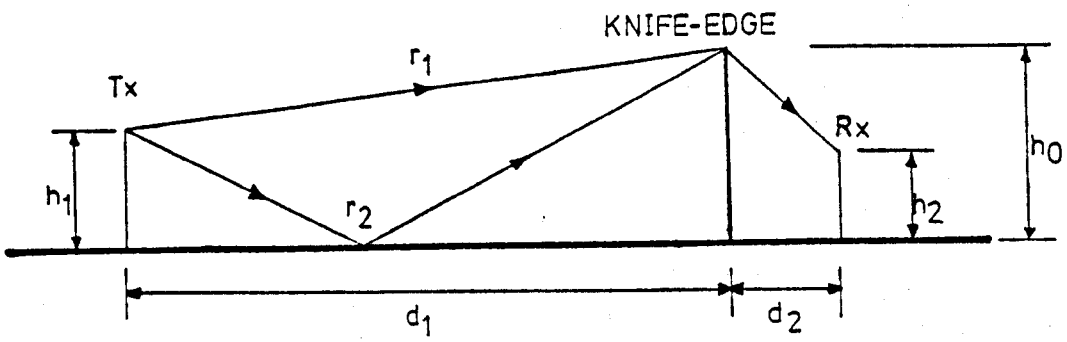

REFLECTIONS OVER A KNIFE-EDGE --FIG 7.3

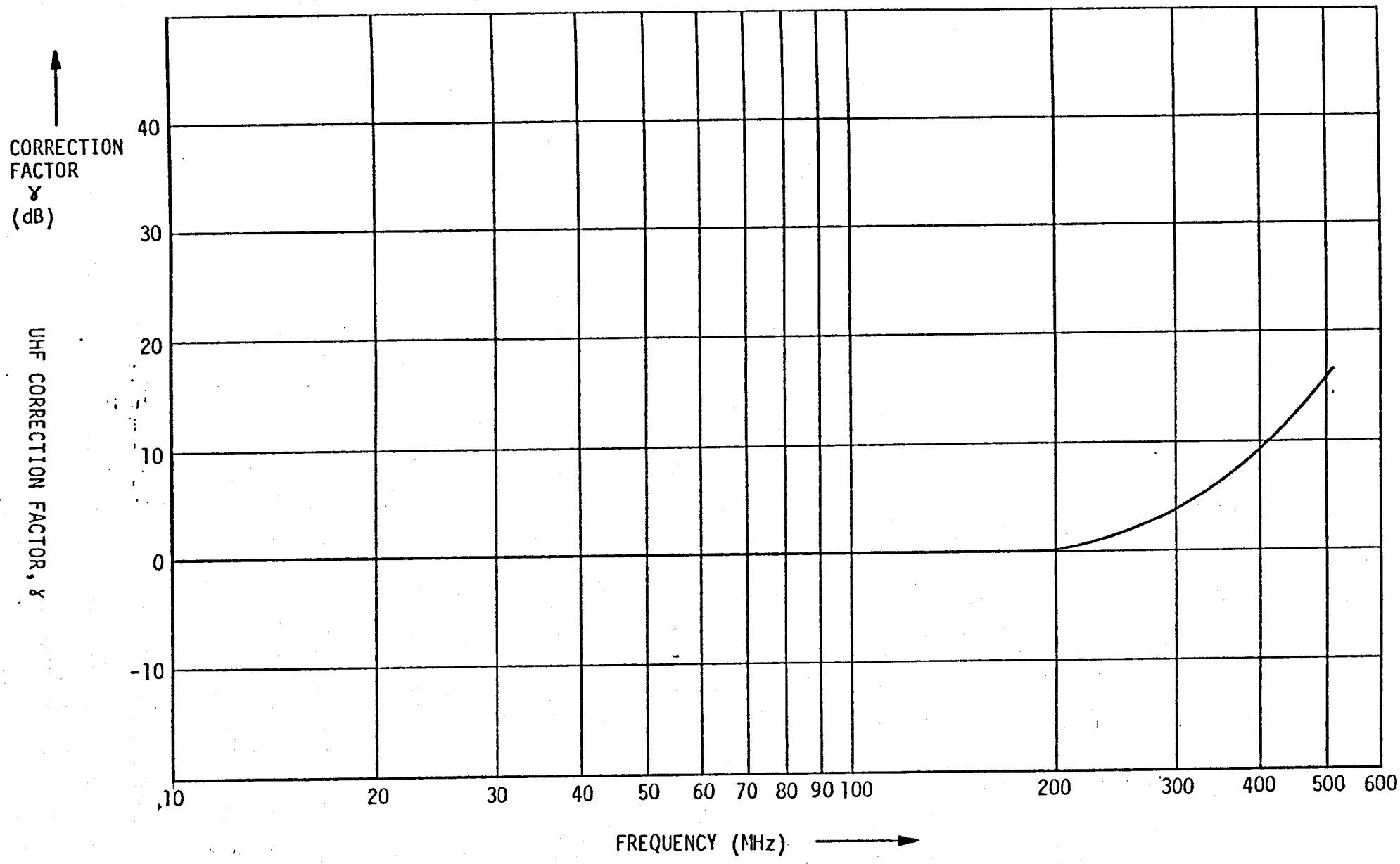

UHF CORRECTION FACTOR, γ

FIG. 7.4

CHAPTER 8

CONCLUSIONS

An investigation aimed at uniquely identifying the so-called slow and fast fading field components of the signal envelope experienced by a moving vehicular receiver using simple filtering techniques has been performed. This has shown thatthe improvement in the filtered output gained by recourse to raised cosine or triangular weighting functions rather than a rectangular window having the same overall width is negligible. In this context an improvement is judged to have been obtained if the magnitudes of the high frequency spectral components of the field are diminished, i.e. the ripple on the filtered waveform is reduced in amplitude.

The width of the window function was noted to influence the output waveform produced and is concluded to be a highly relevant parameter. In order to establish the optimum window width required to isolate the slow and fast fading fields, the autocovariance functions of low-pass filtered waveforms, determined using a 64 m rectangular window, have been calculated. These demonstrated that the slow fading signals changed by negligible amounts over distances of up to approximately 75 m. The optimum weighting function was therefore deduced to be rectangular in shape, and to encompass less than 75 m of the received signal record while containing sufficient data samples to ensure that a valid statistical estimate of the signals properties is obtained.

The fast fading signal patterns produced by high-pass filtering measured signal records using various window shapes and sizes have been examined. These have indicated that the resulting envelope probability

8 (cont'd) distribution, rather than being Rayleigh as anticipated from multi-path constraints, was better described as Weibull of the form:

$$P(x \leqslant X) = 1 - e^{-X^{2.5}} \quad ; \; X \geqslant 0$$

It has been suggested that this distributionis a consequence of the inherent inseparability, by simple filtering methods, of the slow and fast fading fields caused by an overlapping of the two frequency spectra. The terms "slow fading" and "fast fading" were therefore deemed to be inappropriate and it was recommended that the field pattern should be described in terms of the statistical parameters existing within "small sectors" over which all discernable factors influencing the received signal strength remain sensibly constant. The measured data were accordingly analysed in terms of small sector records comprising the equivalent of less than 250 m of the vehicle's movement. This distance was selected because such variables as street width, street orientation and the terrain profile of the transmission path were judged to remain largely unaltered.

The application of curves of the form $P_r \alpha (\text{Range})^{-n}$ to the median values of the small sector measured data using the least squares error method has shown the exponent (n) to have optimum values of 3.8, 3.9 and 2.4 at 85.875, 167.2 and 441.025 MHz respectively. These results lead to the hypothesis that a significant amount of the energy arriving at the receiver has undergonesome form of reflection from the ground surface over nearly all the paths at the two frequencies in the VHF band whereas this infrequently appears to be the case at the 441 MHz

8 (cont'd) frequency. This is perhaps to be expected from consideration of the Rayleigh criterion of roughness which evaluates the amplitudes of the surface irregularities in terms of the transmitted wavelength. As the frequency is raised, therefore, the larger the effective heights of the irregularities become and consequently the surface appears rougher. The magnitude of the coherent reflection from the surface at any given non-zero grazing angle is accordingly reduced.

The use of a curve of the type $P_r \propto (\text{range})^{-4}$ to describe the small sector median path loss measurements was found to produce negligible degradation of the error statistics at VHF over those obtained by the use of the optimum power law. The 441 MHz measured data, perhaps surprisingly, was found to yield only a slight increase in the standard deviation of the errors about the curve fit from 7.8 dB to 8.3 dB. It appears, therefore, that the received signal can be satisfactorily described using a model of the form proposed by Egli:

$$P_r = P_t G_t G_r \left(\frac{h_t h_r}{d^2}\right)^2 \beta$$

where "β" is termed the "urban clutter factor".

The urban clutter factor values for the measured small sector data, assuming that the aerial heights in the above expression are taken above local ground, have been demonstrated to be statistically well described by the diffraction loss over the buildings adjacent to the mobile terminal and lying on the line-of-sight path between the transmitter and the receiver. The use of knife-edge diffraction theory was

8 (cont'd) found to be adequate at the frequencies in the VHF band but grossly underestimated the total loss at UHF, possibly as a result of neglecting the large thickness of the buildings compared with the 60 cm wavelength.

Two mathematical models have been proposed to facilitate the prediction of the median small sector propagation path loss, one empirical and the other semi-theoretical. The empirical method is an extension to the Okumura model formulated to enable all the relevant correction factors to be utilised for any link range greater than 1 km. The semi-theoretical method, on the other hand, is based on a technique accredited to Blomquist and Ladell and includes correction factors found to be necessary from the analysis of the measurements. This latter model evaluates the propagation path loss, in dB, as:

$$\text{Free Space Path Loss} + \left((\text{Plane Earth Path Loss} - \text{Free Space Path Loss})^2 + (\text{Terrain Diffraction Loss})^2\right)^{\frac{1}{2}} + \text{Diffraction Loss over the Adjacent Obstructing Buildings} + \text{UHF Correction Factor}$$

The terrain diffraction loss required as a parameter in the model has been found to be satisfactorily estimated using a construction suggested by the Japanese Postal Service, and this method is recommended even though the Epstein-Peterson construction was advocated in Blomquist and Ladell's original publication. By comparison the Bullington equivalent knife-edge model was thought to underestimate the loss while, over the paths under consideration, the Deygout construction did not warrant the considerable complexity entailed by its use.

8 (cont'd) The UHF correction factor is the deviation of the measured path loss values from predictions based on simple knife-edge diffraction theory and is only significant at frequencies above approximately 200 MHz.

Predictions derived using both models have been compared with the corresponding path loss values measured over the flat terrain of Birmingham, the sloping ground of Bath and the hills of Bradford. In the case of the semi-theoretical model the mean errors were found to be consistantly less than 6 dB in magnitude while the empirical model exhibited a slightly worse performance. The standard deviations of the prediction errors were deemed to be comparable with those produced using a purely statistical approach and, as such, were small. The use of both techniques therefore appears to have been vindicated and little can be seen, insofar as the prediction accuracy is concerned, to recommend one rather than the other. The semi-theoretical model, however, utilises physical urban parameters and may be interpreted to give an indication of the propagation mechanisms existing in an urban mobile radio situation.

It is worth noting that the number of computations required to evaluate the propagation path loss prediction using the empirical Okumura model is far greater than that needed by the semi-theoretical model to obtain a largely similar prediction accuracy. It is therefore concluded that the Okumura prediction model is more complex than is essential for applications involving British cities.

APPENDIX A

AN ANALOGUE-TO-DIGITAL CONVERSION SYSTEM FOR THE ANALYSIS OF STOCHASTIC WAVEFORMS

A.1 INTRODUCTION

The analysis and subsequent characterisation of random signals require that large quantities of data are considered. Even the calculation of such simple parameters as the mean value and standard deviation needsmany hundreds of individual measurements from a single ensemble if negligible statistical errors are to result. In this type of situation the application of digital computers is beneficial both as bulk data storage devices and for the high processing speeds attainable. Analogue waveforms cannot be handled as such, but must be converted into digital form before they are manipulated by digital computers. The monitoring of the analogue-to-digital conversion process and the subsequent transcription to a high capacity storage unit, such as magnetic disc or tape, calls for the total involvement of the computer's central processor unit for the duration of the digitisations. The permanent utilisation of the central processor unit is generally unavailable on large computer installations because of the inefficiency incurred and consequential prohibitive cost.

A system for performing analogue-to-digital conversions using a PDP-11 minicomputer is described in the following sections.

A2 THE ANALOGUE-TO-DIGITAL CONVERTER ASSEMBLY

A2.1 THE SYSTEM REQUIREMENTS

A general purpose analogue-to-digital conversion system having eight multiplexed analogue input channels was required. The assembly was required to operate in conjunction with a PDP-11 minicomputer and must commence conversions upon receipt of either an external (user supplied) or internal (computer supplied) convert command pulse.

A2.2 THE GENERAL INTERFACE UNIT

Operational on the PDP-11 minicomputer at the Department of Electronic and Electrical Engineering during the design phase were a series of general purpose data buffers and status registers connected to the computer's "uni-bus" peripheral communications system. The schematic diagram and a list of the connections to this general interface unit are given in Figs.A1 and A2 respectively.

A2.3 THE ANALOGUE-TO-DIGITAL CONVERTER

An analogue-to-digital converter and eight channel analogue multiplexer with the specifications shown in Table A.1 were connected to the general interface unit (Section A2.2) as detailed in Fig.A3. The quantisation interval available using this system is approximately 5 mV with a peak signal capability of ± 10 V.

Data buffer 1 (Address: 160002) holds the three bit code needed to select the multiplexer input channel. This lies in the range 0 to 7.

Data buffer 2 (Address: 160004) stores the digital output of the analogue-to-digital converter. This is sign extended (bit 12) to

A2.3 Cont'd occupy all the available 16 bits of the standard PDP-11 word. The buffer is loaded only while the converter is inactive, determined by performing a logical 'AND' function on each of the individual bits with the $\overline{\text{STATUS}}$ output from the converter.

Bit 0 of the status register (Address: 160000) flags the current state of the analogue-to-digital converter. It is set while a conversion is in process and is cleared on completion. The bit is loaded by a logical 'AND' operation between the STATUS line of the converter and the logical 'OR' of monostable multivibrators connected to the STATUS and $\overline{\text{STATUS}}$ outputs. The condition of the STATUS function is loaded, therefore, when either conversion starts (STATUS becomes positive) or when conversion stops ($\overline{\text{STATUS}}$ becomes positive).

Conversion may be commanded by a +5 V pulse supplied either externally or by a programmed reference to the 'SELECT 10' pulse (Address: 160010).

A3 THE ANALOGUE-TO-DIGITAL CONVERSION PROGRAMME

The electronic system described in the previous sections is of little use in its own right. To achieve versatility and efficiency of operation, the PDP-11 minicomputer must be programmed to function in conjunction with the converter assembly.

The tasks to be performed by the programme are basically the monitoring of the conversion process and the subsequent storage of the digitised samples on a bulk storage peripheral, in this instance a high packing density magnetic disc. It is vital that no time is wasted during the execution of the real time operations assigned by the programme, a

A3 Cont'd factor which rules out any possibility of using a high level computer language (e.g. FORTRAN IV) and necessitates the utilisation of an efficient coding system such as assembly language.

A3.1 THE PROGRAMME OUTLINE

A general purpose PDP-11 computer programme was required to operate in conjunction with the analogue-to-digital converter system working under externally clocked conditions. The functions performed fall into three sections:-

1. A programme pre-amble comprising the operator commands (input/output functions on teletype), disc file manipulation and checks prior to opening the file for write access.
2. A real time segment composed of recursively setting the multiplexer channel as required, monitoring of the converter status, reading the data word into core memory and transcription onto the disc file. This portion of the programme must fulfill its duties at the maximum speed possible.
3. A programme termination routine consisting of closing the disc file and communications with the operator.

A3.1.1 The Programme Pre-amble

A large number of the operations required by the programme are performed prior to the real time computing section. During this period the converter is assumed inactive, with the consequence that slow execution speed is tolerable. The steps transacted fall into two broad categories:-

A3.1.1 Cont'd

1. Operator - Programme Communications.
2. Magnetic Disc File management.

In order to achieve the minimum time wastage during the real time programme segment, the file on disc must be in the most compact form possible. This uses unformatted binary mode data in a contiguous file, thereby entailing no unnecessary disc head manipulations.

Data files may be easily handled using FORTRAN IV but the subsequent loss of speed during write processes is intolerable. This high level language is therefore restricted in its applicability, as far as this programme is concerned, to teletype management.

On a single disc drive computer installation the data must be written to the same physical magnetic disc as stores the system utility programmes. It is consequently imperative that the greatest care is taken when writing to this disc to ensure that a disc "wreck" does not occur. To guard against this possibility the programme only permits a file to be used which already exists on the disc. A full series of tests can then be performed to check the "start" and "end" disc file addresses, that the "length" is consistent with the difference between these and that it is a contiguous file. These checks are only available when using assembly language instructions.

A3.1.2 The Real Time Programme Segment

In order that the completed analogue-to-digital conversion system be capable of performing at the maximum clock speed attainable, while still maintaining the ability to handle the data output, the minimum

A3.1.2 Cont'd

number of programme steps are employed. The programme applicability and disc security are not sacrificed to achieve the desired speed. The steps necessary are:-

1. The analogue multiplexer input channel is selected prior to a conversion being commanded. This is performed at the earliest moment available within the programme.

   The multiplexer channel may be specified as a sequence of channels determined by the operator for the analysis to be performed.

2. The programme now waits for a conversion to commence. This is signalled when bit 0 of the status register becomes set. In waiting for this event, the programme ensures that only one sample is read from the converter for each digitisation performed.

   The system waits for an external convert command pulse to be supplied. Time can only be guaranteed to be available at this instant in the real time segment and all non-data manipulations must be performed here. One such important facility, hitherto unmentioned, is the ability for the operator to "HALT" the conversion process at any time and to "FINISH" when desired. The former request is required when the operator wishes to blank out a portion of the analogue waveform for any reason. In this case, the digital output of the converter is disregarded until the operator requests the continuation to be undertaken. The "FINISH" command is supplied by the user when no more of the conversions being performed are to be stored in the current disc file. The

A3.1.2. Cont'd

current core buffer is appended with zeros and written to disc as described in the following section. The fastest and most advisable means the operator has of signalling his intentions to the programme is by way of the computer console switch register. Of these, bit 0 is designated the "HALT" switch and bit 1 the "FINISH" switch. Switch down (clear) indicates that no action is required. If the programme finds both bits 0 and 1 set simultaneously, while waiting for a conversion to begin, the segment is exited via the programme termination section. If bit 0 is set and bit 1 is clear, the programme re-examines both bits sequentially until either changes. Bit 0 set prevents any examination of the converter status register being performed. Bit 0 clear, however, results in a recursive examination of the converter status register and bit 0 until either becomes set. The converter status becoming set causes a jump to the next step.

3. Having detected the start of an analogue-to-digital conversion the programme waits for the digitisation to be completed. This is heralded by bit 0 of the status register becoming clear.

4. Upon completion of a conversion, the digitised data sample is read into the next available word in a core memory data buffer. The routine is restarted from step 1 if this buffer is not full. When the data buffer is full, however, it is written to the next section of the disc file. The disc address is automatically incremented and a check made that this is within the file boundary. If this check proves false, an error is generated and

A3.1.2 Cont'd

the programme terminated. Providing that the disc address is valid, the data buffer pointer is reset and the routine restarted from step 1.

The magnetic disc on a PDP-11 installation uses blocks of 256 words regardless of the quantity of data supplied. Efficiency of operation is therefore improved by the use of the full block size, reducing the number of occasions on which the disc is accessed. The use of a single block buffer increases the versatility.

A3.1.3 The Programme Termination Routine

This routine is entered when the operator commands the programme to "FINISH" by use of the console switch register. The data buffer is appended with zeros and written to disc. The file is closed and details of the quantity of data handled are written on the teletype for user reference.

A3.2 THE PROGRAMME

The final programme is realised in two sections. The section manipulating the disc file and monitoring the conversion process is a FORTRAN IV subroutine written in assembly code. The FORTRAN "CALL" statement for this routine is:-

```
CALL ATOD (FILE, IX, ICH, ILOOP, IERR)
```

The variables input to the subroutine are:-

FILE; The disc filename for the data storage. This may be an

A3.2
Cont'd

array containing a Hollerith string in 3A4 format.

ICH; An array containing the required multiplexer sequence.

ILOOP; Four times the length of the multiplexer sequence. The quadruple arises because a FORTRAN variable uses 4 bytes of storage.

The variables output by the subroutines are:-

IX; Number of data points in the last block of file. This does not include the zeros written when the "FINISH" command was encountered.

ILOOP; The number of full and partially filled blocks of file written to disc.

IERR; An error indicator in the range 0 to 7. These values correspond to:-

0 : No error

1 : Filename error - illegal syntax

2 : A non-existant file

3 : A non-contiguous (linked) file

4 : File has an invalid disc start address

5 : File has an invalid disc end address

6 : Disc control was not ready at the time of a disc operation

7 : File is full.

Return to the main program is not possible if the subroutine is entered with an incorrect argument count. The program is commanded to "HALT" with zero displayed in the console register.

A3.2 Cont'd The complete programme is given in Fig.A4 and the outline flow diagram in Fig.A5.

A general purpose FORTRAN IV main programme is given in Fig.A6.

FUNCTION	A/D CONVERTER	ANALOGUE MULTIPLEXER
Power Supply	+15V @30mA -15V@40mA +5V@300mA	+15V@5mA -15V@45mA +5V@13mA
Number of Inputs	1	8
Analogue Input Range	±10V	±10V
Analogue Output Range	-	±10V
Input Impedance	>1MΩ	>1KΩ
Settling Time	-	7μs for 20V step
Digital Output	12 bits (inc. sign) Binary (2's comp.)	-
Conversion Time	30μs	-
Convert command Pulse	>100ms >2.0V	-
Maximum Conversion Rate	4kHz	-

Table A.1

Specifications of the Analogue - to - Digital Converter and Analogue Multiplexer

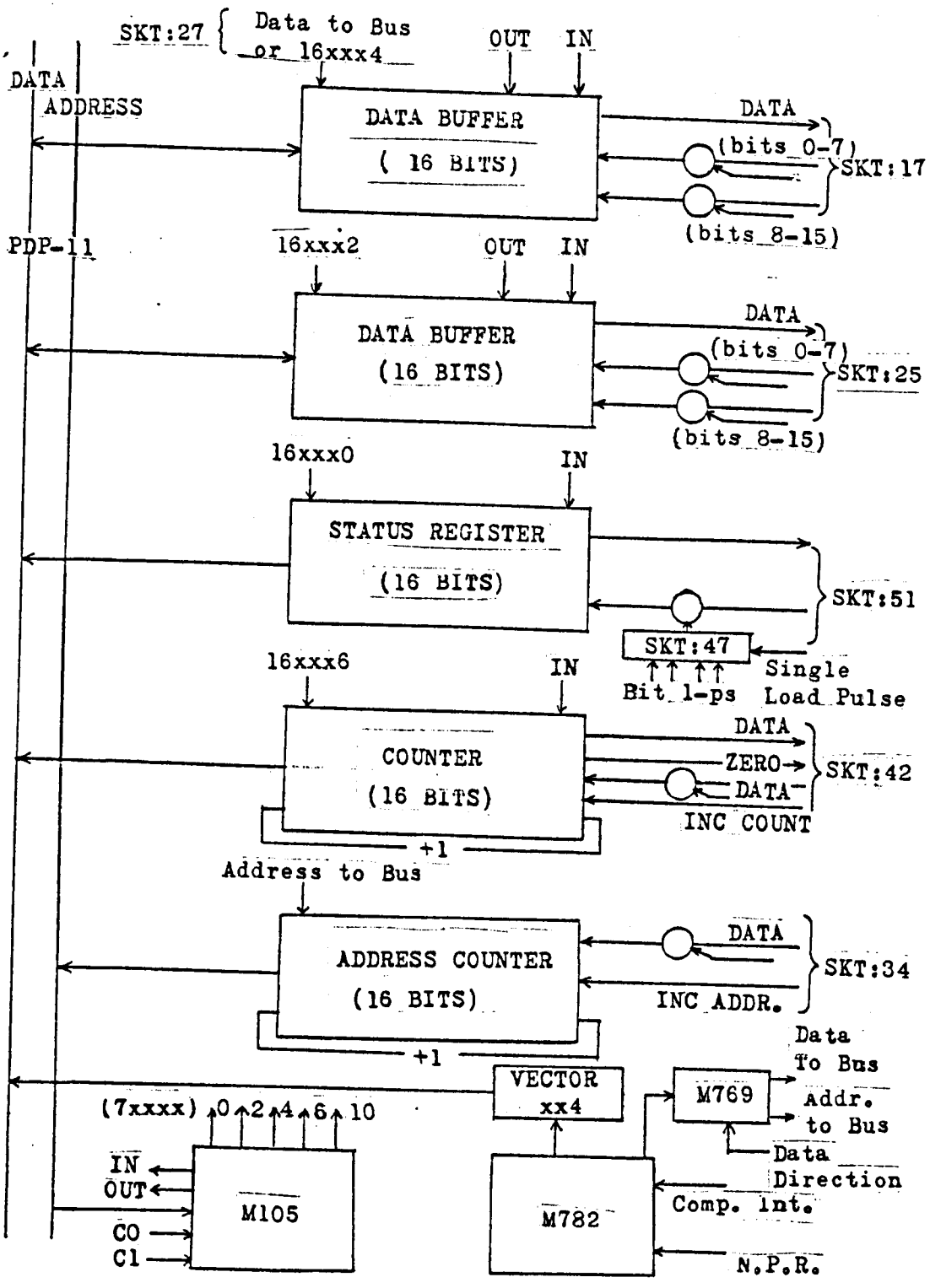

THE GENERAL INTERFACE UNIT

FIG A.1

DATA BUFFER

TWO DATA BUFFERS ARE AVAILABLE, EACH ARE 16 BIT. INPUT AND OUTPUT DATA FOR EXTERNAL USE ARE AVAILABLE AT SKT: POSITIONS 17 & 25 VIA A 43 WAY EDGE CONNECTOR BOARD TYPE:- "CABLE BOARD/8/01".

ALL OUTPUT SIGNALS FROM THIS UNIT ARE VIA OPEN COLLECTOR LOGIC THEREFORE IT IS SUGGESTED THAT ALL USERS NOT WORKING ADJACENT TO THE P.D.P. 11 SHOULD RECIEVE THESE SIGNALS AT THEIR UNIT WITH THE FOLLOWING CIRCUIT. THOSE WHO ARE WORKING ADJACENT TO THE COMPUTER REQUIRE ONLY A 1K RESISTOR TO THE +5V SUPPLY LINE ON EACH SIGNAL RECIEVED.

SIGNALS RECEIVED BY THE INTERFACE, FROM USERS NOT ADJACENT TO THE COMPUTER, ARE ASSUMED TO BE FROM OPEN COLLECTOR LOGIC I.E.

THIS DOES NOT AFFECT OTHER USERS.
PIN CONNECTIONS FOR BOTH DATA BUFFERS ARE AS FOLLOWS. ALL SIGNAL NAMES ARE WITH RESPECT TO THE INTERFACE AND ARE HIGH FOR ASSERTION.
L.S.B.=00

PIN NO:	USE	PIN NO:	USE
1	EARTH	21	I/P LOAD PULSE (HIGH)
2	EARTH	22	SLT 10 PULSE
3	I/P 00	23	COMPUTER INT:
4	I/P 01	24	
5	I/P 02	25	
6	I/P 03	26	O/P 00
7	N/C	27	O/P 01
8	I/P 04	28	O/P 02
9	I/P 05	29	O/P 03
10	I/P 06	30	O/P 04
11	I/P 07	31	O/P 05
12	I/P 08	32	O/P 06
13	I/P 09	33	O/P 07
14	I/P 10	34	O/P 08
15	I/P 11	35	O/P 09
16	I/P 12	36	O/P 10
17	I/P 13	37	O/P 11
18	I/P 14	38	O/P 12
19	I/P 15	39	O/P 13
20	I/P LOAD PULSE (LOW)	40	O/P 14
		41	O/P 15

STATUS BUFFER

ONE 16 BIT STATUS BUFFER IS AVAILABLE. EACH OF THE 16 BITS CAN BE LOADED INDIVIDUALLY OR ONE PULSE CAN BE USED TO LOAD ALL 16 BITS. CONECTIONS FOR I/P DATA & SINGLE PULSE LOAD ARE MADE VIA SKT: POSITION 51 USING A 43 WAY EDGE CONNECTOR BOARD TYPE:- CABLE BOARD/8/01. TO LOAD BITS INDIVIDUALLY THE BOARD IN POSITION 47 IS REMOVED AND A 43 WAY EDGE CONNECTOR BOARD USED TO CONNECT TO THE INDIVIDUAL LOAD LINES.

AS FOR THE DATA BUFFER ALL O/P SIGNALS ARE VIA OPEN COLLECTOR

LOGIC.

PIN CONNECTIONS FOR THE BUFFER ARE AS FOLLOWS. ALL SIGNAL NAMES ARE WITH RESPECT TO THE INTERFACE AND ARE HIGH FOR ASSERTION. L.S.B. =00.

PIN NO:	USE	PIN NO:	USE
1	EARTH	21	COMPUTER INT:
2	EARTH	22	INIT:
3	I/P 00	23	
4	I/P 01	24	
5	I/P 02	25	
6	I/P 03	26	O/P 00
7	N/C	27	O/P 01
8	I/P 04	28	O/P 02
9	I/P 05	29	O/P 03
10	I/P 06	30	O/P 04
11	I/P 07	31	O/P 05
12	I/P 08	32	O/P 06
13	I/P 09	33	O/P 07
14	I/P 10	34	O/P 08
15	I/P 11	35	O/P 09
16	I/P 12	36	O/P 10
17	I/P 13	37	O/P 11
18	I/P 14	38	O/P 12
19	I/P 15	39	O/P 13
20	I/P LOAD PULSE	40	O/P 14
		41	O/P 15

PIN CONNECTIONS FOR THE EDGE CONNECTOR BOARD USED TO LOAD ALL 16 BITS INDIVIDUALLY ARE AS FOLLOWS

PIN NO:	USE
1	EARTH
2	EARTH
3	I/P LOAD PULSE 00
4	I/P LOAD PULSE 01
5	I/P LOAD PULSE 02
6	I/P LOAD PULSE 03
7	N/C
8	I/P LOAD PULSE 04
9	I/P LOAD PULSE 05
10	I/P LOAD PULSE 06
11	I/P LOAD PULSE 07
12	I/P LOAD PULSE 08
13	I/P LOAD PULSE 09
14	I/P LOAD PULSE 10
15	I/P LOAD PULSE 11
16	I/P LOAD PULSE 12
17	I/P LOAD PULSE 13
18	I/P LOAD PULSE 14
19	I/P LOAD PULSE 15

COUNTER

ONE 16 BIT COUNTER IS AVAILABLE. INPUT DATA, INCREMENT CLOCK, AND "COUNTER = ZERO SIGNAL" CONNECTIONS ARE AVAILABLE AT POSITION 42 VIA A 43 WAY EDGE CONNECTOR BOARD TYPE :- CABLE BOARD/3/01 AS FOR THE DATA BUFFER ALL OUTPUT SIGNALS ARE VIA OPEN COLLECTOR LOGIC.

PIN CONNECTIONS FOR THE COUNTER ARE AS FOLLOWS. ALL SIGNAL NAMES

ARE WITH RESPECT TO THE INTERFACE AND ARE HIGH FOR ASSERTION L.S.B=00.

PIN NO:	USE	PIN NO:	USE
1	EARTH	21	COUNTER=ZERO
2	EARTH	22	INC: CLOCK
3	I/P 00	23	
4	I/P 01	24	
5	I/P 02	25	
6	I/P 03	26	O/P 00
7	N/C	27	O/P 01
8	I/P 04	28	O/P 02
9	I/P 05	29	O/P 03
10	I/P 06	30	O/P 04
11	I/P 07	31	O/P 05
12	I/P 08	32	O/P 06
13	I/P 09	33	O/P 07
14	I/P 10	34	O/P 03
15	I/P 11	35	O/P 09
16	I/P 12	36	O/P 10
17	I/P 13	37	O/P 11
18	I/P 14	38	O/P 12
19	I/P 15	39	O/P 13
20	I/P LOAD PULSE	40	O/P 14
		41	O/P 15

ADDRESS COUNTER

ONE 16 BIT ADDRESS COUNTER IS AVAILABLE. THIS IS ONLY REQUIRED WHEN NON-PROCESSOR REQUESTS ARE TO BE CARRIED OUT. INPUT ADDRESS, INCREMENT CLOCK, AND N.P.R CONTROL SIGNAL CONNECTIONS ARE AVAILABLE AT POSITION 34 VIA A 43 WAY EDGE CONNECTOR BOARD TYPE :- CABLE BOARD/8/01. AS FOR THE DATA BUFFER ALL OUTPUT SIGNALS ARE VIA OPEN COLLECTOR LOGIC.

PIN CONNECTIONS FOR THE COUNTER ARE AS FOLLOWS. ALL SIGNAL NAMES ARE WITH RESPECT TO THE INTERFACE AND ARE HIGH FOR ASSERTION L.S.B=00.

PIN NO:	USE	PIN NO:	USE
1	EARTH	21	
2	EARTH	22	INC: CLOCK
3	I/P 00	23	
4	I/P 01	24	
5	I/P 02	25	TIME OUT
6	I/P 03	26	N.P.R DIRECTION
7	N/C	27	END CYCLE
8	I/P 04	28	OBTAIN BUS FOR N.P.R
9	I/P 05	29	
10	I/P 06	30	
11	I/P 07	31	
12	I/P 08	32	
13	I/P 09	33	
14	I/P 10	34	
15	I/P 11	35	
16	I/P 12	36	
17	I/P 13	37	
18	I/P 14	38	
19	I/P 15	39	
20	I/P LOAD PULSE	40	

M 105'

THE M 105' ADDRESS SELECTOR PROVIDES GATING SIGNALS FOR INPUT AND OUTPUT OF DATA FROM THE P.D.P. 11. THE ADDRESS OF THE INTERFACE CAN BE CHANGED BY THE POSITION OF THE CONNECTORS ON THE FRONT. THIS ADDRESS CAN BE SET BETWEEN 160000 & 177760 OCTAL AS THE 4 L.S.B. ARE NOT CHANGABLE BY HARDWARE.
A LINK INSERTED = 0

4	5	6	7	8	9	10	11	12

M 782

THE M 782 INTERUPT BOARD PROVIDES INTERUPT OF THE P.D.P 11 AND ALSO A UNIQUE VECTOR ADDRESS BETWEEN 004 & 374 OCTAL.
A LINK INSERTED = 0

VECTOR =	X	X	4

LOCATION 27

IF A N.P.R IS TO BE CARRIED OUT BY THE INTERFACE THE BOARD IN LOCATION 27 SHOULD BE REPLACED BY THE ONE MARKED "N.P.R" FOR ALL OTHER USES THE BOARD IN THAT LOCATION SHOULD BE THE ONE MARKED "INT".

NON-PROCESSOR REQUESTS

TRANSFER OF DATA BETWEEN THE INTERFACE AND MEMORY CAN BE CARRIED OUT VIA A N.P.R. THE DATA TO BE TRANSFERED SHOULD BE PLACED IN,OR RECEIVED FROM,THE DATA BUFFER USING LOCATION 17 THE ADDRESS OF THE TRANSFER SHOULD BE IN THE ADDRESS COUNTER. THE DIRECTION OF TRANSFER IS DETERMINED BY A LEVEL ON PIN 26 OF LOCATION 34. +3.6VOLTS =TO MEMORY GROUND= FROM MEMORY

TIME OUT

THIS SIGNAL WILL BE ASSERTED (H) BEFORE A N.P.R IS CARRIED OUT, IF AN ERRONEOUS ADDRESS IS IN THE ADDRESS REGISTER,OR IF THE SLAVE FAILS TO RESPOND IN 20 MICROSECONDS.

END CYCLE

AN END CYCLE PULSE WILL BE ASSERTED AT THE END OF EACH N.P.R DATA TRANSFER AND IS USUALLY USED TO RELEASE CONTROL OF THE BUS.

INITIALIZATION (INIT)
---------- ------

THIS SIGNAL IS ASSERTED BY THE PROCESSOR WHEN THE START KEY ON THE CONSOLE IS DEPRESSED, WHEN A REST INSTRUCTION IS EXECUTED, OR WHEN THE POWER FAIL SEQUENCE OCCURS. IT CAN BE USED TO CLEAR AND INITIALIZE PERIPHERAL DEVICES.

I/P LOAD PULSE
--- ---- -----

A PULSE OF AT LEAST 150 NANOSECONDS DURATION AND LOGICAL "1" LEVEL >2.0VOLTS IS REQUIRED AS AN INPUT LOAD PULSE TO ALL BUFFERS AND REGISTERS.

THE DATA TO BE LOADED SHOULD BE PRESENT ON THE INPUT LINES FOR THE COMPLETE DURATION OF THE LOAD PULSE.

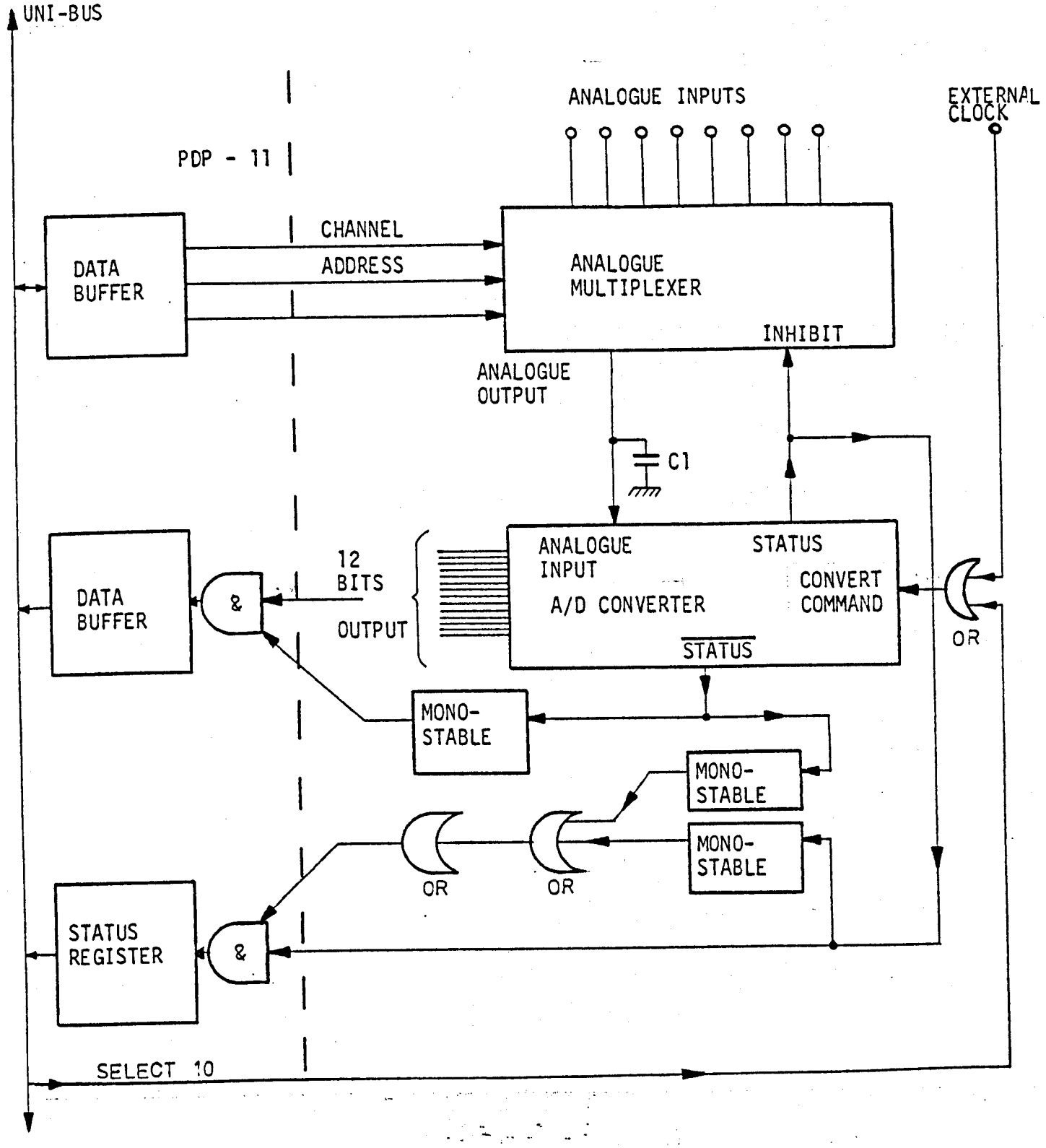

THE A - D CONVERTER

FIG. A. 3

```
;ATOD.MAC

;ANALOG TO DIGITAL FORTRAN SUBROUTINE
; - FOR USE WITH EXTERNAL CLOCK PULSES

;ALLOCATE CONTIGUOUS FILE BEFORE CALLING:
;       CALL ATOD('FILE.EXT',IX,ICH,ILOOP,IERR)
;'FILE.EXT' MAY BE INSTEAD A REAL ARRAY DIMENSION 3
;(READ INTO ARRAY IN 3A4)
;IX RETURNS FINAL DATA POSITION WITHIN FINAL BLOCK (<256.)
;ARRAY ICH CONTAINS MULTIPLEXER CHANNEL SEQUENCE
;ILOOP IS FOUR TIMES THE DIMENSION OF ICH,
; AND RETURNS NUMBER OF BLOCKS TRANSFERRED.
;IERR RETURNS 0 FOR NO ERROR OR:
;       1 FILENAME ERROR
;       2 FILE DOES NOT EXIST
;       3 FILE NOT CONTIGUOUS
;       4 INVALID START BLOCK
;       5 INVALID END BLOCK
;       6 DISK CONTROL WAS NOT READY
;       7 FILE FULL
;       HALT WITH 0 IN DISPLAY REGISTER: WRONG NO OF ARGUMENTS
;       DITTO WITH 177777: DISK DRIVE NOT READY
;       - OTHERWISE DISPLAYS RKER AFTER A DISK ERROR
;SWITCH REGISTER BIT 0: UP = PAUSE
;                      DOWN = GO / CONTINUE
;SWITCH REGISTER BIT 1: UP = FINISH
;(CURRENT BLOCK APPENDED WITH ZEROS)
;                      DOWN = NORMAL OPERATION

        .TITLE ATOD
        .GLOBL ATOD
        .MCALL  .INIT,  .LOOK

R0=%0
R1=%1
R2=%2
R3=%3
R4=%4
R5=%5
SP=%6
PC=%7

STATUS=160000
BUF=STATUS!4
CHAN=STATUS!2
SWR=177570

RKDS=177400     ;DRIVE STATUS
RKER=177402     ;ERROR REGISTER
RKCS=177404     ;CONTROL REGISTER
RKWC=177406     ;WORD COUNT
RKBA=177410     ;BUS ADDRESS
RKDA=177412     ;DISK ADDRESS
RKDB=177416     ;DATA BUFFER

        0,0
FILBLK: 0,0,0
        0
```

```
        0

        0
LNKBLK: 0
        0
        .BYTE 1,0
        .RAD50 /DK/

FILE:   0,0,0,0,0

ATOD:   CLR R0          ;HALT WITH 0 IN DISPLAY REGISTER
        CMPB (R5),#5    ;5 ARGS ?
        BEQ .+4
        HALT
        CLR @12(R5)     ;NO ERRORS YET !,IERR=0
        MOV 2(R5),R0            ;FILENAME.EXT
        MOV #FILE,R1
        MOV #7,R2       ;7CHARACTERS (+'.') MAXIMUM
NCHAR:  TSTB (R0)       ;ANY CHARACTERS LEFT (' ')
        BEQ FIN         ;NO
        CMPB (R0),#40
        BEQ FIN
        CMPB (R0),#56   ;='.'?
        BEQ EXT         ;YES
        MOVB (R0)+,(R1)+        ;NO,UNPACK NAME
        DEC R2
        BNE NCHAR
ERR1:   MOV #1,@12(R5)  ;FILENAME ERROR
        RTS R5
EXT:    INC R0
        MOV #4,R2
SPCHR:  CMP R1,#FILE+6
        BEQ NCHAR
        BHI ERR1
        MOVB #40,(R1)+
        BR SPCHR
FIN:    CMP R1,#FILE+11 ;LAST CHARACTER?
        BEQ PACK                ;YES
        BHI ERR1                ;TOO MANY!
        MOVB #40,(R1)+
        BR FIN
PACK:   MOV #FILBLK,R3
        MOV #FILE,-(SP)
NPK:    CLR -(SP)
        EMT 42          ;.RADPK
        BCS ERR1
        MOV (SP)+,(R3)+
        CMP R3,#FILBLK+6
        BLO NPK
        TST (SP)+       ;REMOVE ARG FROM STACK

        CLR BLOCKS      ;BLOCKS TRANSFERRED COUNTER
        CLR ENDFL       ;EOF TEST
        .INIT #LNKBLK
        .LOOK #LNKBLK,#FILBLK,1         ;FIND FILE ON DISK
        MOV (SP)+,START         ;START BLOCK NO.
        MOV (SP)+,LENGTH                ;NO. OF BLOCKS
        TSTB (SP)+
        BMI E1
```

```
        MOV #2,@12(R5)  ;FILE DOES NOT EXIST
        RTS R5
E1:     ASL -2(SP)
        TSTB -2(SP)
        BMI E2
        MOV #3,@12(R5)  ;LINKED FILE
        RTS R5
E2:     CMP START,#4800.
        BLO E3
        MOV #4,@12(R5)  ;INVALID START BLOCK
        RTS R5
E3:     MOV START,R0
        ADD LENGTH,R0
        DEC R0
        MOV R0,BLK
        JSR PC,BLOCK
        MOV @#RKDA,END
        CMP R0,#4800.
        BLO E4
        MOV #5,@12(R5)  ;INVALID END BLOCK
        RTS R5
E4:     MOV START,BLK
        JSR PC,BLOCK
        TSTB @#RKCS     ;WAIT FOR CONTROL
        BPL .-4

        MOV @10(R5),R2  ;R2=4*CHANNELS
        MOV #BUFA,R4
        CLR R1          ;FIRST CHANNEL
RTN:    CLR R3
RET:    MOV 6(R5),CH
        MOV 2(R1),@#CHAN
CH=.-4
        ADD #4,R1
        CMP R1,R2
        BLT WAIT
        CLR R1

WAIT:   BIT #2,@#SWR            ;FINISHED?
        BNE DUMP                ;YES
        BIT #1,@#SWR            ;NO,PAUSE?
        BNE WAIT                ;YES
        BIT #1,@#STATUS         ;NO,WAIT FOR A-D TO START
        BEQ WAIT
        BIT #1,@#STATUS         ;WAIT FOR A-D TO FINISH
        BNE .-6
        BIT #10,@#CHAN          ;BINARY OR ANALOGUE INPUT?
        BNE PHASE               ;BINARY WORD TO STATUS REGISTER
        MOV @#BUF,(R4)+
CONT:   INC R3
        CMP R3,#256.            ;FULL BLOCK?
        BLT RET         ;NO
        JSR PC,DKWRT            ;YES,WRITE BLOCK TO DISK
        CMP R4,#BUFB+512.               ;END OF BUFB?
        BLO .+6
        MOV #BUFA,R4            ;YES,START ON BUFA
        BR RTN

PHASE:  MOV @#STATUS,PH
```

```
        ASR PH
        ASR PH
        ASR PH
        BIC #177770,PH
        MOV PH,(R4)+
        BR CONT

DUMP:   MOV R3,@4(R5)    ;IX=R3
CLEAR:  CMP R3,#256.
        BGE EXIT
        CLR (R4)+                ;APPEND BLOCK WITH ZEROS
        INC R3
        BR CLEAR
EXIT:   COM ENDFL        ;NO EOF ERROR
        JSR PC,DKWRT             ;PREPARE TO WRITE
        MOV BLOCKS,@10(R5)
        TSTB @#RKCS      ;WAIT FOR END OF TRANSFER !
        BPL .-4
        RTS R5

PH:     0
START:  0
LENGTH: 0
END:    0
BLOCKS: 0
ENDFL:  0
BLK:    0
CYL:    0
SUR:    0
SECTR:  0

DKWRT:  TSTB @#RKDS      ;DRIVE READY ?
        BMI DKWT
        MOV #-1,R0       ;DRIVE NOT READY
        HALT
DKWT:   TSTB @#RKCS      ;CONTROL NOT READY ?
        BMI DKC
        MOV #6,@12(R5)
        TST (SP)+
        TSTB @#RKCS
        BPL .-4
        RTS R5
DKC:    TST @#RKCS               ;DISK ERROR?
        BPL DKWT1
        MOV @#RKER,R0            ;DISPLAY RKERR IN CONSOLE
        HALT
DKWT1:  CMP @#RKBA,#BUFB+512.            ;BUFA OR BUFB?
        BLO .+8.                 ;WRITE BUFB
        MOV #BUFA,@#RKBA                 ;WRITE BUFA
        MOV #177400,@#RKWC               ;WORD COUNT =-256.
        INC BLOCKS
        CMP @#RKDA,END
        BLO DKWT2
        TST ENDFL        ;DUMP SW USED ?
        BNE DKWT2
        MOV #3,@#RKCS    ;WRITE,GO
        MOV R3,@4(R5)    ;IX=R3
        MOV BLOCKS,@10(R5)
        MOV #7,@12(R5)   ;FILE FULL
```

```
        TST (SP)+
        TSTB @#RKCS      ;WAIT !!
        BPL .-4
        RTS R5
DKWT2:  MOV #3,@#RKCS    ;WRITE,GO
        RTS PC

BLOCK:  MOV BLK,R2       ;INTERPRET MON BLOCK NUM
        CLR R1           ;SEE DISK DRIVER FOR COMMENTS
        BR DKIN20
DKIN10: ADD R2,R1
        ASR R2
        ASR R2
        ADD R4,R2
DKIN20: MOV R2,R4
        BIC #177760,R4
        BIC R4,R2
        BNE DKIN10
        CMP R4,#12.
        BLT .+6
        ADD #4,R4
        ADD R4,R1        ;RKDA IN R1 NOW
        CLR SECTR        ;LOAD SECTR
        BIS R1,SECTR
        BIC #177760,SECTR
        CLR SUR          ;LOAD SUR
        BIT #20,R1
        BEQ .+6
        INC SUR
        CLR CYL          ;LOAD CYL
        BIS R1,CYL
        ASR CYL
        ASR CYL
        ASR CYL
        ASR CYL
        ASR CYL
        BIC #177400,CYL
        TSTB @#RKCS      ;RK11 CONTROL READY ?
        BPL .-4
        MOV R1,@#RKDA
        MOV #BUFA,@#RKBA
        RTS PC

BUFA:
.=.+512.
BUFB:
.=.+512.

        .END
```

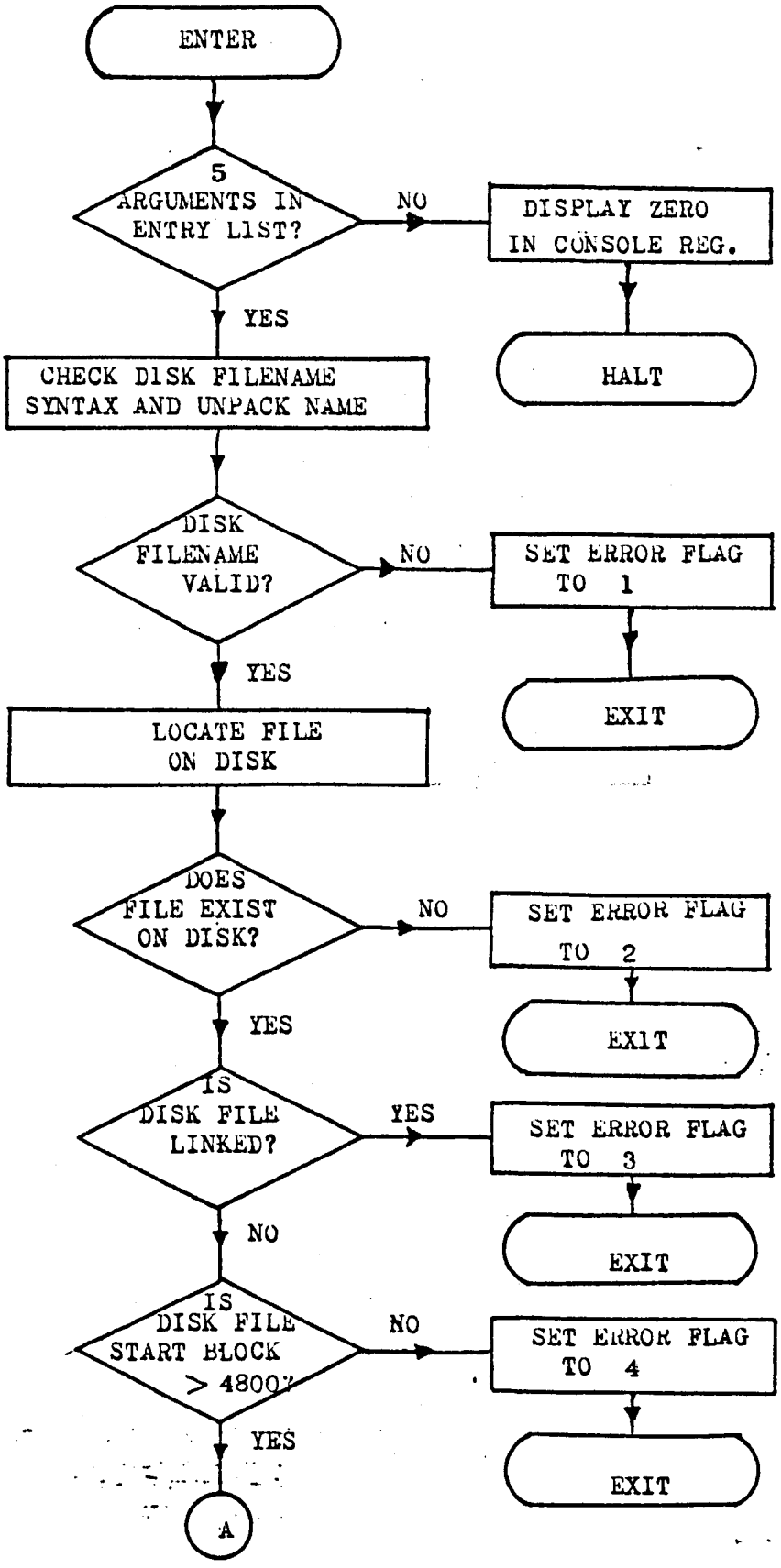

ANALOGUE-TO-DIGITAL CONVERSION PROGRAMME

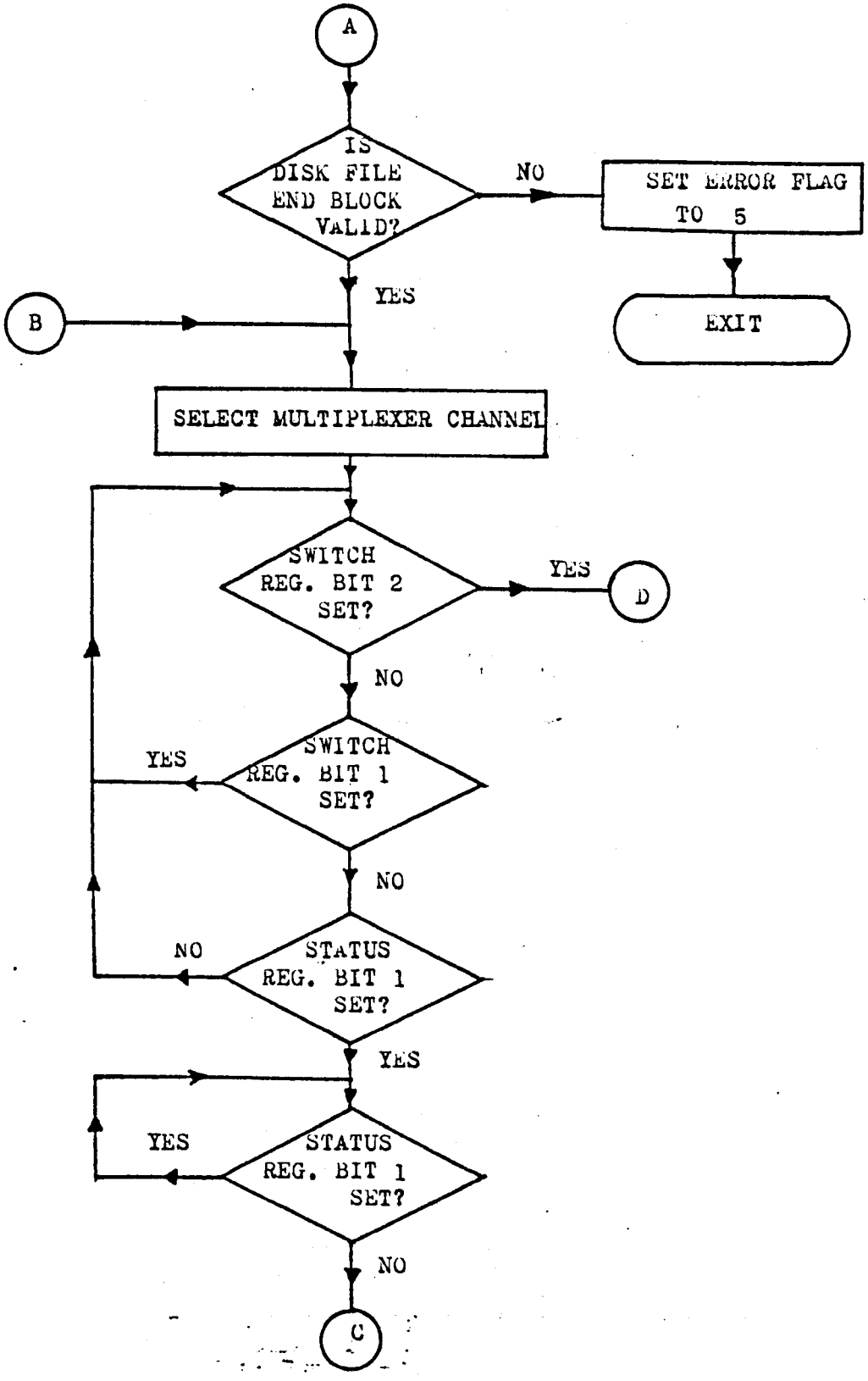

ANALOGUE-TO-DIGITAL CONVERSION PROGRAMME

FIG. A.5
Page 2 of 3

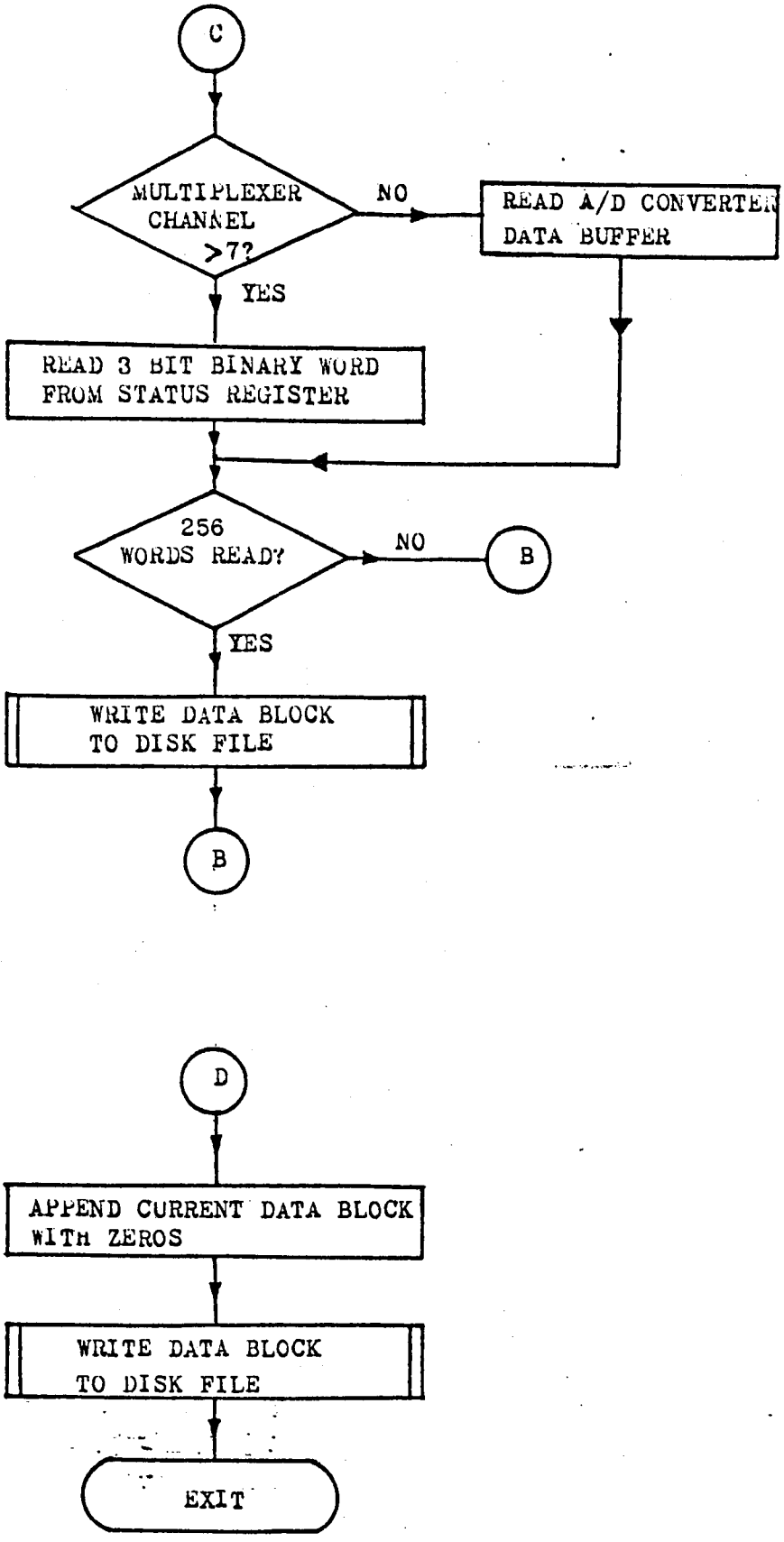

ANALOGUE-TO-DIGITAL CONVERSION PROGRAMME

```
C       ADC.FTN
C       GENERAL ANALOG TO DIGITAL CONVERSION PROGRAM
        DIMENSION FILE(3),ICH(10)
        WRITE(6,103)
103     FORMAT(1H$,' LENGTH OF SEQUENCE?: ')
        READ(6,104)IL
104     FORMAT(I1)
        WRITE(6,105)
105     FORMAT(1H$,' WHAT IS THE SEQUENCE?:(1 FORMAT,1 SPACE) ')
        READ(6,106)(ICH(J),J=1,IL)
106     FORMAT(10(I1,1X))
5       WRITE(6,101)
101     FORMAT(1H$, ' FILENAME?: ')
        READ(6,102)FILE
102     FORMAT(3A4)
        ILOOP=IL*4
        CALL ATOD(FILE,IX,ICH,ILOOP,IERR)
        IF(IERR.EQ.0)GOTO20
        IF(IERR.GT.7)WRITE(6,107)IERR
107     FORMAT(1X,' UNKNOWN ERROR: ',I2,/)
        WRITE(6,108)IERR
108     FORMAT(1X,' ERROR NUMBER: ',I2,/)
        GOTO(11,12,13,14,15,16,17)IERR
11      WRITE(6,111)
111     FORMAT(1X,' FILENAME ERROR',/)
        GOTO5
12      WRITE(6,112)
112     FORMAT(1X,' NO FILE!',/)
        GOTO5
13      WRITE(6,113)
113     FORMAT(1X,' FILE NOT CONTINGUOUS',/)
        GOTO5
14      WRITE(6,114)
114     FORMAT(1X,' INVALID START BLOCK',/)
        GOTO5
15      WRITE(6,115)
115     FORMAT(1X,' INVALID END BLOCK',/)
        GOTO5
16      WRITE(6,116)
116     FORMAT(1X,' DISK WAS NOT READY',/)
        GOTO5
17      WRITE(6,117)
117     FORMAT(1X,' FILE FULL!',/)
        GOTO5
20      WRITE(6,21)
21      FORMAT(1X,'FINISHED!!!!!',/)
        WRITE(6,22)ILOOP,IX
22      FORMAT(///,1X,I2,' BLOCKS FILLED; ',I3,
        1' DATA SAMPLES IN LAST BLOCK',/)
        GOTO5
        END
```

ANALOGUE-TO-DIGITAL CONVERSION
MAIN PROGRAMME

FIG. A.6

APPENDIX B

TRANSFER OF DATA FROM A PDP-11 TO A 1906A COMPUTER USING 7-TRACK INDUSTRIALLY COMPATIBLE MAGNETIC TAPE

Digital computers are commonly interfaced using industrially compatible magnetic tape systems, even though their internal and tape character codes may differ. The immediate problem of finding a medium suitable for both machines is of prime importance, a problem which may be solved by recourse to magnetic tape insofar as the physical dimensions of the tape are machine independent, e.g. tape width, number of tracks, inter-track gap, packing density, etc., but are only a function of the tape transporter.

The two computers to be interfaced were a PDP-11 minicomputer and a 1906A general purpose installation, the latter having both 7 and 9 track magnetic tape stations at packing densities of 800 and 1600 bpi respectively. A PDP-11 was available on campus with a 7-track, 800 bpi magnetic tape unit, therefore enabling this mode of transfer to be employed. The basic differences in the character sets and the word storage bit patterns between the two computers required that assembly language instructions be used for all data manipulations.

B1 MAGNETIC TAPE FORMAT

The single reel file structure of FORTRAN IV on the 1906A is shown in Fig.B1. It must comprise, in sequence, a header label to define the tape to the operating system, a start-of-data sentinel to define the data file structure, as many data blocks as are required, with the

B1 Cont'd proviso that the tape is physically long enough to contain them, and finally, an end-of-file trailer label.

B1.1 THE HEADER LABEL

The header label defines the magnetic tape to the GEORGE III operating system (1906A). It must, therefore, contain information which makes it unique within the system, i.e. serial number and tape name, together with housekeeping information such as date written and retention period.

This block must have 9 (or more) words of data. These are:-

WORD	
0	The 4 characters 'HDDR'
1	The tape serial number ($\leq$ 37777777 Octal)
2	The filename (12 characters)
3	
4	
5	Reel sequence number (0 to 511)
6	File generation number ($\geq$ 0)
7	Retention period
8	Date written

The tape serial number must be unique within the 1906A operating system and should be obtained from the chief operator.

The filename may be any 12 alphanumeric characters, the first being a letter. The name 'TRANSFERTAPE' is implicit in the programme.

B1.1 Cont'd The reel sequence number for a single reel file (the only form permitted under FORTRAN IV) is 0.

The file generation number and retention period are set to zero.

The date written is given as the number of days since 31st December 1899.

B1.2 START-OF-DATA SENTINEL

The start-of-data sentinel must contain 20 words and follow the header label and a tape mark. The words required are:-

WORD	
0	Bit 0 = 1 Bits 18 - 23 = the character '2'
1	Maximum Data Block Size to follow or zero
2, 3	zero
4-19	user information (set to zero).

B1.3 THE DATA BLOCKS

There may be as many sequential data blocks on a magnetic tape as are required by the application, provided that the tape is physically long enough to accommodate them. Each data block must contain between 5 and 32767 words with at least one complete record of between 2 and 512 words.

It should be noted that the maximum number of words in any data block

B1.3 Cont'd has been defined as word 1 of the start-of-data sentinel (if not given as zero). A formatted data block is as follows:-

WORD	
0	Number of words in a record
1	Space, Space, Space, Carriage Control
≥2	Records space filled to the record boundary.

The carriage control character (Byte 4 of Word 1) may be 41 to 47 or 51 to 57 giving 1 to 7 lines or page advances respectively when the tape is listed on a line printer.

B1.4 END-OF-FILE TRAILER LABEL

The trailer label indicates that the end of the data has been reached. No further read operations should be performed unless a REWIND or BACKSPACE command is executed.

The trailer label should be the last valid block on the tape and should be preceded by a tape mark. It contains:-

WORD	
0	Trailer identification (Bit 0 = 1)
1	Data block count (excluding labels, sentinels, tape marks and dumps)
2, 3	zero
4-19	User information (set to zero).

B2 THE PROGRAMME REQUIREMENTS

A PDP-11 programme was required which would write a header label and start-of-data sentinel to a magnetic tape, read data blocks from disc file as formatted or random access records, reformat these using 1906A tape character codes and write them onto the tape. It should correctly terminate the tape by an end-of-file trailer label when the data is exhausted.

The serial number of the tape must be a variable and the data files should be easily accessible on the 1906A.

Binary (random access) data stored on the disc should be written to tape in the equivalent format to 8 (I6, 1X) for a FORTRAN IV programme.

B2.1 THE PROGRAMME REALISATION

The programme assumes that a linked disc file consists of formatted ASCII records while a contiguous disc file contains unformatted binary records. These are the only two file types permitted.

Each data record written to tape starts with either a 0 or 1. The character 0 indicates that the next line is a data line whereas a 1 denotes the last record of the file. Each data file on tape is preceded by its filename as shown in Fig.B.2.

As no pre-knowledge of the number of data files to be written is available, each data file is terminated by a tape mark, an end-of-file trailer label and two backspaces of the tape. Any attempt to write another data file in the input chain will then overwrite these two

B2.1 Cont'd blocks, whereas termination of the programme will result in a valid single reel data file.

B3 THE PROGRAMME "MAG"

B3.1 INPUT/OUTPUT ON TELETYPE

Control Commands are accepted from the keyboard and error messages are displayed on the teletype. The programme may be terminated in the normal manner at any time.

Input data is required in response to the BATCH stream prompt "#" printed on the teletype. The first data record entered must be the required tape serial number. Any error at this point will result in an error message or, if undetected, an incorrectly labeled magnetic tape. Subsequent keyboard inputs are taken to be data filenames on the PDP-11 disc filestore. Errors in the filenames are signalled on the teletype.

All inputs may be given as a BATCH stream.

After each file has been written to the tape, a count of the total number of blocks written is printed on the console as an octal integer. This provides the capability of verifying that all the data records in the files have been handled.

Console switch register bit 0 controls the monitoring of data transfers. With bit 0 up (logical 1) and a contiguous disc file, the data records, after formatting, are written to the teletype and the magnetic tape.

B3.1 Cont'd Bit 0 clear (down) condition causes this facility to be cancelled.

B3.2 PROGRAMME OPERATION

A simplified flow diagram is given in Fig.B3 for the programme of Fig.B4.

B3.2.1 Tape Initialisation

To ensure that the tape is correctly loaded, no operations are allowed unless the tape is at the beginning-of-tape (BOT) mark. Failure of this condition causes an error to be flagged and the programme loops until corrective action is taken.

B3.2.2 The Header Block and Start-of-Data Sentinel

The various parameters for the header block are now calculated. The date given by the PDP-11 is converted to the number of days since 31st December 1899 and placed into a buffer store.

A character "#" is printed on the teletype and the tape serial number read from the keyboard and checked for eight octal digits. Failure at this point causes the programme to be terminated. The tape is given the label "TRANSFERTAPE" while the reel generation number, the file generation number and the retention period are set to zero.

The header block, a tape mark and the start-of-data sentinel are now written to tape.

B3.2.3 Data Blocks

The prompt character "#" is printed on the teletype and the name of a disc file read from the keyboard. This is scrutinised for legal structure, syntax and to ensure that a file of that name exists. This file is then examined and its disc location and length noted. Failure to this point results in an error diagnostic on the teletype and a restart from the "#" prompt.

The file is examined to determine if it is linked (formatted ASCII mode) or contiguous (unformatted binary random access mode) and a block of the file read in whichever mode is appropriate.

The filename is preceded by the character "0" and written to tape in 1906A 7-track tape code.

A block of contiguous file (if a contiguous file has been read) is formatted to be the equivalent of FORTRAN 8 (I6, 1X) format and each line preceded by "0", unless it is the final line of the file in which case it is preceded by "1".

Each line of a linked file is preceded by "0" or "1" as indicated above but reformatting is unnecessary.

This block of data file is now converted from PDP-11 internal machine code to ICL 1906A 7-track tape code. The block is transferred to the magnetic tape.

B3.2.3 Cont'd If more data is present in the disc file it is read and the process of reformatting repeated. If the file is exhausted, however, the programme continues by writing a tape mark and a trailer label on the magnetic tape, followed by two backspaces. The next filename is requested and the program either terminated or continued.

The total number of blocks written to tape is printed on the teletype.

B3.2.4 The End-of-File Trailer Label

This block is set up in a buffer and is now transferred to the tape to signify the end of the data records. It is accompanied by a tape mark and two backspaces.

Termination of the program results in the tape being correctly written. Any subsequent attempt to write on the tape will overwrite the trailer and permit more data to be placed on the tape. A new trailer will be required at the end of this new data.

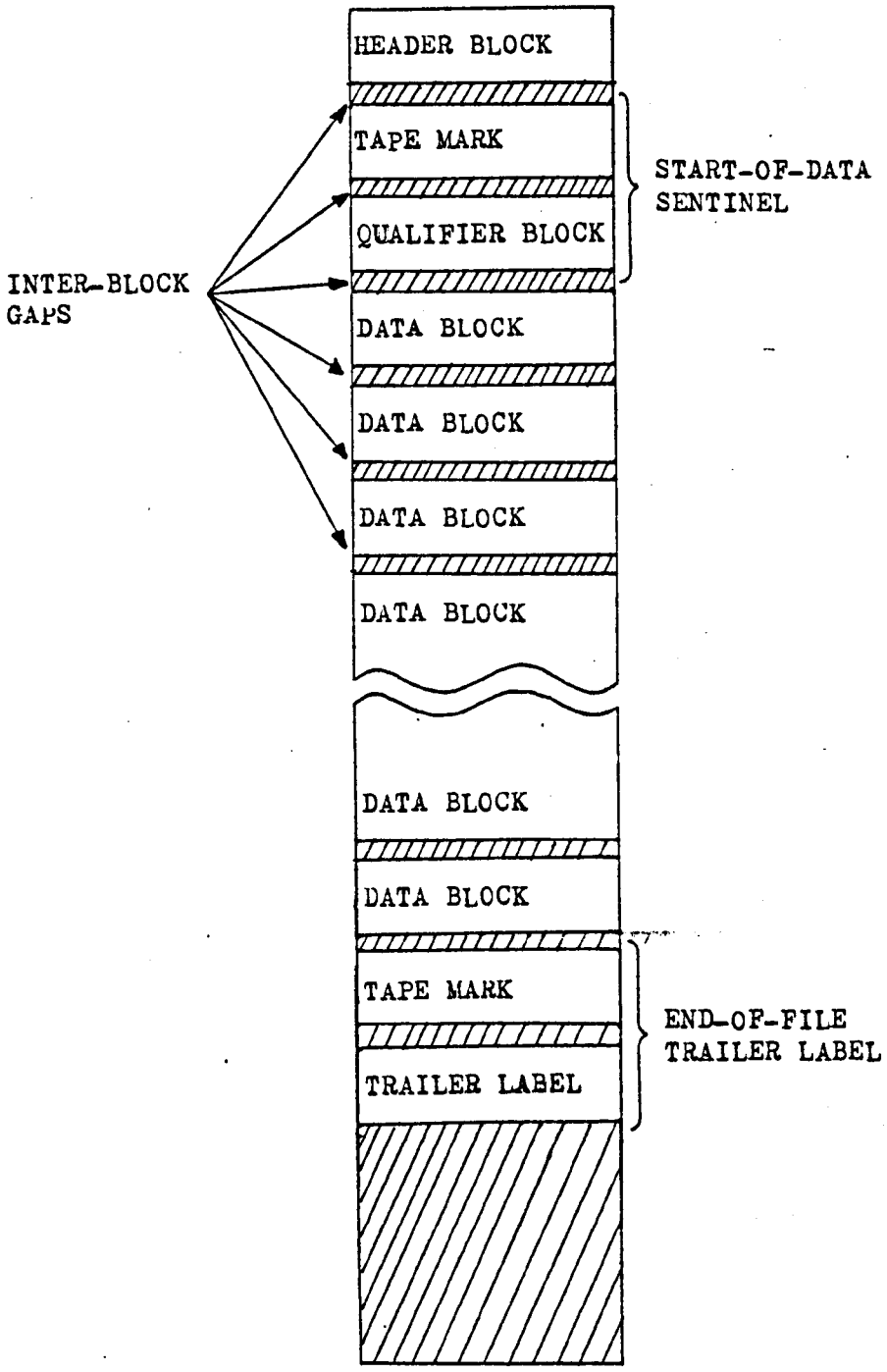

SINGLE REEL FORTRAN DATA FILE

FIG. B.1

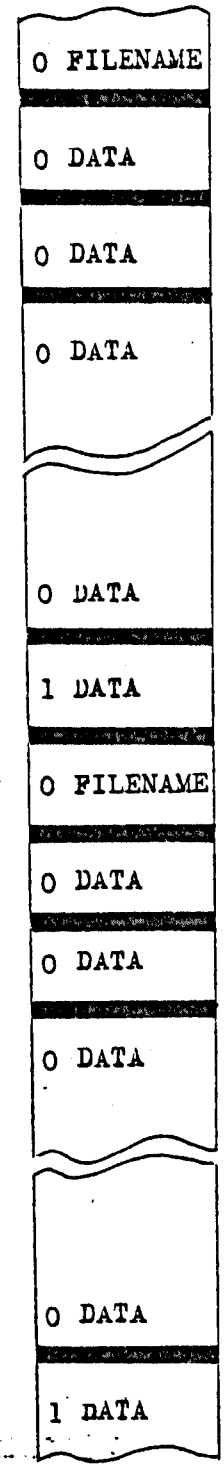

MAGNETIC TAPE DATA STRUCTURE

FIG. B.2

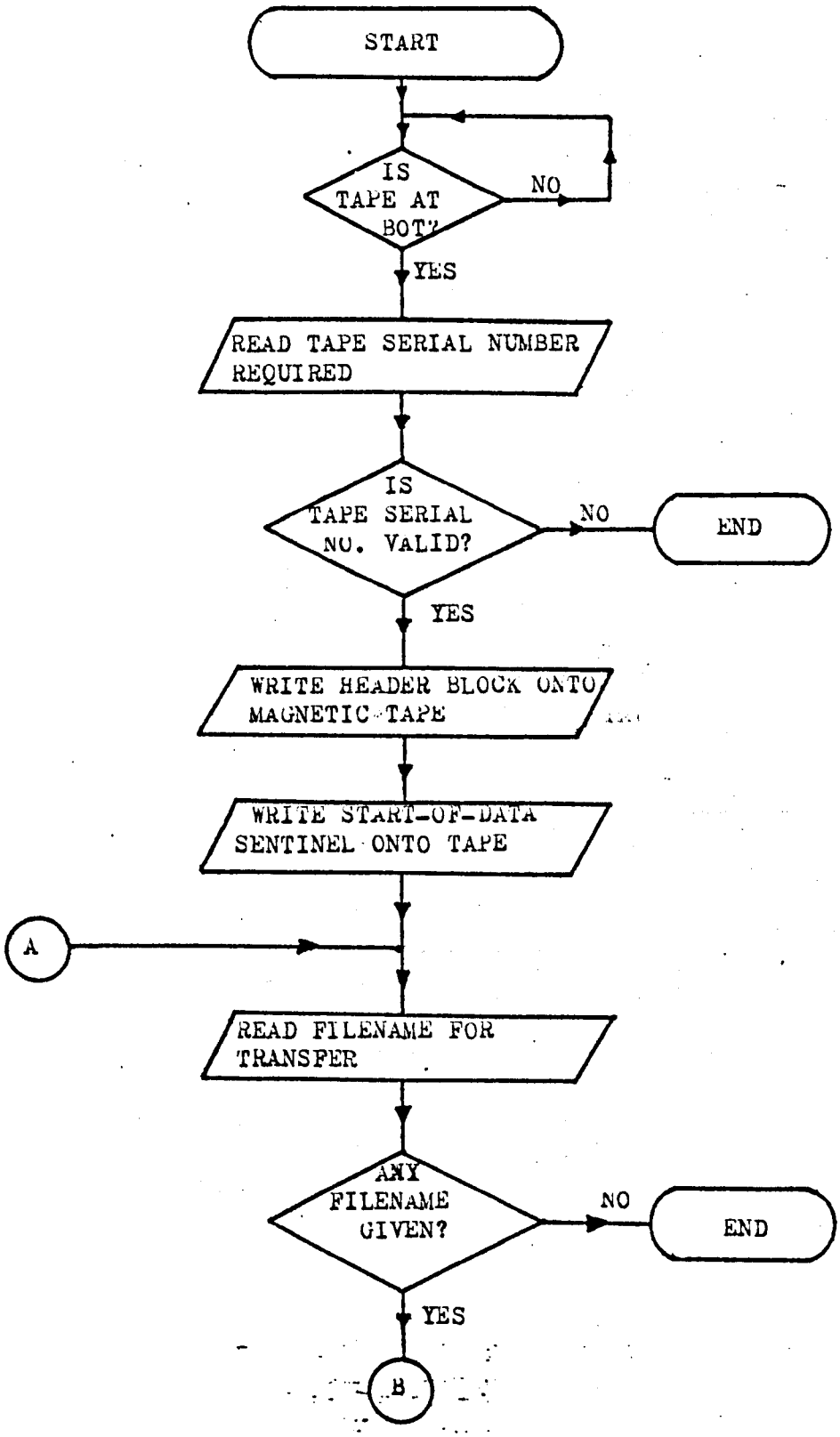

MAGNETIC TAPE TRANSFER PROGRAMME

FIG. B.3
-Page 1 of 3

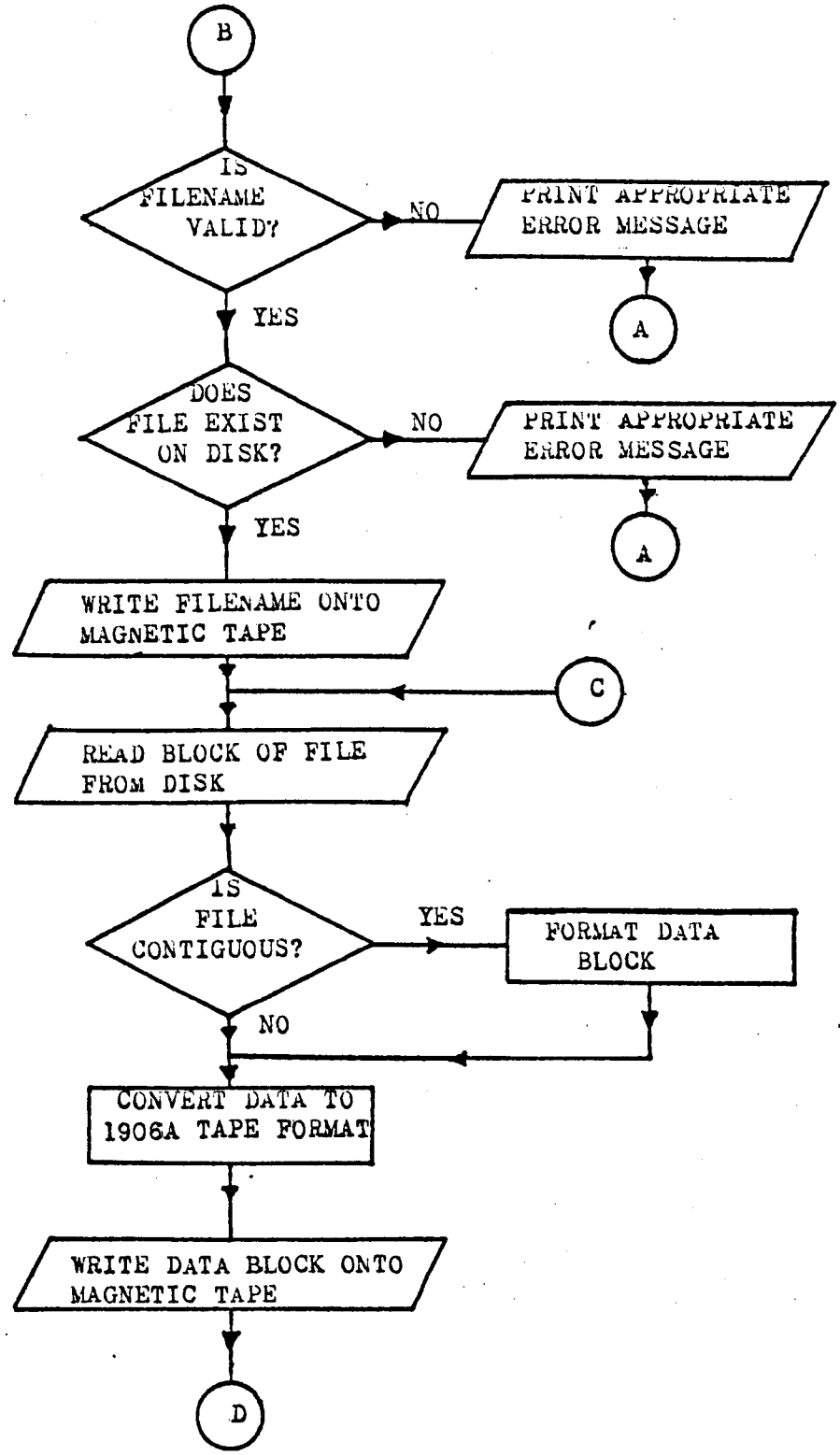

MAGNETIC TAPE TRANSFER PROGRAMME

FIG. B.3
Page 2 of 3

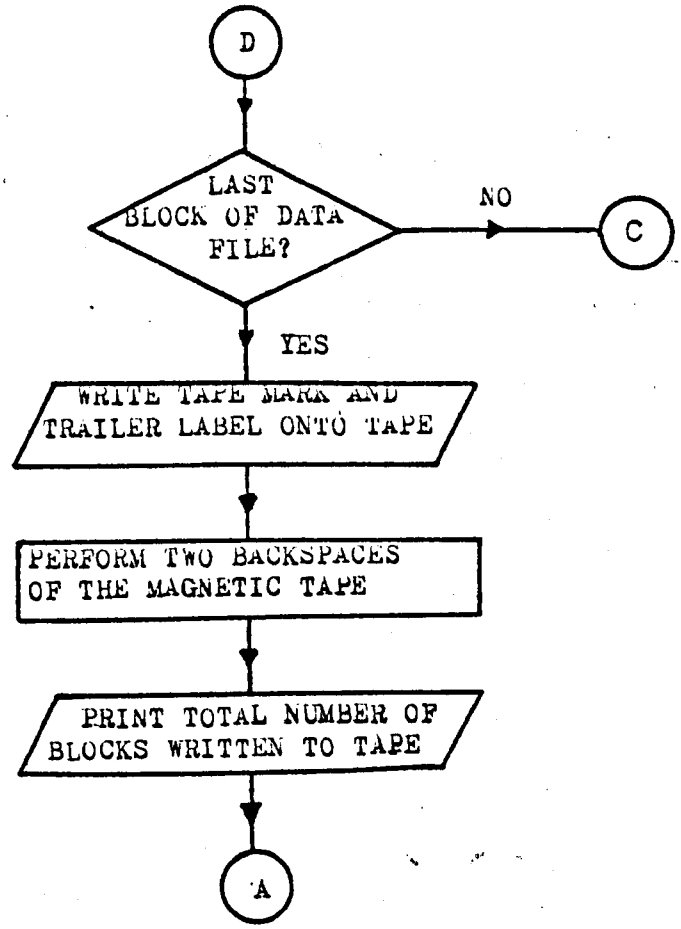

MAGNETIC TAPE TRANSFER PROGRAMME

FIG. B.3
Page 3 of 3

```
        .TITLE MAG
        .NCALL  .PARAM, .OPENI, .TRAN,  .SPEC,  .INIT
        .NCALL  .WRITE, .READ,  .CLOSE, .CSI1,  .BLOCK
        .NCALL  .CSI2,  .WAIT,  .RLSE,  .LOOK
        .PARAM

;PROGRAM TO TRANSFER DATA FROM A PDP-11 FILE ONTO
;MAGTAPE IN ICL 1900 FORTRAN DATA FILE FORMAT.

;MAGTAPE FILENAME: TRANSFERTAPE
;TAPE SERIAL NUMBER IS REQUIRED FOLLOWING FIRST '#'
;ENTER IT AS 8 OCTAL DIGITS

;  DATA STRUCTURE:
;LINKED FILE - MUST CONTAIN FORMATTED ASCII LINES (TAB ALLOWED)
;       EACH LINE COPIED DIRECTLY. 100 CHARACTERS MAX.
;CONTIGUOUS FILE - MUST CONTAIN UNFORMATTED BINARY DATA
;       EACH WORD IS CONVERTED TO FORTRAN I6 CHARACTER FORMAT
;       EACH LINE HAS 8 NUMBERS - 8(1X,I6)
;EVERY FILE HAS A DATA LINE INSERTED AT THE BEGINNING
;       CONTAINING THE FILENAME CHARACTERS AS TYPED
;       FOLLOWING THE '#' SYMBOL TO THE CSI.
;EVERY DATA LINE HAS A CHARACTER INSERTED AT THE BEGINNING:
;       0 - NEXT LINE IS ANOTHER DATA LINE
;       1 - NEXT LINE IS THE FILENAME

CR=15
LF=12
VT=13
MTS=172520

START:  .INIT   #LNKIP
        .INIT   #LNKUP1
        .INIT   #LNKMT
        CLR     DBLKS
        CLR     DBUVF
        .WRITE  #LNKUP1,#B1
        .WAIT   #LNKUP1

        .SPEC   #LNKMT,#SF800
        BIT #400,SF800+2
        BNE WTHD
        .WRITE  #LNKUP1,#B4     ;TAPE NOT AT BOT
        .WAIT   #LNKUP1
BOTWT:  BIT #40,@#MTS   ;WAIT FOR BOT MARKER
        BEQ BOTWT
WTHD:   MOV @#40,R0
        MOV 52(R0),R2   ;OBTAIN DATE
        ADD #54704,R2   ;1906A IS MUCH OLDER !!
        MOV R2,R0
        BIC #177700,R0
        JSR PC,CHCOMP
        MOVB R0,DATE+3
        ASR R2
        ASR R2
        ASR R2
        ASR R2
        ASR R2
```

```
        ASR R2
        MOV R2,R0
        BIC #177700,R0
        JSR PC,CHCOMP
        MOVB R0,DATE+2
        ASR R2
        ASR R2
        ASR R2
        ASR R2
        ASR R2
        ASR R2
        MOV R2,R0
        BIC #177700,R0
        JSR PC,CHCOMP
        MOVB R0,DATE+1
        .WRITE  #LNKOP1,#NINPT
        .WAIT   #LNKOP1
        .READ   #LNKIP,#BUF1
        .WAIT   #LNKIP
        CMP     BUF1+4,#10.     ;MUST HAVE 8 CHARS + CR,LF
        BEQ     TSNOK
BADTSN: .WRITE  #LNKOP1,#86     ;BAD TSN
        .WAIT   #LNKOP1
        BR      EXIT
TSNOK:  MOV #4,R4
        MOV #BUF1+6,R5
        MOV #TSN,R3
TSN1:   MOVB (R5)+,R0
        CMPB R0,#60
        BLO BADTSN
        CMPB R0,#67
        BHI BADTSN
        BIC #177770,R0
        ASL R0
        ASL R0
        ASL R0
        MOVB (R5)+,R1
        CMPB R1,#60
        BLO BADTSN
        CMPB R1,#67
        BHI BADTSN
        BIC #177770,R1
        ADD R1,R0
        JSR PC,CHCOMP
        MOVB R0,(R3)+
        DEC R4
        BNE TSN1
        .TRAN   #LNKMT,#TRANHD  ;WRITE HEADER
        .SPEC   #LNKMT,#TMARK
        .TRAN   #LNKMT,#SODS
        .WRITE  #LNKOP1,#NINPT
BEGIN:  .WAIT   #LNKOP1
        .READ   #LNKIP,#BUF1
        .WAIT   #LNKIP
        BITB    #100,BUF1+3     ;END OF BATCH INPUT ?
        BEQ     STRGET
EXIT:   .WAIT   #LNKMT
        .RLSE   #LNKMT
```

```
        .RLSE   #LNKOP1
        .RLSE   #LNKIP
        EMT     66
STRGET: CMP     BUF1+4,#2
        BGT     A1          ;ANY INPUT ?
        .WRITE  #LNKOP1,#NINPT
        BR      BEGIN
A1:     .CSI1   #CBH
        TST     (SP)+       ;ANY ERRORS ?
        BEQ     IP
        .WRITE  #LNKOP1,#ERRM1   ;SYNTAX ERROR
        BR      BEGIN

IP:     MOV #2,CBH          ;GET OUTPUT DATASET
        MOV     #LNKBK,CSIBK+2
        MOV     #FILBK,CSIBK+4
        .CSI2   #CSIBK
        MOV     (SP)+,R1
        BIT     #1,R1
        BNE     E5
        .WRITE  #LNKOP1,#ERRM6   ;2 OR MORE I/P FILES
        JMP     BEGIN
E5:     BIT     #2,R1
        BEQ     E6
        .WRITE  #LNKOP1,#ERRM7   ;2 OR MORE SWITCHES
        JMP     BEGIN
E6:     CMP     FILBK,#52
        BNE     C1
        .WRITE  #LNKOP1,#CERR1   ;'*' IN FILENAME
        JMP     BEGIN
C1:     CMP     FILBK+4,#52
        BNE     C2
        .WRITE  #LNKOP1,#CERR2   ;'*' IN EXTENSION
        JMP     BEGIN
C2:     CMPB    FILBK+6,#377
        BEQ     C3
        CMPB    FILBK+7,#377
        BNE     CX
C3:     .WRITE  #LNKOP1,#CERR3   ;'*' IN UIC
        JMP     BEGIN
CX:     NOP

        .INIT   #LNKBK
        .LOOK   #LNKBK,#FILBK
        MOV (SP)+,LENGTH
        TSTB (SP)+
        BMI OPEN
        .RLSE   #LNKBK
        .WRITE  #LNKOP1,#B2
        JMP BEGIN
OPEN:   CLR BLK+2           ;FIRST BLOCK
        MOV #4,BLK          ;READ
        CLR CONTIG
        ASL -(SP)
        TSTB (SP)+
        BMI .+6
        COM CONTIG
        MOV #FILBK,R0
```

```
        .OPENI  #LNKBK,R0
        JSR R5,LNCNV
        BUF1+6
        DATA
        BR WTDATA
NULINE: JSR R5,LNCNV
        BUF+0
        DATA
WTDATA: JSR PC,READ
        MOVB #75,DATA+10
        BITB #100,BUF+3 ;EOF ?
        BNE TRAN
        MOVB #74,DATA+10
TRAN:   .TRAN   #LNKMT,#TRNDAT
        .WAIT   #LNKMT
        INC DBLKS
        BNE .+6
        INC DBOVF
        CMPB DATA+10,#74
        BEQ NULINE
        JMP CLOSE

LENGTH: 0
CONTIG: 0
READ:   TST CONTIG
        BPL CON
LKRD:   .READ   #LNKBK,#BUF
        .WAIT   #LNKBK
        BITB #1,BUF+3   ;EXCESSIVE LINE LENGTH ?
        BNE .+4
        RTS PC
        .WRITE  #LNKOP1,#03
        .WAIT   #LNKOP1
        BR LKRD
CON:    TST CONTIG
        BNE CONLN
        DEC LENGTH
        BPL CONC
        BISB #100,BUF+3
        RTS PC
CONC:   .BLOCK  #LNKBK,#BLK
        .WAIT   #LNKBK
        TSTB BLK+1
        BEQ CON1
        .WRITE  #LNKOP1,#05     ;BLOCK READ ERROR
        .WAIT   #LNKOP1
        TST (SP)+       ;RESET STACK
        JMP CLOSE
CON1:   INC BLK+2
        MOV #32.,CONTIG
        MOV BLK+4,POINT
CONLN:  MOV #8.,R4
        MOV #BUF+6,R3
CON2:   JSR PC,FMTLN
        DEC R4
        BNE CON2
        MOVB #CR,(R3)+
        MOVB #LF,(R3)+
```

```
        DEC CONTIC
CONS:   BIT #1,@#177570
        BNE .+4
        RTS PC
        MOV #58.,BUF+4
        .WRITE  #LNKUP1,#BUF
        .WAIT   #LNKUP1
        RTS PC

POINT:  0
FMTLN:  MOV @POINT,R0
        ADD #2,POINT
        MOVB #' ,(R3)+
        MOVB #' ,(R3)+
        TST R0
        BPL FMT1
        MOVB #'-,-1(R3)
        NEG R0
FMT1:   JSR PC,DOCT
        RTS PC

DOCTX:  0
DOCT:   MOV #10000.,DIVOCT
        JSR PC,DECDIV
        MOVB DOCTX,(R3)+
        MOV #1000.,DIVOCT
        JSR PC,DECDIV
        MOVB DOCTX,(R3)+
        MOV #100.,DIVOCT
        JSR PC,DECDIV
        MOVB DOCTX,(R3)+
        MOV #10.,DIVOCT
        JSR PC,DECDIV
        MOVB DOCTX,(R3)+
        ADD #60,R0
        MOVB R0,(R3)+
        RTS PC

DIVOCT: 0
DECDIV: CLR DOCTX
        CMP DIVOCT,R0
        BHI .+12.
        SUB DIVOCT,R0
        INC DOCTX
        BR .-14.
        ADD #60,DOCTX
        RTS PC

CLOSE:  .SPEC   #LNKMT,#TMARK
        MOV #6+T2-T1,BUF+4      ;CHAR COUNT
        MOV #BUF+14+T2-T1,R5
        MOV #T2,R4
SHIFT:  MOVB -(R4),-(R3)
        CMP R4,#T1
        BHI SHIFT
        MOV DBLKS,R0
        MOV R0,R2
        JSR PC,WTBLK
```

```
        JSR PC,CHCOMP
        MOVB R0,DBCNT+3
        MOV DBOVF,R4
        ROR R4
        ROR R2
        ROR R4
        ROR R2
        ASR R2
        ASR R2
        ASR R2
        ASR R2
        MOV R2,R0
        JSR PC,WTBLK
        JSR PC,CHCOMP
        MOVB R0,DBCNT+2
        ASR R2
        ASR R2
        ASR R2
        ASR R2
        ASR R2
        ASR R2
        MOV R2,R0
        JSR PC,WTBLK
        JSR PC,CHCOMP
        MOVB R0,DBCNT+1
        MOVB #74,DBCNT
        .WRITE  #LNKOP1,#BUF    ;WRITE BLOCKS ON TAPE
        .WAIT   #LNKOP1
        .TRAN   #LNKMT,#EOFTL
        .SPEC   #LNKMT,#BKSP
        .CLOSE  #LNKBK
        .RLSE   #LNKBK
        .WRITE  #LNKOP1,#MINPT
        JMP BEGIN

WTBLK:  MOV R0,R4
        BIC #177770,R4
        ADD #60,R4
        MOVB R4,-(R3)
        MOV R0,R4
        ASR R4
        ASR R4
        ASR R4
        BIC #177770,R4
        ADD #60,R4
        MOVB R4,-(R3)
        RTS PC

LNCNV:  CLR R4              ;CHAR COUNT
        MOV (R5)+,R2
        MOV (R5)+,R3
        ADD #9.,R3          ;SPACE FOR REC LENGTH & CARR CNTRL & 1 C
                                -HAR

DLN:    MOVB (R2)+,R0
        BIC #177000,R0
        BEQ DLN
        CMPB R0,#11         ;TAB ?
        BEQ TAB
```

```
        CMPB R0,#177    ;RUBOUT ?
        BEQ DLN
        CMPB R0,#CR
        BEQ ENDLN
        JSR PC,CHCNV
        MOVB R0,(R3)+
        INC R4
        BR DLN
TAB:    MOVB #54,(R3)+
        INC R4
        BIT #7,R4
        BEQ DLN
        BR TAB
ENDLN:  ADD #9.,R4      ;INCLUDE WORD COUNT,CARR CTRL & 1 CHAR
PAD:    CMP R4,#88.     ;80 CHARS MIN
        BLO PADSP
        BIT #3,R4
        BEQ DLGTH
PADSP:  MOVB #54,(R3)+
        INC R4
        BR PAD
DLGTH:  CMP R4,#20.     ;MIN BLOCK SIZE = 5 WORDS
        BHIS BLKOK
        MOVB #74,(R3)+
        INC R4
        BR DLGTH
BLKOK:  ASR R4          ;= PDP 11 WORDS
        MOV R4,TRNDAT+4
        ASR R4          ;= 1906 WORDS
        MOV R4,R0
        JSR PC,CHCOMP   ;= 1906 TAPE CODE
        MOVB R0,DATA+3  ;MAX 63 WORDS = 252 CHARS
        RTS R5

CHCNV:  BIC #177600,R0
        CMP R0,#100
        BLO CHLOW
        CMP R0,#134
        BEQ CHERR
        CMP R0,#137
        BHI CHERR
        SUB #40,R0
        BR CHCOMP
CHLOW:  CMP R0,#60
        BHIS CHNUM
        CMP R0,#40
        BLO CHERR
        CMP R0,#44
        BEQ DOLLAR
        SUB #20,R0
        BR CHCOMP
DOLLAR: MOV #74,R0
        BR CHCOMP
CHNUM:  SUB #60,R0
CHCOMP: MOV R0,R1
        BIC #3,R1
        BIS #74,R0
        BIC R1,R0
```

```
        RTS PC
CHERR:  MOV #77,R0
        BR CHCOMP


        0
LNKIP:  0
        .RAD50 /CMI/
        .BYTE 1,0
        .RAD50 /KB/

        0
LNKOP1: .WORD 0
        .RAD50  /CMO/
        .BYTE   1,0
        .RAD50 /KB/

        0
LNKBK:  0
        .RAD50 /DSF/
        .BYTE 1,0
        0


        0
LNKMT:  0
        0
        .BYTE 1,0
        .RAD50 /MT/

        0       ;FATAL ERROR
        .BYTE 2,0
FILBK:  .WORD 0,0,0,0,0,0

CSIBK:  CBH
        LNKBK
        FILBK

CBH:    .WORD 0,0,0,0,0,0,0     ;CSI BUF HEADER
BUF1:   84.             ;MAX BYTE COUNT
        0
        0
.=.+84.         ;I/P BUFFER

BUF:    100.    ;MAX CHAR COUNT
        0
        0
.=.+100.

SF800:  .BYTE 6,5
        .WORD 0
        .BYTE 0,2       ;800 BPI, ODD PARITY
        .WORD 0

TRANHD: .WORD 0,HEADER,40.,2,0
HEADER: .BYTE 24,30,30,16       ;HDDR
TSN:    .BYTE 74,74,74,74       ;TAPE SERIAL NUMBER
        .BYTE 10,16,35,22,17,32 ;FILENAME = TRANSFERTAPE
        .BYTE 31,16,10,35,14,31
```

```
        .BYTE 74,74,14,74          ;REEL GENERATION NO. = 0
        .BYTE 74,74,14,74          ;FILE GENERATION NO. = 0
        .BYTE 74,74,14,74          ;RETENTION PERIOD =0
DATE:   .BYTE 74,74,14,74          ;DATE WRITTEN
        .BYTE 10,74,14,74
        .BYTE 74,74,14,74          ;PADDING...
        .BYTE 74,74,14,74
        .BYTE 74,74,14,74
        .BYTE 74,74,14,74
        .BYTE 74,74,14,74
        .BYTE 74,74,14,74
        .BYTE 74,74,14,74
        .BYTE 74,74,14,74
        .BYTE 74,74,14,74
        .BYTE 74,74,14,74

SODS:   .WORD 0,SOD,40.,2,0
SOD:    .BYTE 34,74,14,76          ;START OF DATA SENTINEL
        .BYTE 74,74,14,74          ;MAX BLOCK SIZE
        .BYTE 74,74,14,74
        .BYTE 74,74,14,74
.=.+64.

TRNDAT: .WORD 0,DATA,0,2,0
DATA:   .BYTE 74,74,14,74          ;WORDS IN RECORD
        .BYTE 74,74,14,35          ;CARRIAGE CONTROL
.=.+110.

BLK:    .WORD 4 ;INPUT FUNCTION
        0       ;BLK NUMBER
        0       ;BUFFER ADDRESS
        0       ;BUFFER LENGTH

TMARK:  .BYTE 2,5
        .WORD 0,0,0

DBLKS:  0
DBOVF:  0
EOFTL:  .WORD 0,EOF,40.,2,0
EOF:    .BYTE 34,74,14,74          ;TRAILER
DBCNT:  .BYTE 74,74,14,74          ;DATA BLOCK COUNT
        .BYTE 74,74,14,74
        .BYTE 74,74,14,74
.=.+64.

BKSP:   .BYTE 5,5
        .WORD 0,2,0

OFFLN:  .BYTE 1,5
        .WORD 0,0,0

B1:     .WORD 0,0,B2-B1-6
        .ASCII '1906 MAGTAPE - V002A'
        .BYTE CR,LF
B2:     .WORD 0,0,B3-B2-6
        .ASCII 'FILE NOT FOUND !'
        .BYTE CR,LF,'#,VT
B3:     .WORD 0,0,B4-B3-6
```

```
        .ASCII 'EXCESSIVE LINE LENGTH '
        .BYTE CR,LF
B4:     .WORD 0,0,B5-B4-6
        .ASCII 'TAPE NOT AT BOT MARKER !'
        .BYTE CR,LF
B5:     .WORD 0,0,B6-B5-6
        .ASCII 'BLOCK READ ERROR !'
        .BYTE CR,LF
B6:     .WORD 0,0,NINPT-B6-6
        .ASCII 'BAD TSN !!'
        .BYTE CR,LF

NINPT:  .WORD 0,0,ERRM1-NINPT-6
        .BYTE '#,VT
ERRM1:  .WORD 0,0,ERRM2-ERRM1-6
        .ASCII  /SYNTAX ERROR !/
        .BYTE   CR,LF,'#,VT
ERRM2:  .WORD 0,0,ERRM3-ERRM2-6
        .ASCII /ONE OUTPUT DEVICE ONLY !/
        .BYTE CR,LF,'#,VT
ERRM3:  .WORD 0,0,ERRM4-ERRM3-6
        .ASCII /NO OUTPUT SWITCHES ALLOWED !/
        .BYTE CR,LF,'#,VT
ERRM4:  .WORD 0,0,ERRM6-ERRM4-6
        .ASCII /SPECIFY OUTPUT DEVICE ! /
        .BYTE CR,LF,'#,VT
ERRM6:  .WORD 0,0,ERRM7-ERRM6-6
        .ASCII  /TOO MANY INPUT FILES !/
        .BYTE   CR,LF,'#,VT
ERRM7:  .WORD 0,0,CERR1-ERRM7-6
        .ASCII  /TOO MANY SWITCHES ! /
        .BYTE   CR,LF,'#,VT
CERR1:  .WORD 0,0,CERR2-CERR1-6
        .ASCII  /* NOT ALLOWED FOR FILENAME/
        .BYTE   CR,LF,'#,VT
CERR2:  .WORD 0,0,CERR3-CERR2-6
        .ASCII  /* NOT ALLOWED FOR EXTENSION /
        .BYTE   CR,LF,'#,VT
CERR3:  .WORD 0,0,T1-CERR3-6
        .ASCII  /* NOT ALLOWED IN UIC/
        .BYTE   CR,LF,'#,VT
T1:     .ASCII ' DATA BLOCKS ON TAPE'
        .BYTE CR,LF
T2:

        .END START
```

APPENDIX C

TRANSFER OF DATA FROM A PDP-11 TO A 1906A COMPUTER USING A DATA LINK

The ICL 1900 series of computers allow remote job entry terminals, comprising a line printer, a card reader and an operator's teletype, to be linked to the main frame installation via telephone lines. These are known as "7020" terminals; the block diagram of the basic hardware configuration is presented in Fig.C1.

It is possible, by the use of a synchronous interface, to replace the transmission control unit of Fig.C1 by another computer. This is commercially available for PDP-11 computers as depicted in Fig.C2.

C1 THE PDP-11 CONFIGURATION

The system block diagram shown in Fig.C2 must be modified to cater for the real peripheral configuration of the computer employed as the line termination. The system incorporating the PDP-11 in the Department of Electronic and Electrical Engineering is given in Fig.C3.

It should be noted that the 1906A requires a card reader as the input peripheral and a line printer as the remote output peripheral (Fig.C1). These both operate on "card image" records in "GRAPHIC" (formatted ASCII) mode on the data link. Any string of characters input or output via the PDP-11 must therefore be in this format if it is to be compatible with the 1906A.

C2 THE PDP-11 PROGRAMMES

A suite of programmes, known as the "7020 Emulator Package", was developed by the University of Nottingham to permit a PDP-11 minicomputer to operate as a standard 1906A remote installation. The package operates in a time-shared (multiplexed) mode under the control of an executive programme (PIPIT). Data flow is achieved by a system of hardware priority interrupts, the DP-11 synchronous transmitter/receiver having the highest priority level and the input/output devices having the lowest.

The programmes read data records (in formatted ASCII mode) from disc, teletype or card reader and transmit them along the data link to the 1906A. Data strings received from the line are written to a line printer or teletype as required by the operational context. The PDP-11 employed, however, did not have a line printer or a card reader, thereby necessitating slight modifications in the programmes to re-route all output to the operator's console. This means that the single low speed device is performing a multiplicity of input and output functions and, as a consequence, becomes very congested.

The keyboard has to perform three input duties:-

(1) Control of the PDP-11 programmes and system

(2) Remote operator control of the cluster

(3) Pseudo-card reader data input to the 1906A.

To indicate which of the above facilities is required, the separate duties have differing programmed input channels on the same keyboard. These are numbered 0, 1 and 2 for the three input duties listed,

C2 Cont'd these being preceded by the character "*" to change the conceptual teletype. All data strings commencing with an asterisk (cf. the GEORGE III default file terminator of ****) are consequently misinterpretted as requests for a change of input function.

C3 TRANSFER OF FILES FROM PDP-11 TO 1906A

The default terminator of **** is forbidden via the teletype. To overcome this a terminator must be specified, e.g. ////. The GEORGE III input command is required on the card reader channel (*2):

*2 INPUT : username, filename, T////

where : username is the 1906A user's registered name and filename is the required name for the 1906A file.

The statement has the effect of opening, for input, a file under the GEORGE III operating system. It is now required that the file on the PDP-11 disc store is opened for read access:

. OPI PDP-11 file / FA

where PDP-11 file is the PDP-11 filename and the /FA switch indicates that the file is stored in formatted ASCII mode. Note that all character strings typed on keyboard 2 commencing with '.' are interpretted as commands.

The transfers must now be started:

.GO

The file is transmitted along the data link until it is exhausted. At this point the message:-

C3 Cont'd

ITP ← END OF FILE

is printed. The PDP-11 and 1906A files must be closed:

```
.CLO
////
```

The "card reader" is devoid of cards at this instant and causes the main installation to signal:

UNIT I115 FREE

where I115 is the unit number of the pseudo-card reader for the cluster.

C3.1 CLOSING A 1906A FILE WITH UNKNOWN TERMINATOR

If the terminator option (T or S parameter to the INPUT command) is neglected for any reason, it is possible to close the file correctly by typing, in response to the message "ITP ← END OF FILE", the statement:-

*1TE I115

where I115 is the unit number of the cluster card reader on the 1906A.

C3.2 MULTIPLE FILE INPUTS TO THE 1906A FILESTORE

When many files are to be transferred to the 1906A filestore from the PDP-11 disc, the instructions detailed above may be typed for each one. The ensuing process is lengthy and requires an operator's presence to respond to the 1906A prompts. It would be advantageous, obviously, to structure the system in a manner allowing automatic data transfers to be performed.

C3.2 Cont'd The 1906A treats all inputs along the line as if they had been issued by a card reader. Knowledge of the real peripheral used is, insomuch as the 1906A is concerned, irrelevant. If it were possible to place all the commands and data records into one large file, they could be sequentially transmitted to line and decoded upon reception by the 1906A.

In this case, the default file terminator of **** is permitted because it is not handled by the teletype decoder.

A sample data file on PDP-11 disc would appear as Fig.C4 with the files destined to : USER with filenames of FILEA, FILEB and FILEC.

To send the records in this file to line, all that is needed is to provide read access to it and to start the operation:-

```
.OPI filename/FA
.GO
```

and in response to the end-of-file message to close the file:-

```
.CLO
```

C4 CONVERSION OF BINARY TO FORMATTED ASCII DATA

The analogue-to-digital conversion programme of Appendix A writes to PDP-11 disc in unformatted binary (random access) mode whereas the data link requires formatted ASCII records. A basic restructuring of the data files must be performed before the latter may be used.

C4 Cont'd

The basic method is straightforward, requiring that the data is read from disc in random access mode and written back in formatted ASCII. The process necessitates a DEFINE FILE statement and a random access read operation while the latter needs a formatted WRITE only.

A programme demonstrating this and the data file stacking of Section C3.2 is given in Fig.C5 with an outline flow diagram in Fig.C6.

The data files specified by the user in response to the teletype questions are each read from disc and written back into a file called G3FILE.ASC. Each individual original file (presumed to have ".BIN" as the filename extension) is preceded by a GEORGE III INPUT command and trailed by the default terminator ****.BATCH mode operation is permitted by the programme.

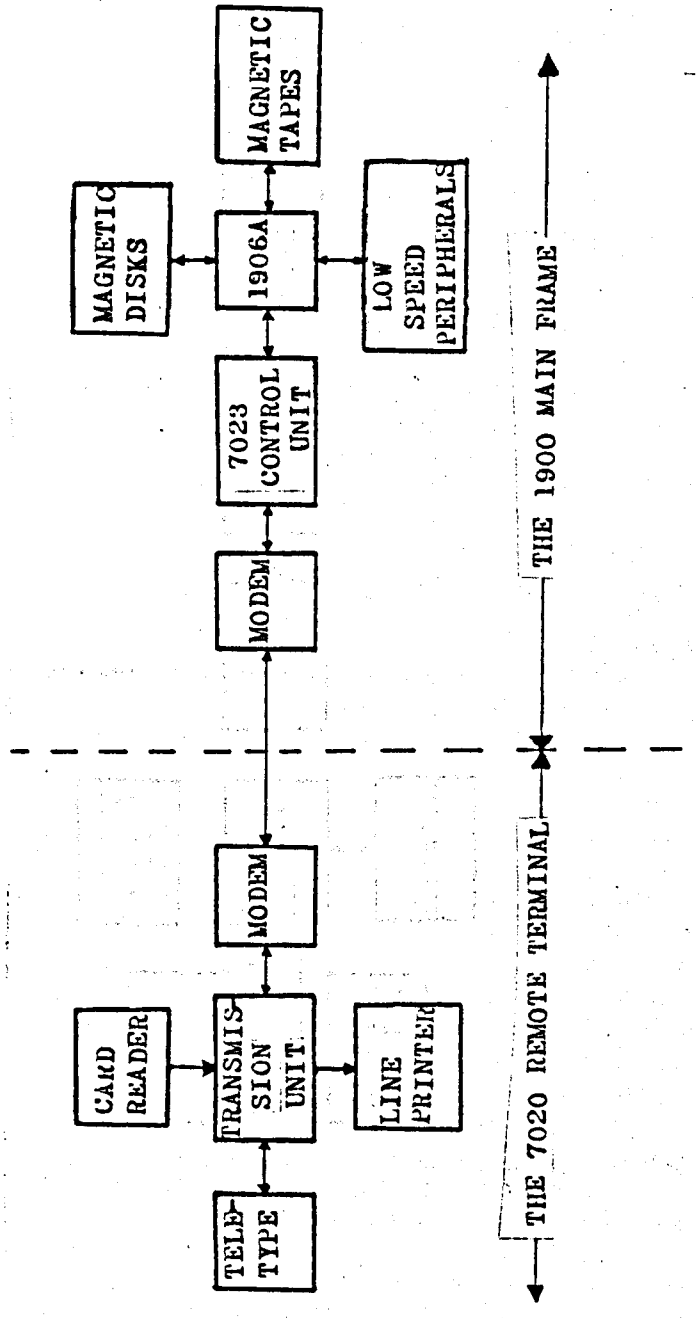

A CONVENTIONAL 1900 SERIES REMOTE JOB ENTRY TERMINAL

FIG. C.1

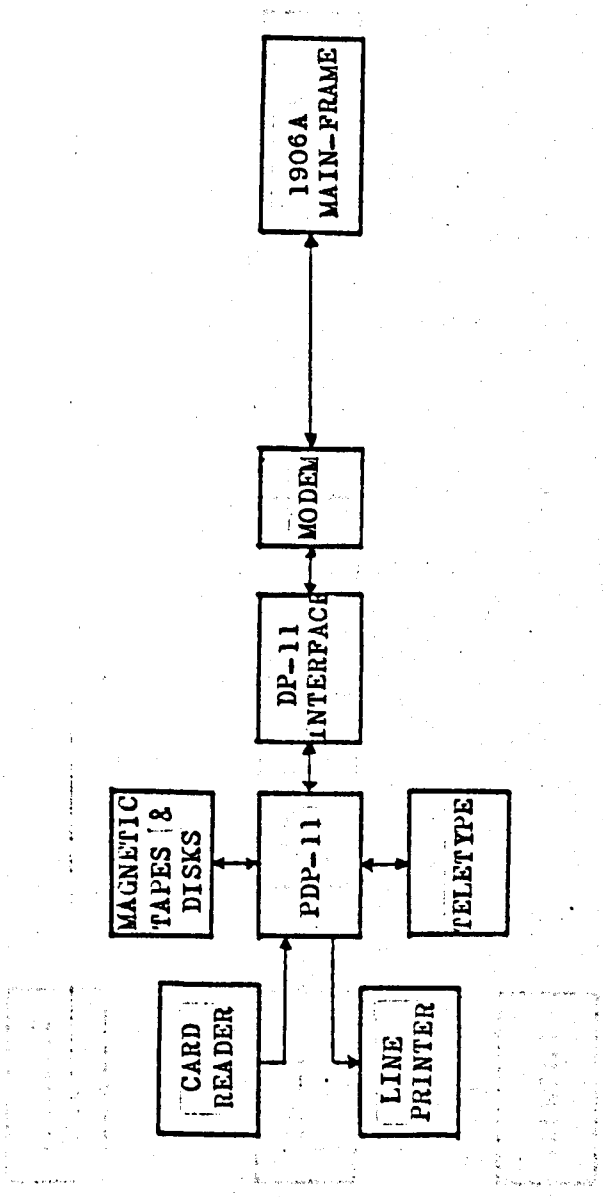

THE PDP-11 AS A REMOTE TERMINAL

FIG. C.2

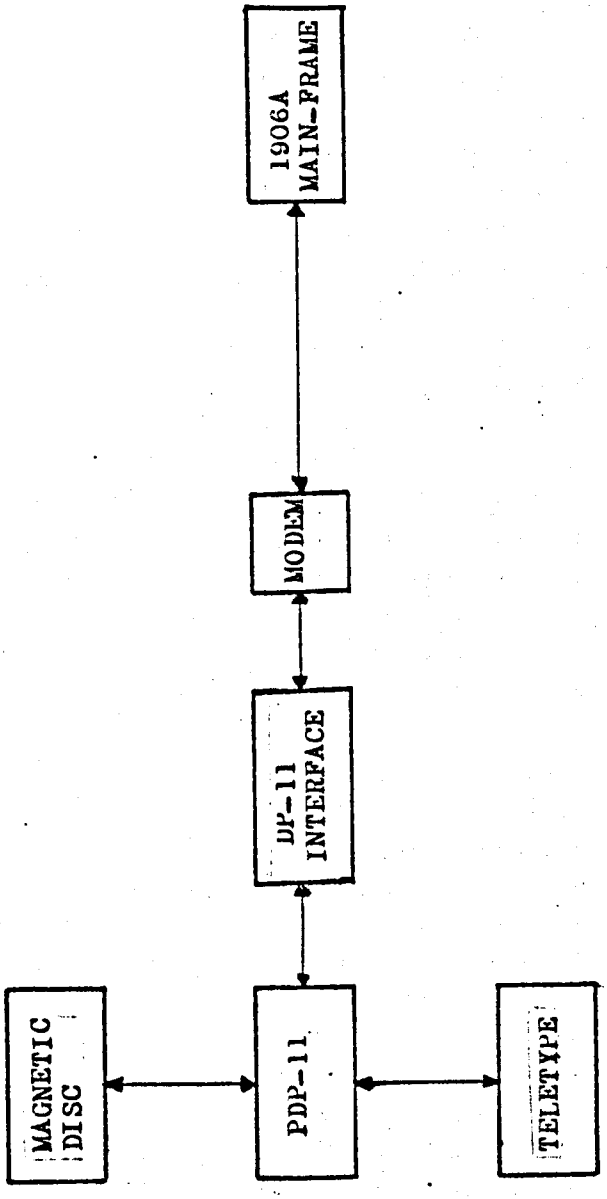

THE BASIC PDP-11 CONFIGURATION USED AS A REMOTE TERMINAL

-FIG. C.3

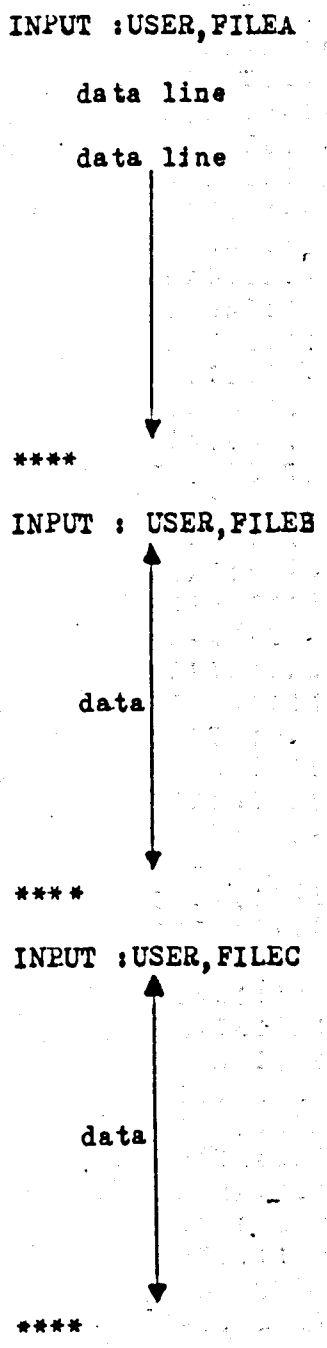

STACKING OF DATA FILES TO FACILITATE MULTIPLE TRANSFERS

– FIG. C.4

```
C       WRITE FILES FROM DEVICE #1 ONTO DEVICE #3
C       EACH PRECEDED BY THE GEORGE 3 INPUT COMMAND
C       AND TERMINATED BY "*****"
C
C       INPUT FILENAME MUST BE 4CHARACTERS,DEFINED EXT =.BIN
C
C
C
      DIMENSION INT(3),FILE1(3),FILE2(3),G3NAME(3),GFILE(3)
      DATA FILE1(2),FILE1(3)/'.BIN','    '/
      DATA STARS/'*****'/
      DATA END/'FIN1'/
      WRITE(6,10)
10    FORMAT(1HS,'GEORGE USERNAME?:')
      READ(8,11)G3NAME
11    FORMAT(3A4)
      WRITE(5,12)
12    FORMAT(1X,12X,'OUTPUT INTO G3FILE.ASC',///)
      CALL SETFIL(3,'G3FILE.ASC',1ERR,'DK')
111   WRITE(6,4)
4     FORMAT(1HS,' FILENAME?:')
      READ(8,5)FILE1(1)
5     FORMAT(1A4)
      IF(FILE1(1).EQ.END)GOTO112
      WRITE(6,23)
23    FORMAT(1HS,'G3 FILENAME?:')
      READ(8,11)GFILE
      CALL SETFIL(1,FILE1,1ERR,'DK')
      WRITE(6,25)
25    FORMAT(1HS,'HOW MANY BLOCKS(1S)?:')
      READ(8,26)NB
26    FORMAT(I3)
      NR=NB*32
      WRITE(5,27)NB,FILE1(1),G3NAME,GFILE
27    FORMAT(1X,I3,' BLOCKS OF ',1A4,' INTO ',3A4,'.',3A4,/)
      WRITE(3,56)G3NAME,GFILE
56    FORMAT('IN ',3A4,',',3A4)
      DEFINE FILE 1(NR,8,U,IVAR)
      DO 300 JAS=1,NB
      IR=JAS
      IRS=(IR-1)*32+1
      IRT=IR*32
      DO 3 J=IRS,IRT
      READ(1'J)(INT(I),I=1,8)
      WRITE(3,101)(INT(I),I=1,8)
101   FORMAT(8(1X,I6))
3     CONTINUE
300   CONTINUE
      WRITE(3,57)STARS
57    FORMAT(1A4)
      ENDFILE 1
      GOTO111
112   ENDFILE3
      CALL EXIT
      END
```

PROGRAMME TO PERMIT THE SEMI-AUTOMATIC DATA TRANSFERS BETWEEN THE PDP-11 AND THE 1906A COMPUTERS

FIG. C.5

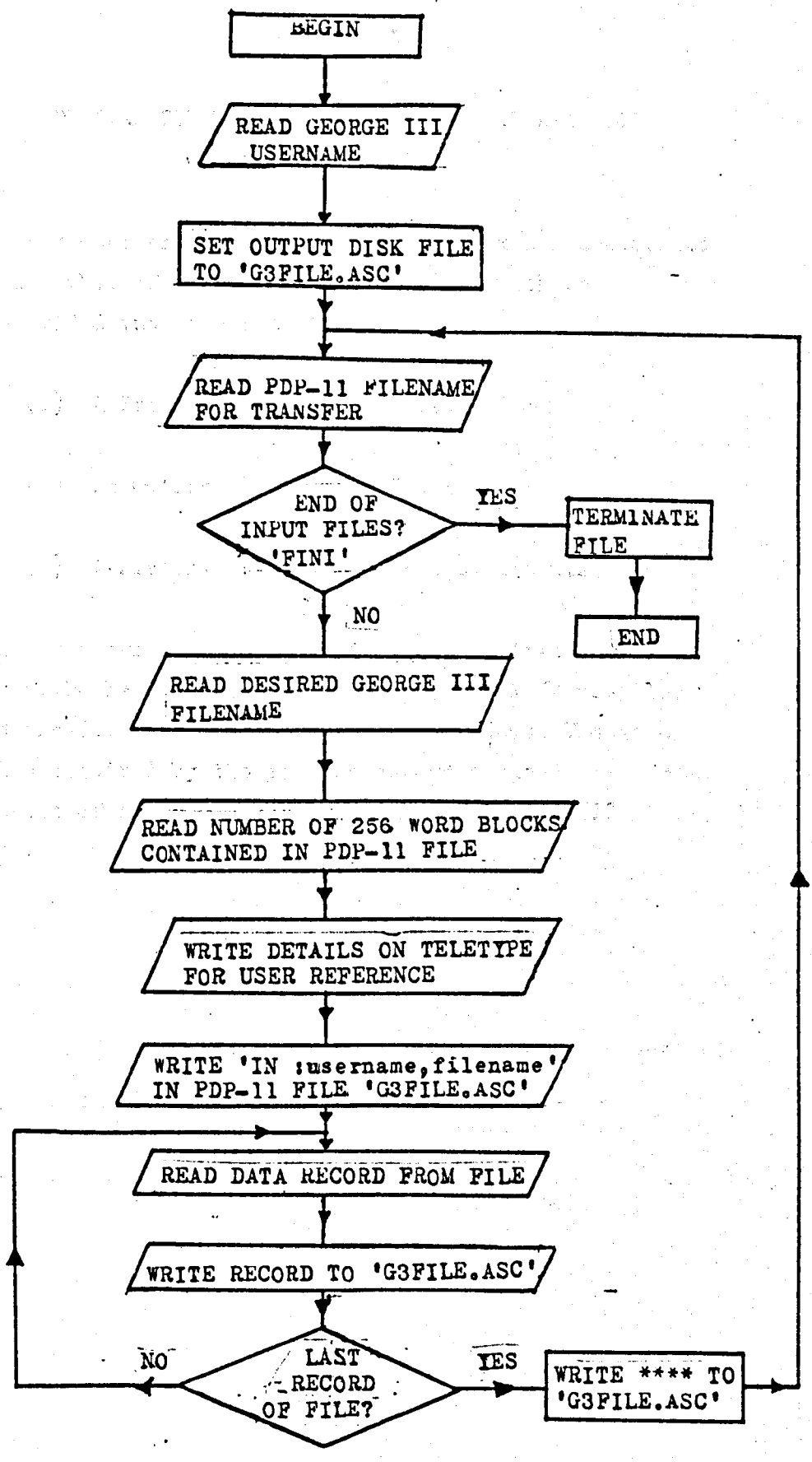

LOGIC FLOW DIAGRAM FOR PROGRAMME FACILITATING MULTIPLE FILE TRANSFERS

FIG. C.6

APPENDIX D

DIGITAL COMPUTER PROGRAMMES FOR THE ANALYSIS OF THE MEASURED DATA

The computer programmes in this appendix are documented as a number of illustrations, each of which is subdivided into three sections:

(a) A Brief Programme Description

(b) An Outline Logic Flow Diagram

(c) A Listing of the Programme Statements

All the programmes reported here are written for use with the ICL 1906A background FORTRAN IV compiler and the GEORGE III or IV operating systems. The data files required by the programmes are assumed to consist of card image records written in GRAPHIC mode.

D.1 DATA ANALYSIS PROGRAMMES

The following programmes are documented:

FIG. NO.	Programme Purpose	Name
D.1.1	Graphical plot of the measured signal (dB above 1μV) against distance travelled.	PLOTFL
D.1.2	Graphical plot of the signal after weighting (dB above 1μV) against distance travelled.	AVPLOT
D.1.3	Determination of the mean and median values for many data files	ALLMEANS
D.1.4	Determination of the pdf histograms of many data files.	ALLPDFS
D.1.5	Determination of the pdf histogram of a high-pass filtered signal.	REMNANT
D.1.6	Determination of the auto-covariance function of a low-pass filtered signal.	AUTOAV

D.2 GENERALLY USED SUBROUTINES

The following generally used sub-programmes are reported:

Fig.No.	Programme purpose	Name
D.2.1	Conversion of stored data to dB above 1μV	CONVRT
D.2.2	Conversion of signal from volts to dB above 1μV	RECONV
	Conversion of signal from dB above 1μV to volts	DECONV
D.2.3	Sorting of stored data and discarding of spurious points	ADJ
D.2.4	Rectangular window function	AVS
D.2.5	Triangular weighting function	AVS
D.2.6	Raised cosine weighting function	AVS
D.2.7	Calculation of median values along signal record	MEDS
D.2.8	Determination and plotting of the pdf histogram for a given data set	PDF
D.2.9	Scaled plot routine on graphical display	PLOT
D.2.10	Issuing of GEORGE commands	IGECOM

RAW SIGNAL PLOT

(i) INPUT/OUTPUT CHANNEL ASSIGNMENT

Input channel 5 : On-Line Card Reader

Input Channel 7 : Card Reader For Data File

Output Channel 6 : On-Line Line Printer

Additional Output : File Writer Channel For Incremental Graph Plotter

(ii) ON-LINE CARD READER INPUT REQUIRED

Card No. 1 : A title consisting of 80 alphanumeric characters to be written onto the graphical output.(This cannot be a totally blank card!)

Card No. 2 : Three variables read in free field format. NB,NS,ATTEN

where NB=the number of 256 word blocks of the file containing valid data samples.

NS=the number of valid data samples within the NB^{th} block of the file.

ATTEN=the setting of the receiver input attenuator at measurement time.

Card No. 3 : The character L,H or U representing data at the frequencies 85.875,167.2 and 441.025MHz respectively.

(iii) ON-LINE LINE PRINTER OUTPUT GIVEN

The total number of spurious points detected in the data file are printed.

PROGRAMME PLOTFL

(iv) SUB-PROGRAMMES REQUIRED

Routine Called	Fig. No.	Routines required by Called routine	
ADJ	D.2.3	-	
CONVRT	D.2.1	-	
PLOT	D.2.9	COMP8	(FORTRAN library)
		REGION	GHOST LIBRARY
		LIMITS	
		BORDER	
		CURPTO	
		AXESSI	
		CRSIZE	
		PLOTCL	
GREND	-	-	GHOST LIBRARY

(v) PURPOSE

To convert a data file to dB above 1μV and plot it on the incremental graph plotter using the LEEDS GHOST plotter package.

PROGRAMME PLOTFL

- FIG. D.1.1(a)

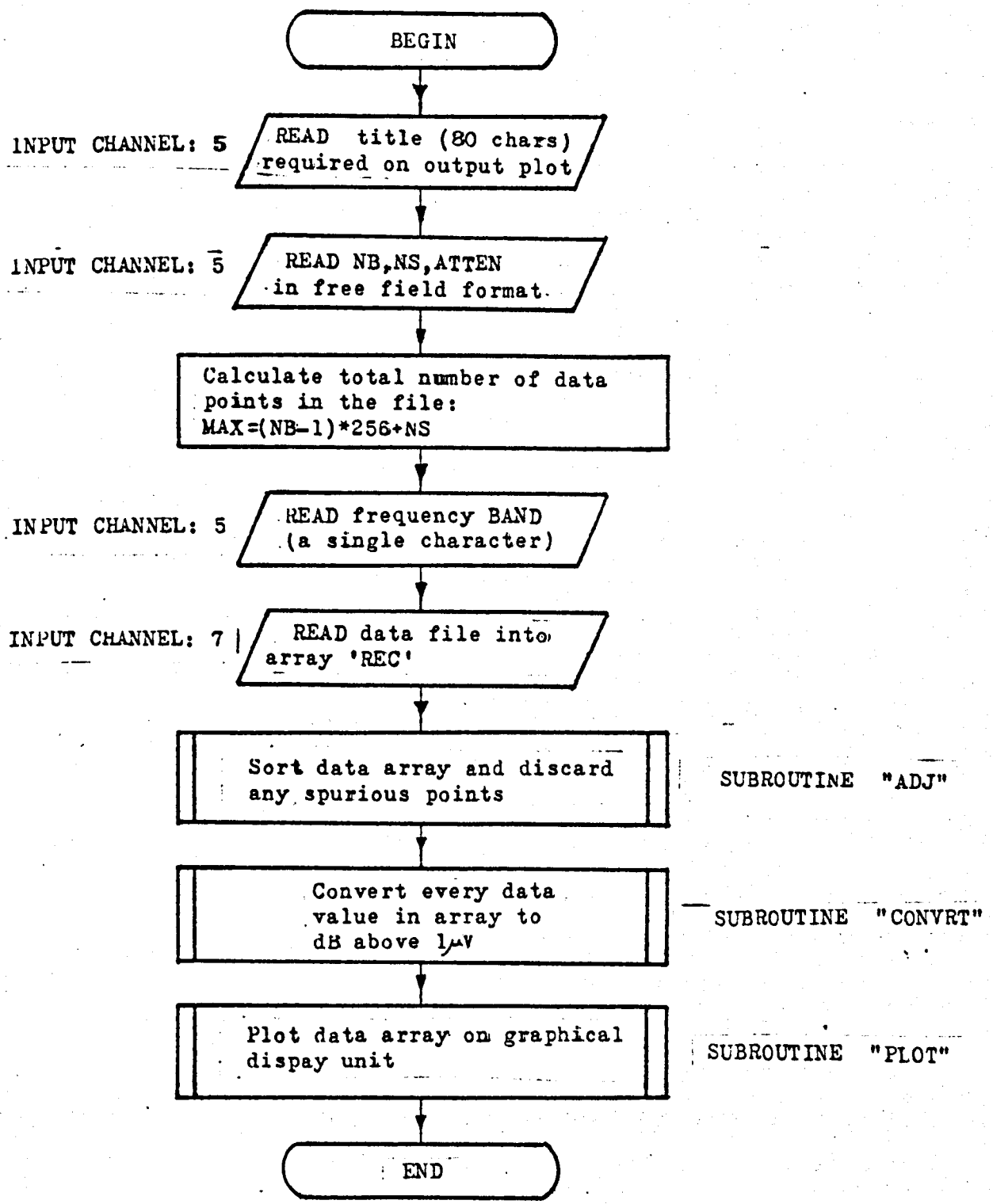

RAW SIGNAL PLOTTING PROGRAMME (PLOTFL)

FIG D.1.1(b)

```
      PROGRAM (FORT)
      INPUT 5 = CRO
      OUTPUT 6 =LPO
      INPUT 7 = CR1
      END

      MASTER MAIN
      COMMON RARR(8192),X(8192),CHAR(10)
      READ(5,6)CHAR
      READ(5,2)NB,NS,ATTEN
2     FORMAT(2I0,F0.0)
      MAX=256*(NB-1)+NS
      READ(5,7)BAND
7     FORMAT(1A8)
      READ(7,1)(RARR(I),I=1,MAX)
1     FORMAT(8192F0.0)
6     FORMAT(10A8)
      CALL ADJ(L,MAX)
      MAX=MAX-L
      WRITE(6,5)L
5     FORMAT(1H1,I3,16H SPURIOUS POINTS       )
      DO 3 J=1,MAX
3     CALL CONVRT(RARR(J),RARR(J),ATTEN)
      J=NB
      MAXM=J*256
      IF(J.EQ.NB)MAXM=MAX
      CALL PLOT(MAXM,BAND)
      CALL GREND
      STOP 'OK'
      END
```

RAW SIGNAL PLOTTING PROGRAMME (PLOTFL)

FIG. D.1.1(c)

WEIGHTED SIGNAL PLOT

(i) INPUT/OUTPUT CHANNEL ASSIGNMENT

Input channel 5 : On-Line Card Reader
Input Channel 7 : Card Reader For Data File
Output Channel 6 : On-Line Line Printer
Additional Output : File writer Channel For Incremental Graph Plotter

(ii) ON-LINE CARD READER INPUT REQUIRED

As shown in FIG. D.1.1(a)

(iii) ON-LINE LINE PRINTER OUTPUT GIVEN

As shown in FIG. D.1.1(a)

(iv) SUB-PROGRAMMES REQUIRED

Routine called	Fig. No.	Routines required by called routine	
ADJ	D.2.3	-	
CONVRT	D.2.1	-	
DECONV, RECONV	D.2.2	-	
AVS	D.2.4, D.2.5 & D.2.6	-	
PLOT	D.2.9	COMP8	FORTRAN LIBRARY
		REGION	GHOST SYSTEM LIBRARY
		LIMITS	
		BORDER	
		CURPTO	
		AXESSI	
		CRSIZE	
		PLOTCL	
GREND	-	-	

(v) PURPOSE

To weight a data file and plot on the graph plotter.

PROGRAMME AVPLOT

-- FIG. D.1.2(a)

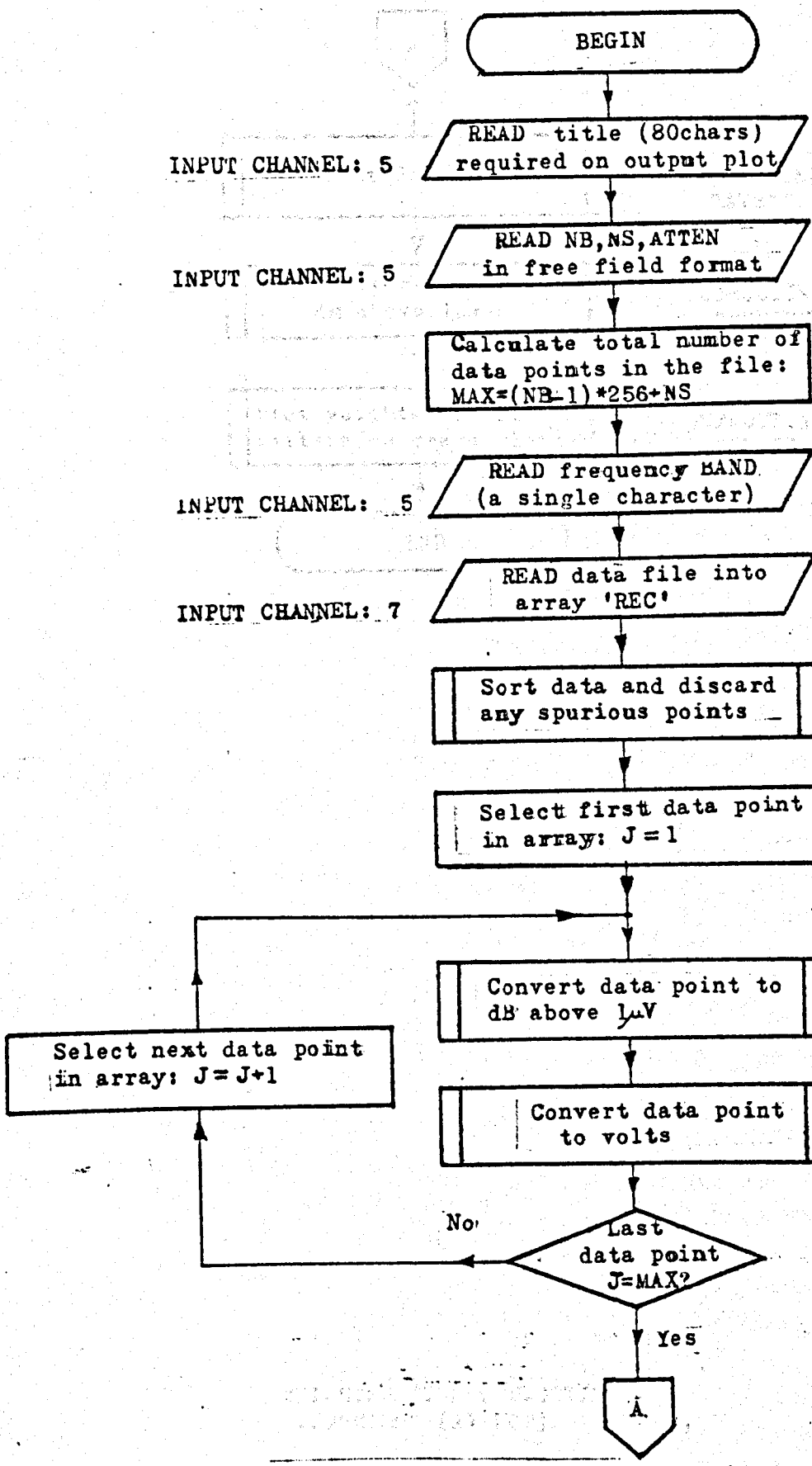

WEIGHTED SIGNAL PLOTTING PROGRAMME (AVPLOT)

FIG D.1.2(b)
Page 1 of 2

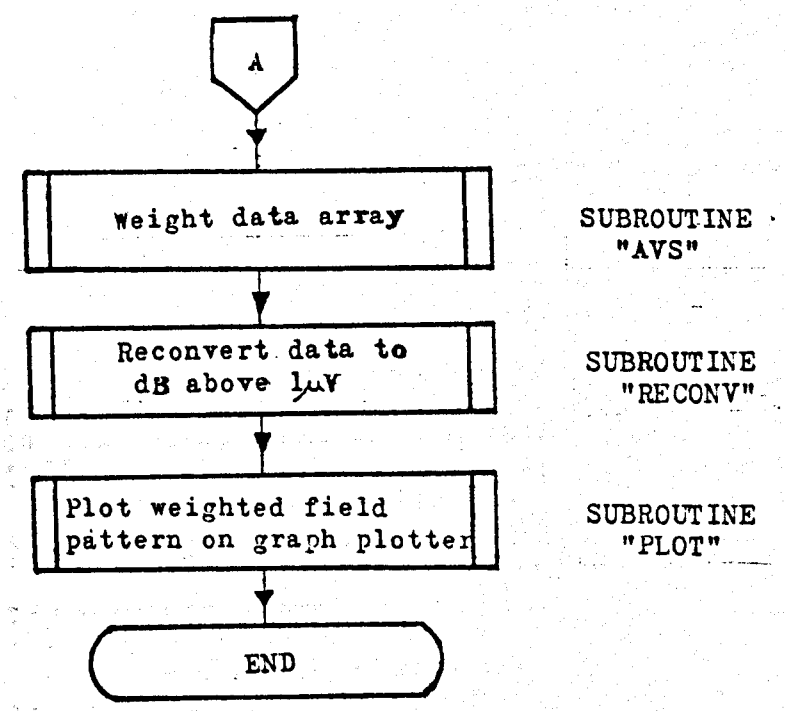

WEIGHTED SIGNAL PLOTTING PROGRAMME (AVPLOT)

FIG D.1.2(b)
Page 2 of 2

```
      PROGRAM (FORT)
      INPUT 5=CRO
      OUTPUT 6=LPO
      INPUT 7=CR1
      END
      MASTER MAIN
      COMMON REC(8192),RM(8192),CH(10)
C     NEEDS;
C     NB,NS,ATTEN
C     BAND(L,H,U)
C     TITLE
      MEAN=256
      READ(5,1)(CH(I),I=1,10)
    1 FORMAT(10A8)
      READ(5,2)NB,NS,ATTEN
    2 FORMAT(2I0,F0.0)
      MAX=256*(NB-1)+NS
      READ(5,7)BAND
    7 FORMAT(1A8)
      READ(7,3)(REC(I),I=1,MAX)
    3 FORMAT(1024(8F0.0))
      CALL ADJ(L,MAX)
      WRITE(6,5)L
    5 FORMAT(1H1,I4,15HSPURIOUS POINTS)
      MAX=MAX-L
      DO 4 J=1,MAX
      XXX=REC(J)
      CALL CONVRT(XXX,REC(J),ATTEN)
    4 CALL DECONV(REC(J))
      CALL AVS(MAX,MEAN)
      DO 6 J=1,MAX
    6 CALL RECONV(RM(J))
      CALL PLOT (MAX,     ,BAND)
      CALL GREND
      STOP 'OK AFTER PROGRAM'
      END
```

WEIGHTED SIGNAL PLOTTING PROGRAMME (AVPLOT)

FIG D.1.2(c)

DETERMINATION OF MEAN AND MEDIAN VALUES

(i) INPUT/OUTPUT CHANNEL ASSIGNMENT

Input channel 5 : On-Line Card Reader.

Input channel 7 : Card Reader (1) unassigned at start
- this will be switched by the programme.

Input channel 8 : Card Reader (2) assigned to a file containing all the GEORGE III "ASSIGN" commands required by input channel 7.

Output channel 6 : On-Line Line Printer.

Output channel 9 : Card Punch (0) assigned to an output file.

(ii) CARD READER INPUT REQUIREMENTS

1. On-Line Card Reader (Unit No. 5)

The input required on unit 5 consists of two cards for each data file to handled.These are:

Card 1 : A series of 80 alphanumeric characters to be printed on the output (not all blanks!)

Card 2 : Three variables to be read in free field format.

NB,NS,ATTEN

where these are described in FIG.D.1.1(a).

At the end of the input data ,i.e. when no more files are to be handled and the programme is to be terminated, a card containing the alphanumeric character string NOMORE is needed.

2. The GEORGE Assignments File (Unit No. 8)

The inputs required on unit no. 8 are the GEORGE III commands to be issued by the programme. Firstly the directory must be selected (e.g. :USER say) and then each file of data must be assigned to the relevant card reader (say filenames FILE1,FILE2 and FILE3 are required on card reader 1).The file would then contain:

DY :USER
AS *CR1,FILE1
AS *CR1,FILE2
AS *CR1,FILE3

and so on for all the input files.The files assigned by the programme in this manner must be synchronised to unit 5.

PROGRAMME ALLMEANS

(iii) ON-LINE OUTPUT GIVEN

The mean and median values of the file currently assigned to the card reader on input channel 7 are written on the card punch alongside the annotation requested on input channel 5.

(iv) SUB-PROGRAMMES REQUIRED

Routine called	Fig. No.	Routines required by called routine	
COMP8	-	-	FORTRAN COMPILER LIBRARY
IGECOM	D.2.10	SGEUCI	SYSTEM LIBRARY 'BHAMLIB'
ADJ	D.2.3	-	
CONVRT	D.2.1	-	
DECONV, RECONV	D.2.2	-	
MEDS	D.2.7	-	

(v) PURPOSE

To calculate the mean and median values of files read from input channel 7.

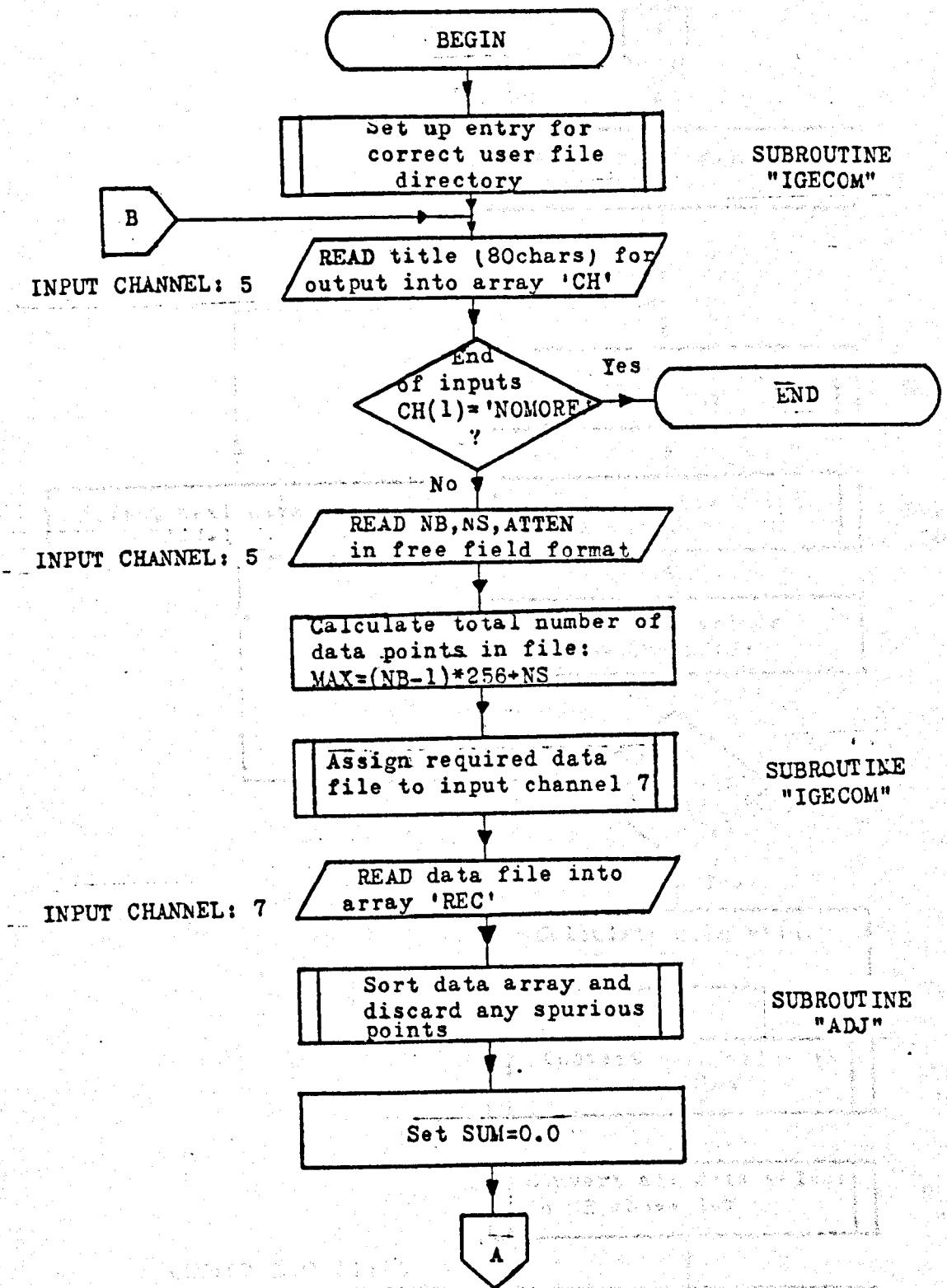

DETERMINATION OF MEAN AND MEDIAN VALUES (ALLMEANS)

FIG D.1.3(b)
Page 1 of 2

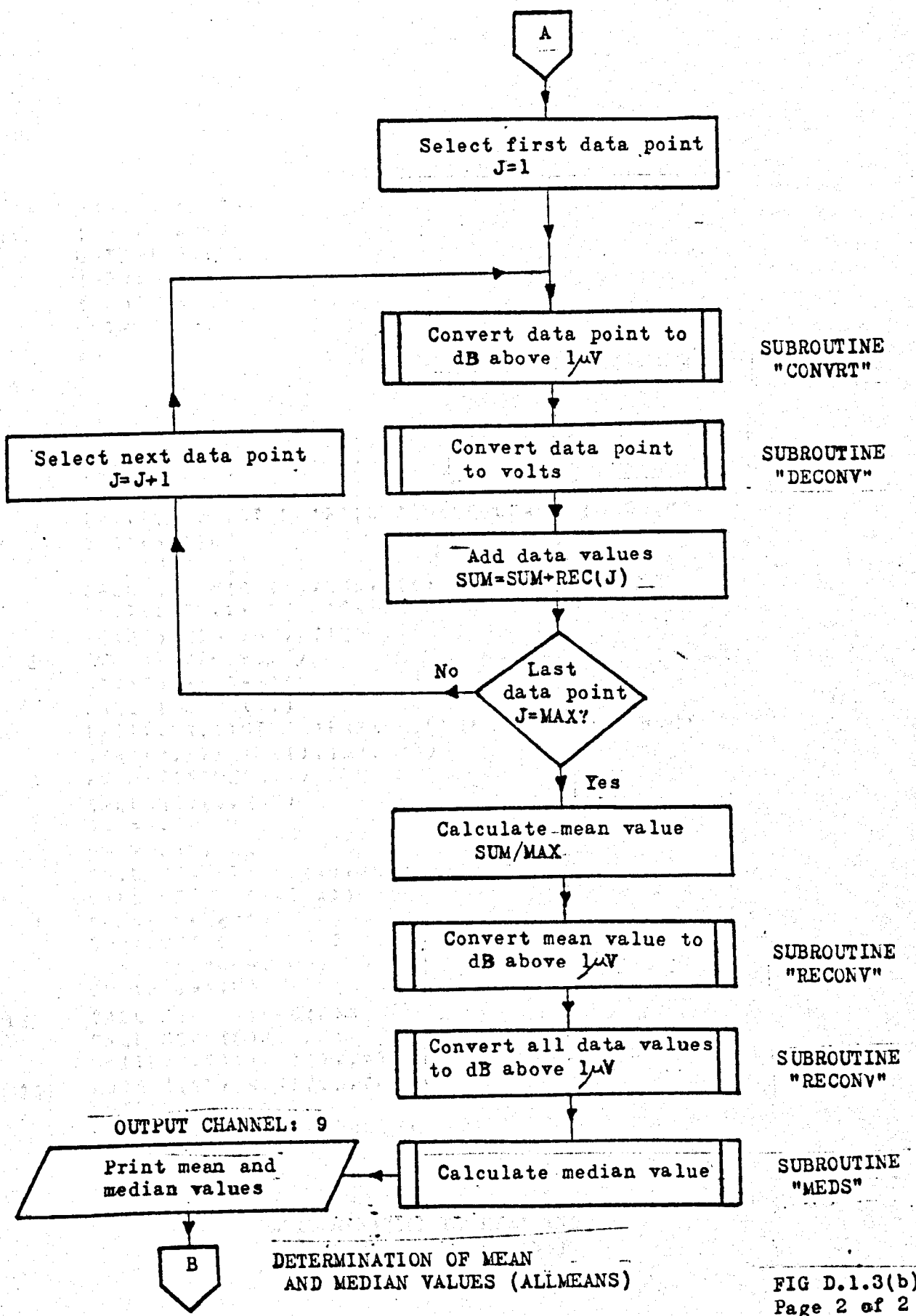

DETERMINATION OF MEAN AND MEDIAN VALUES (ALLMEANS)

FIG D.1.3(b)
Page 2 of 2

```
      PROGRAM(,,VRG)
      INPUT 5=CR0
      OUTPUT 6=LP0
      INPUT 7=CR1
      INPUT 8=CR2
      OUTPUT 9=CP0
      END


      MASTER MAIN
      COMMON REC(81*2),RN(81*2),CH(10)
      DATA END/'NORMOF  '/
      CALL IGECOM(II)
      IF(II.EQ.1)STOP 'FAIL GEORGE ERROR IN "DY"'
10    READ(5,1)CH
 1        FORMAT(10A8)
      CALL COMP8(CH(1),END,III)
      IF(III.EQ.1)STOP 'OK AFTER PROGRAM'
      READ(5,2)NB,NS,ATTEN
 2    FORMAT(2I0,F0.0)
      MAX=256*(NB-1)+NS
      CALL IGECOM(II)
      IF(II.EQ.1)STOP 'FAIL GEORGE COMMAND ERROR'
      READ(7,3)(REC(I),I=1,MAX)
 3    FORMAT(81*2F0.0)
      CALL ADJ(L,MAX)
      SUM=0.0
      DO 9 J=1,MAX
      CALL CONVRT(REC(J),REC(J),ATTEN)
      CALL DECONV(REC(J))
 9    SUM=SUM+REC(J)
      SUM=SUM/FLOAT(MAX)
       CALL RECONV(SUM)
      DO 12 J=1,MAX
12    CALL RECONV(REC(J))
      CALL MEDS(MAX,MAX)
      WRITE(9,11)(CH(I),I=1,9),SUM,RN(1)
 11   FORMAT(1X,9A8,F7.3,F8.3)
      GOTO10
      STOP 'OK AFTER PROGRAM'
      END
```

DETERMINATION OF MEAN AND MEDIAN VALUES (ALLMEANS)

FIG D.1.3(c)

RAW SIGNAL PLOT

(i) INPUT/OUTPUT CHANNEL ASSIGNMENTS

Channels 5,6,7 and 8 are the same as shown in FIG. D.1.3(a).

(ii) CARD READER INPUT REQUIREMENTS

These requirements are as shown in FIG. D.1.3(a)

(iii) ON-LINE LINE PRINTER OUTPUT GIVEN

The histogram of the pdf of the data file input on channel 7 is plotted in 1dB steps.

(iv) SUB-PROGRAMMES REQUIRED

Routine Called	Fig. No.	Routines required by routine called	
IGECOM	D.2.10	SGEUCI	SYSTEM LIBRARY 'BHAMLIB'
COMP8	-	-	FORTRAN LIBRARY
ADJ	D.2.3	-	
CONVRT	D.2.1	-	
PDF	D.2.8	-	

(v) PURPOSE

To determine the pdf of data files read in on input channel 7.

PROGRAMME ALLPDFS

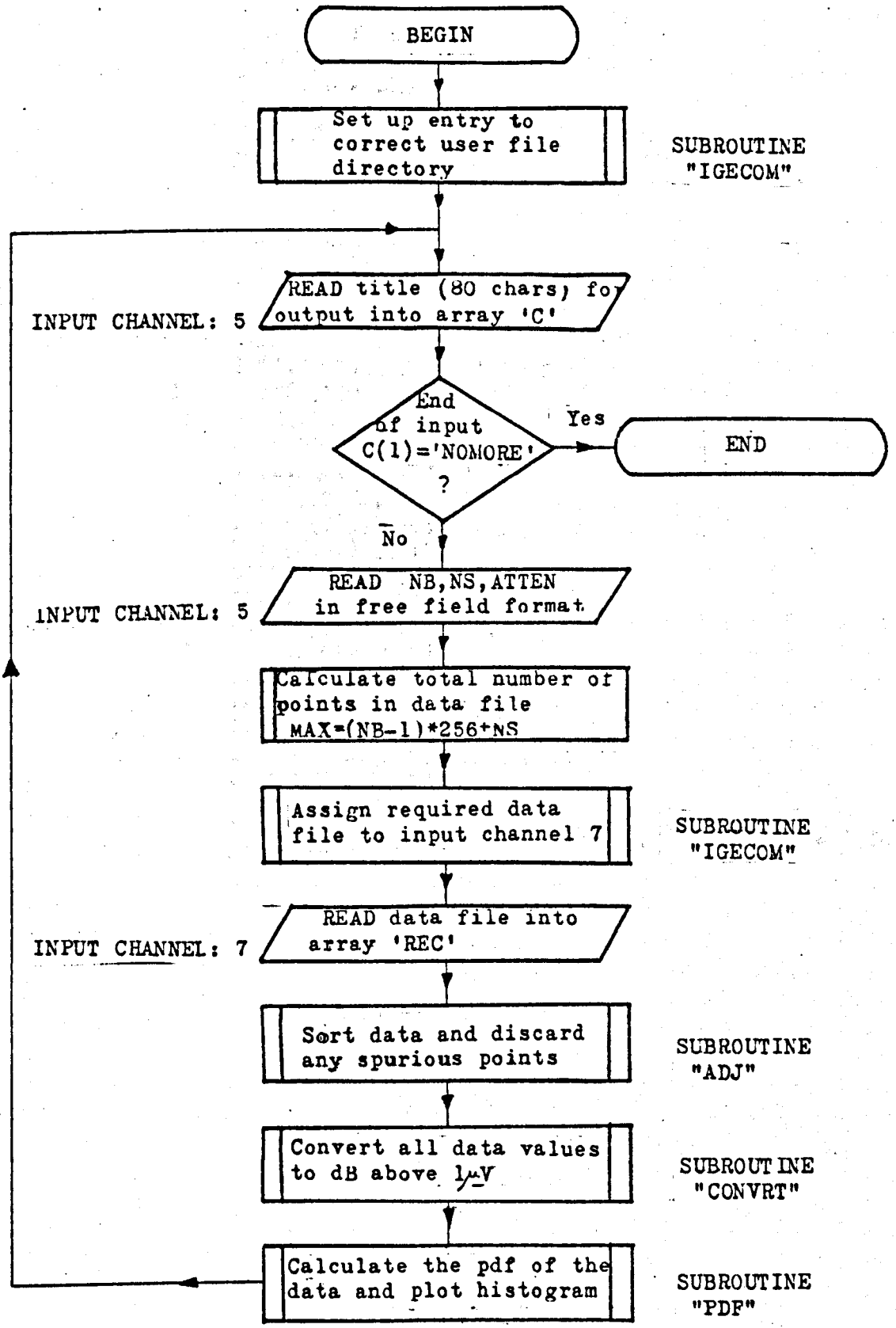

DETERMINATION OF THE PDF HISTOGRAM (ALLPDFS)

FIG D.1.4(b)

```
      PROGRAM (PDFS)
      INPUT 5 = CRO
      OUTPUT 6 = LPO
      INPUT 7 = CR1
      INPUT 8 = CR2
      END


      MASTER MAIN
      COMMON REC(8192)
      DIMENSION C(3)
      DATA END/'NOMORE  '/
      CALL IGECOM(I)
      IF(I.EQ.1)STOP 'FAIL IN DY'
10    READ(5,1)C
 1    FORMAT(3A8)
      CALL COMP8(C(1),END,I)
      IF(I.EQ.1)STOP 'OK'
      READ(5,2)NB,NS,ATTEN
 2    FORMAT(2I0,F0.0)
      MAX=(NB-1)*256+NS
      CALL ICECOM(I)
      IF(I.EQ.1)STOP 'FAIL COMERR'
      READ(7,3)(REC(I),I=1,MAX)
 3    FORMAT(8192F0.0)
      CALL ADJ(L,MAX)
      MAX=MAX-L
      DO 4 J=1,MAX
 4    CALL CONVRT(REC(J),REC(J),ATTEN)
      CALL PDF(MAX,REC,0,80,MM,4.0)
      WRITE(6,5)C,MAX
 5    FORMAT(1HO,'PDF OF ARRAY ',3A8,',TOTAL POINTS = ',I4)
      GO TO 10
      END
```

DETERMINATION OF THE PDF HISTOGRAM (ALLPDFS)

FIG. D.1.4(c)

HIGH PASS FILTERING

(i) INPUT/OUTPUT CHANNEL ASSIGNMENTS

Input Channel 5 : On-Line Card Reader

Input Channel 7 : Card Reader For Data File

Output Channel 6 : On-Line Line Printer

(ii) ON-LINE CARD READER REQUIREMENTS

Card No. 1 : The Filter width (i.e. no. of points) required for the filter in free field format. This is required to be a power of 2.

Card No. 2 : Three variables read in free field format. NB,NS,ATTEN where these are described in FIG. D.1.1(a).

(iii) ON-LINE LINE PRINTER OUTPUT GIVEN

Histograms of the low pass filtered and high pass filtered versions of the field envelope are given.

(iv) SUB-PROGRAMMES REQUIRED

Routine Called	Fig. No.	Routines required by routine called
ADJ	D.2.3	-
CONVRT	D.2.1	-
DECONV, RECONV	D.2.2	-
AVS	D.2.4, D.2.5 & D.2.6	-
PDF	D.2.8	-

(v) PURPOSE

To plot the pdf of the filtered signal envelope.

PROGRAMME REMNANT

FIG. D.1.5(a)

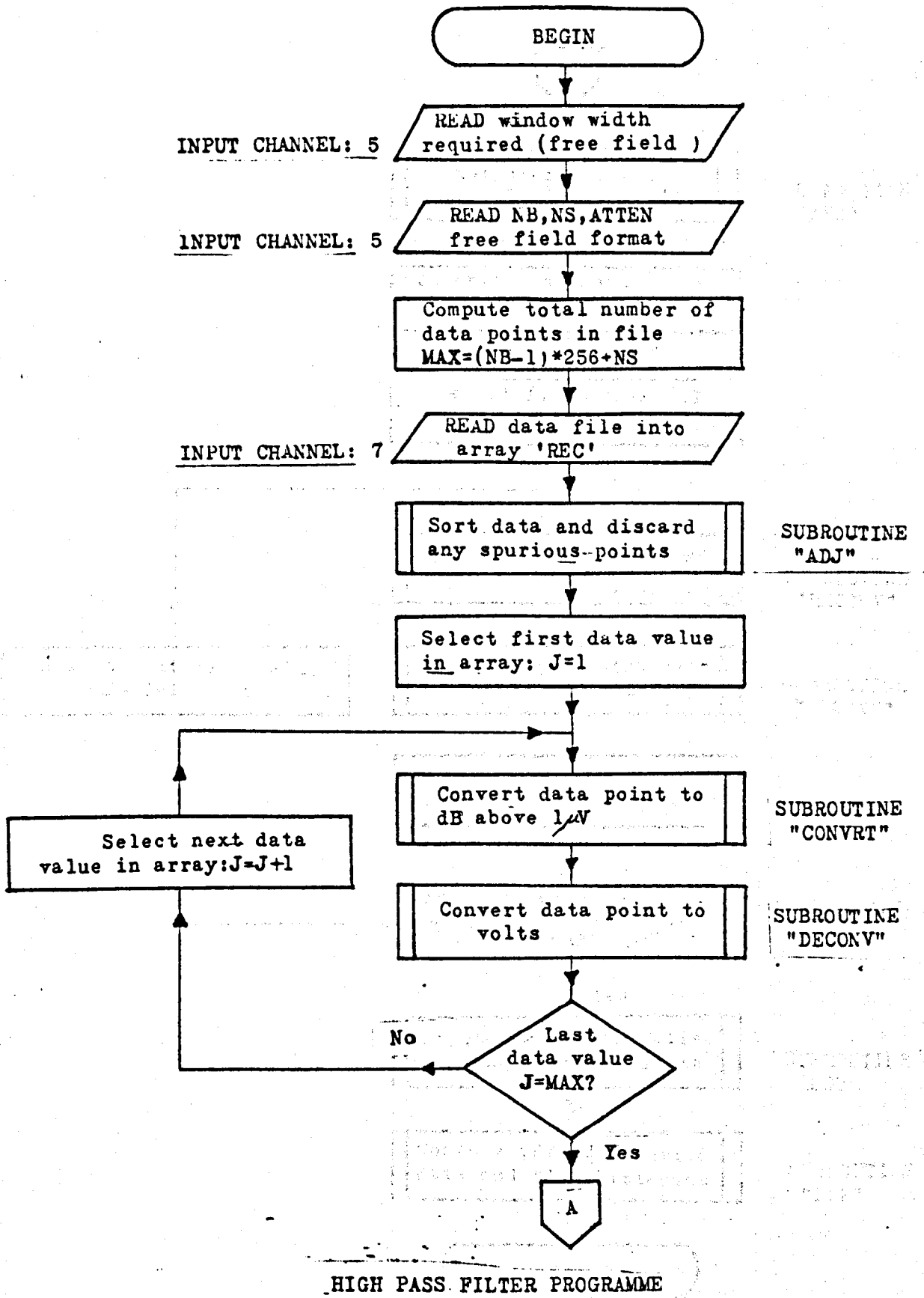

HIGH PASS FILTER PROGRAMME

FIG D.1.5(b)
Page 1 of 2

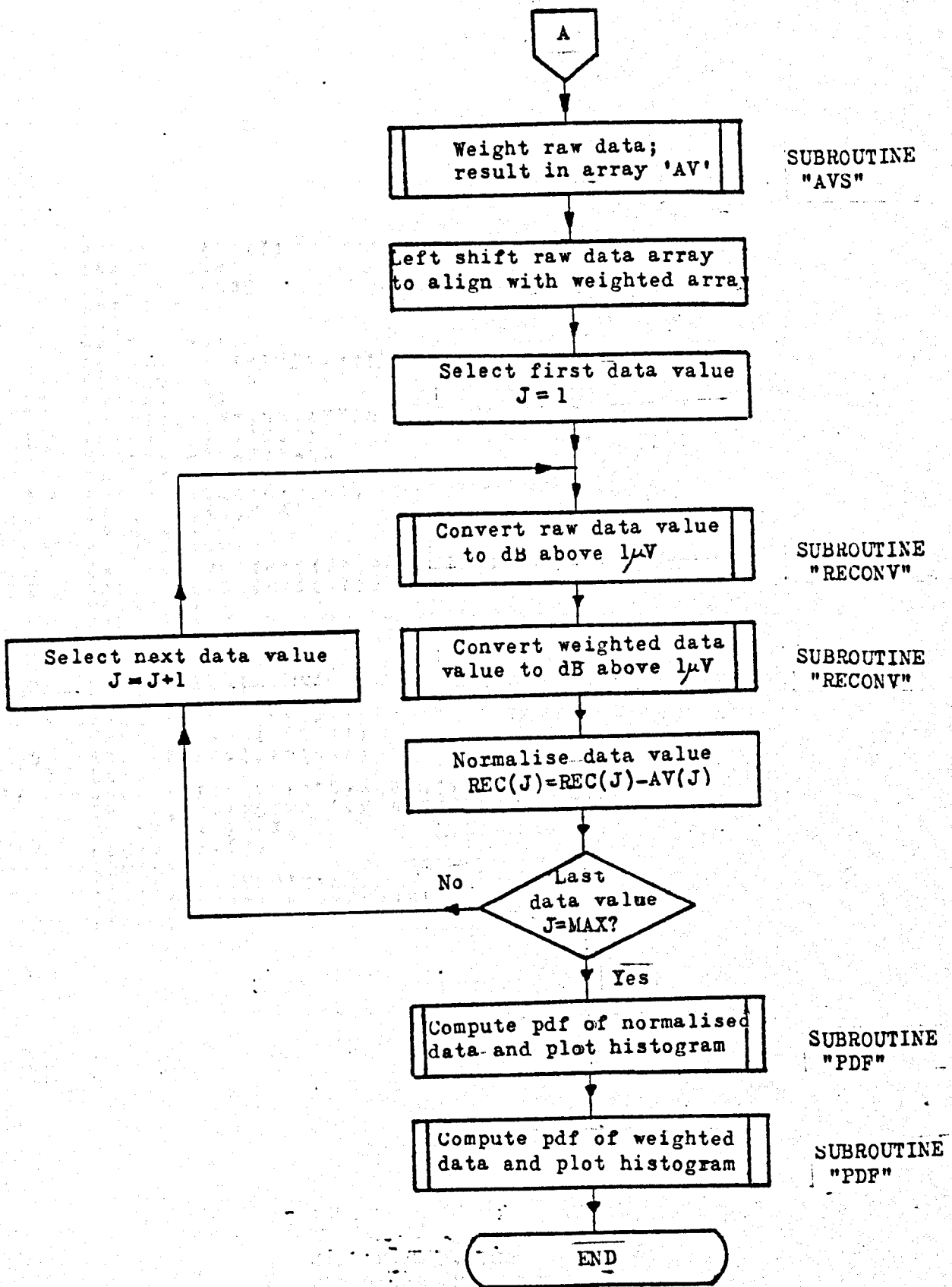

HIGH PASS FILTER PROGRAMME

FIG D.1.5(b)
Page 2 of 2

```
      PROGRAM (FORT)
      INPUT 5=CR0
      OUTPUT 6=LP0
      INPUT 7=CR1
      END
      MASTER MAIN
      COMMON REC(8192),AV(8192)
      READ(5,20)NN
   20 FORMAT(I0)
      READ(5,1)NB,NS,ATTEN
    1 FORMAT(2I0,F0.0)
      MAX=(NB-1)*256+NS
      READ(7,3)(REC(I),I=1,MAX)
    3 FORMAT(1024(6F0.0))
      CALL ADJ(L,MAX)
      MAX=MAX-L
      DO 2 J=1,MAX
      CALL CONVRT(REC(J),REC(J),ATTEN)
    2 CALL DECONV(REC(J))
      MAXM=MAX
      CALL AVS(MAXM,NN)
      MAXL=MAXM
      DO 4 J=1,MAXM
    4 REC(J)=REC(J+NN/2)
      DO 5 J=1,MAXM
      CALL RECONV(AV(J))
      CALL RECONV(REC(J))
    5 REC(J)=REC(J)-AV(J)
      LL=0
   18 CALL PDF(MAXM,REC,-40,60,MAXK,2.0)
      IF(LL.EQ.1)STOP 'OK AFTER PROGRAM'
      DO 17 J=1,MAXL
   17 REC(J)=AV(J)
      LL=LL+1
      IF(LL.EQ.1)GOTO18
      STOP 'OK AFTER PROGRAM'
      END
```

HIGH PASS FILTER
PROGRAMME (REMNANT)

FIG D.1.5(c)

AUTOCOVARIANCE OF THE AVERAGED FIELD

(i) INPUT/OUTPUT CHANNEL ASSIGNMENTS

Input Channel 5 : On-Line Card Reader

Input Channel 7 : Card Reader for Data File

Output Channel 6 : On-line Line Printer

Additional Output : File Writer Channel for the Incremental Graph Plotter

(ii) ON-LINE CARD READER INPUT REQUIRED

Card No. 1 : A title consisting of 80 alphnumeric characters to be written onto the graphical output (this may not be blank).

Card No. 2 : Three variables read in free field format.
NB,NS,ATTEN
where these are defined in FIG. D.1.1(a).

((iii) ON-LINE LINE PRINTER GIVEN

The maximum value of the covariance function is printed.

(iv) SUB-PROGRAMMES REQUIRED

Routines called	Fig. No.	Routines required by routine called	
MEAN AUTO PLOTA	Internal	LIMITS REGION FRAME BORDER CRSIZE GRAPHN AXESSI PLOTCL GREND	SYSTEM LIBRARY GHOST
ADJ	D.2.3	-	
CONVRT	D.2.1	-	
DECONV	D.2.2	-	
AVS	D.2.4,D.2.5&D.2.6	-	

(v) PURPOSE

To calculate and plot the autocovariance function of a weighted data file on an incremental graph plotter using the LEEDS GHOST package.

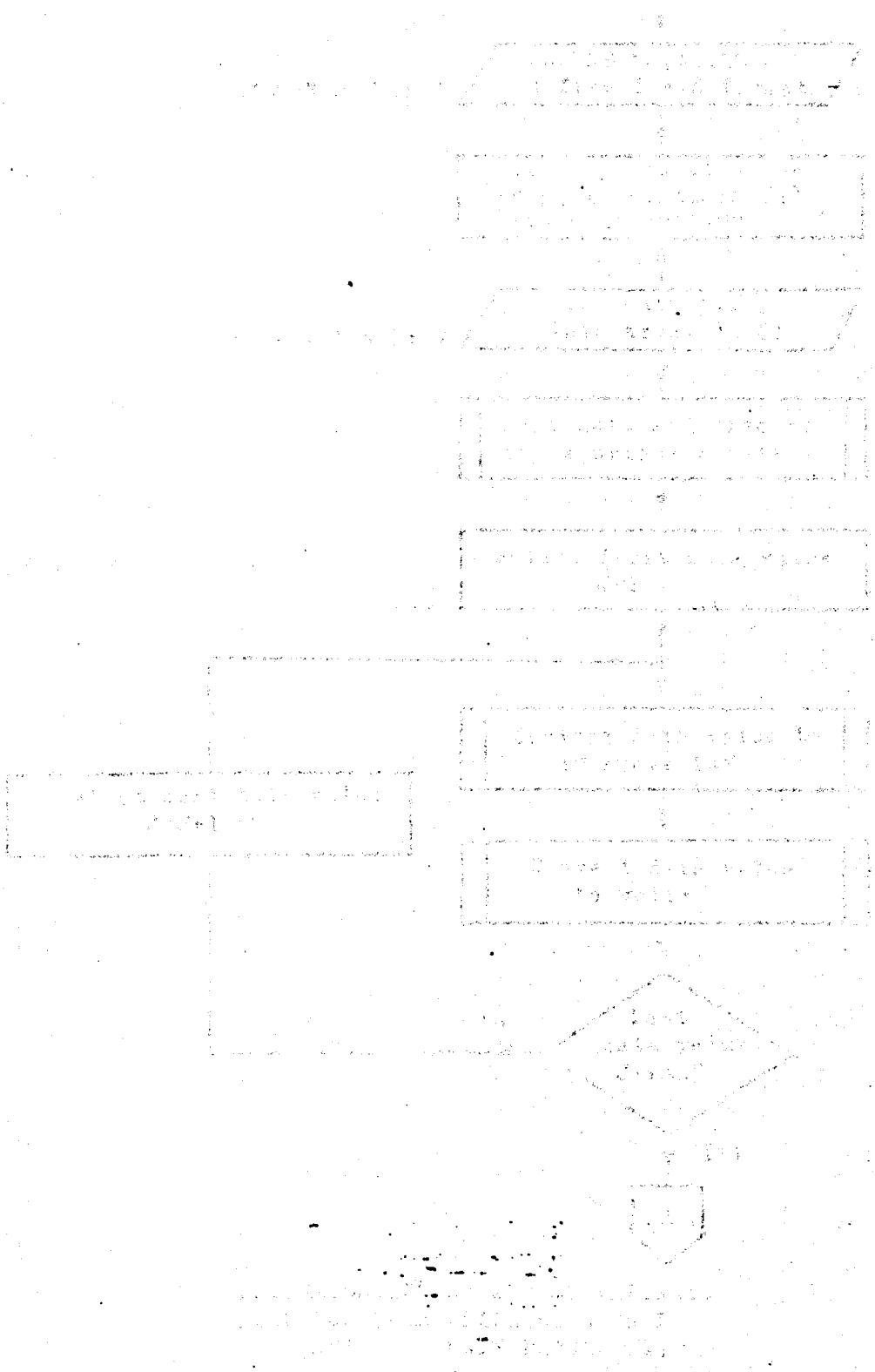

PROGRAMME AUTOAV

FIG. D.1.6(a)
Page 2 of 2

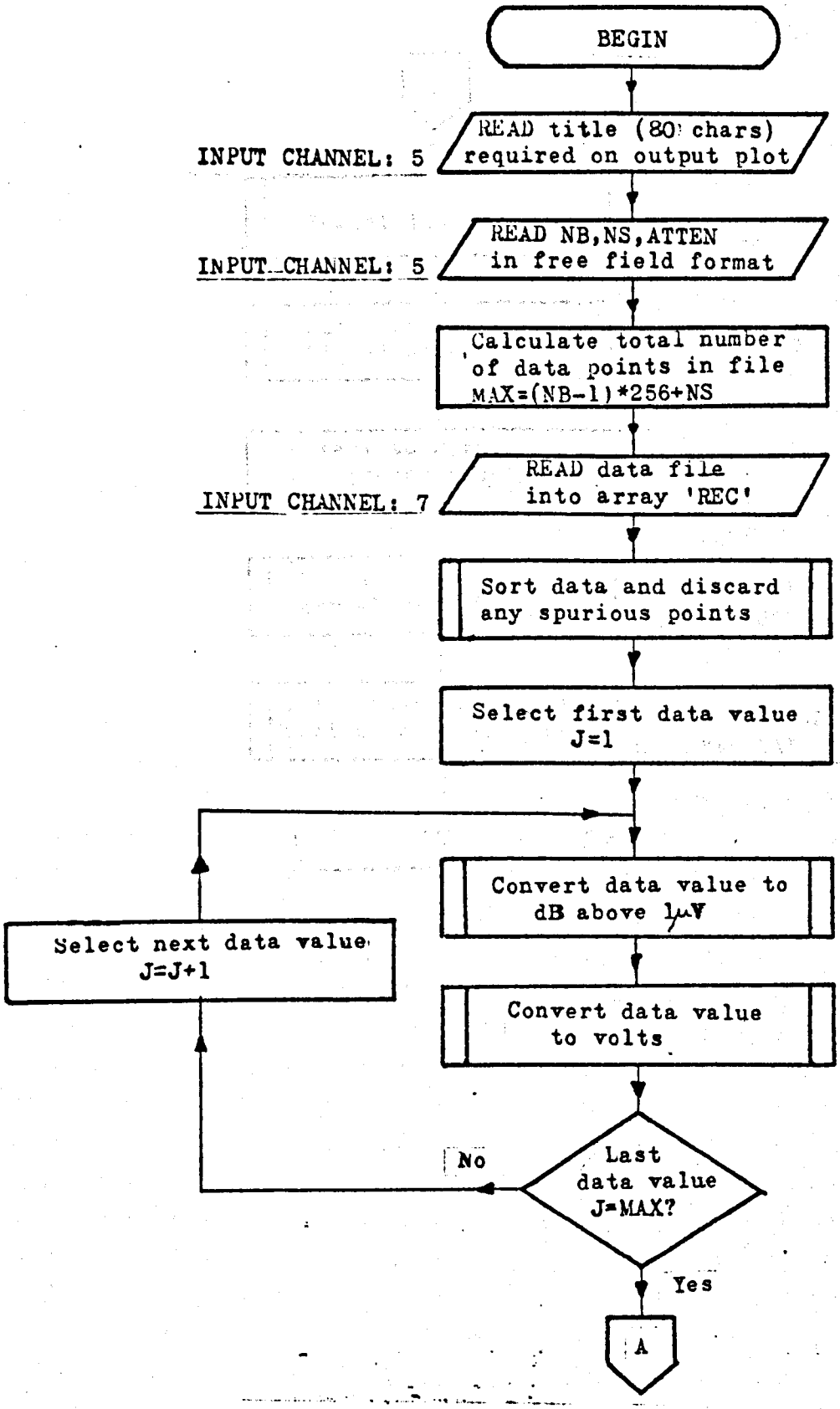

DETERMINATION OF AUTO-COVARIANCE FUNCTION OF A WEIGHTED SIGNAL
(AUTOAV - MAIN PROGRAMME)

FIG D.1.6(b)
Page 1 of 5

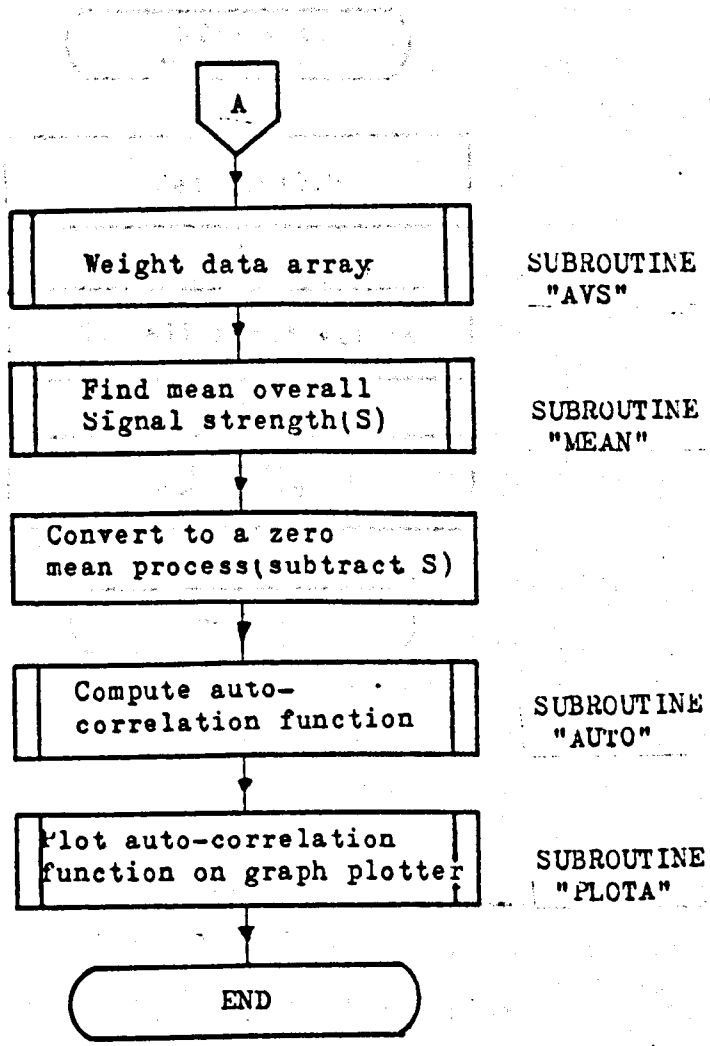

DETERMINATION OF AUTO-COVARIANCE FUNCTION OF A WEIGHTED SIGNAL (AUTOAV - MAIN PROGRAMME)

FIG D.1.6(b)
Page 2 of 5

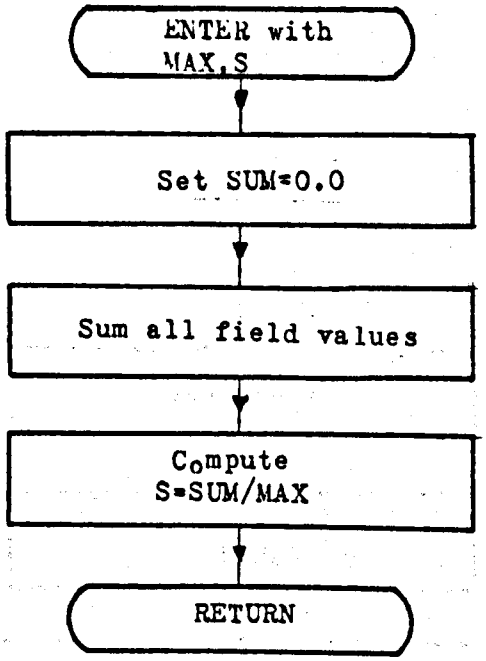

DETERMINATION OF AUTO-COVARIANCE
FUNCTION OF A WEIGHTED SIGNAL
(AUTOAV - SUBROUTINE MEAN)

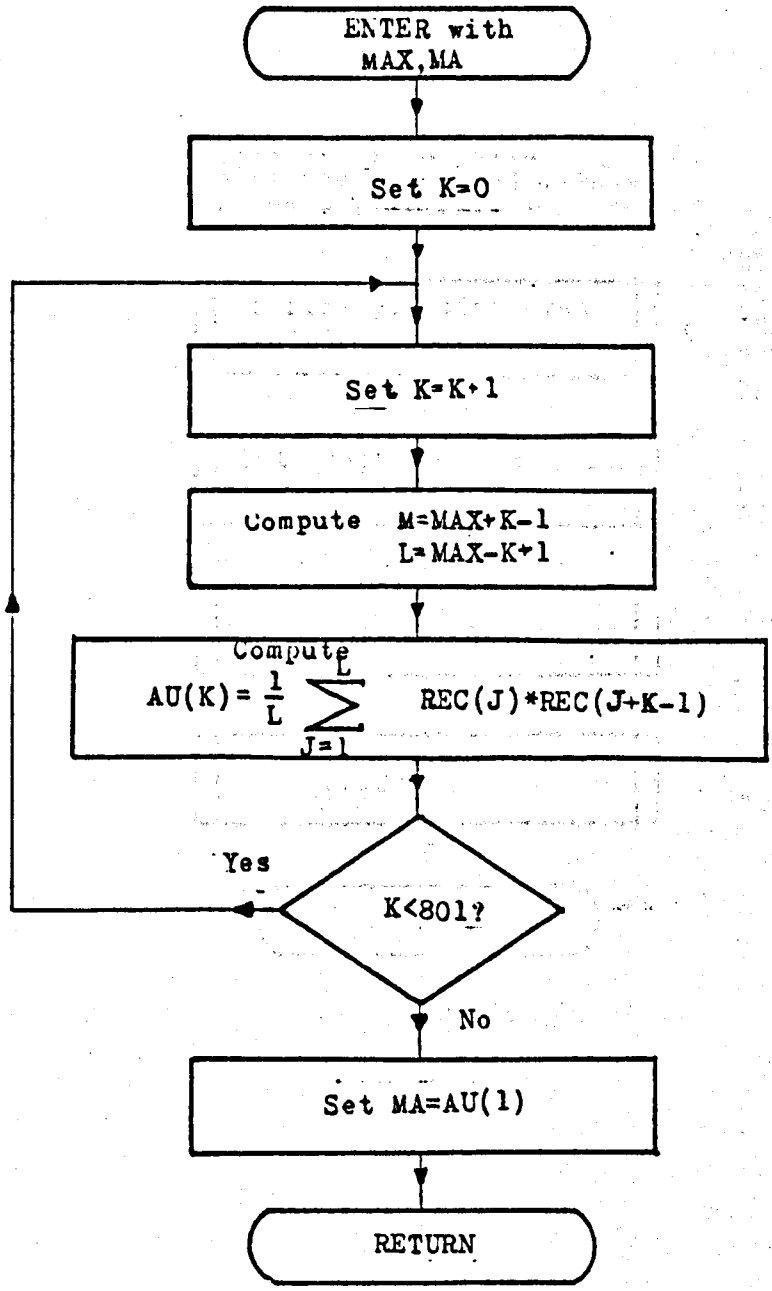

DETERMINATION OF AUTO-COVARIANCE FUNCTION OF A WEIGHTED SIGNAL (AUTOAV - SUBROUTINE AUTO)

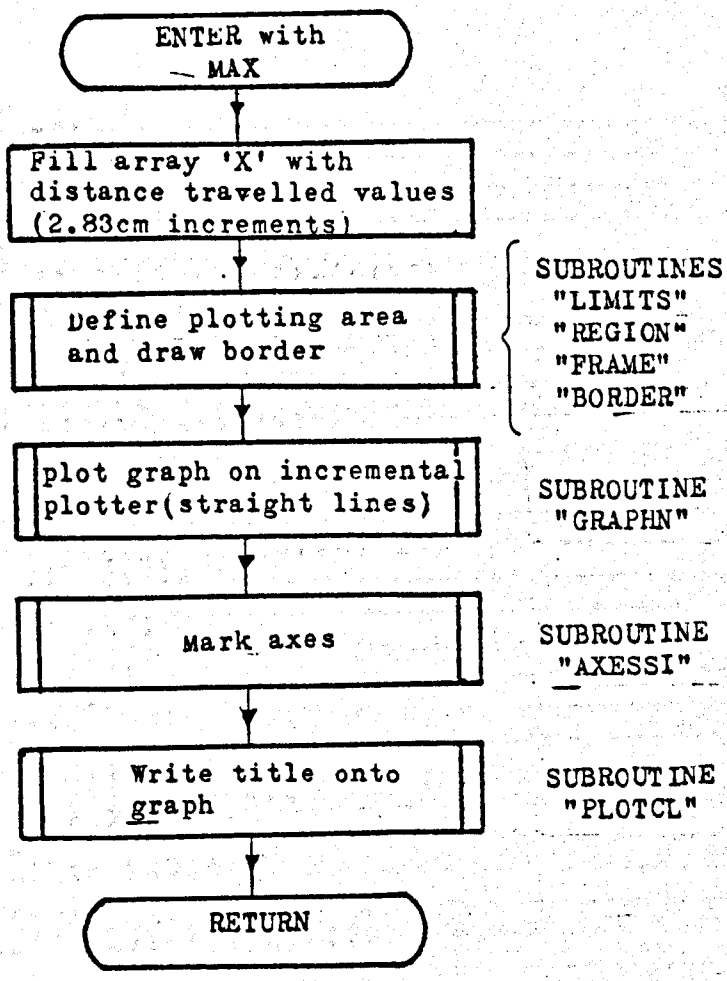

DETERMINATION OF AUTO-COVARIANCE FUNCTION OF A WEIGHTED SIGNAL (AUTOAV - SUBROUTINE PLOTA)

FIG D.1.6(b)
Page 5 of 5

```
      PROGRAM (AUTOC)
      INPUT 5=CRD
      OUTPUT 6=LPO
      INPUT 7=CR1
      END
      MASTER MAIN
      COMMON REC(8192),AU(8192),CH(10)
      READ(5,1)(CH(I),I=1,10)
    1 FORMAT(10A8)
      READ(5,2)NB,NS,ATTEN
    2 FORMAT(2I0,F0.0)
      MAX=(NB-1)*256+NS
      READ(7,3)(REC(I),I=1,MAX)
    3 FORMAT(1024(8F0.0))
      CALL ADJ(L,MAX)
      MAX=MAX-L
      DO 6 J=1,MAX
      CALL CONVRT(REC(J),REC(J),ATTEN)
    6 CALL DECONV(REC(J))
      IAV=256
      CALL AVS(MAX,IAV)
      DO 9 JJK=1,MAX
    9 REC(JJK)=AU(JJK)
      CALL MEAN(MAX,S)
      DO 7 J=1,MAX
    7 REC(J)=REC(J)-S
      CALL AUTO(MAX,RMA)
      IF(RMA.EQ.0.0)STOP 'FAIL MAX. AUTOCORRELATION NOT AT ZERO'
      CALL PLOTA(MAX)
      CALL GREND
      STOP 'OK AFTER PROGRAM'
      END
      SUBROUTINE MEAN(MAX,S)
      COMMON REC(8192),A(8192),C(10)
      SUM=0.0
      DO 1 J=1,MAX
    1 SUM=SUM+REC(J)
      S=SUM/FLOAT(MAX)
      RETURN
      END
      SUBROUTINE AUTO(MAX,MA)
      REAL MA
      COMMON REC(8192),AU(8192),CH(10)
      DO 4 J=1,801
    4 AU(J)=0.0
      N=MAX
      K=0
   10 K=K+1
      M=N+K-1
      L=N-K+1
      SUM=0.0
      DO 9 J=1,L
    9 SUM=SUM+REC(J)*REC(J+K-1)
      AU(K)=SUM/FLOAT(L)
      IF(K.LT.801)GOTO10
      MA=AU(1)
      DO 11 J=2,801
      IF(AU(J).GT.MA)GOTO14
   11 CONTINUE
      DO 12 J=1,801
   12 AU(J)=AU(J)/MA
      WRITE(6,13)MA
   13 FORMAT(1X,12HMAX. VALUE=,F20.10)
      RETURN
   14 MA=0.0
      RETURN
      END
```

DETERMINATION OF AUTO-COVARIANCE FUNCTION OF A WEIGHTED SIGNAL
(AUTOAV - MAIN PROGRAMME)
(AUTOAV - SUBROUTINES MEAN AND AUTO)

FIG D.1.6(c)
Page 1 of 2

```
      SUBROUTINE PLOTA(MAX)
      COMMON X(8192),Y(8192),C(10)
      DO 1 J=1,MAX
    1 X(J)=FLOAT(J-1)*0.0283
      CALL LIMITS(0.0,20.0,2.0,17.0)
      CALL REGION(0.0,20.0,-0.5,1.0)
      CALL FRAME
      CALL BORDER
      CALL CRSIZE(0.02)
      CALL GRAPH(X,Y,1,301)
      CALL AXESSI(1.0,0.1)
      CALL PLOTCL(20.0,0.9,24HAUTOCORRELATION FUNCTION,24)
      CALL PLOTCL(20.0,0.85,C(1),80)
      RETURN
      END
```

DETERMINATION OF AUTO-COVARIANCE FUNCTION OF A WEIGHTED SIGNAL (AUTOAV – SUBROUTINE PLOTA)

FIG D.1.6(c)
Page 2 of 2

CONVERSION OF DATA TO dB ABOVE 1μV

(i) ARGUMENT LIST

SUBROUTINE CONVRT(X,Y,ATTEN)

INPUT
- X = Signal level stored in the 1906A filestore using the systems described in Appendices A,B and C.
- ATTEN = Input attenuator setting on the field strength receiver at measurement time.

OUTPUT : Y = Signal strength in dB relative to 1μV.

(ii) OTHER INFORMATION REQUIRED

None

(iii) OTHER INFORMATION GIVEN

None

(iv) OTHER SUB-PROGRAMMES REQUIRED

None

(v) PURPOSE

To convert the signal strength values stored in the 1906A filestore as a result of the processing described in Chapter 5 into dB values referred to 1μV.

SUBROUTINE CONVRT

FIG. D.2.1(a)

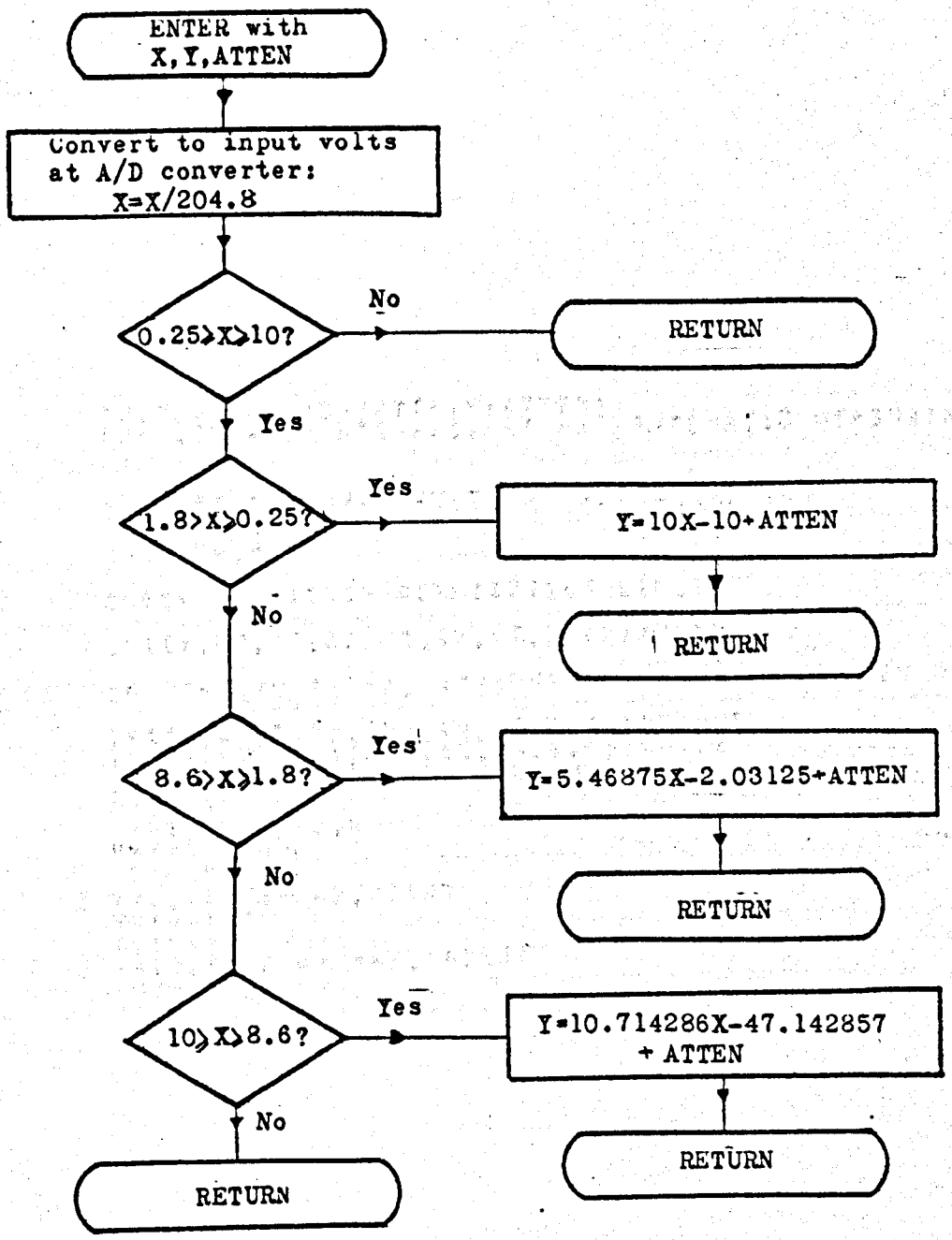

CONVERSION OF STORED DATA
TO dB ABOVE 1μW
(SUBROUTINE CONVRT)

FIG D.2.1(b)

```
      SUBROUTINE CONVRT(X,Y,ATTEN)
C     FOR USE WITH R*S F.S. RX AND AUTOMATIC MEASURING EQUIPMENT
C
C
C     CONVERT TO INPUT VOLTS AT A/D CONVERTER
C
      X=X/204.8
C
C     CHECK IF WITHIN PERMISSIBLE LIMITS
C
      IF((X.GT.10.0).OR.(X.LT.0.25))RETURN
C
C     CONVERT TO SIGNAL STRENGTH AT INPUT TO RX IN DBU
C
      IF((X.LT.1.8).AND.(X.GE.0.25))GOTO1
      IF((X.LT.6.6).AND.(X.GE.1.8))GOTO2
      IF((X.LE.10.0).AND.(X.GE.6.6))GOTO3
      RETURN
    1 Y=10.0*X-10.0
      Y=Y+ATTEN
      RETURN
    2 Y=3.46875*X-2.0312
      Y=Y+ATTEN
      RETURN
    3 Y=10.714286*X-47.142857
      Y=Y+ATTEN
      RETURN
      END
```

CONVERSION OF STORED DATA TO dB RELATIVE TO 1μV (SUBROUTINE CONVRT)

FIG D.2.1(c)

CONVERSION OF SIGNAL STRENGTH BETWEEN VOLTS AND dB

(i) ARGUMENT LISTS

SUBROUTINE RECONV(X)

SUBROUTINE DECONV(X)

X = Signal strength value

INPUT: Volts for RECONV

dB above 1μV for DECONV

OUTPUT: dB above 1μV for RECONV

Volts for DECONV

(ii) OTHER INFORMATION REQUIRED

None

(iii) OTHER INFORMATION GIVEN

None

(iv) OTHER SUB-PROGRAMMES REQUIRED

None

(v) PURPOSE

RECONV: To convert field strength in volts to dB above 1μV.

DECONV: To convert field strength in dB above 1μV to volts.

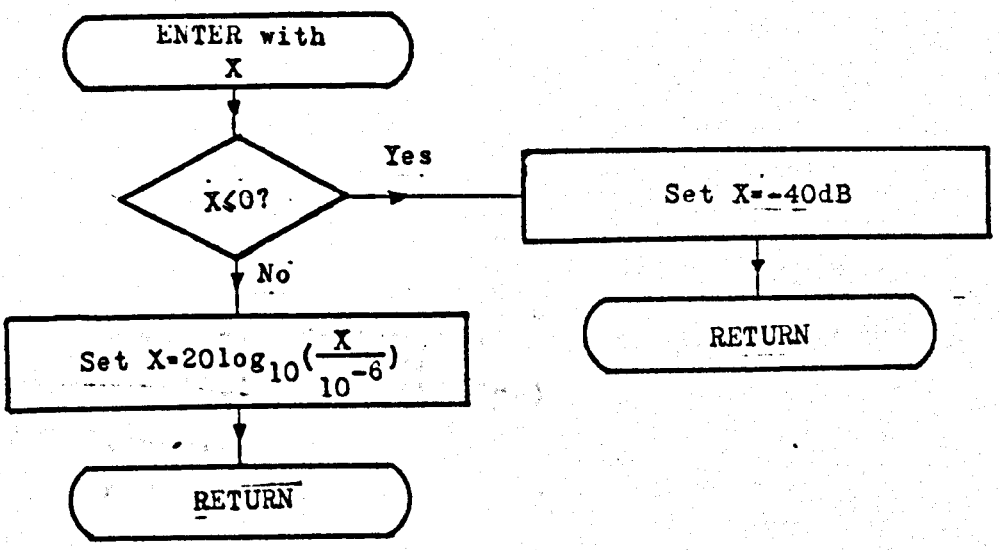

SUBROUTINE RECONV

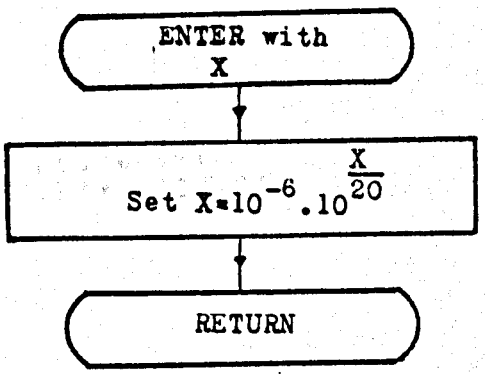

SUBROUTINE DECONV

CONVERSION OF DATA FROM dB ABOVE 1 V
TO VOLTS(DECONV) AND VICE-VERSA(RECONV)

FIG D.2.2(b)

```
      SUBROUTINE RECONV(X)
      IF(X.LE.0.0)GOTO1
      X=20.0*ALOG10(X/1.0E-06)
      RETURN
1     X=-40.0
      RETURN
      END
```

```
      SUBROUTINE DECONV(X)
      X=1.0E-6*10.0**(X/20.0)
      RETURN
      END
```

CONVERSION OF DATA FROM dB W.R.T. μV TO VOLTS (DECONV)
CONVERSION OF DATA FROM VOLTS TO dB W.R.T. μV (RECONV)

FIG D.2.2(c)

DATA SORTING PROGRAMME

(i) ARGUMENT LIST

SUBRCUTINE ADJ(L,MAX)

INPUT: MAX = Number of data points in array.

OUTPUT: L = Number of spurious data points contained within the MAX data points.

(ii) OTHER INFORMATION REQUIRED

COMMON RARR(8192)

RARR = Array containing the data to be sorted.

(iii) OTHER INFORMATION GIVEN

None

(iv) OTHER SUB-PROGRAMMES REQUIRED

None

(v) PURPOSE

To locate spurious data points in an array and to exclude them from that array.

SUBROUTINE ADJ

FIG. D.2.3(a)

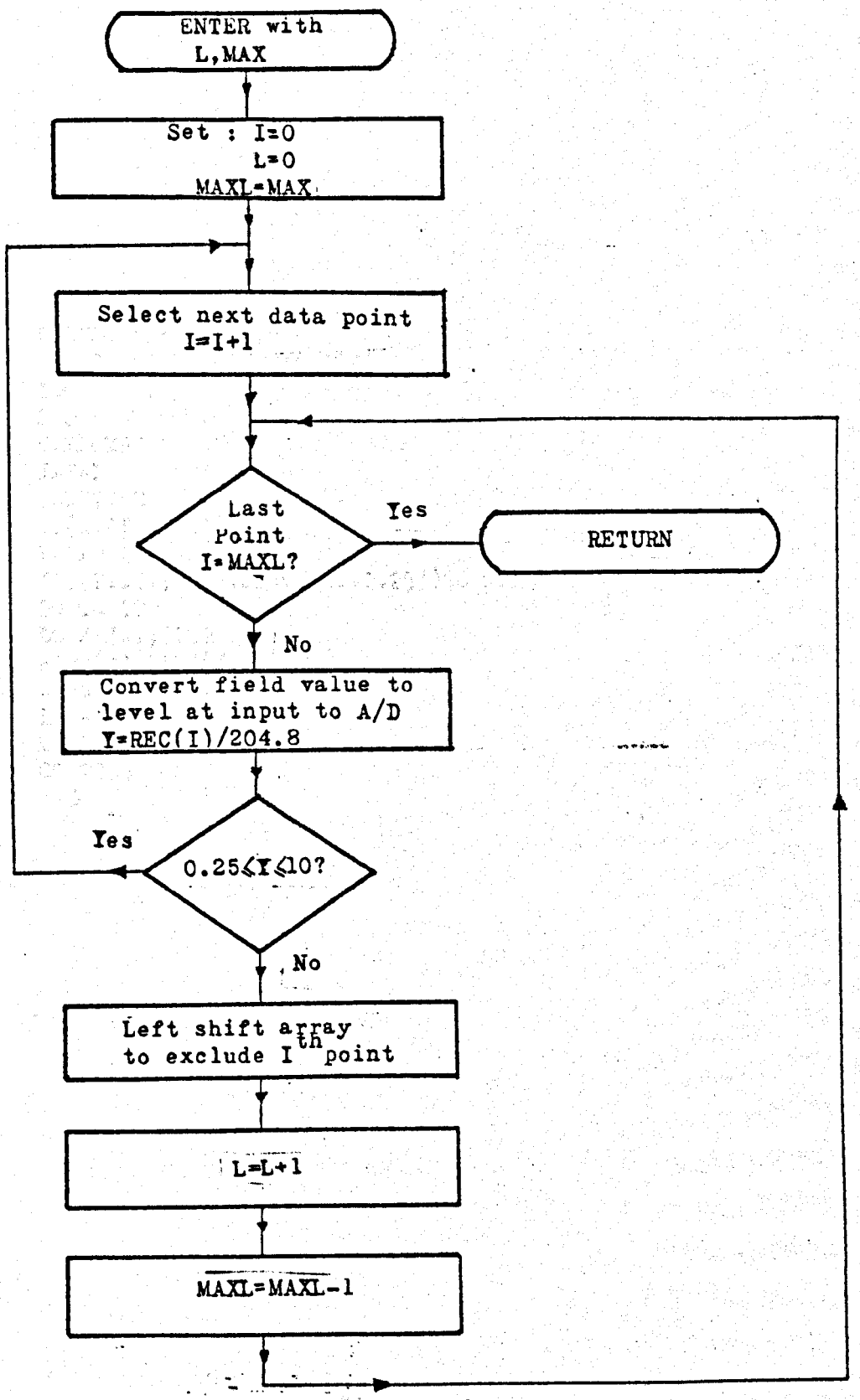

SORTING OF DATA AND EXCLUSION OF SPURIOUS VALUES(ADJ)

FIG D.2.3(b)

```
      SUBROUTINE ADJ(L,MAX)
      COMMON RARR(8192),X(8192)
      I=0
      L=0
      MAXL=MAX
10    I=I+1
 9    CONTINUE
      IF(I.GT.MAXL)RETURN
      Y=RARR(I)/204.8
      IF((Y.GT.10.0).OR.(Y.LT.0.25))GO TO 3
      GO TO 10
3     DO 4 J=I,8192
4     RARR(J)=RARR(J+1)
      RARR(8192)=0.0
      L=L+1
      MAXL=MAXL-1
      GO TO 9
      END
```

SORTING OF DATA VALUES AND EXCLUSION OF SPURIOUS POINTS (ADJ)

FIG. D.2.3(c)

RECTANGULAR WEIGHTING FUNCTION

(i) ARGUMENT LIST

SUBRCUTINE AVS(MAX,IAV)

INPUT { IAV = Width of the weighting function required (No. of points)
MAX = Number of data points in the input array.

OUTPUT : MAX = Number of data points in the weighted array.

(ii) OTHER INFORMATION REQUIRED

COMMON RARR(8192),AV(8192)

RARR = Array of data to be weighted.

(iii) OTHER OUTPUT GIVEN

COMMON RARR(8192),AV(8192)

AV = Array of the weighted data.

(iv) OTHER SUB-PROGRAMMES REQUIRED

None

(v) PURPOSE

To weight an array of data using a rectangular window function.

SUBROUTINE AVS

FIG. D.2.4(a)

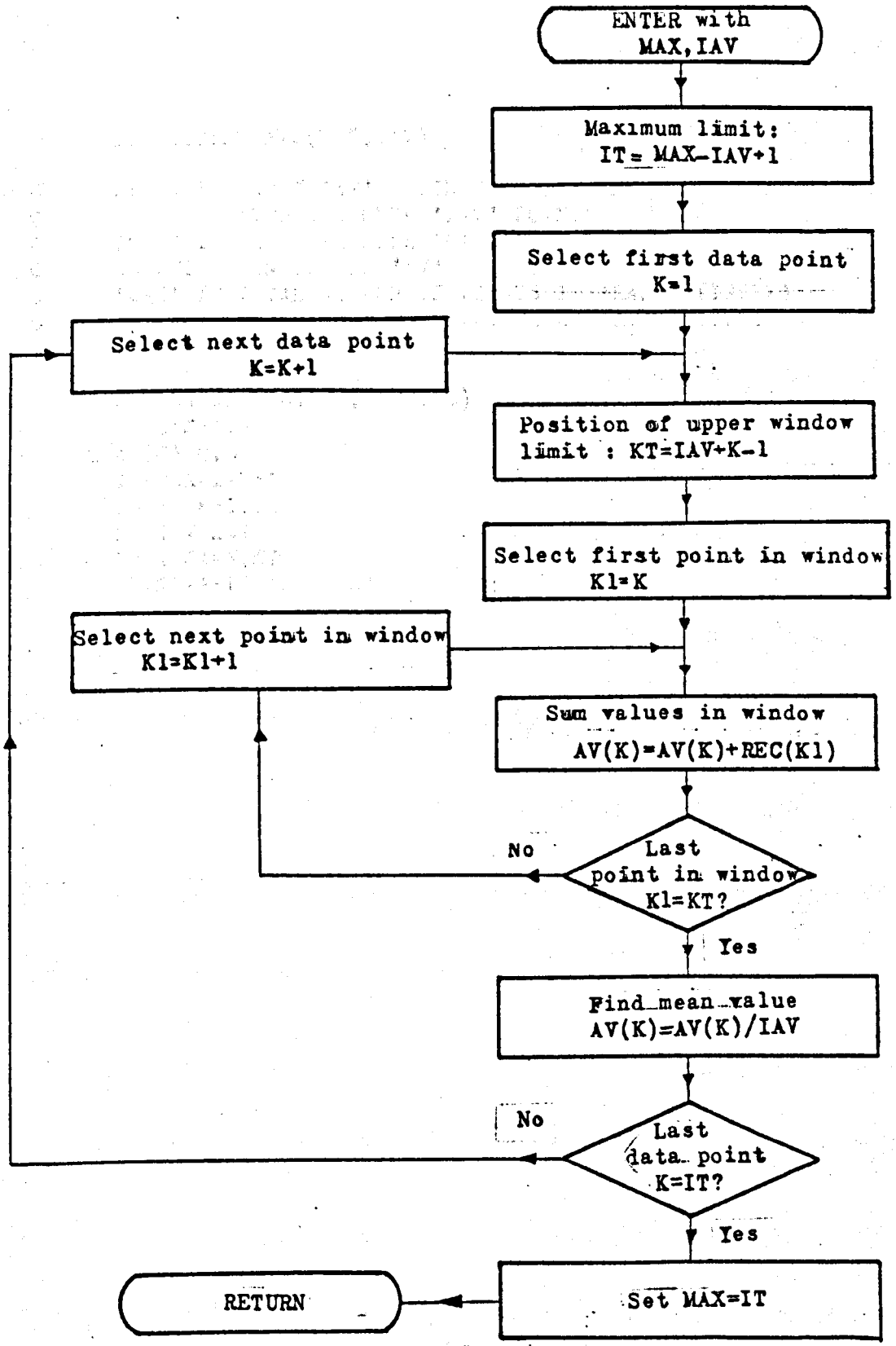

RECTANGULAR WEIGHTING
FUNCTION (AVS)

FIG D.2.4(b)

```
      SUBROUTINE AVS(MAX,IAV)

C     FINDS AN ARRAY 'AV' WHICH CONTAINS THE ARRAY 'RARR'
C              AVERAGED OVER 'IAV' POINTS.
C     INPUT IS RAW DATA FILE 'RARR'
C     OUTPUT IS IN DBU TO 'AV'
C     'MAX' IS TOTAL NUMBER OF POINTS IN 'RARR' (INPUT)
C     'MAX' IS TOTAL NUMBER OF POINTS IN 'AV' (OUTPUT)
C

      COMMON RARR(8192),AV(8192)
      DO 2 J=1,8192
    2 AV(J)=0.0
      IT=MAX-IAV+1
      DO 10 K=1,IT
      KT=IAV+K-1
      DO 1 K1=K,KT
    1 AV(K)=AV(K)+RARR(K1)
   10 AV(K)=AV(K)/FLOAT(IAV)
      MAX=IT
      RETURN
      END
```

RECTANGULAR WEIGHTING
FUNCTION (AVS)

FIG D.2.4(c)

TRIANGULAR WEIGHTING FUNCTION

This routine is identical in its requirements to the rectangular window shown in Fig. D.2.4(a) except that a triangular function is employed with a width (IAV) which must be specified as a power of 2 in the calling statement.

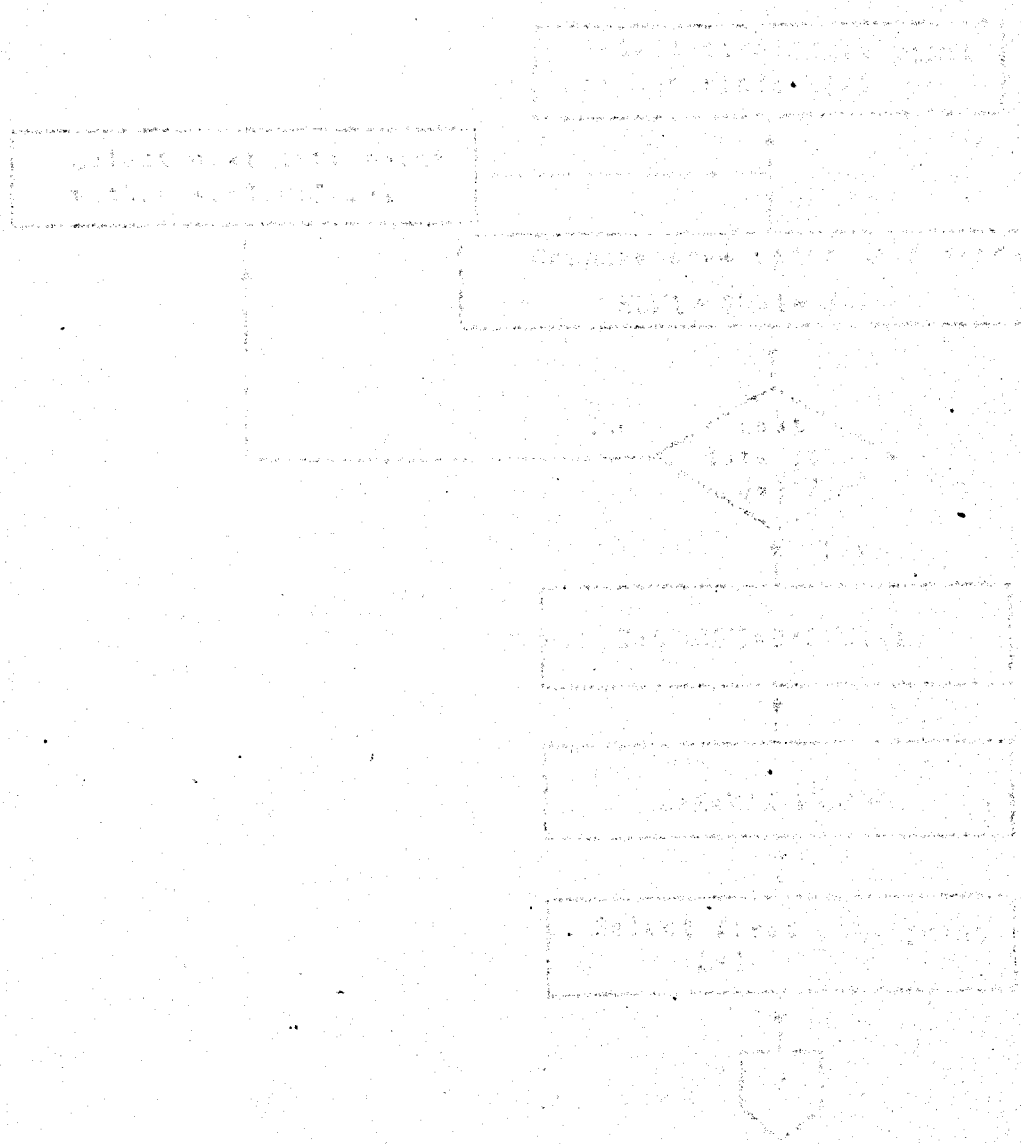

SUBROUTINE AVS

FIG. D.2.5(a)

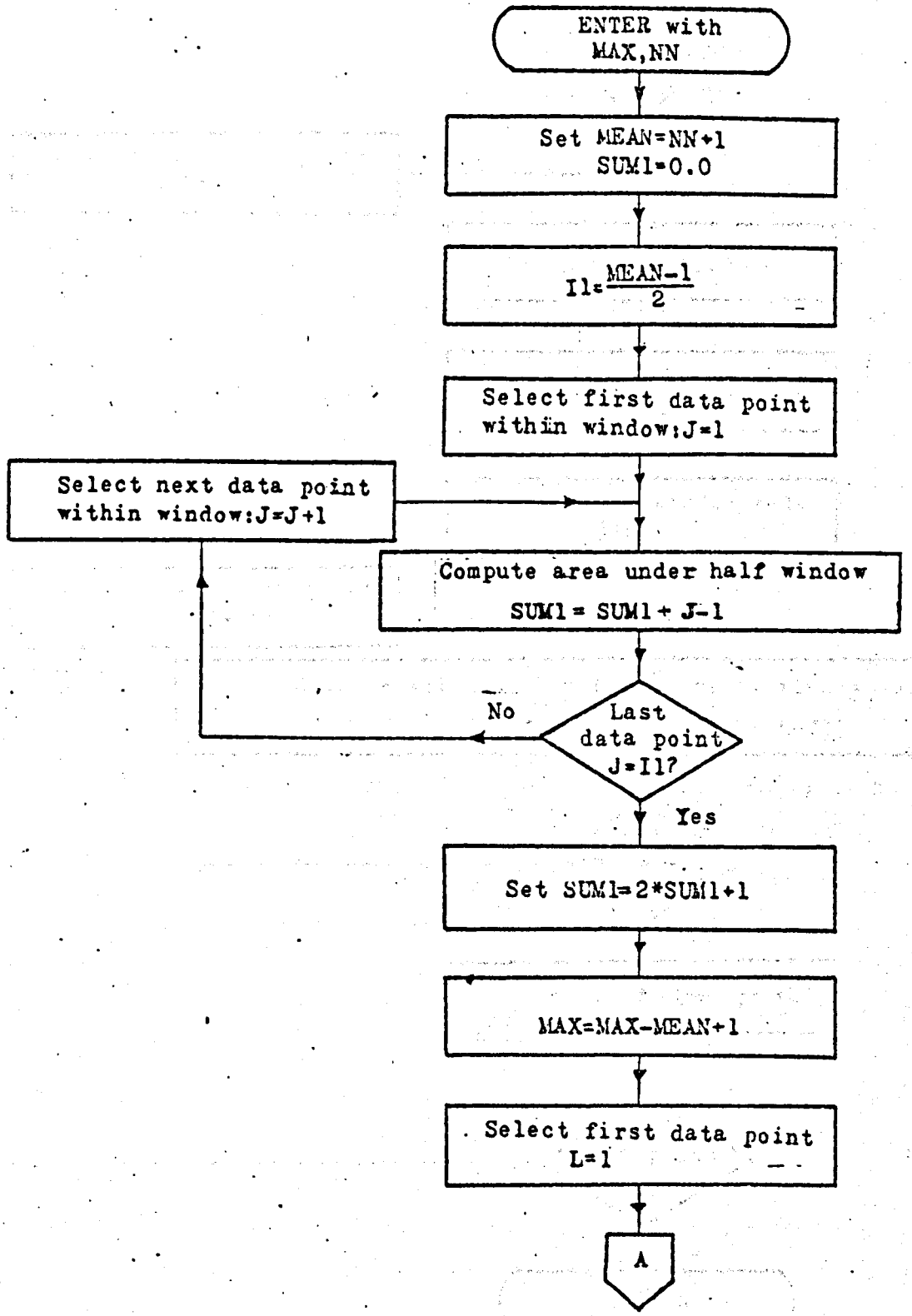

TRIANGULAR WEIGHTING FUNCTION (AVS)

FIG D.2.5(b)
Page 1 of 2

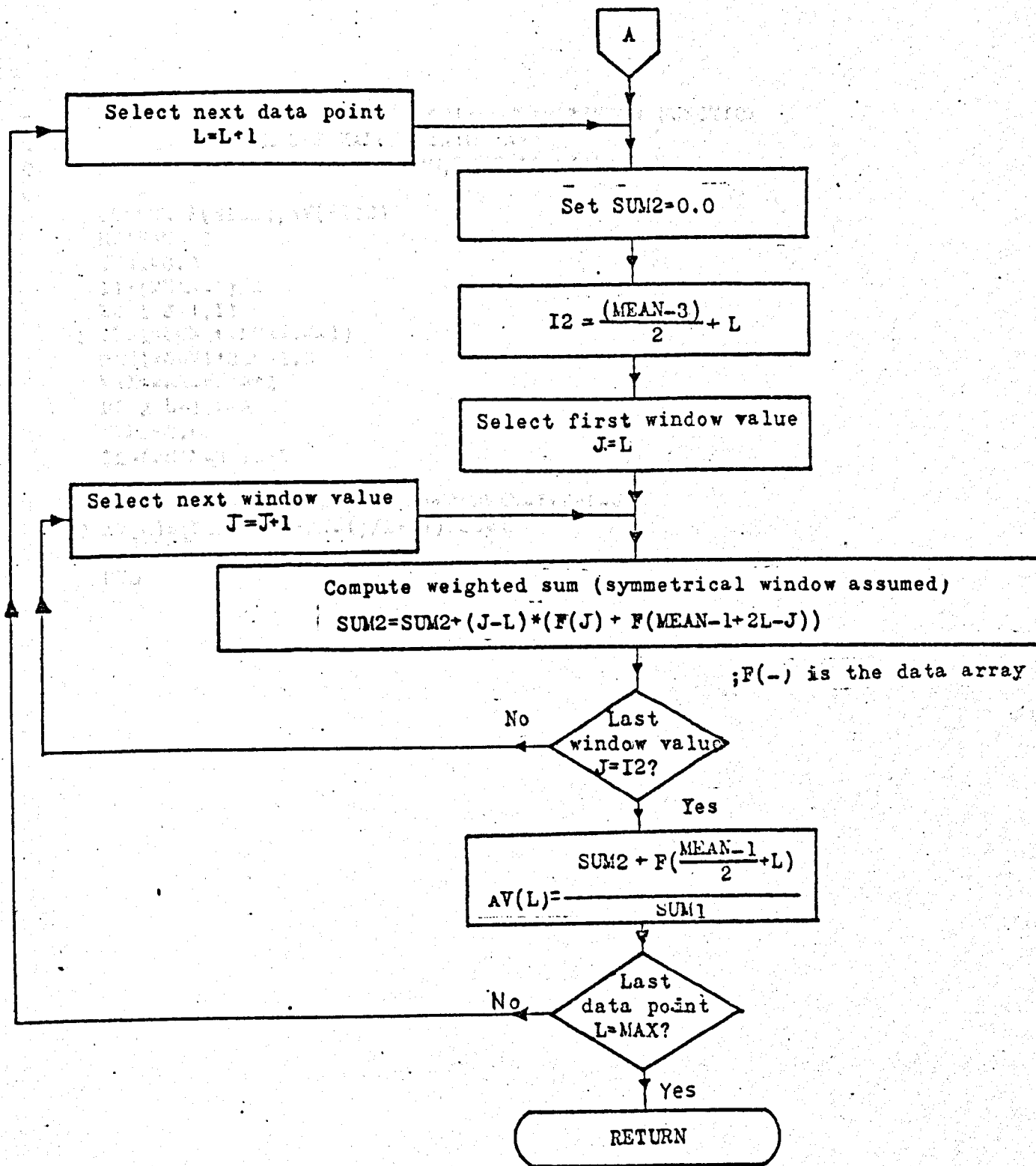

TRIANGULAR WEIGHTING FUNCTION (AVS)

FIG D.2.5(b)
Page 2 of 2

```
      SUBROUTINE AVS(MAX,NN)
C     WEIGHTS ARRAY 'F' USING A TRIANGULAR WINDOW FUNCTION
C             AND PLACES VALUES INTO 'AV'
C     NN INPUT TO ROUTINE AS 2**N,USED AS 2**N+1
C
      COMMON F(8192),AV(8192)
      MEAN=NN+1
      SUM1=0.0
      I1=(MEAN-1)/2
      DO 1 J=1,I1
    1 SUM1=SUM1+FLOAT(J-1)
      SUM1=SUM1*2.0+1.0
      MAX=MAX-MEAN+1
      DO 2 L=1,MAX
      SUM2=0.0
      I2=(MEAN-3)/2+L
      DO 3 J=L,I2
    3 SUM2=SUM2+FLOAT(J-L)*(F(J)+F(MEAN-1+2*L-J))
    2 AV(L)=(SUM2+F(MEAN-1)/2+L))/SUM1
      RETURN
      END
```

TRIANGULAR WEIGHTING FUNCTION (AVS)

FIG D.2.5(c)

RAISED COSINE WEIGHTING FUNCTION

This routine is identical in its requirements to the rectangular window shown in Fig. D.2.4(a) except that a raised cosine function is employed with a width (IAV) which must be specified as a power of 2 in the calling statement.

SUBROUTINE AVS

-FIG. D.2.6(a)

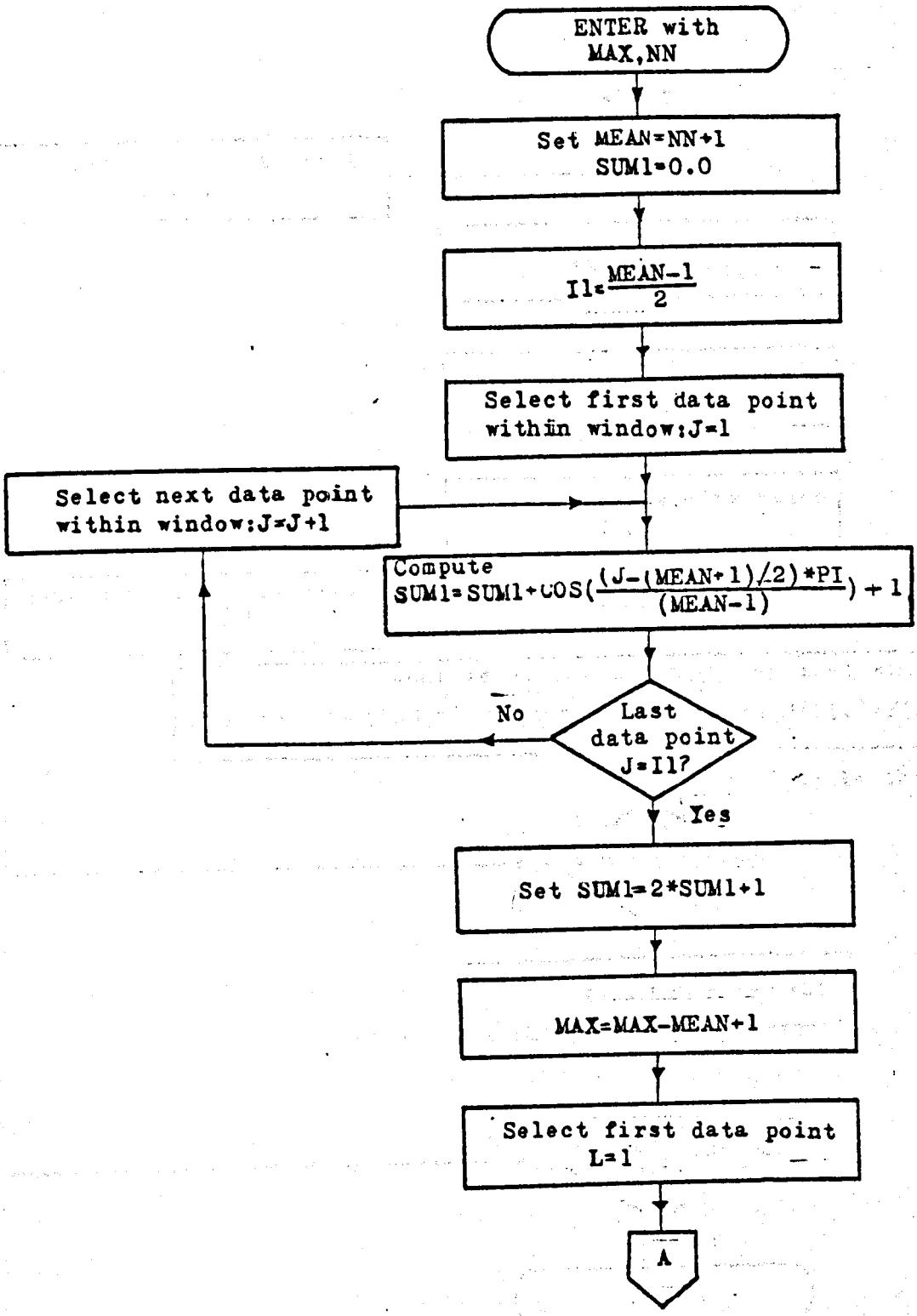

RAISED COSINE WEIGHTING FUNCTION (AVS)

FIG D.2.6(b)
Page 1 of 2

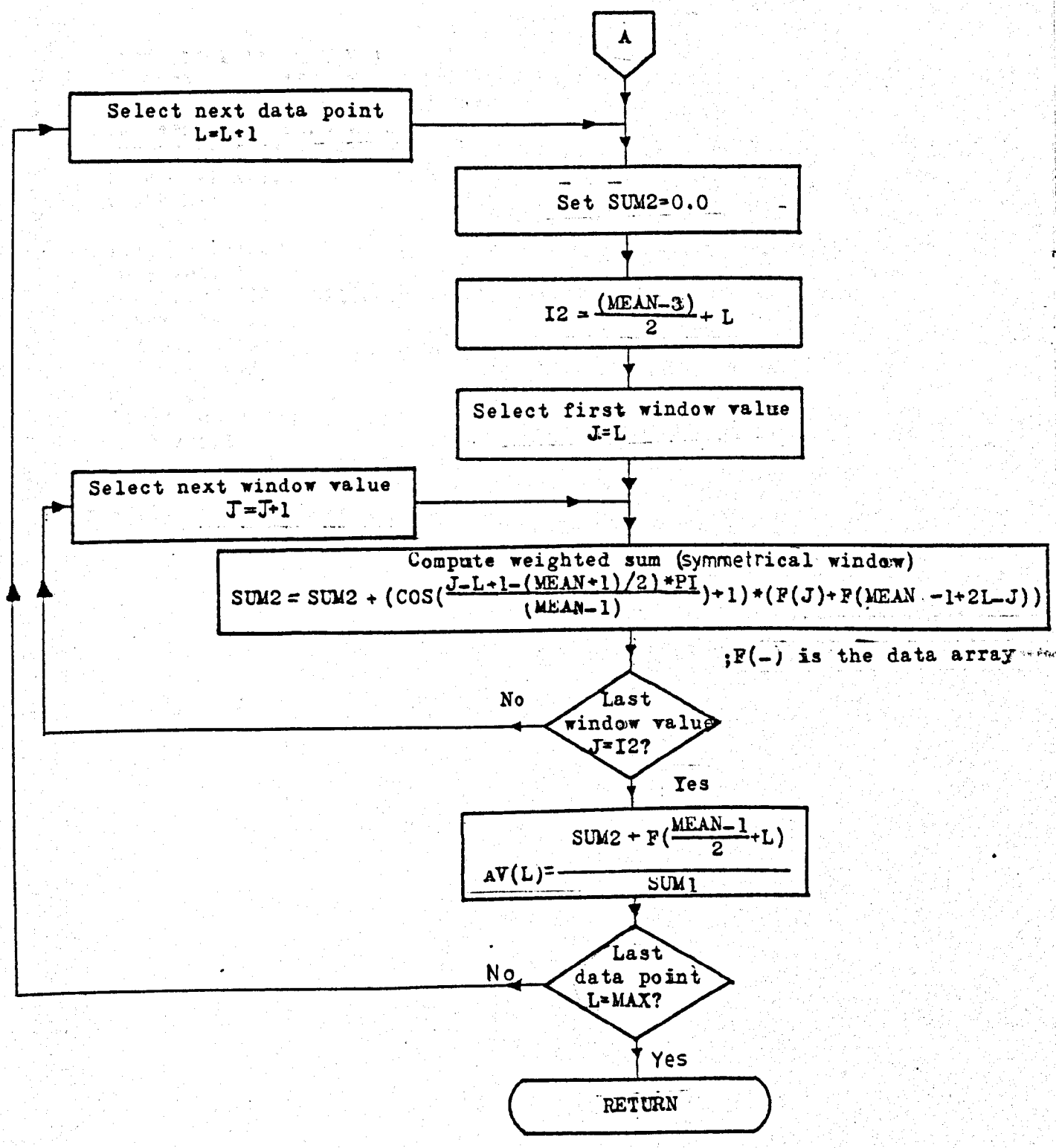

RAISED COSINE WEIGHTING FUNCTION (AVS)

FIG D.2.6(b)
Page 2 of 2

```
      SUBROUTINE AVS(MAX,NN)
C     WEIGHTS ARRAY 'F' BY A RAISED COSINE FUNCTION AND
C             PLACES VALUES INTO 'AV'
C     NN=2**N INPUT USED AS 2**N+1 WINDOW WIDTH
      COMMON F(8192),AV(8192)
      PI=4.0*ATAN(1.0)
      MEAN=NN+1
      SUM1=0.0
      I1=(MEAN-1)/2
      DO 1 J=1,I1
    1 SUM1=SUM1+COS(FLOAT(J-(MEAN+1)/2)*PI/FLOAT(MEAN-1))+1
      SUM1=2.0*SUM1+1
      MAX=MAX-MEAN+1
      DO 2 L=1,MAX
      SUM2=0.0
      I2=(MEAN-3)/2+L
      DO 3 J=L,I2
    3 SUM2=SUM2+(COS(FLOAT(J-L+1-(MEAN+1)/2)*PI/FLOAT(MEAN-1))+1)
     1*(F(J)+F(MEAN-1+2*L-J))
    2 AV(L)=(SUM2+F((MEAN-1)/2+L))/SUM1
      RETURN
      END
```

RAISED COSINE WEIGHTING FUNCTION (AVS)

FIG D.2.6(c)

DETERMINATION OF MEDIAN VALUES

(i) ARGUMENT LIST

SUBROUTINE MEDS(MAX,MED)

INPUT { MAX = Total number of data points in input array.
MED = Number of data points over which the median value is to be determined.

OUTPUT : MAX = Total number of points in output array.

(ii) OTHER INFORMATION REQUIRED

COMMON RARR(8192),RMEDN(8192)

RARR = Array of data to be processed.

(iii) OTHER INFORMATION GIVEN

COMMON RARR(8192),RMEDN(8192)

RMEDN = Array of median values of array RARR determined over MED points at stepped intervals.

(iv) OTHER SUB-PROGRAMMES REQUIRED

None

(v) PURPOSE

To determine the median values of an array of data over a fixed interval which is stepped along the data record.

SUBROUTINE MEDS

FIG. D.2.7(a)

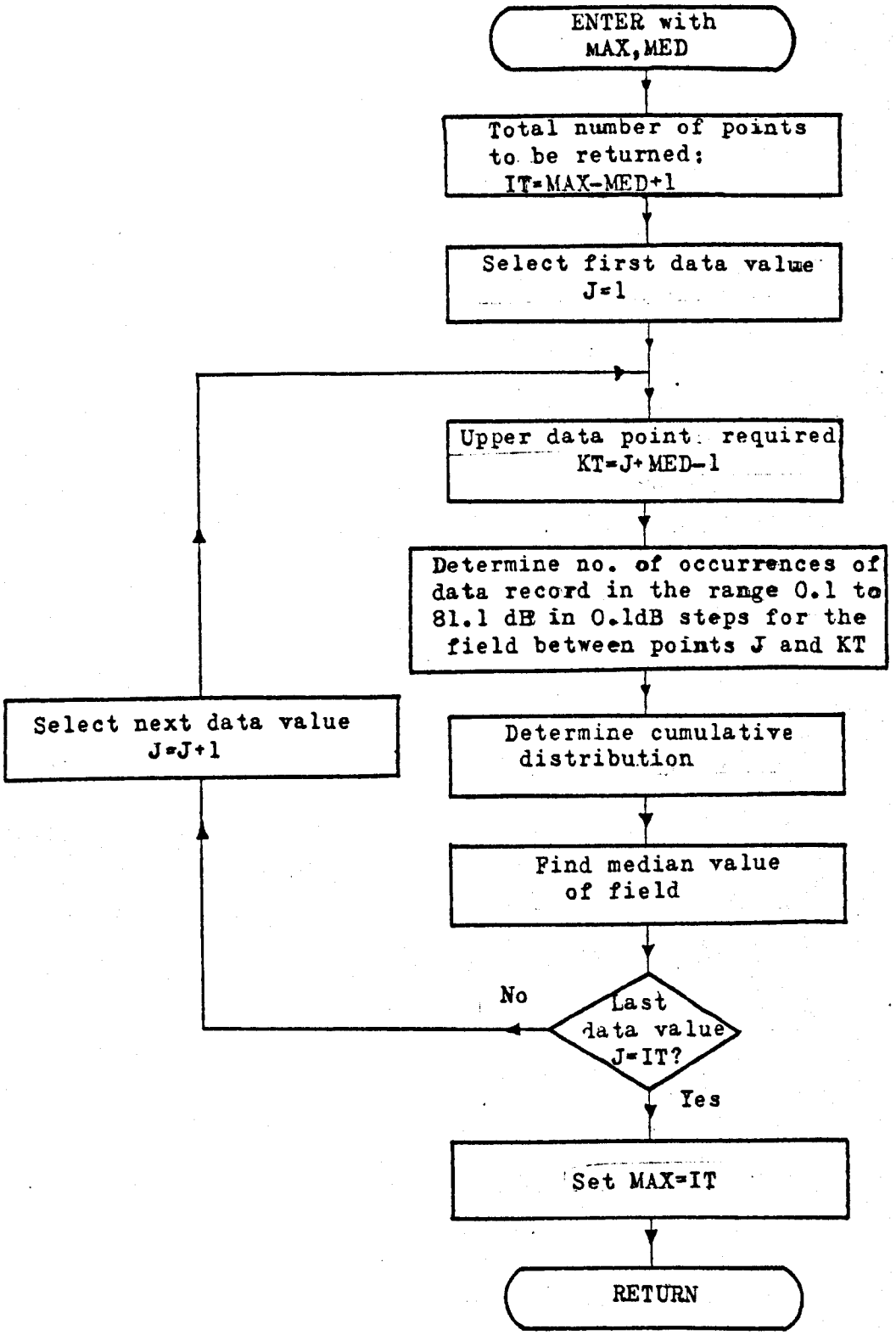

DETERMINATION OF MEDIAN VALUES
AT 0.1dB STEPPED INTERVALS
ALONG THE DATA RECORD (MEDS)

FIG D.2.7(b)

```
      SUBROUTINE MEDS(MAX,MED)
      COMMON RARR(8192),RMEDN(8192)
      DIMENSION IC(811),P(811),Q(811)
      DO 2 J=1,8192
    2 RMEDN(J)=0.0
      IT=MAX-MED+1
      DO 10 J=1,IT
      DO 3 J1=1,811
      IC(J1)=0
      P(J1)=0.0
    3 Q(J1)=0.0
      KT=J+MED-1
      DO 11 K=J,KT
      I=NINT(RARR(K)*10.0)
      IF((I.LT.1).OR.(I.GT.811))GOTO20
      IC(I)=IC(I)+1
      GOTO11
   20 CONTINUE
   11 CONTINUE
      DO 12 K=1,811
   12 P(K)=FLOAT(IC(K))/FLOAT(MED)*100.0
      Q(1)=0.0
      DO 13 K=2,811
      M1=K-1
   13 Q(K)=Q(M1)+P(M1)
      DO 10 K=1,810
      IF((Q(K).LE.50.0).AND.(Q(K+1).GE.50.0))RMEDN(J)=FLOAT(K)/10.0
   10 CONTINUE
      MAX=IT
      RETURN
      END
```

DETERMINATION OF MEDIAN VALUES
ALONG A DATA RECORD (MEDS)

FIG D.2.7(c)

DETERMINATION OF THE PDF HISTOGRAM

(i) ARGUMENT LIST

SUBROUTINE PDF(MAX,A,IZ,IS,MAXM,SCALE)

INPUT
- MAX = Total number of data points in input array.
- A = Input data array (8192 points)
- IZ = Minimum value anticipated in array A ($\leqslant$ 0dB)
- IS = Maximum value anticipated in array A (dB)
- SCALE = Scale factor for output histogram
  (1.0 = 100% full scale)
  (2.0 = 50% full scale , etc.)

OUTPUT : MAXM = Number of points in the range IZ to IS which have been used to determine the histogram.

(ii) OTHER INFORMATION REQUIRED

None

(iii) OTHER INFORMATION GIVEN

COMMON /PDFCOM/ P(501),IC(501),ALINE(101)

P = Matrix of probabilities of occurrences.

IC = Matrix of number of occurrences of the event.

ALINE = Used internally.

A histogram of the pdf is also printed on output channel No. 6.

(iv) OTHER SUB-PROGRAMMES REQUIRED

None

(v) PURPOSE

To calculate the pdf of an array of data and to plot the resulting histogram on the line printer.

SUBROUTINE PDF

FIG. D.2.8(a)

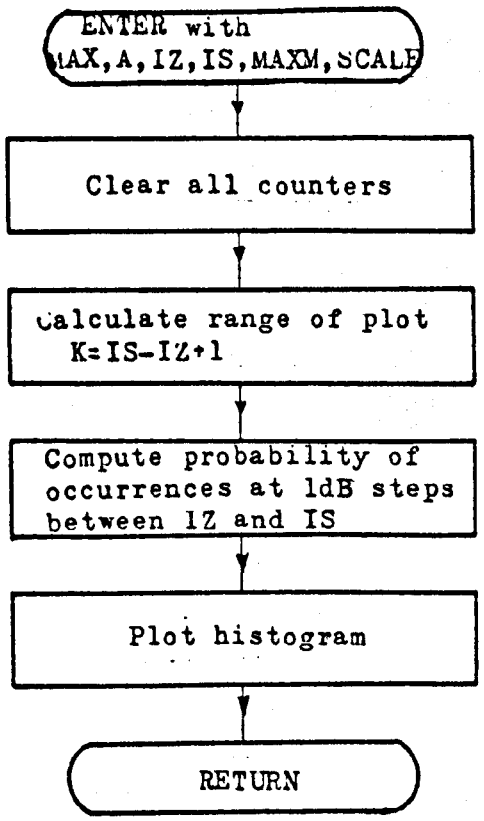

OUTPUT CHANNEL: 6

CALCULATION OF PDF
HISTOGRAM (PDF)

FIG D.2.8(b)

```
      SUBROUTINE PDF(MAX,A,IZ,IS,MAXM,SCALE)
C
C     IZ=MINIMUM VALUE ALLOWED IN A(J), <0
C     A=ARRAY OF DATA
C     IS=MAXIMUM VALUE OF A(J) FOR PDF TO BE FOUND
C      MAX=POINTS INCLUDED IN PLOT
C     SCALE=SCALE FACTOR FOR GRAPH.1.0=100% FULL SCALE
C                                   .2.0=50% FULL SCALE
C
C
      DIMENSION A(8192)
      COMMON/PLOT00/P(500),IC(500),ALINE(101)
      DATA SP,EYE,STAR,DASH/' ','I','*','-'/
      DO 1 J=1,500
      P(J)=0.0
    1 IC(J)=0
      LGT=0
      LLT=0
      COM=0.0
      K=IS-IZ+1
      DO 2 J=1,MAX
      I=MINT(A(J))-IZ+1
      IF(I.GT.K)GOTO3
      IF(I.LT.1)GOTO4
      GOTO5
    3 LGT=LGT+1
      GOTO2
    4 LLT=LLT+1
      GOTO2
    5 IC(I)=IC(I)+1
    2 CONTINUE
      MAXM=MAX-LGT-LLT
      DO 6 J=1,500
    6 P(J)=FLOAT(IC(J))/FLOAT(MAXM)*100.0
      WRITE(6,7)
    7 FORMAT(1H1)
      DO 100 L=1,K
      IF(L.EQ.(1-IZ))GOTO20
      DO 9 J=1,101
    9  ALINE(J)=SP
      GOTO25
   20 DO 21 J=1,101
   21  ALINE(J)=DASH
      DO 22 J=1,101,10
   22 ALINE(J)=EYE
   25 ALINE(1)=EYE
      I=MINT(SCALE*P(L))+1
      ALINE(I)=STAR
      M=L+IZ-1
      IF(L.NE.1)COM=COM+P(L-1)
      WRITE(6,50)COM,P(L),M,(ALINE(J),J=1,101)
   50 FORMAT(1X,F7.3,F7.3,1X,I5,1X,101A1)
  100 CONTINUE
      RETURN
      END
```

FIG D.2.8(c)

CALCULATION AND PLOTTING OF PDF HISTOGRAM (PDF)

SCALED PLOT ROUTINE

(i) ARGUMENT LIST

SUBROUTINE PLOT(MAX,BAND)

INPUT
- MAX = Number of data points to be plotted.
- BAND = Frequency designation : L = 85.875MHz
  H = 167.2MHz
  U = 441.025MHz

(ii) OTHER INFORMATION REQUIRED

COMMON RARR(8192),X(8192),CHAR(10)

RARR = Array of data to be plotted.

X = Used internally.

CHAR = Array of alphanumeric characters to be plotted as a title on the output.

(iii) OTHER INFORMATION GIVEN

A plot is given on the incremental plotter.

(iv) OTHER SUB-PROGRAMMES REQUIRED

COMP8 (From the FORTRAN Compiler Library)

REGION,LIMITS,BORDER,CURPTO,AXESSI,CRSIZE,PLOTCL (All from the GHOST system library).

(v) PURPOSE

To produce a plot of the data on the incremental graph plotter using the LEEDS GHOST package.

SUBROUTINE PLOT

FIG. D.2.9(a)

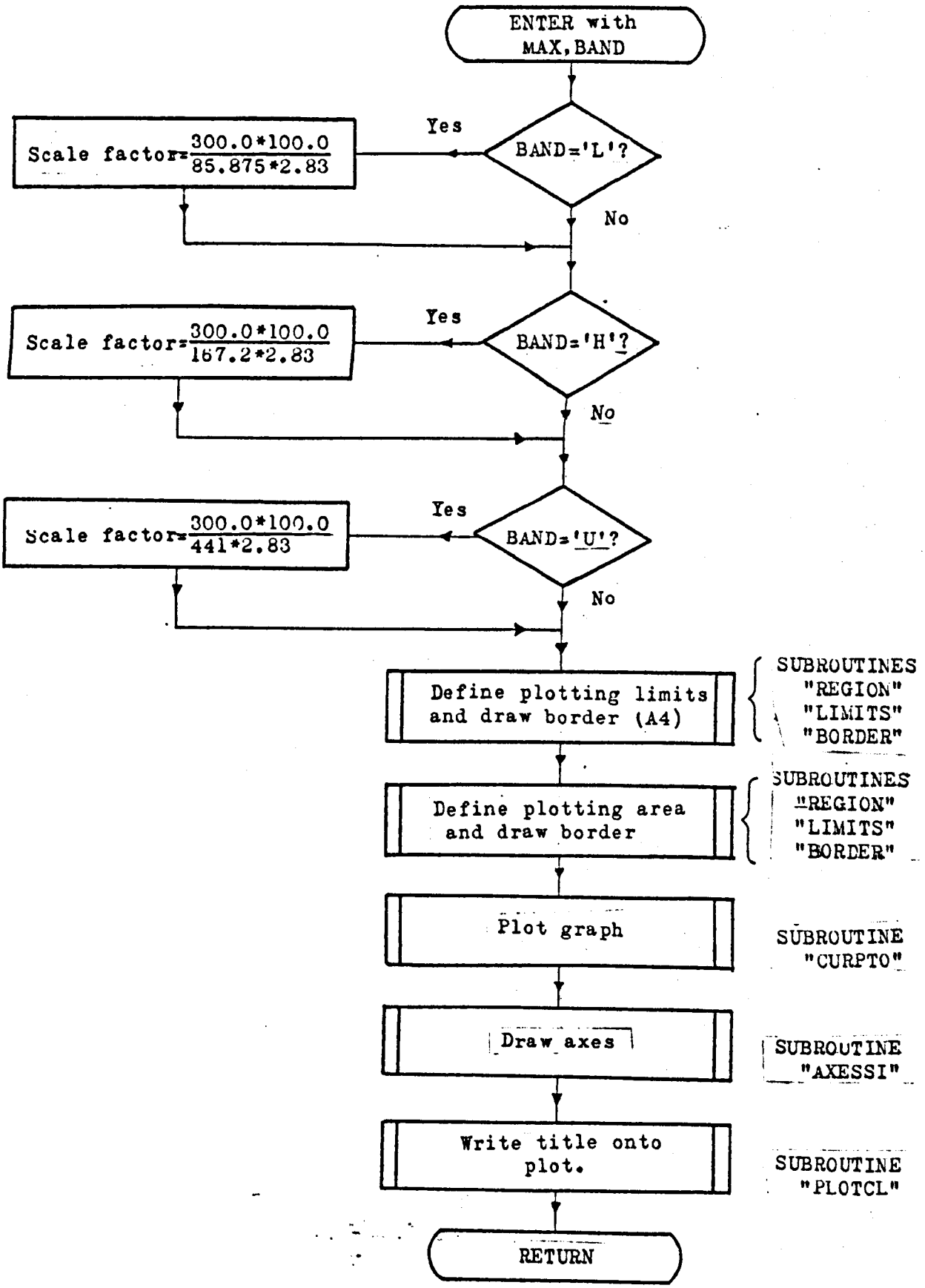

SCALED PLOTTING ROUTINE (PLOT)

FIG D.2.9(b)

```
      SUBROUTINE PLOT(MAX,BAND)
      COMMON RARR(8192),X(8192),CHAR(10)
      DATA VLO,VHI,UHF/'L       ','H       ','U       '/
      CALL COMPS(VLO,BAND,II)
      IF(II.EQ.1)SCALE=300.0/85.875/2.83*100.0
      CALL COMPS(VHI,BAND,II)
      IF(II.EQ.1)SCALE=300.0/167.2/2.83*100.0
      CALL COMPS(UHF,BAND,II)
      IF(II.EQ.1)SCALE=300.0/441.025/2.83*100.0
      CALL REGION(0.0,1.0,0.0,0.1.0)
      CALL LIMITS(0.0,29.7,0.0,22.9)
      CALL BORDER
      XLMAX=FLOAT(MAX-1)*27.7/8192.0+2.5
      XMAX=FLOAT(MAX-1)/SCALE
      DO 1 J=1,MAX
    1 X(J)=FLOAT(J-1)/SCALE
      CALL REGION(0.0,XMAX,-10.970.0)
      CALL LIMITS(2.3,XLMAX,2.0,17.0)
      CALL BORDER
      CALL CURPTO(X,RARR,1,MAX,-10)
      CALL AXESST(10.0,10.0)
      CALL CRSIZE(1.0)
      CALL PLOTCL(20.0,65.0,CHAR(1),30)
      RETURN
      END
****
```

SCALED PLOTTING
ROUTINE (PLOT)

FIG D.2.9(c)

GEORGE COMMAND ISSUER

(i) ARGUMENT LIST

SUBROUTINE IGECOM (I)

OUTPUT : I = 0 ; Command issued successfully.
= 1 ; Command failure.

(ii) OTHER INFORMATION REQUIRED

Card image records are required on input channel 8 giving the GEORGE commands to be issued.

(iii) OTHER INFORMATION GIVEN

None

(iv) OTHER SUB-PROGRAMMES REQUIRED

SGEUCI (From system library BHAMLIB)

(v) PURPOSE

To read character strings on unit 8 and to issue them as GEORGE commands.

SUBROUTINE IGECOM

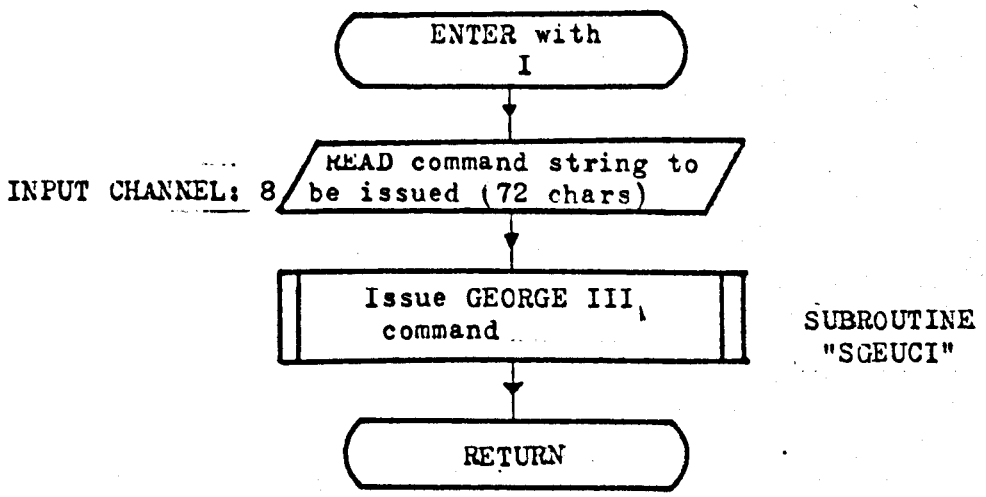

ISSUE GEORGE COMMANDS
(IGECOM)

FIG D.2.10(b)

```
      SUBROUTINE IGECOM(I)
C
C     ISSUES A GEORGE COMMAND READ FROM A FILE USING 'SGEUCI'
C     THE INDIVIDUAL COMMANDS MUST NOT BE GREATER THAN 72 CHARACTERS
C
C     CALLING ROUTINE SHOULD BE AS FOLLOWS:-
C
C     CALL IGECOM(I)
C     IF(I.EQ.1)STOP 'FAIL GEORGE COMMAND ERROR'
C
C
C     NEEDS THE FOLLOWING:-
C
C     *CR'N' ASSIGNING TO THE FILE CONTAINING THE COMMANDS
C     LIB BHAMLID
C     INPUT 8 ON CR'N'
C
C     I=0 RETURNED 'OK';I=1 RETURNED 'FAIL GEORGE COMMAND ERROR'
C
      DIMENSION COMMAND(9)
      READ(8,1)COMMAND
    1 FORMAT(9A8)
      CALL SGEUCI(COMMAND(1),72,I)
      RETURN
      END
```

ISSUING OF A
GEORGE III COMMAND
(IGECOM)

FIG D.2.10(c)

APPENDIX E

TECHNICAL PUBLICATIONS

The following paper has been accepted for publication in the Proceedings of the IEE and it is anticipated that this will occur in the first quarter of 1977.

MOBILE RADIO PROPAGATION IN BRITISH CITIES AT FREQUENCIES IN THE VHF AND UHF BANDS

K. ALLSEBROOK, M.Sc., Associate Member
British Aircraft Corporation Limited
Guided Weapons Division
Electronic Systems Group
Bristol

and

J.D. PARSONS, M.Sc., Associate Member
Department of Electronic and Electrical Engineering
University of Birmingham

SUMMARY

Measurements of propagation path losses made in three British cities at VHF and UHF are described. An analysis of the factors influencing the transmission loss leads to the formulation of a prediction model. This is shown to be simpler to use than the Okumura technique while giving comparable prediction errors.

ABSTRACT

Measurements of the received signal envelope magnitude have been made in three British cities at frequencies of 85.875, 167.2 and 441.025 MHz. In all cases unmodulated carrier waves were radiated from aerials atop tall buildings or prominent terrain features and detected using a vehicle-mounted receiver. These measurements have provided the basis for an analysis of the factors affecting the transmission loss in urban/suburban areas which, in turn, has enabled a propagation prediction model to be constructed. Close agreement between measured and predicted path losses has been found for the various terrain situations investigated.

The statistical prediction errors produced by the proposed model for the three British cities analysed are shown to be similar in magnitude to those obtained using an extrapolation of the Okumura method. Because the proposed model is much less complex and procedurally simpler, it is recommended for use, in the first instance, in British cities.

LIST OF PRINCIPAL SYMBOLS

d = Range

d_1 = Range from Transmitter to Obstacle

d_2 = Range from Receiver to Obstacle

h_o = Height of Obstacle above Ground

h_r = Height of Receiving Aerial above Ground

h_t = Height of Transmitting Aerial above Ground

k = A constant

L_B = Diffraction Loss over Buildings (dB)

L_D = Diffraction Loss over Terrain Obstacles (dB)

L_F = Free Space Path Loss (dB)

L_p = Plane Earth Path Loss (dB)

n = An exponent

P_r = Power Received

P_t = Power Transmitted

W = Street Width

W^1 = Effective Street Width $\left(\frac{W}{2\sin\alpha}\right)$

α = Street Orientation

β = Excess Path Loss Correction Factor (Urban Clutter Factor)

β^1 = Frequency Corrected Value of β

γ = UHF Correction Factor (dB)

λ = Wavelength

θ = Diffraction Angle

σ = The mode of a Rayleigh Distribution

1 INTRODUCTION

A vehicle mounted radio receiving system moving through the streets of a town or city experiences a spatially distributed field pattern. Typical examples of received signal envelope waveforms are given in Figs.1, 2 and 3 for transmission frequencies of 85.875, 167.2 and 441.025 MHz respectively. Observation of the closely spaced interference minima in the signal magnitude distribution as a time series has led to the term "fast-fading" coming into common use.

Fast-fading may be considered as the result of interference between a number of incoming waves which have been scattered from obstacles in close proximity to the vehicle. The resulting interference situation has been analysed by many authors[1,2] and mathematical models have ensued [3-5] which permit the prediction of various statistical properties of the signal pattern. Of these fast-fading models, that proposed by Clarke[4] has been widely quoted, probably because it is based on physically reasonable assumptions. In this model the signal at any point in space is considered to be the vector sum of a number of horizontally travelling plane waves having equal amplitudes, random phases and arriving from random directions in the azimuthal plane. If the phase angles of the component waves are further assumed uniformly distributed in the range 0 to 2π radians, the model predicts that the signal envelope will be Rayleigh distributed; a property which has been substantiated over short distances of travel in areas where no line-of-sight path between the transmitter and receiver exists[1,6].

Large area variations of the received signal envelope are determined by calculating a series of "local mean" values at points along a large

1 Cont'd signal record[6,17,18], i.e. greater than approximately 1km of the receiver's travel. These "local mean" signal values along the received envelope waveform are evaluated by performing a convolution between the "raw" signal record and a weighting function whose width is sufficiently small to satisfy the criterion that the signal envelope is Rayleigh distributed within it (and therefore no variation in the mode "σ" of the distribution has occurred[4]) while being large enough to ensure that a valid statistical estimate is obtained. The low-pass filtered waveform resulting from this process exhibits variations over distances of many tens of metres and accordingly derives the term "slow-fading". For comparison the slow-fading patterns of the "raw" signals in Figs.1, 2 and 3 are shown in Fig.4.

The ability to predict the slow-fading pattern, and to provide a quantitive measure of the variations about it[18], are highly relevant in the planning of mobile radio communications links and in estimating the subsequent overall system performance. Of paramount importance is the capability of the systems engineer to predict the coverage area achieved by a base station at a given position[22], and in locating the radio "black-spots" within that area.

2 LOCAL MEAN PREDICTION TECHNIQUES

A number of prediction methods have been proposed in the literature[6-10] for the estimation of propagation path loss at VHF and UHF over irregular terrain. These may be broadly classified as empirical[6,7] and semi-theoretical[8-10], the latter relying on the determination of terrain diffraction loss by approximations[11-14] rather than the exact solution[15,16] which becomes very complex for two or more obstacles.

2 Cont'd Whichever form of model is to be used, it is usually necessary to obtain a terrain profile of the path under investigation, either to determine the diffraction loss over the terrain obstacles or to calculate correction factors for the ground roughness and undulations. When operations are to be performed on many paths within a specified region, e.g. in the determination of coverage areas[22], a need is established for the existence of large terrain data bases stored on, and consequently using, digital computers. Fast terrain profile acquisition and high speed evaluation of the path loss prediction are accordingly achieved.

Propagation prediction techniques for receivers located in urban and suburban areas are very sparsely documented. In this area only the model by Okumura[6], empirical in nature, has achieved any renown[17,18] although the broadcasting authorities have formulated their own technique[19]. Both these models are intended for use with tall transmitting aerials remote from the receiver and therefore outside the city limits. The latter model[19] is intended for use at UHF with a receiving aerial at roof-top height (10 m) and re-optimisation for use with lower frequencies and aerials would be a major task. While obviously being satisfactory for their own purposes, the BBC model[19] requires very specialised and detailed topographic information which cannot be obtained by merely reading data from an Ordnance Survey map of the city.

In the case of the Okumura model[6], the methods of determining the various factors are limited to applications involving radio links operating at frequencies above 100 MHz and over ranges greater than

2 Cont'd approximately 10 km. The basic method involves the reading of values from numerous correction curves and adding these, or subtracting, depending upon the context, to the free space propagation path loss[18]. Three of these curves, however, do not directly utilise the variables of link range and transmission frequency but require the computation of intermediate parameters. These are as follows:-

(1) Base Station Effective Antenna Height

This is evaluated as the height of the base station aerial above the average ground level calculated over the range interval of 3 to 15 km from the base station site (or less if the entire link range is below 15 km).

(2) Average General Slope Angle of Terrain

This is determined as the average slope of the terrain over "at least 5 to 10 km" of the path closest to the mobile terminal.

(3) Terrain Undulation Height

The terrain undulation height may be found from the difference between 10% and 90% of the peak excursions of the terrain undulations away from their average value within a distance of 10 km from the mobile terminal to the base station.

If the Okumura model is to be made generally applicable, extrapolations to the original curves and careful interpretations of the parameter definitions must be made. It should be noted, however, that extensive data regarding the performance of this new model must be obtained before its use may be advocated.

2 Cont'd It is the purpose of this paper to report a series of measurements made at 85.875, 167.2 and 441.025 MHz in the British cities of Birmingham, Bath and Bradford. A simple model is subsequently derived from these measurements and is compared with an extrapolated version of the Okumura model.

3 MEASUREMENT OF THE RECEIVED SIGNAL ENVELOPE

Measurements have been made of the signal envelope magnitude received at a moving vehicle using frequencies of 85.875, 167.2 and 441.025 MHz in the British cities of Birmingham, Bath and Bradford. Base stations utilizing suitable transmitting aerials at the three frequencies were erected on the roof of a prominent building in the appropriate city and unmodulated carriers broadcast. Transmitter powers measured at the aerial terminals of approximately 30, 30 and 3.8 watts (in order of increasing frequency) were radiated by monopoles on ground planes at the two VHF frequencies, and by a colinear array of four folded dipoles orientated to provide an omnidirectional radiation pattern at the UHF frequency. The aerials were sited approximately 35, 20 and 50 m above local ground for the cities of Birmingham, Bath and Bradford respectively.

The cities were chosen as being representative of three commonly occurring mobile radio situations. Birmingham is basically a large flat city (Fig.5) with a compact, heavily built-up urban centre. It should be noted that this central area is very much less congested than is typical of the larger North American type of cities where much of the previous work has been based, but is typical of the centre of many European cities.

3 Cont'd Bath, on the other hand, is much smaller than Birmingham, sits in a valley and has a centre composed mainly of three or four storey buildings with narrow streets. A terrain profile drawn through Bath city centre and the transmitter site is given in Fig.6 and demonstrates that a frequently encountered base station siting philosophy has been used, i.e. atop a prominent terrain feature.

Bradford, like Bath, is much smaller than Birmingham in total area and, as demonstrated by the terrain profiles of Fig.7, is extremely hilly. The transmitter was mounted on a tall building in the valley and was intended to be representative of the situation where a central urban base station radiated to outlying districts beyond the surrounding terrain obstructions, possibly unintentionally as r.f. interference.

The field strength measuring system is depicted in the upper half of Fig.8. The signal was received using a quarter wavelength whip aerial mounted in the centre of the vehicle's roof, detected by calibrated field strength measuring receiver and recorded using a multi-channel analogue f.m. tape recorder.

The automatic distance measuring system is shown in the lower portion of Fig.8. The rotation of a fifth wheel towed behind the vehicle was photoelectrically sensed and recorded on the tape recorder. Pulses were derived by this means at intervals corresponding to approximately 2.8 cm of the vehicle's movement, acting later as an aid to relative position fixing. This fine positional information was supplemented by recording a commentary on the voice track of the tape recorder while the measurements were being performed. The commentary took the

3 Cont'd form of local details which were readily locatable on a street map of the area, e.g. street intersections and local geographical information.

The record of received signal magnitude was later analysed in "small sectors" corresponding to less than 250 m of the vehicle's movement, the intention being that parameters such as street width, street orientation and terrain features should remain sensibly constant. When sampled at the 2.8 cm distance marker rate sufficient data points were made available in each of the "small sector" records (approximately 8000) to enable the calculation of various statistical parameters. The equivalent detectable average fade depths[18] obtained by these means for a vehicle speed of 9 m/sec (20 mph) were 34, 28 and 20 dB at 85.875, 167.2 and 441.025 MHz respectively. Approximately 300 "small sector" records have been processed at each of the frequencies to provide values of median path loss referred to half-wave dipole aerials. The relationship between this path loss and the various influencing parameters is investigated.

4 FACTORS INFLUENCING THE MEDIAN PATH LOSS IN BIRMINGHAM

4.1 DEPENDENCE OF MEDIAN ATTENUATION ON RANGE AND FREQUENCY

The total range over which a radio link operates will be an important factor in determining the total propagation path loss experienced. It is therefore desirable to establish the relationship between the measured loss values and the spatial separation of the aerials. To this end, a curve fit of the form $k \times (\text{link range})^{-n}$ was performed by the least squares error method on the Birmingham "small sector" median attenuations. The values of the exponent (n) were found to be 3.8,

4.1 Cont'd

3.9 and 2.4 at frequencies of 85.875, 167.2 and 441.025 MHz respectively. The corresponding rms errors between the measured values and the appropriate curve fits were found to be 7.5, 6.2 and 7.8 dB. Application of a curve of the form k x (Range)$^{-4}$ to the UHF data caused a rise in the rms error at this frequency to 8.3 dB. These results appear to indicate that an inverse fourth power range law will provide a good estimate of the path loss values, and a model of the form proposed by Egli[7] is appropriate:-

$$P_r = P_t \{ \frac{h_t h_r}{d^2} \}^2 \beta$$

This equation forces agreement between the well known "plane earth" path loss and the measured loss by the use of an "urban clutter factor" (β). This is shown with the "small sector" median attenuations in Figs.9, 10 and 11 at 85.875, 167.2 and 441 MHz respectively.

The variation of the "urban clutter factor" (β) with frequency is shown in Fig.12 and may be seen to be similar in form to measurements reported by Young[1], Okumura[6] and Parker and Roper[10]. The non-linearity of the curve suggests that above approximately 200 MHz the propagation mechanism changes, a point which will be examined later.

4.2 FACTORS INFLUENCING THE URBAN CLUTTER FACTOR

Having determined the range and frequency dependencies of the measured "small sector" median path loss values, it is possible to compensate the measurements accordingly by normalisation processes using the curves shown in Figs.9, 10, 11 and 12. Approximately 900 frequency corrected urban clutter factor (β^1) values are now analysed further.

4.2 Cont'd To simplify the analysis, it has been assumed that the receiver was located exactly in the centre of the road under consideration. While never being exactly true, this obviates the need to know the direction of travel and on which side of the street the vehicle is positioned. An "effective street width" (W^1) is also defined, for the purposes of the investigation, as the distance between the vehicle-mounted receiver and the buildings measured along the direct path between transmitter and receiver (Fig.13).

If large structures or terrain features obstruct the transmission path, the total loss experienced can be much larger than that predicted using simple "free space" or "plane earth" concepts. This excess loss is often the results of the diffraction of the radio waves over or around the obstacle and, for the idealised situation of a knife-edge shown in Fig.14, can be conveniently calculated in terms of the Fresnel-Kirchoff ν parameter, defined as:-

$$\nu = \theta \sqrt{\frac{2}{\lambda} \cdot \left(\frac{d_1 \, d_2}{d_1 + d_2}\right)}$$

In a typical operational mobile radio-telephone link with no coarse terrain obstructions, the buildings adjacent to the receiver will act as the diffractor. These, in turn, are distant from the transmitter, i.e.

$$d_1 >> d_2, \quad \theta \doteq \frac{h_o - h_r}{d_2}$$

The Fresnel ν parameter can therefore be approximated as:-

$$\nu = \frac{k}{\sqrt{\lambda \, d_2}}$$

4.2 Cont'd and the corresponding transmission loss becomes:-

$$\text{constant} - 10 \log_{10} (\lambda d_2) \text{ , dB}$$

This curve is compared in form with the mean of the frequency corrected urban clutter factor values at quantized intervals of effective street width in Fig.15 and may be seen to be in good agreement. Furthermore, consideration of an "average street" (h_o = 10m, h_r = 2m, d_2 = 30m) yields values of 13, 16 and 21 dB diffraction loss at 85, 167 and 441 MHz respectively. This is shown in Fig.12 as the dashed line and indicates that close approximation between the VHF measured values is obtained by recourse to knife-edge diffraction theory. The simplified solution, however, underestimates the loss at UHF, probably as a result of ignoring the thickness of the buildings which, at the higher frequencies, is many wavelengths[20]. The departure of the theoretical and measured curves in Fig.12 is shown in Fig.16 and forms the basis of a UHF correction factor, γ.

5 THE URBAN PREDICTION MODELS

5.1 EXTENSIONS TO THE OKUMURA PREDICTION MODEL FOR APPLICATION TO THE PATH'S MEASURED

The Okumura prediction model[16] was formulated for use in the frequency range 100 to 3000 MHz. Extrapolation of the curves for use down to 75 MHz is a straightforward exercise and will not be detailed. It is further required that all the correction factors, and consequently the physical parameters, are applicable with any link range greater than 1 km. The intervals over which these have been calculated are given.

5.1.1 Base Station Aerial Height Gain

For a link of range 'd', the base station effective aerial height is determined as the height above the least squares regression line to the terrain computed over the following intervals:-

$\frac{d}{4}$ to d	for 1 km < d ≤ 8 km	
3 km to d	for 8 km < d ≤ 15 km	'd' in km
3 km to 15 km	for 15 km < d	

5.1.2 Rolling Hilly Terrain Correction

The interdecile terrain undulation height is evaluated over the intervals:-

(d-10) to d	for d > 12 km	
2 km to d	for 6 km < d ≤ 12 km	'd' in km
1 km to d	for 1 km < d ≤ 6 km	

5.1.3 Vehicular Ground Slope Correction

The average ground slope at the vehicle is calculated in the regions:-

1 km to d	for 1 km < d < 4 km	
2 km to d	for 4 km ≤ d < 7 km	'd' in km
(d-5) to d	for 7 km ≤ d < 9 km	

For d ≥ 9 km, the larger of the computed slope values over the following intervals is chosen:-

(d-5) to d

and

(d-10) to d	for d ≥ 12 km	'd' in km

or

2 km to d	for d < 12 km	

5.2 THE FLAT CITY PREDICTION MODEL

The results obtained in Birmingham and analysed in the previous sections suggest that predictions may be made by summing the plane earth and building diffraction losses. This is similar in form to the model proposed by Edwards and Durkin[8] for propagation over irregular terrain where the diffraction loss term is that for the terrain obstacles:-

$$\text{Loss} = L_P + L_D \ , \quad \text{dB}$$

The urban model, proposed in this paper for comparison, is given by:-

$$\text{Loss} = L_P + L_B + \gamma \ , \quad \text{dB}$$

where L_B is the diffraction loss incurred by propagation over the buildings next to the mobile unit and between the two terminals.

Appendix 1 demonstrates that this model gives a reasonable approximation to the true propagation loss if a single coherent reflection from the ground surface can be supported, although it must be stated that this is in no way truly representative of the existing situation, i.e. it is not being suggested that a single coherent reflection actually exists.

5.3 THE FLAT CITY PREDICTIONS

5.3.1 The Birmingham Predictions

The 900 small sector median path loss values measured in Birmingham have been compared with predictions obtained using the flat city model. For simplicity, and in the absence of a complete knowledge, the buildings have been assumed to be 10 m tall and the aerial heights

5.3.1 Cont'd have been taken as their heights above local ground. A suburban rather than urban area is therefore implied; a statement which is realistic for the large areas occupied by suburban Birmingham in comparison with urban Birmingham. An analysis of the prediction errors (measured-predicted path loss) obtained using these assumptions is presented in Table 1.

Individual measurements were selected from the small sector median path loss values such that the spacing between any two of the corresponding locations was greater than 1 km. Approximately 180 values were accordingly chosen for comparison with the Okumura extended model and the flat city model. The respective mean prediction errors were found to be 4.9 dB and 2.2 dB with corresponding standard deviations of 7.7 dB and 6.75 dB.

The low statistical errors produced in these comparisons appear to validate the use of the Okumura extension but also demonstrate that the flat city model is similar in accuracy while being much simpler to apply.

5.3.2 The Bath Predictions

The small sector median path loss values measured in Bath have been statistically compared with predictions using the flat city model. The prediction error performance is shown in Table 1.

The low prediction errors obtained appear to justify the treatment of the Bath situation as a flat city on a sloping base. The total area covered by the measurements, however, is small and is not amenable to prediction using the Okumura extended model.

5.4 THE HILLY CITY PREDICTION MODEL

The prediction model presented for the flat city situation takes no account of terrain obstacles. Any attempt to do so must, when the magnitude of the terrain obstructions is negligible, reduce to the flat city model if compatibility is to be achieved. The Okumura extended model is formulated for operation over irregular terrain and is directly applicable.

5.4.1 Detailed Analysis of Selected Bradford Paths

The following methods of predicting the small sector median path loss have been investigated:-

(a) Durkin and Edwards Models[8]

(1) Loss = $L_F + L_D$ + Flat City Correction, dB

(2) Loss = $L_P + L_D$ + Flat City Correction, dB

(b) Modified Blomquist and Ladell Model[9]

Loss $L_F + (L_P - L_F)^2 + L_D^2)^{\frac{1}{2}}$ + Flat City Correction, dB.

In all the above cases, the flat city correction is given as:-

Flat City Loss = $L_B + \gamma$, dB

where the UHF correction, γ, is obtained from Fig.16 and is included to compensate for the obstacle thickness.

The selected paths shown in Fig.7 are analysed in detail in Table 2 by the three methods mentioned and the Okumura extension. Also included in Table 2 are values of terrain diffraction loss computed by various documented constructions[11-14].

5.4.1 Cont'd Comparison of the terrain diffraction loss values reveals that the Bullington method[11] produces the smallest loss whereas the remaining three models[12-14] predict roughly similar losses. Of these, the Deygout method[14] is particularly cumbersome to use, especially on a digital computer. Of the remaining diffraction models, the Japanese method[13] has been shown to be more accurate[15,21] than the Epstein-Peterson method[12], both of which are easily programmed on a digital computer. The Japanese method is therefore recommended for the computation of the terrain diffraction loss values although the original presentations[8,9] advocated the use of the Epstein-Peterson method[12].

Further statistical comparison shows that the Blomquist and Ladell method[9] with flat city correction produces the minimum overall error and may be seen to provide a measure of "smoothing" between the two Edwards and Durkin[8] forms. The suggested hilly city prediction model is accordingly given by:-

$$\text{Loss} = L_F + ((L_p - L_F)^2 + L_D^2)^{\frac{1}{2}} + L_B + \gamma \text{ , dB}$$

In the case of a flat city, $L_D = 0$ and the predicted loss reduces to:-

$$\text{Loss} = L_p + L_B + \gamma \text{ , dB}$$

showing that full compatibility is attained with the flat city model used earlier.

5.4.2 The Bradford Predictions

The measured small sector measured median path loss values have been statistically compared with the hilly city model's predictions. The prediction behaviour is given in Table 1.

6 CONCLUSIONS

Measurement of the 'small sector' (250 m) median propagation loss at VHF and UHF frequencies in Birmingham have indicated that, for the case of a flat city, the diffraction loss over the buildings adjacent to the mobile terminal is of importance. Furthermore, predictions made by a simple technique involving the summation of the plane earth and building diffraction losses have yielded small mean prediction errors and low rms errors for both Birmingham (flat city) and Bath (sloping city).

An extension of the simple flat city model to cover the situation of a hilly city has been suggested as the sum of the path loss predicted using a technique based on the Blomquist and Ladell model and the building diffraction loss. The terrain diffraction loss, needed as a factor in the calculation of the Blomquist and Ladell irregular terrain loss, has been found to be adequately evaluated using the method proposed by the Japanese Postal Service. Comparison of hilly city predictions and "small sector" measurements has again shown close agreement.

The extension to the Okumura model for operation with links greater than 1 km has also given small prediction errors but the computational processes needed in its evaluation are much more numerous. This method, in essence taken by many as a standard, is concluded to be far more complex than is necessary and therefore inappropriate for use in British cities.

7 ACKNOWLEDGEMENTS

The authors wish to acknowledge many useful discussions, particularly with Dr. C.J. Hall of AWRE (Aldermaston), Messrs. R.A. Burberry and C. Felix of BAC (Bristol) and Prof. E.D.R. Shearman of the University of Birmingham. Thanks are also due to Prof. W. Gosling of the University of Bath and Prof. D.P. Howson of the University of Bradford for the use of equipment and facilities at their respective Universities. The work was carried out under the terms of a research contract from the UK Atomic Energy Authority at the University of Birmingham.

The Universities of Bath, Bradford and Birmingham are members of the Universities Mobile Radio Research Consortium.

8 REFERENCES

1 Young, W.R. Jnr.
"Comparison of Mobile Radio Transmission at 150, 450, 900 and 3700 MHz" B.S.T.J., Vol.31, Nov.1952.

2 Nylund H.W.
"Characteristics of Small Area Signal Fading on a Mobile Circuit in the 150 MHz Band" IEEE Trans.Veh.Tech. Vol. VT-17, Oct.1968.

3 Ossanna J.F. Jnr.
"A Model for Mobile Radio Fading due to Building Reflections: Theoretical and Experimental Fading Waveform Power Spectra"
B.S.T.J., Vol.43, Nov.1964.

4 Clarke R.H.
"A Statistical Theory of Mobile Radio Reception"
B.S.T.J., Vol.47, July 1968.

5 Gans M.J.
"A Power-Spectral Theory of Propagation in a Mobile Radio Environment"
IEEE Trans. Veh. Tech. Vol. VT-21, Feb.1972.

6 Okumura Y., Ohmori E., Kawano T. and Fukuda K.
"Field Strength and its Variability in VHF and UHF Land Mobile Service"
Rev. Elec.Comm. Lab. 16, Sept.-Oct.1968.

7 Egli J.J.
"Radio Propagation Above 40 Mc over Irregular Terrain"
Proc. IRE, Oct.1957.

8 Edwards R. and Durkin J.
"Computer Prediction of Service Areas for VHF Mobile Radio Networks"
Proc. IEE, Vol.116, No.9, Sept.1969.

9 Blomquist A. and Ladell L.
"Prediction and Calculation of Transmission Loss in Different Types of Terrain" NATO AGARD Conference Publ. CP144, Research Institute of National Defence, Dep.3, S-10450, Stockholm 80, Sweden, March 1974.

10 Parker R.E. and Roper, G.B.
"Vehicular Radio Communication in London"
SDE/X/B70/1, AWRE Aldermaston, Feb.1970

11 Bullington K.
"Radio Propagation at Frequencies above 30 Mc/s"
Proc. IRE, Oct.1947.

12 Epstein J. and Peterson D.W.
"An Experimental Study of Wave Propagation at 850 Mc/s"
Trans. IRE, Ant and Prop. April 1955.

13 The Radio Research Lab.
"Atlas of Radio Wave Propagation Curves for Frequencies between 30 and 10000 Mc/s"
Ministry of Postal Services - Tokyo, Japan.

14 Deygout J.
"Multiple Knife Diffraction of Microwaves"
IEEE Trans. Ant. and Prop. Vol. AP-14, No.4 , July 1966.

15 Millington G., Hewitt, R. and Immirzi F.S.
"Double Knife-Edge Diffraction in Field Strength Predictions"
IEE Monograph No. 507E, March 1962.

16 Millington, G., Hewitt R. and Immirzi F.S.
"The Fresnel Surface Integral"
IEE Monograph No. 508E, March 1962.

17 Reudink D.O.
"Properties of Mobile Radio Propagation above 400 MHz"
IEE Trans. Veh.Tech. Vol. VT-23, No.4, Nov.1971.

18 Jakes W.C. Jr.
"Microwave Mobile Communications"
Published by John Wiley and Sons

19 Sofaer E. and Davis B.
"Computer Method of Service Area Predic tion at UHF"
BBC Research Dept., Service Planning Section, Tech.Memo RA-1010
August 1967.

20 Hacking K.
"UHF Propagation over Rounded Hills"
Proc. IEE, Vol.117, No.3, March 1970

21 Hacking K.
"Approximate Methods for Calculating Multiple Diffraction Losses"
Electronics Letters, May 1966, Vol.2, No.5.

22 Barsis A.P.
"Determination of Service Area for VHF/UHF Land Mobile and Broadcast Operations over Irregular Terrain"
IEEE Trans. Veh. Tech. Vol. VT-22, No.2, May 1973.

APPENDIX 1

Consider the situation depicted in Fig. 17 where a knife-edge diffractor is placed adjacent to the receiver. All heights are measured above the perfectly conducting plane as shown.

Assuming that no reflections occur on the receiver's side of the obstacle, and that $d_1 \gg d_2, h_o, h_1, h_2$, the diffraction loss for ray path r_1 is given by:

$$A(\sigma_1) \doteq \sqrt{\frac{\lambda d_2}{2\pi(h_o - h_2)}}$$

Similarly for the reflected path r_2:

$$A(\sigma_2) \doteq \sqrt{\frac{\lambda d_2}{2\pi(h_o - h_2)}}$$

The path loss is therefore given by (isotropic radiators assumed):

$$20 \log_{10}\left(2\pi \frac{d_1^2}{\sqrt{\lambda d_2}} \cdot \frac{(h_o - h_2)}{h_o \cdot h_1} \right) \quad , \text{dB}$$

The proposed flat city model, for comparison, gives a path loss of:

$$20 \log_{10} \left(\frac{2\pi d_1^2}{\sqrt{\lambda d_2}} \cdot \frac{(h_o - h_2)}{h_1 \cdot h_2} \right) \quad , \text{dB}$$

The error between these is consequently:

$$20 \log_{10} \left(\frac{h_o}{h_2} \right) \quad , \text{dB}$$

The magnitude of this error term is dependant upon the location of the reflecting plane; a parameter which is extremely difficult to determine in an urban area. Assuming that the reflecting plane is local ground, and that $h_o = 10\text{m}$, $h_2 = 2\text{m}$, the error would be a constant 14dB.

City	Mean Error of Prediction (dB)	Standard Deviation of Prediction Errors (dB)
Birmingham	0.8	8.0
Bath	3.6	7.9
Bradford	5.5	10.7

Table 1

Statistical Analysis of the Prediction Errors Incurred Using the Proposed Model

				DIFFRACTION LOSS				PATH LOSS PREDICTIONS						
				Bullington[11] Method	Epstein-Peterson[12] Method	Japanese Atlas[13] Method	Deygout[14] Method	Edwards and Durkin[8]		Blomquist & Ladell[9]	Okumura Model[6]			
Region	Terrain Profile Fig.No.	Free Space Path Loss dB	Plane Earth Path Loss dB	dB	dB	dB	dB	Free Space + Diffraction + Urban Correction	Plane Earth + Diffraction + Urban Correction	+ Urban Correction dB	dB	Measured Path Loss Values dB	Number Of Obstacles	Frequency MHz
Cottingley	7(a)	86.7 92.5 101.0	110 110 110	20.5 23.4 27.6	27.0 31.5 39.0	28.4 33.0 40.7	30.8 35.5 43.3	126.5 141.0 176.3	140.8 158.5 185.3	133.0 145.0 177.0	130.6 137.4 147.8	135.5 145.2 148.7	2	85.875 167.2 441.025
Greengates	7(b)	85.4 91.2 99.7	107.6 107.6 107.6	16.4 19.1 23.1				113.7 126.2 157.7	135.9 142.6 165.6	125.0 132.0 159.0	128.4 134.4 144.7	145.0 154.5 –	1	85.875 167.2 441.025
Eccleshill	7(c)	83.2 89.0 97.4	103.0					92.2 102.0 129.4	112.0 116.0 135.0	112.0 116.0 135.0	111.5 117.5 127.8	114.8 117.9 119.7	0	85.875 167.2 441.025
Undercliffe	7(d)	84.5 90.3 98.7	105.6	14.9 17.5 21.4				116.3 128.6 159.9	137.4 144.0 166.8	127.0 134.4 161.0	123.0 129.0 139.3	140.0 150.7 –	1	85.875 167.2 441.025
Shipley	7(e)	86.0 91.7 100.0	108.5	13.7 16.0 19.9	23.7 25.6 29.3	25.4 27.8 32.2	24.5 26.6 29.9	119.5 131.3 161.9	142.0 148.1 170.4	128.0 136.0 163.0	123.2 129.2 139.5	136.8 142.2 150.0	3	85.875 167.2 441.025
Bingley	7(f)	89.2 95.0 103.4	115.0	12.7 14.9 18.7	22.7 24.4 27.8	24.5 26.8 30.9	25.1 27.5 31.9	123.3 135.5 167.3	149.0 155.5 147.0	134.0 142.0 169.0	130.0 136.0 146.2	141.3 143.0 –	3	85.875 167.2 441.025
Illingworth Moor	7(g)	90.9 96.6 105.1	118.4	17.4 20.0 24.1	20.7 23.7 29.6	22.3 25.8 32.5	25.8 29.7 36.2	125.7 139.3 173.3	153.2 161.1 186.6	137.6 146.5 175.7	139.5 145.4 155.6	136.0 148.0 –	2	85.875 167.2 441.025

TABLE 2 COMPARISON OF PREDICTION METHODS FOR THE BRADFORD RESULTS

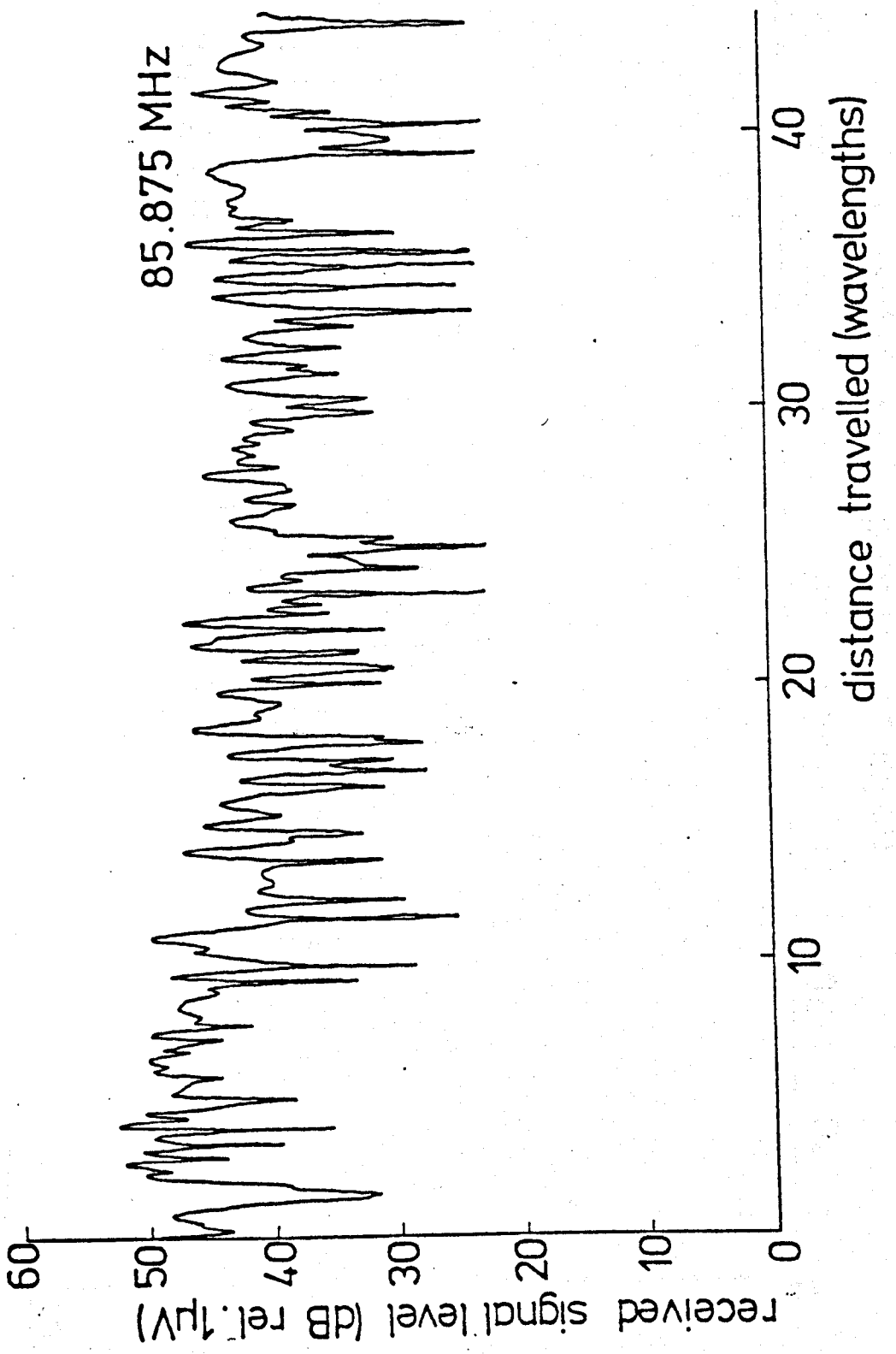

A MEASURED SIGNAL ENVELOPE AT 85.875MHz

.FIG. 1

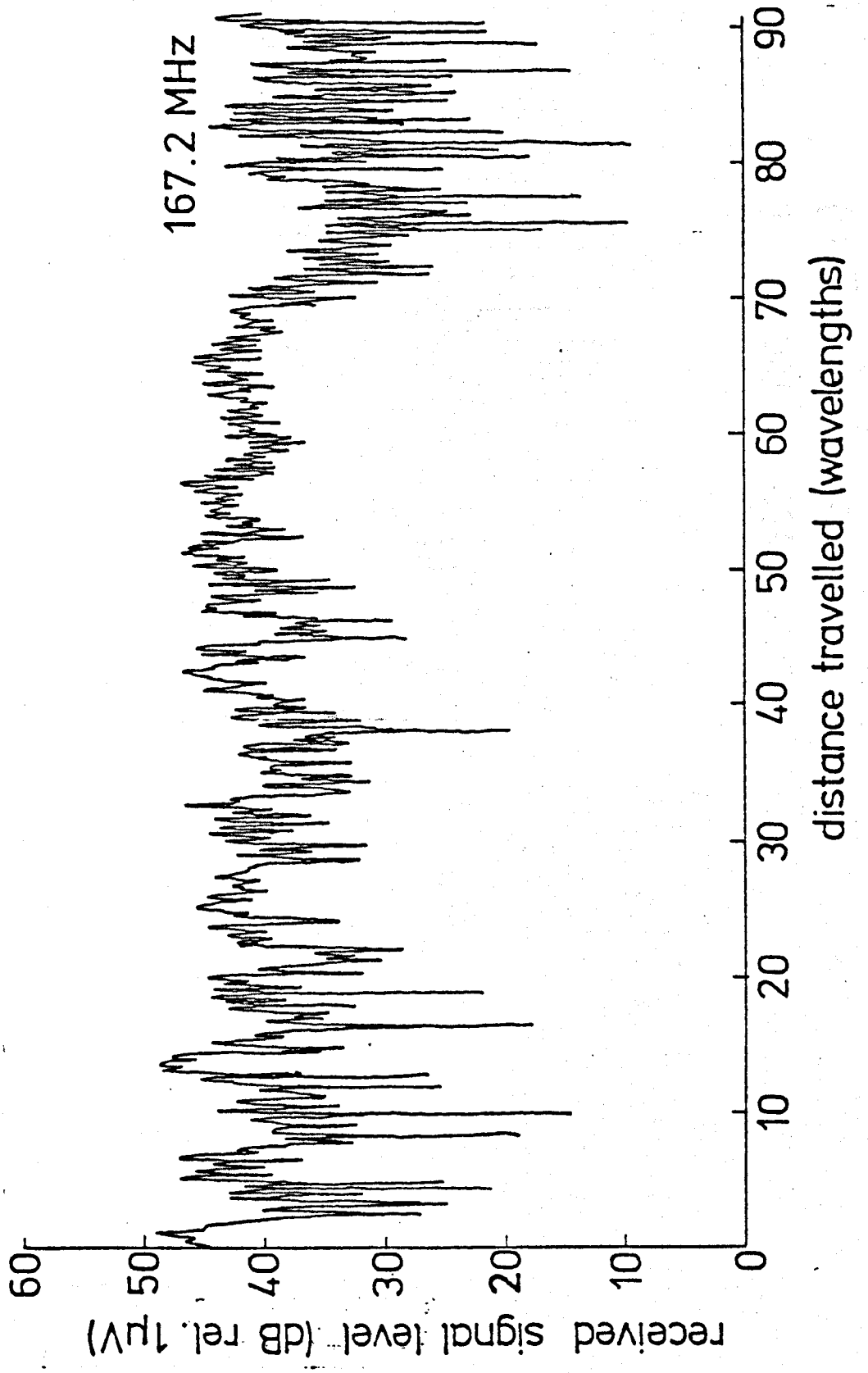

A MEASURED SIGNAL ENVELOPE AT 167.2MHz

FIG. 2

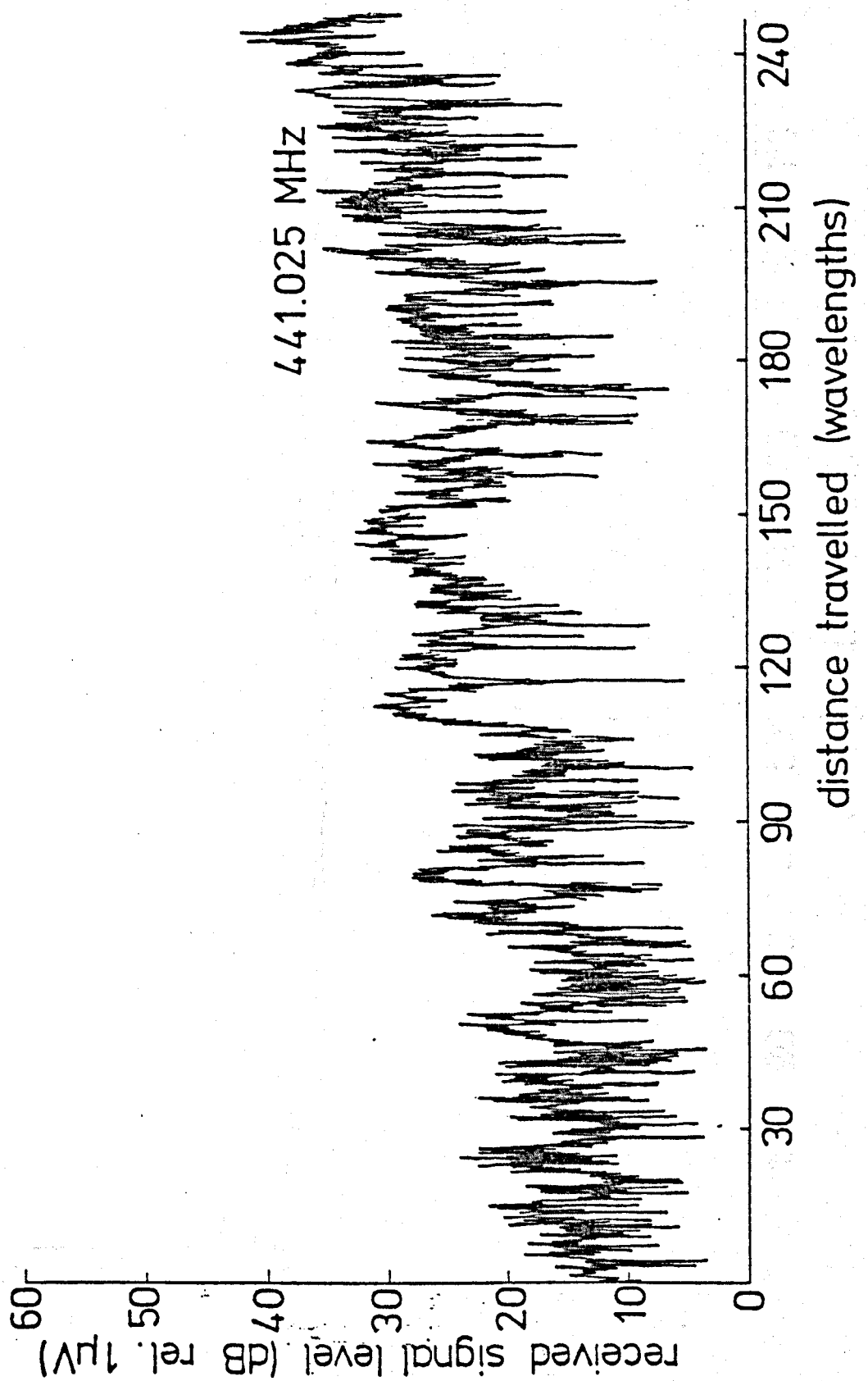

A MEASURED SIGNAL ENVELOPE AT 441.025MHz

-- FIG. 3

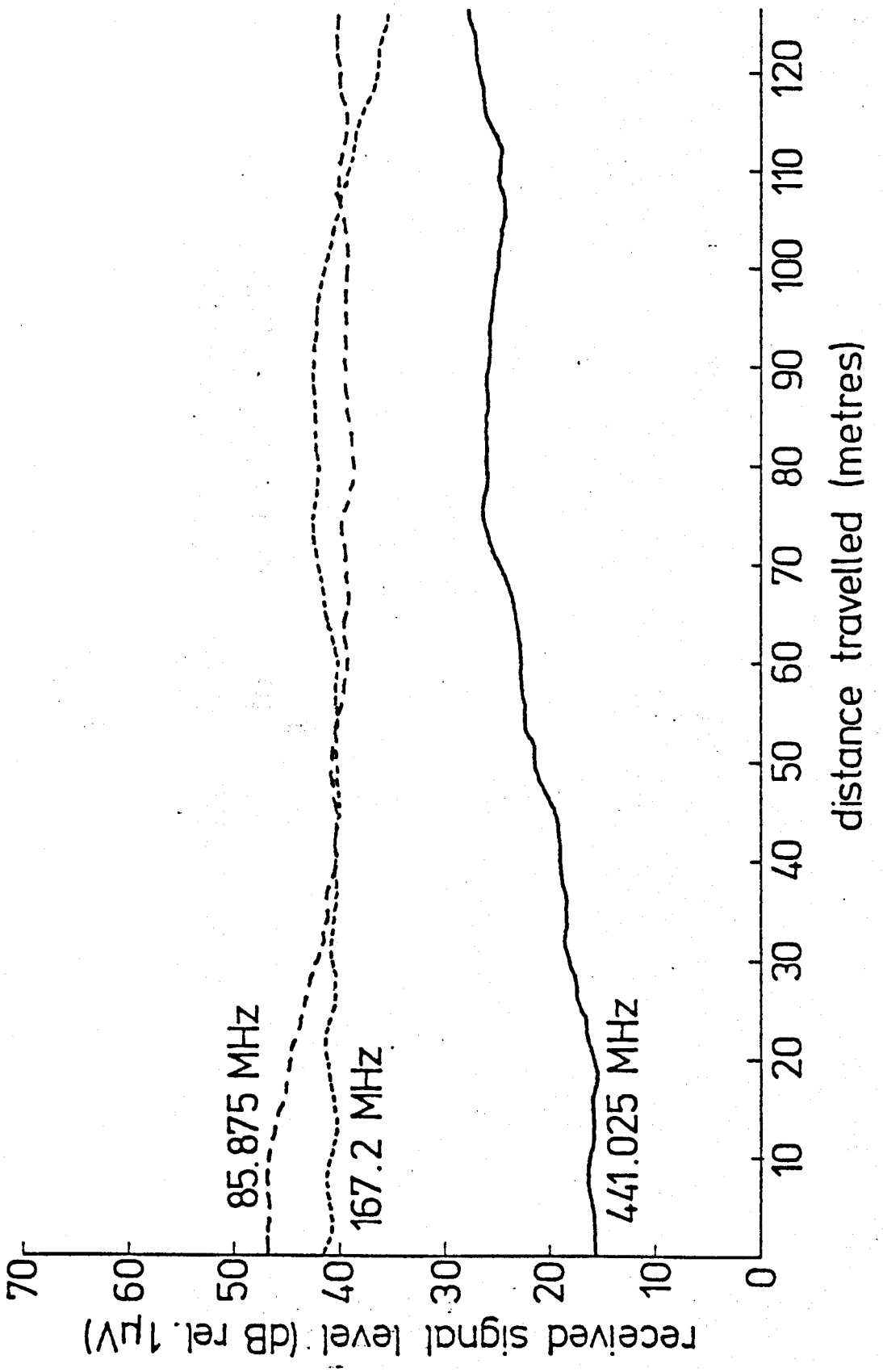

EXAMPLES OF SLOW FADING SIGNALS

FIG. 4

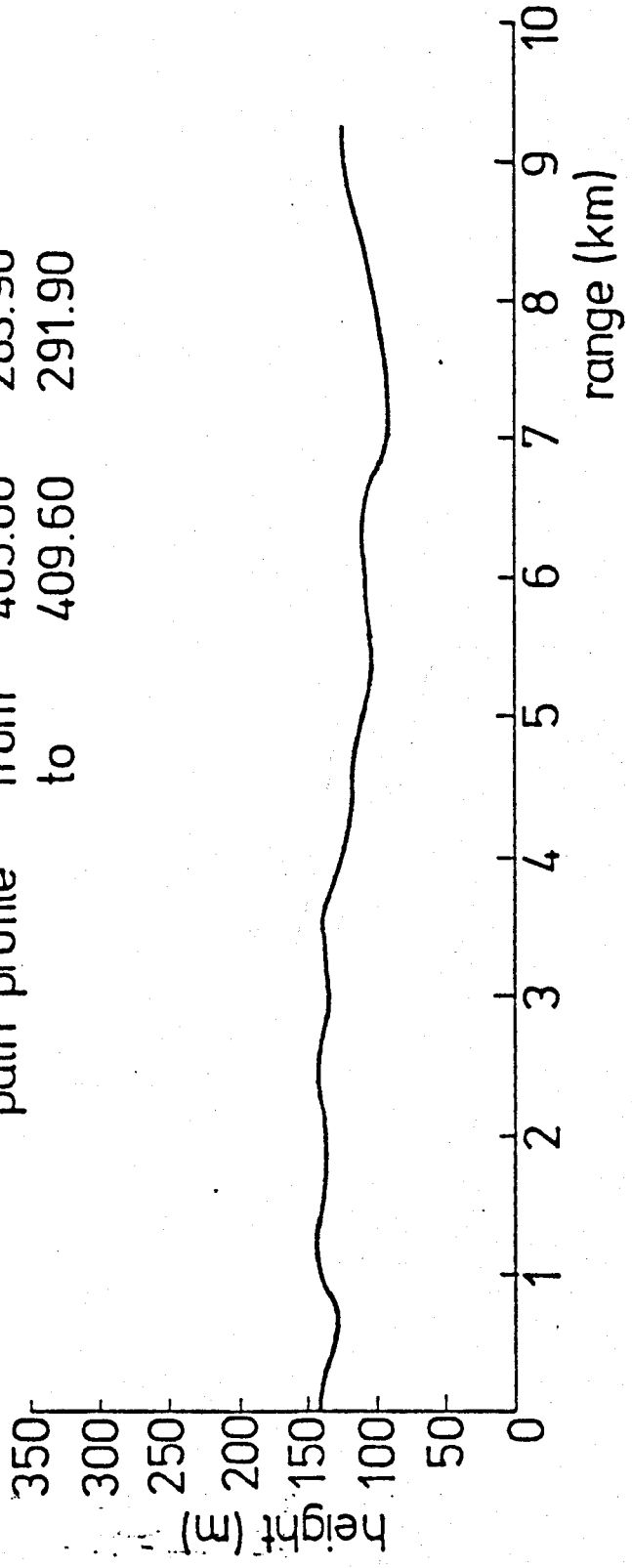

A BIRMINGHAM PATH PROFILE

FIG.5

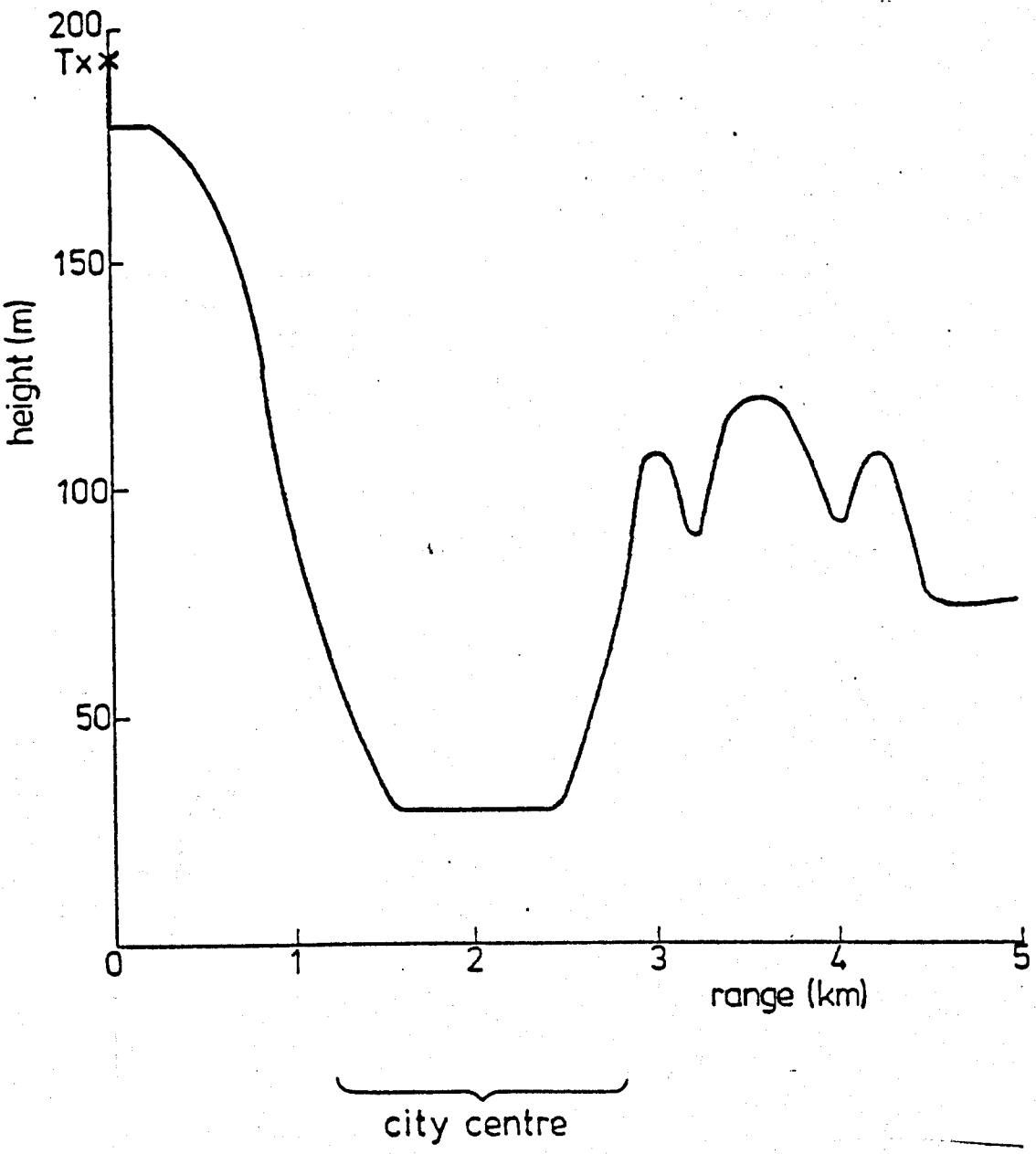

A TERRAIN PROFILE OF BATH

FIG. 6

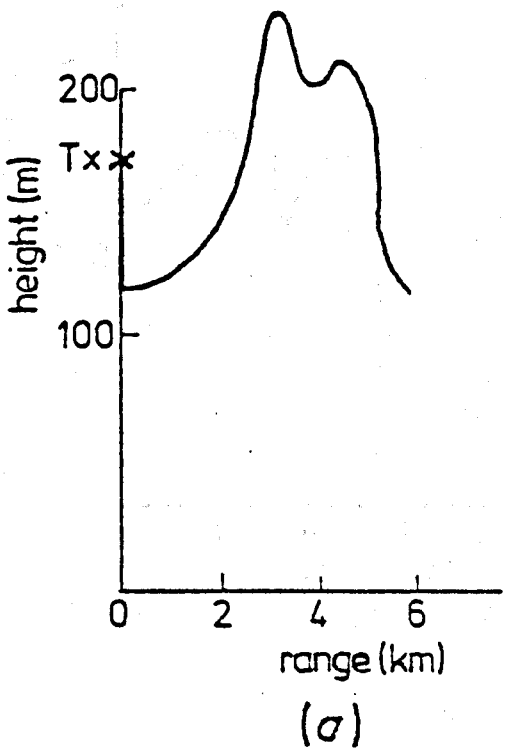

(a)

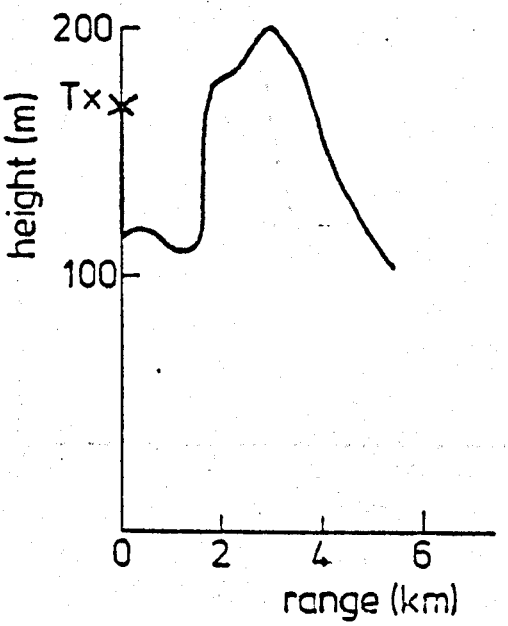

(b)

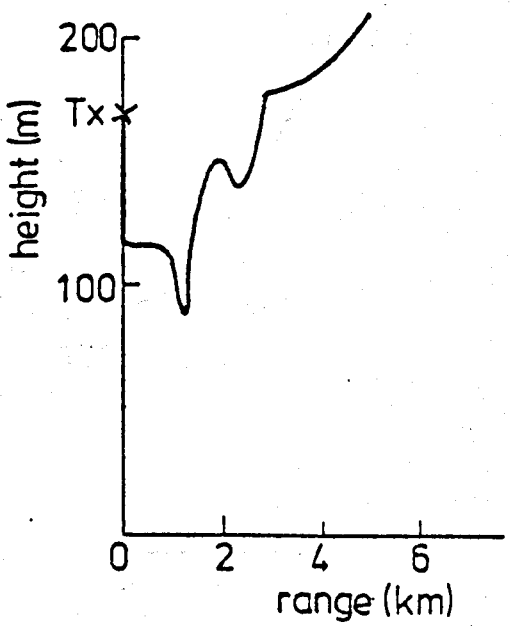

(c)

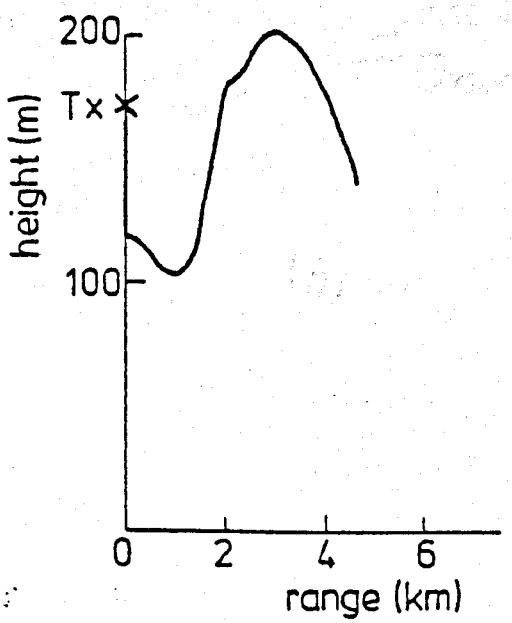

(d)

TERRAIN PROFILES OF BRADFORD
(a) Cottingley (b) Greengates (c) Eccleshill (d) Undercliffe

-- FIG. 7

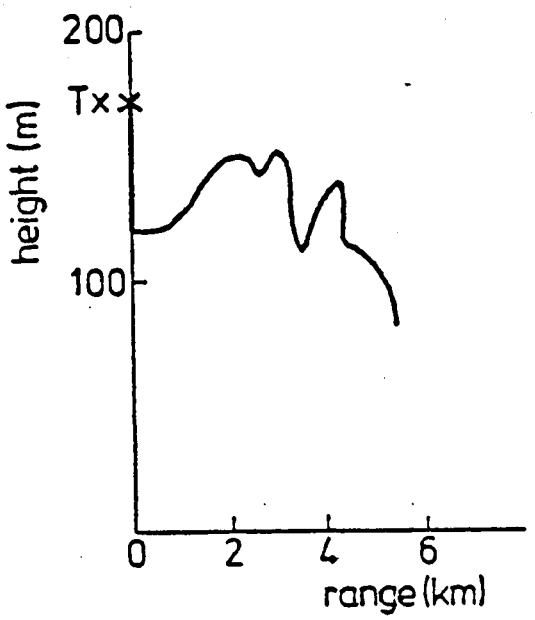

(e)

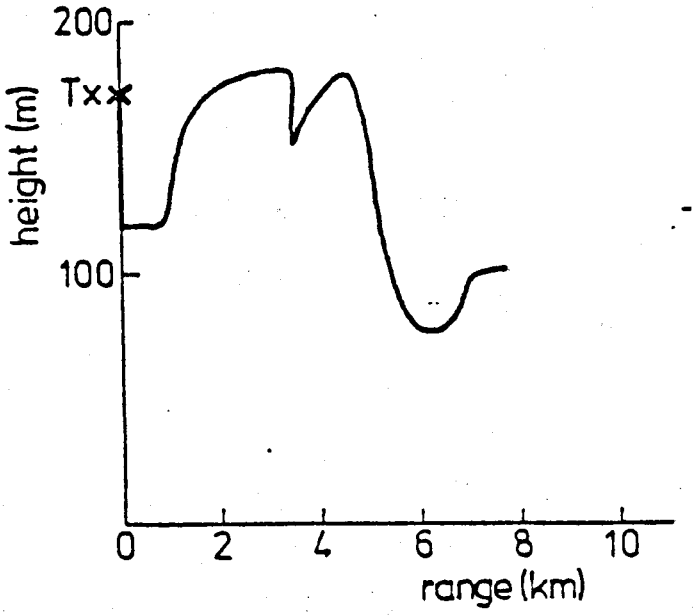

(f)

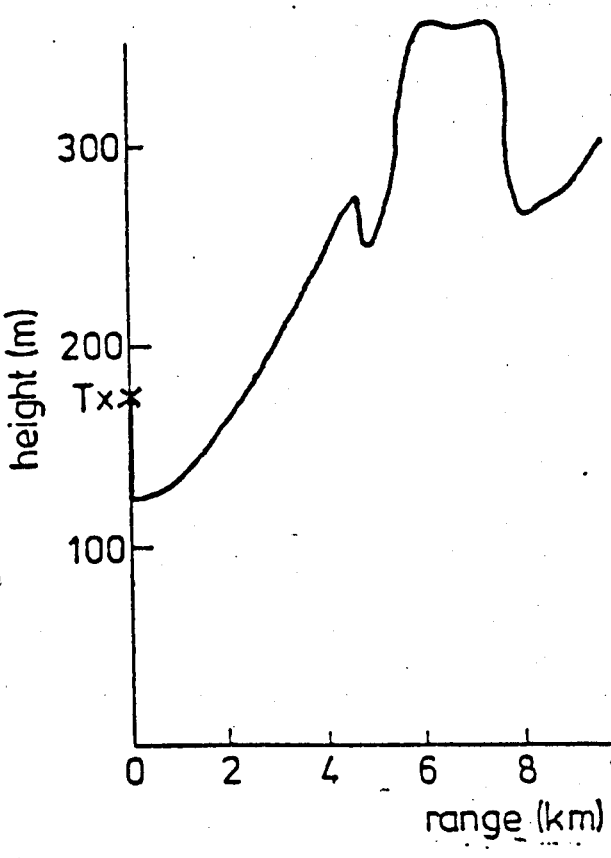

(g)

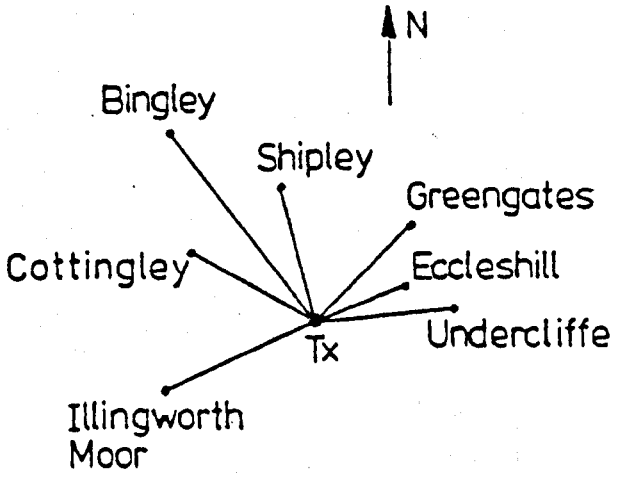

(h)

TERRAIN PROFILES OF BRADFORD
(e) Shipley (f) Bingley (g) Illingworth Moor
(h) Bradford Regional Plan

FIG. 7
(cont.)

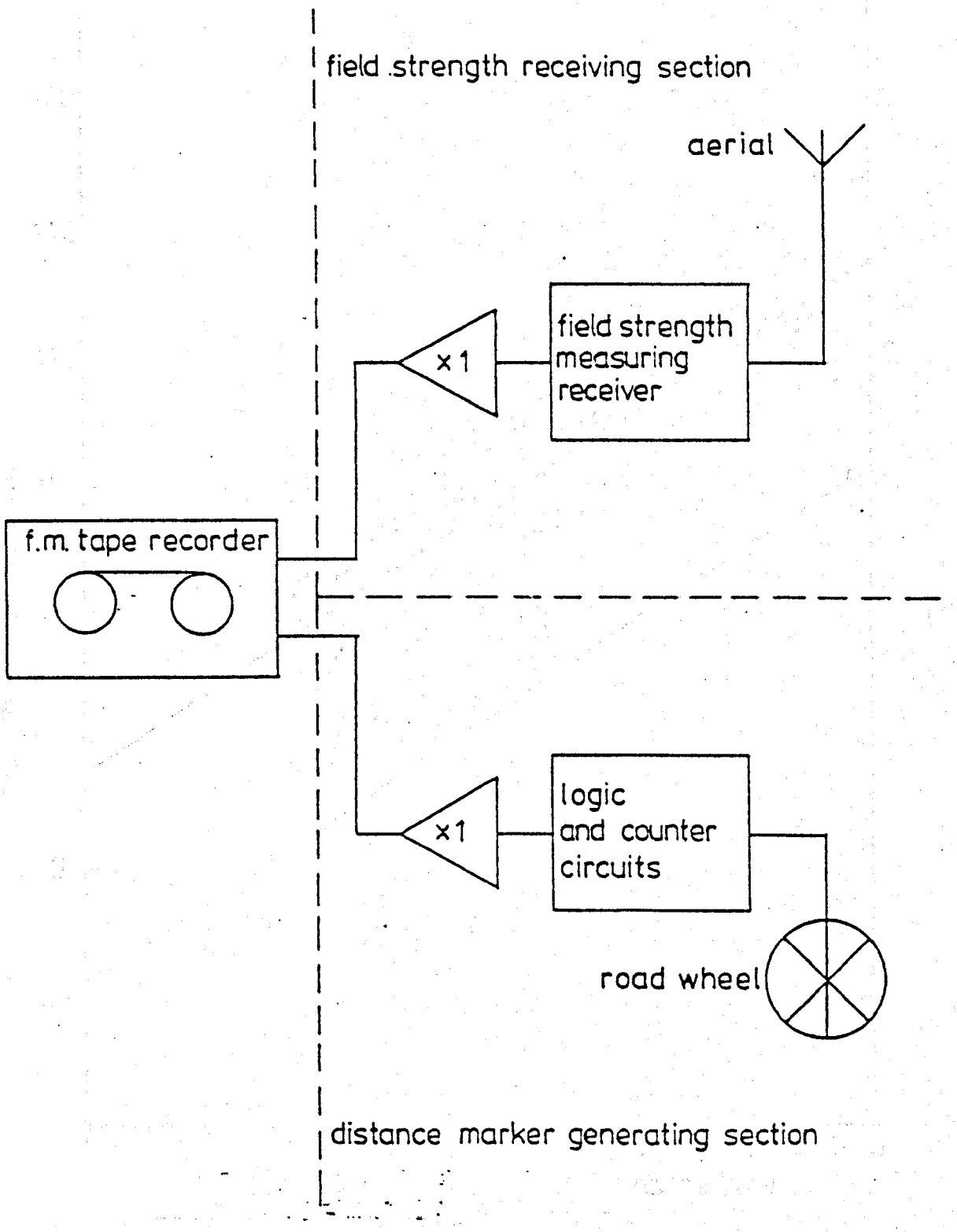

THE RECEIVING SYSTEM

- FIG. 8

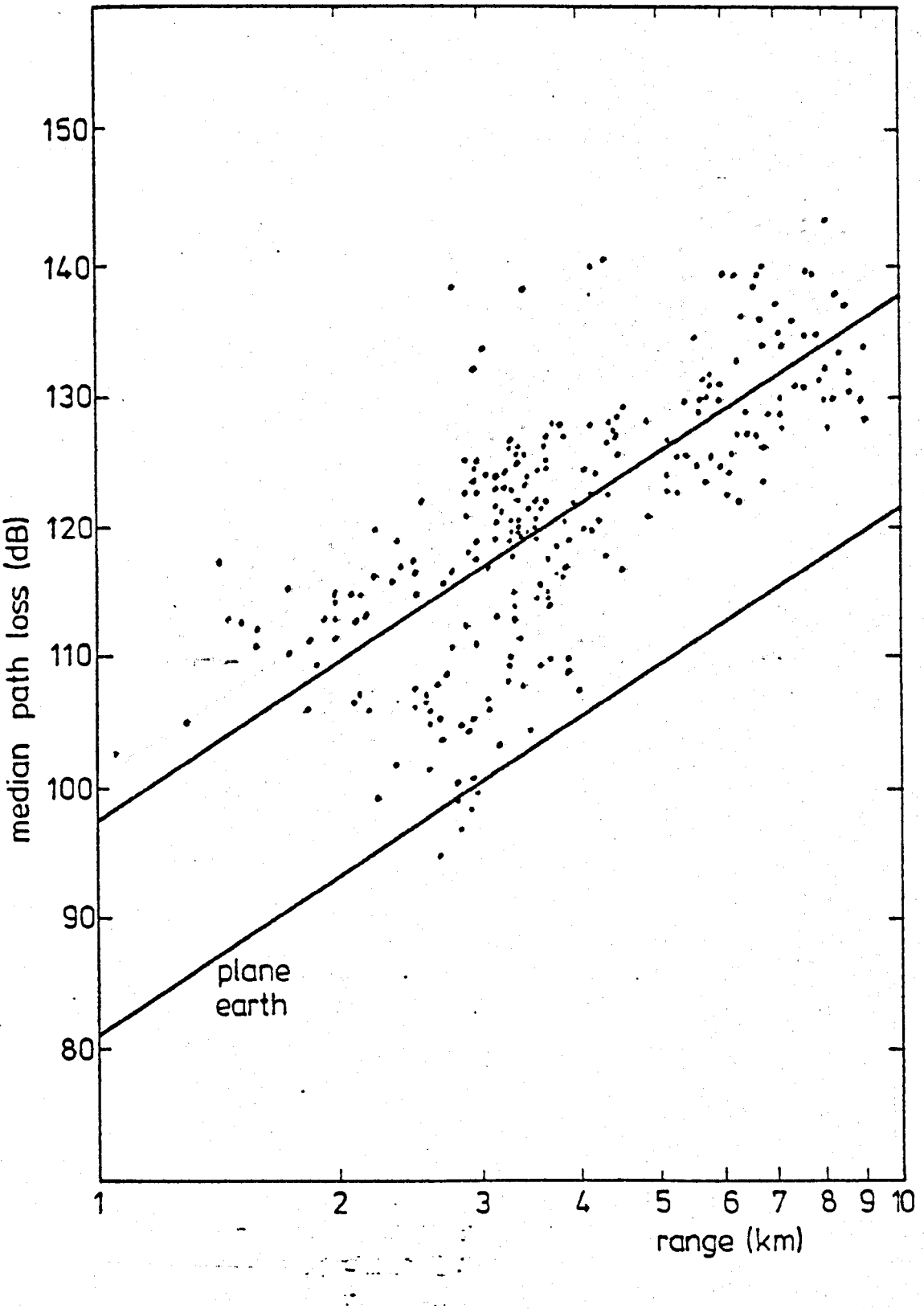

MEDIAN PATH LOSS BETWEEN HALF-WAVE DIPOLES
Vs. RANGE AT 85.875MHz

FIG. 9

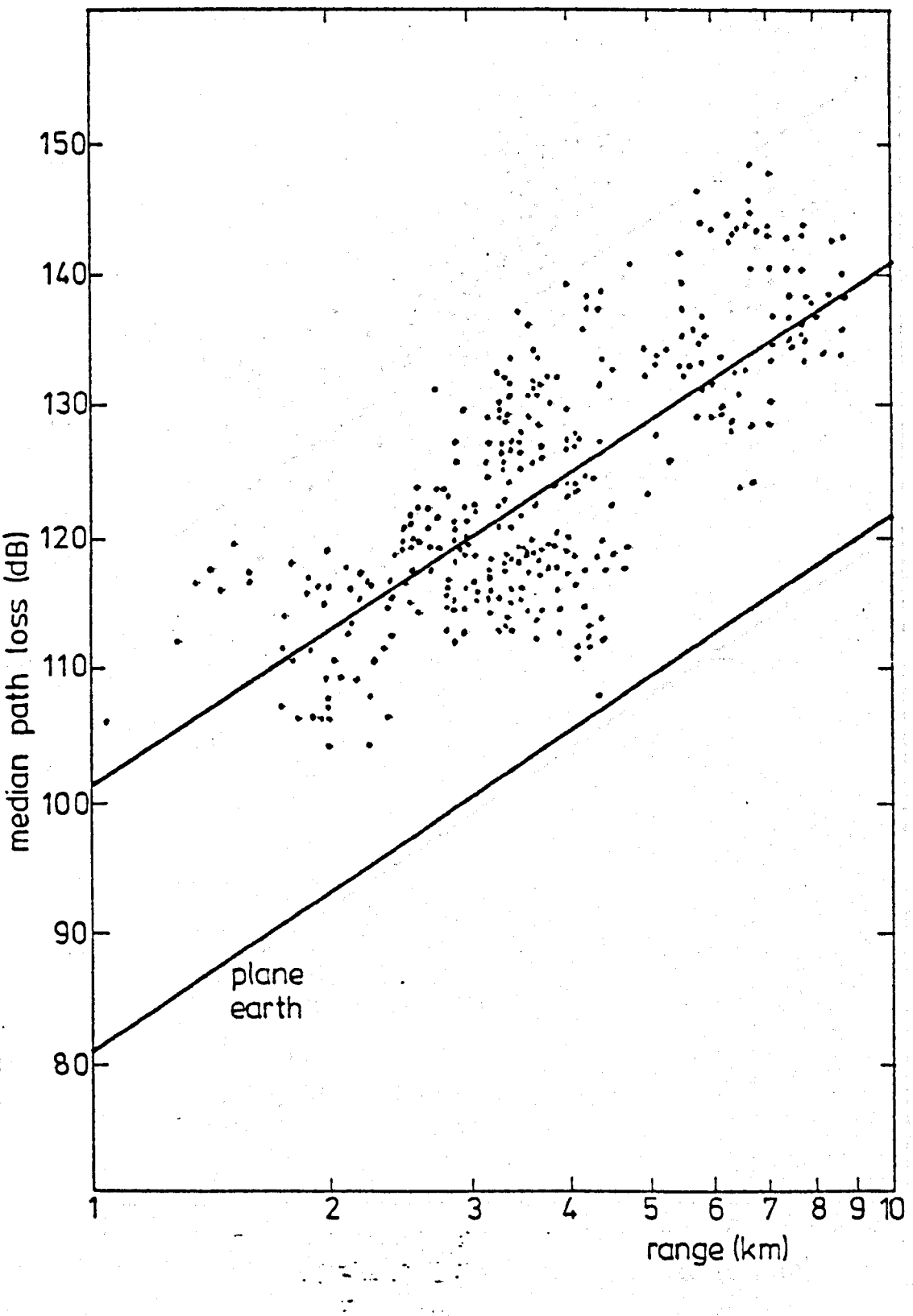

MEDIAN PATH LOSS BETWEEN HALF-WAVE DIPOLES
Vs. RANGE AT 167.2MHz

FIG. 10

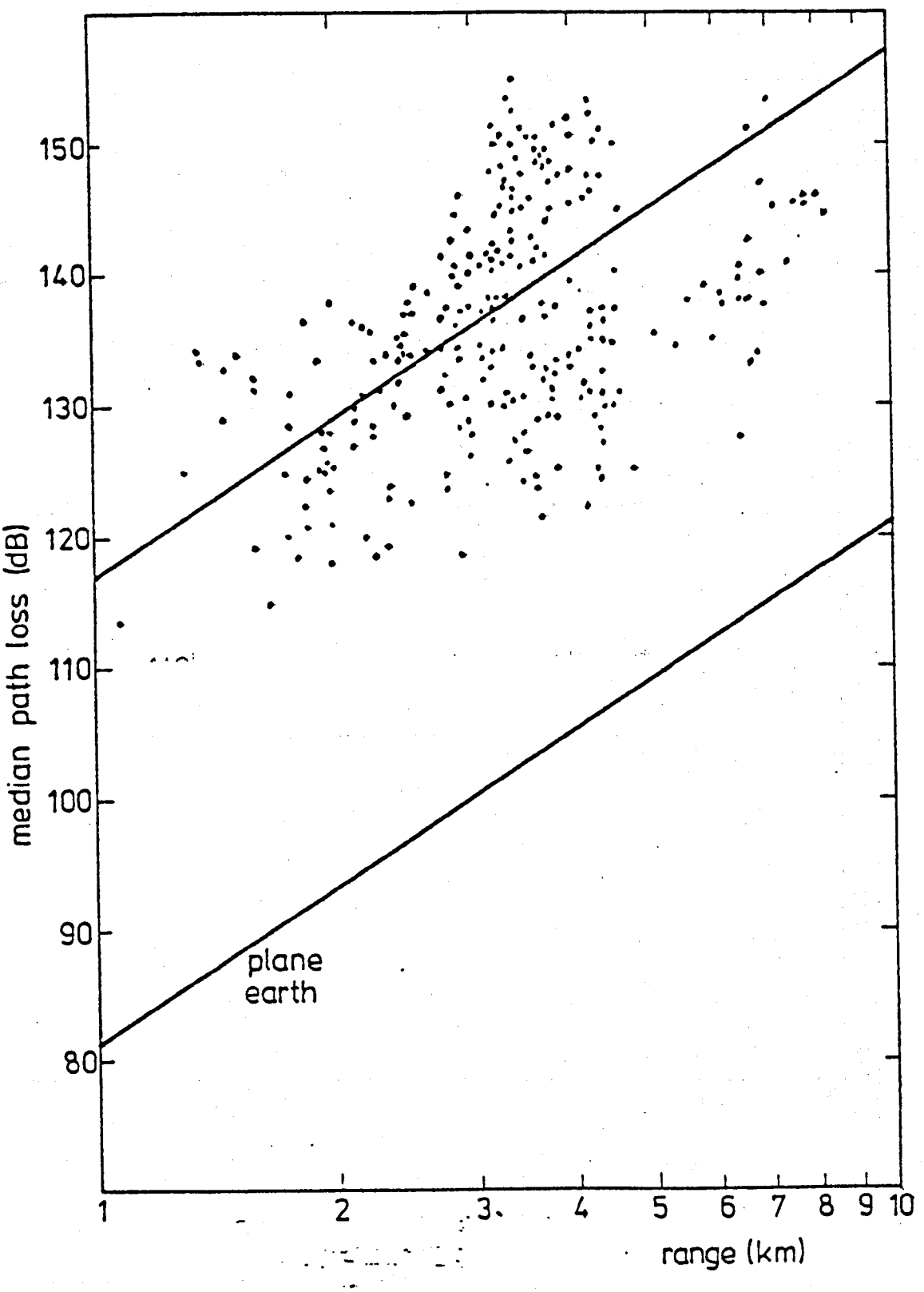

MEDIAN PATH LOSS BETWEEN HALF-WAVE DIPOLES
Vs. RANGE AT 441.025MHz

-- FIG. 11

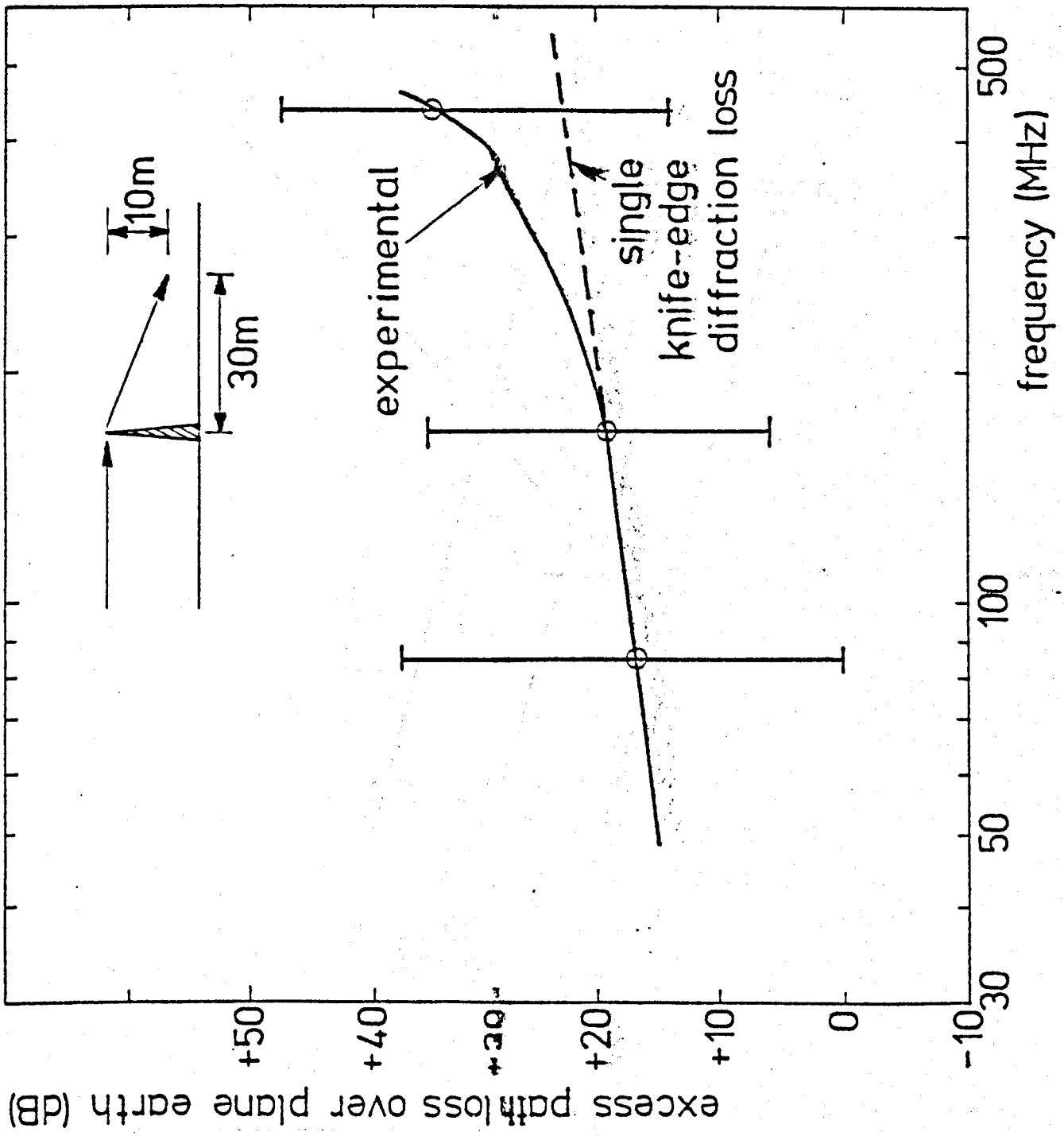

FREQUENCY DEPENDENCE OF THE URBAN CLUTTER FACTOR (β)

.. FIG. 12

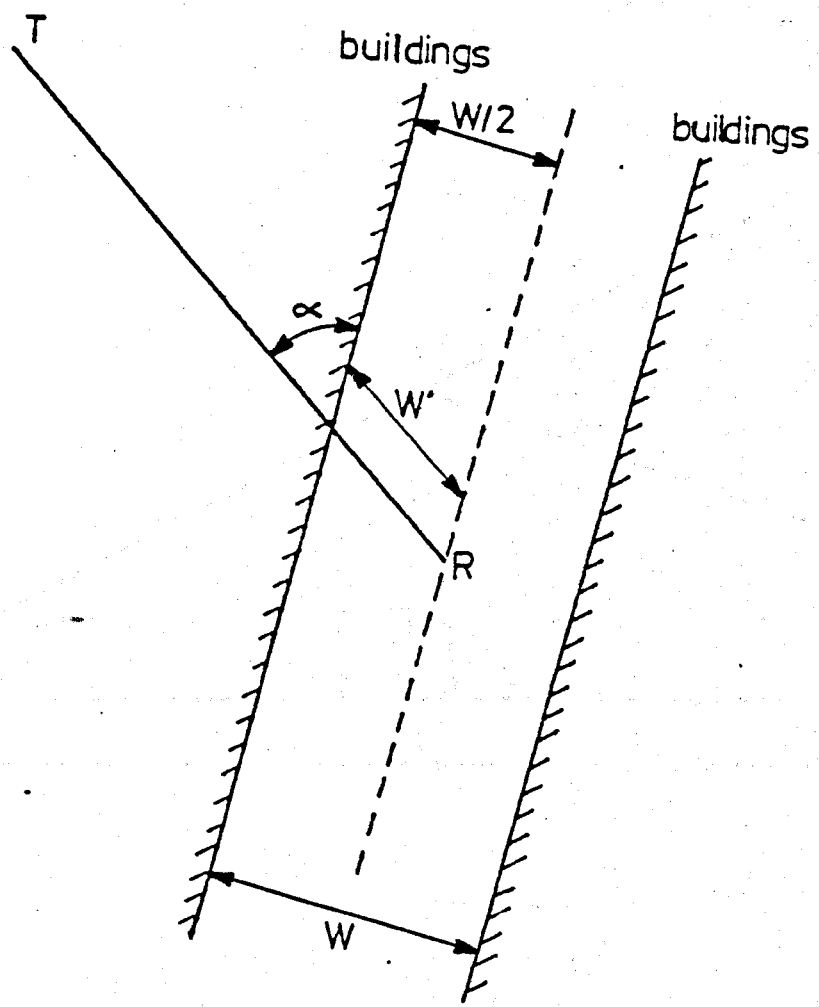

$$W' = \frac{W}{2 \sin \alpha}$$

DEFINITION OF EFFECTIVE STREET WIDTH (W')

FIG. 13

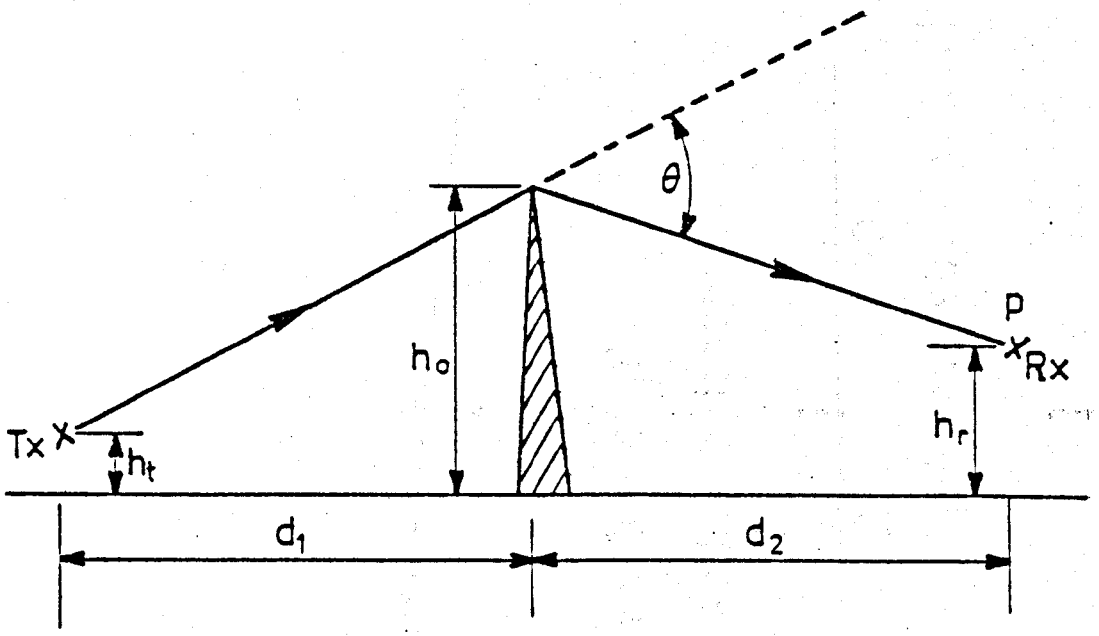

$$v = \sqrt{\frac{2d_1 d_2}{\lambda(d_1 + d_2)}}\,\theta$$

KNIFE-EDGE DIFFRACTION

-- FIG. 14

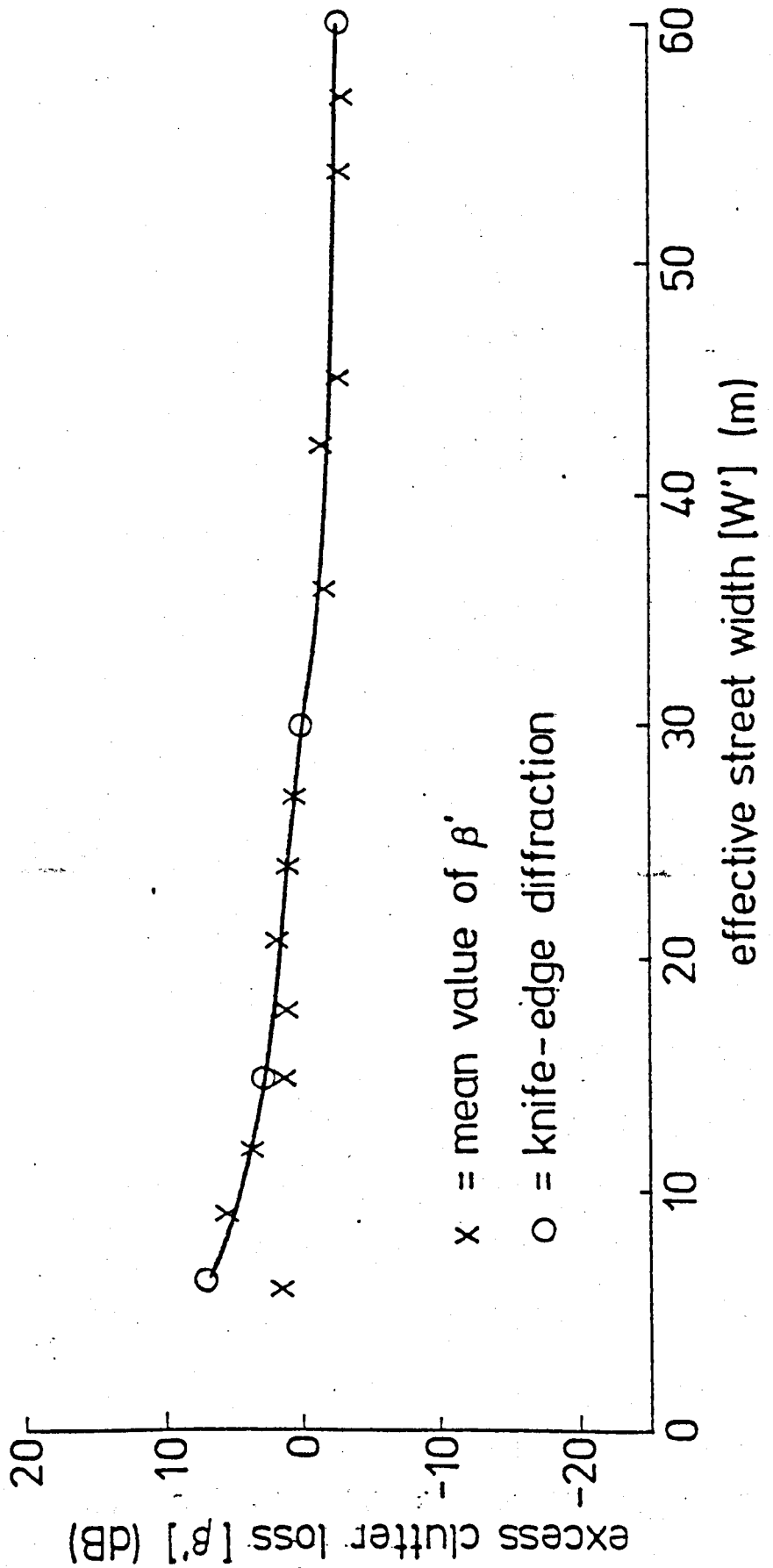

VARIATION OF FREQUENCY CORRECTED URBAN CLUTTER FACTOR (β) WITH EFFECTIVE STREET WIDTH (W')

FIG. 15

THE UHF CORRECTION FACTOR (γ)

FIG. 16

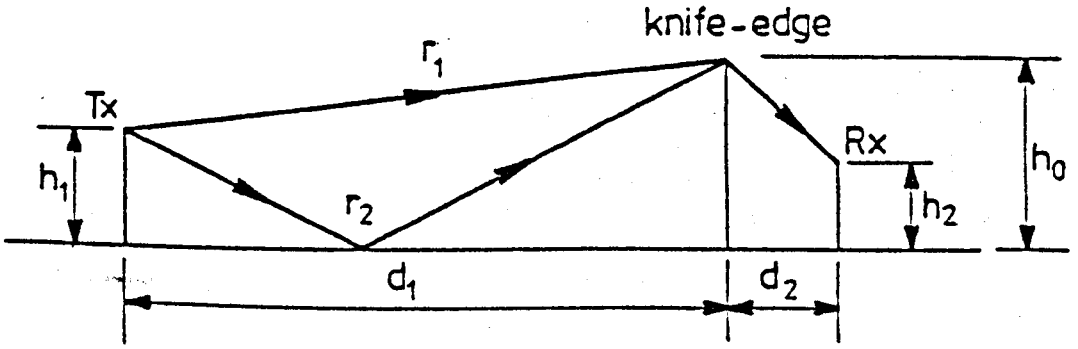

REFLECTIONS OVER A KNIFE-EDGE

FIG. 17